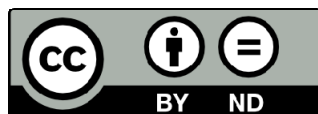




UNIVERSITAT DE
BARCELONA

Novel nanoscale therapeutic approaches to treat liver diseases

Meritxell Perramón Corominas



Aquesta tesi doctoral està subjecta a la llicència Reconeixement- SenseObraDerivada 4.0. Espanya de Creative Commons.

Esta tesis doctoral está sujeta a la licencia Reconocimiento - SinObraDerivada 4.0. España de Creative Commons.

This doctoral thesis is licensed under the Creative Commons Attribution-NoDerivatives 4.0. Spain License.



UNIVERSITAT DE
BARCELONA



Novel nanoscale therapeutic approaches to treat liver diseases

Memòria presentada per

MERTXELL PERRAMÓN COROMINAS

Per a optar al títol de Doctora per la Universitat de Barcelona

Treball realitzat sota la supervisió del **Dr. Wladimiro Jiménez Povedano**
i del **Dr. Pedro Melgar Lesmes**

Servei de Bioquímica i Genètica Molecular del Hospital Clínic

Fundació Hospital Clínic de Barcelona

Institut d'Investigacions Biomèdiques Pi i Sunyer (IDIBAPS)

Departament de Biomedicina, Universitat de Barcelona

Programa de Doctorat de Medicina i Recerca Translacional

Facultat de Medicina i Ciències de la Salut de la Universitat de Barcelona

Barcelona, Juny 2022

A tots els qui m'han acompanyat en aquest camí.

I en especial als meus pares i al Ferran.

INDEX

FIGURES AND TABLES INDEX	v
ABBREVIATIONS	ix
PUBLICATIONS	xiii
RESUM DE LA TESI	xvii
INTRODUCTION	2
1. LIVER DISEASES.....	3
1.1 Overview.....	3
1.2 Liver fibrosis	4
1.2.1 Cellular and molecular mechanisms	5
1.2.2 Fibrosis regression	8
1.2.3 PTTG1/DLK1 axis	9
1.3 Liver cirrhosis and complications	14
1.3.1 Role of nitric oxide in liver cirrhosis	16
1.4 Hepatocellular carcinoma	19
1.4.1 Genetic landscape.....	21
1.4.2 Cellular and molecular mechanisms	23
2. GENE THERAPY	26
2.1 Overview	26
2.2 Types of vectors.....	28
2.2.1 Viral vectors.....	29
2.2.2 Non-viral vectors	30
2.2.2.1 Genetic therapy technologies	33
2.3 Gene therapy in liver fibrosis	36
3. NANOPARTICLES	37
3.1 Overview	37
3.2 Cerium oxide nanoparticles	39
3.2.1 Characteristics	39
3.2.2 Applications in liver diseases	40

3.3 Poly(beta-amino ester) nanoparticles.....	43
3.3.1 Characteristics.....	43
3.3.2 Applications in liver diseases	45
HYPOTHESES	47
OBJECTIVES	51
MATERIALS, METHODS, AND RESULTS	55
ARTICLE 1: The pituitary tumor-transforming gene 1 / delta like homolog 1 pathway plays a key role in liver fibrogenesis	57
ARTICLE 2: Bespoke Nanoceria: An Effective Treatment in Experimental Hepatocellular Carcinoma	87
UNPUBLISHED MANUSCRIPT: Liver-targeted nanoparticles delivering nitric oxide reduce portal hypertension in cirrhotic rats	129
DISCUSSION	163
CONCLUSIONS	177
REFERENCES	183

FIGURES AND TABLES INDEX

Figure 1. Schematic representation of the stages of CLDs.....	3
Figure 2. Transmission electron microscopy (TEM) images of a human liver. .	4
Figure 3. Activation of an HSC.	6
Figure 4. Schematic representation of the human PTTG1 protein in domains..	9
Figure 5. Schematic representation of the human DLK1 protein in domains..	12
Figure 6. Pathophysiology of portal hypertension in cirrhosis.....	15
Figure 7. NO synthesis and effects in endothelial and HSCs.	18
Figure 8. Incidence of primary liver cancer worldwide	20
Figure 9. Barcelona Clinic Liver Cancer staging algorithm	21
Figure 10. Mechanisms of malignant transformation in HCC	22
Figure 11. Mechanisms influencing tumor growth and progression	25
Figure 12. Different strategies used in gene therapy.	27
Figure 13. Schematic representation of processes of non-viral vectors gene therapy.....	31
Figure 14. Schematic representation of a pDNA design..	33
Figure 15. Schematic siRNA-mediated gene silencing.....	35
Figure 16. Design of a nanoparticle.....	38
Figure 17. Oxidation and reduction states of cerium.	40
Figure 18. Schematic representation of the signaling pathways involved in oxidative stress-mediated inflammation and CeO ₂ NP effects.	41
Figure 19. Schematic representation of the synthesis of a linear pBAE.	44
Figure 20. Schematic representation of the proposed mechanism underlying PTTG1/DLK1 axis role in liver fibrosis induction	168
Figure 21. Schematic representation of CeO ₂ NPs effects on experimental HCC.....	172
Table 1. Main characteristics of the most used viral vectors.....	29

ABBREVIATIONS

ABBREVIATIONS

AAVs	Adeno-associated viruses
AD	Adenovirus
AFP	Alpha-fetoprotein
<i>ARID1A</i>	AT-rich interaction domain 1A
α -SMA	Alfa smooth muscle actin
BCLC	Barcelona Clinic Liver Cancer
CCl ₄	Carbon tetrachloride
CE	Cholesterol esters
CeO ₂ NPs	Cerium oxide NPs
CO	Cardiac output
CLDs	Chronic liver diseases
cGMP	Cyclic guanosine monophosphate
CYP	Cytochrome
DAMPs	Damage-associated patterns
DEN	Diethylnitrosamine
DLK1	Delta like non-canonical notch ligand 1
ECM	Extracellular matrix
EGF	Epidermal growth factor
EMT	Epithelial to mesenchymal transition
ET-1	Endothelin 1
eNOS/Nos3	Endothelial oxide synthase
ERK	Extracellular signal-regulated kinase
FA	Fatty acid
HCC	Hepatocarcinoma
HDAC	Histone deacetylases
HSCs	Hepatic stellate cells
IL-1 β	Interleukin 1 beta
iNOS/Nos2	Inducible nitric oxide synthase
KC	Kupffer cell
KO	Knock out
LD	Lipid droplet
LSECs	Liver sinusoidal endothelial cells
MAPK	Mitogen-activated protein kinase

ABBREVIATIONS

MMPs	Metalloproteinases
mRNA	Messenger RNA
mTOR	Mammalian target of rapamycin
NAFLD	Non-alcoholic fatty liver disease
NEFA	Non-esterified fatty acid
NO	Nitric oxide
NOS	Nitric oxide synthase
NP	Nanoparticle
pBAE	Poly(beta-amino ester)
PDI	Polydispersity index
PDGF	Platelet-derived growth factor
PDGFR β	Platelet-derived growth factor receptor beta
pDNA	Plasmid DNA
PI3K	Phosphatidylinositol 3-kinase
PUFA	Polyunsaturated fatty acid
PTTG1	Pituitary tumor-transforming gene 1
RISC	RNA-induced silencing complex
ROS	Reactive oxygen species
RNS	Reactive nitrogen species
siRNA	Small interfering RNA
TACE	Tumor necrosis factor alpha converting enzyme
TAMs	Tumor-associated macrophages
TEM	Transmission electron microscopy
TERT	Telomerase reverse transcriptase
TGF β	Transforming growth factor beta
TIMPs	Tissue inhibitors of metalloproteinases
TNF α	Tumor necrosis factor alpha
VEGF	Vascular endothelial growth factor

PUBLICATIONS

Aquesta tesi en format de compendi d'articles, presentada per a optar al títol de Doctora per la Universitat de Barcelona, consta de tres objectius generals, de dos articles publicats i un sense publicar.

1st Article: **Perramón M**, Carvajal S, Reichenbach V, Fernández-Varo G, Boix L, Macías L, Melgar-Lesmes P, Bruix J, Melmed S, Lamas S, Jiménez W. The pituitary tumor-transforming gene 1 / delta like homolog 1 pathway plays a key role in liver fibrogenesis. *Liver Int.* 2022 Mar;42(3):651-662.

- *Journal impact factor (2020):* 5.828
- *Quartile:* Q2
- *Area of knowledge:* Gastroenterology & Hepatology

2nd Article: Fernández-Varo G, **Perramón M**, Carvajal S, Oró D, Casals E, Boix L, Oller L, Macías-Muñoz L, Marfà S, Casals G, Morales-Ruiz M, Casado P, Cutillas PR, Bruix J, Navasa M, Fuster J, Garcia-Valdecasas JC, Pavel MC, Puentes V, Jiménez W. Bespoke Nanoceria: An Effective Treatment in Experimental Hepatocellular Carcinoma. *Hepatology.* 2020 Oct;72(4):1267-1282

- *Journal impact factor (2020):* 17.425
- *Quartile:* Q1
- *Area of knowledge:* Gastroenterology & Hepatology

Unpublished manuscript: **Perramón M**, Navalón-López M, Fernández-Varo G, Moreno-Lanceta A, Fornaguera C, Melgar-Lesmes P, Borrós S, Jiménez W. Engineered poly(beta-amino ester) nanoparticles containing a nitric oxide donor ameliorate portal hypertension in rats with decompensated cirrhosis.

RESUM DE LA TESI

Títol: Noves aproximacions terapèutiques en la nanoescala per a tractar malalties hepàtiques.

Introducció: Les malalties hepàtiques cròniques, sent la fibrosi la base patològica més comuna, representen la desena causa de mortalitat mundial. La fisiopatologia de la fibrosi és complexa ja que hi intervenen gran multitud de mediadors i tipus cel·lulars. D'altra banda, la fibrosi pot progressar a cirrosi i/o hepatocarcinoma (HCC), les quals són condicions més severes i potencialment mortals. Actualment, no hi ha cap tractament queaturi el curs natural de la malaltia ni l'esdeveniment de complicacions. L'estudi més profund de les vies de senyalització implicades pot donar lloc a noves dianes terapèutiques per frenar-ne l'evolució. Altrament, noves estratègies terapèutiques, com l'ús de nanopartícules podrien ser útils pel seu tractament.

Hipòtesis: La via de senyalització de PTTG1/DLK1 podria tenir un paper important en el procés fibrogènic i per tant, la seva interferència podria ser una bona estratègia terapèutica per a atenuar la progressió de la fibrosi hepàtica experimental. Per altra part, les nanopartícules d'òxid de ceri (CeO₂NPs) són potents antioxidants potencialment beneficiosos per a tractar l'estrès oxidatiu i mitigar la progressió tumoral en l'HCC. I per últim, NPs polimèriques de poli(beta-amino ester) (pBAE) contenint un donador d'òxid nítric i funcionalitzades amb retinol podrien mitigar la hipertensió portal característica de la cirrosi així com millorar la funció hepàtica.

Objectius: En primer lloc, avaluar el paper de la via de senyalització PTTG1/DLK1 en el desenvolupament de la fibrosi hepàtica i el potencial efecte antifibròtic de la interferència de PTTG1. En segon lloc, investigar el potencial efecte de les CeO₂NPs sobre la progressió tumoral i supervivència en rates amb HCC; així com els mecanismes de senyalització involucrats en els seus efectes. A més a més, valorar la capacitat d'internalització i distribució cel·lular d'aquestes NPs en fetges humans. En tercer lloc, avaluar la biodistribució i l'efecte de les NPs pBAE contenint un donador d'òxid nítric en l'hemodinàmica portal i sistèmica així com en els processos inflamatoris i fibroproliferatius de la cirrosi descompensada.

Mètodes: Anàlisi de l'expressió de PTTG1 i DLK1 en la fibrosi/cirrosi experimental i humana. Determinació de la signatura molecular fibròtica en ratolins amb fibrosi deficients i salvatges pel gen PTTG1. Avaluació de la interferència de *Pttg1* com a nova teràpia antifibrogènica. Anàlisi de la biodistribució *in vivo* de les CeO₂NPs. Determinació dels efectes de les CeO₂NPs a nivell genòmic, fosfoproteòmic, lipidòmic i en la supervivència en l'HCC experimental. Anàlisi de la distribució a nivell microscòpic en fetges humans perfosos *ex vivo* i administrats amb CeO₂NPs. Determinació de la distribució *in vivo* així com avaluació de l'efecte del donador d'òxid nítric dirigit amb NPs pBAE en l'hemodinàmica sistèmica i portal, en la funció hepàtica i vies de senyalització profibrogèniques i proinflamatòries en la cirrosi descompensada experimental.

Resultats: L'expressió de PTTG1 i DLK1 augmenta de manera paral·lela a la progressió de la fibrosi experimental i selectivament al fetge, sent majoritària en hepatòcits i cèl·lules hepàtiques estelades. A més a més, en el fetge cirròtic humà ambdós transcrits estan augmentats. Ratolins amb fibrosi deficients pel gen PTTG1 presenten una disminució significativa en la deposició de col·lagen en comparació amb ratolins salvatges amb fibrosi. L'anàlisi de la firma molecular fibròtica mostra una expressió més baixa dels gens *Mmp8*, *Mmp9* i *Timp4*, i un augment en *eotaxina* i *Mmp13* en comparació amb els ratolins salvatges amb fibrosi. Finalment, la interferència de *Pttg1* resulta en la disminució significativa de la fibrosi hepàtica, de la hipertensió portal i de la transcripció de *Dlk1*, *col·làgens I i III*, *Pdgfrβ*, *Tgfrβ*, *Timp1*, *Timp2* i *Mmp2* en rates amb fibrosi. Les CeO₂NPs s'acumulen majoritàriament en el fetge al administrar-les de manera intravenosa en el HCC experimental. Aquestes NPs disminueixen la inflamació i la proliferació, al mateix temps que augmenten l'apoptosi en el fetge de rates amb HCC. A més, les CeO₂NPs afecten a la fosforilació de proteïnes majoritàriament relacionades amb l'adhesió cel·lular i l'empalmament del RNA. Així mateix, la producció d'àcid araquidònic del component lipídic fosfatidilcolina i d'àcid linoleic de diferents components es veuen disminuïts de manera significativa amb el tractament. Les CeO₂NPs també redueixen la concentració d'alfa-proteïna sèrica i milloren la supervivència de rates amb HCC. Finalment, el fetge humà és capaç de captar les CeO₂NPs, les quals es localitzen al citoplasma i dins d'òrgànuls intracel·lulars tipus endosoma. L'administració intravenosa de les NPs pBAE

funcionalitzades amb retinol en rates cirròtiques amb ascites resulta en una transfecció elevada del fetge i la melsa, i en menor intensitat del ronyó. No es localitzen NPs en el cervell, pulmó, cor ni en artèries. Addicionalment, el tractament amb donador d'òxid nítric dirigit disminueix de manera significativa la pressió portal sense afectar a la pressió arterial mitja ni al cabal cardíac. La determinació sèrica de marcadors de funció hepàtica revela una reducció significativa dels enzims aspartat transaminasa i lactat deshidrogenasa en resposta al tractament. Finalment, el tractament també disminueix l'activació de les cèl·lules hepàtiques estelades, i l'expressió de gens relacionats amb inflamació incloent *Cox2*, *Il-6*, *Tnfa* i *Nos2*.

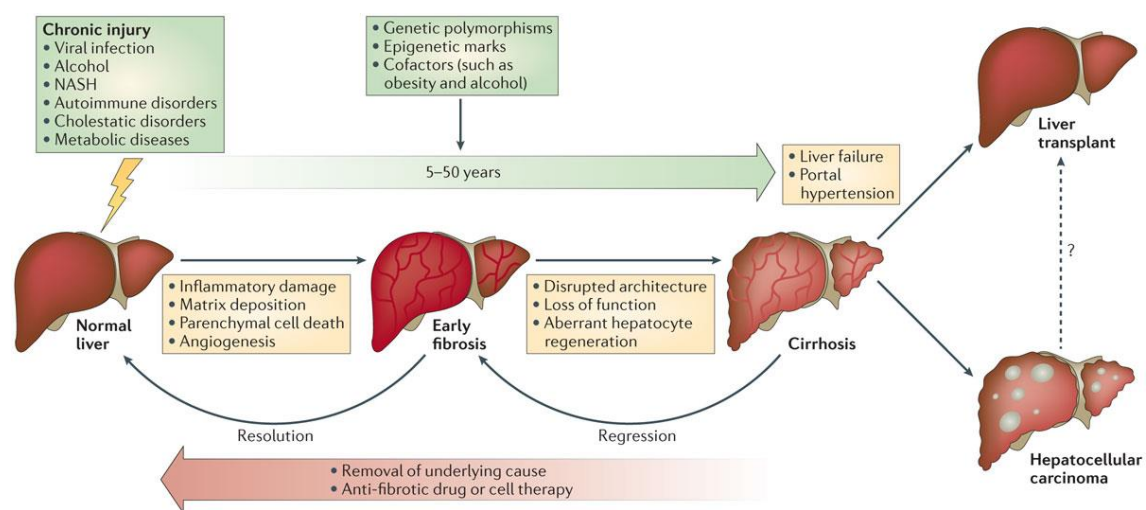
Conclusions: La via de senyalització de PTTG1/DLK1 és una nova diana terapèutica per frenar la progressió de la fibrosi hepàtica. Les CeO₂NPs reverteixen parcialment els mecanismes moleculars relacionats amb l'HCC i són una teràpia prometedora per frenar la progressió tumoral. Les pBAE NPs contenint nitrats orgànics es dirigeixen al fetge de manera selectiva disminuint la pressió portal, així que podrien ser útils per mitigar la hipertensió portal característica de la cirrosi hepàtica.

INTRODUCTION

1. LIVER DISEASES

1.1 Overview

Chronic liver diseases (CLDs) are the consequence of a long-standing process of sustained inflammation with a characteristic phenomenon of destruction and regeneration of the hepatic parenchyma to limit chronic liver injury (1). Liver fibrosis is the common pathological basis of all CLDs, taking years of chronic injury (15 to 20 years) to progress towards cirrhosis, hepatocarcinoma (HCC) and/or hepatic failure (**Figure 1**).



Nature Reviews | Immunology

Figure 1. Schematic representation of the stages of CLDs. Original image from: Pellicoro A, Ramachandran P, Iredale JP, Fallowfield JA. Liver fibrosis and repair: immune regulation of wound healing in a solid organ. *Nat Rev Immunol.* 2014;14(3):181-94.

CLDs are estimated to affect 844 million people and are the 10th cause of mortality worldwide with a mortality rate of 2 million deaths per year (2). However, the estimated incidence and prevalence largely varies depending on factors such as geographic area, etiology, and genetics. In Western countries, non-alcoholic fatty liver disease (NAFLD), recently referred as metabolic dysfunction-associated fatty liver disease, is the most common cause of CLDs (3). NAFLD consists of the presence of hepatic fat accumulation in addition to obesity, type 2 diabetes mellitus or evidence of metabolic dysregulation; with the absence of concomitant liver diseases (4). Other principal culprits of CLDs include chronic viral hepatitis (mostly hepatitis B, C or D virus infections), alcoholic liver disease, genetic causes (like haemochromatosis, Wilson's disease, and α 1-anti-trypsin

deficiency), autoimmune diseases (such as primary biliary cirrhosis, primary sclerosing cholangitis, and autoimmune hepatitis) and others (5).

Despite that elimination or removal of the etiologic agent has shown reversibility of liver fibrosis (6), the morbidity and mortality related to CLDs remain a challenge and identifying an effective treatment is a major unmet medical need.

1.2 Liver fibrosis

Liver fibrosis consists in a wound-healing response characterized by exuberant synthesis of extracellular matrix (ECM) components and continuous degradation to limit the consequences of acute or chronic hepatic injury (7). It is a dynamic process that entails the interplay of a multitude of mediators, cellular subsets and signaling pathways (**Figure 2**). Following liver injury, damaged hepatocytes release cytokines, chemokines, reactive oxygen species (ROS), damage-associated patterns (DAMPs), extracellular vesicles and many other substances that induce the apoptosis of injured cells as well as the recruitment and the activation of innate and adaptive immune responses, triggering all together transdifferentiation and activation of hepatic stellate cells (HSCs), the major effector cells of liver wound healing and repair (6). When the damage becomes chronic, the hepatic parenchyma function is lost, and the tissue architecture is distorted.

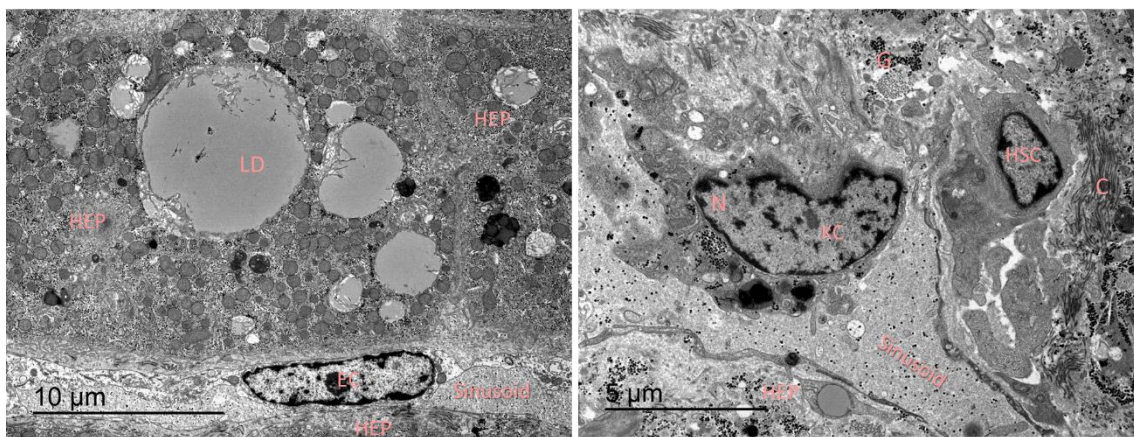


Figure 2. Transmission electron microscopy (TEM) images of a human liver. HEP: hepatocyte, KC: Kupffer cell, HSC: Hepatic stellate cell, EC: endothelial cell, LD: lipid droplet, C: collagen, N: nuclei, G: glycogen.

Liver biopsy, first introduced in 1923, remains the actual gold standard for the diagnosis and staging of liver fibrosis (1). Over the years, several scoring systems

such as METAVIR or Ishak (modified Knodell score) have been developed to classify patients according to histopathological assessment (8,9). For example, METAVIR score system is widely used to score patients with chronic hepatitis C infection because it combines the evaluation of necroinflammation and fibrosis. METAVIR is constituted by two letter and two number coding system: A= histological activity (A0: no activity, A1: mild, A2: moderate, A3: severe) and F= fibrosis (F0: no fibrosis, F1: portal fibrosis, F2: portal fibrosis with rare septa, F3: numerous septa without cirrhosis, F4: cirrhosis) (10). But the liver biopsy has several drawbacks, including it is invasive, costly, prone to sampling error (small representation of the liver = 1/50.000) and inter-observer and intra-observer variable (11). Alternative methods for the diagnosis of liver fibrosis had been proposed over the years including serological markers and imaging techniques. However, the sensibility and specificity of most of them remains low.

1.2.1 Cellular and molecular mechanisms

Quiescent HSC are pericytes residing in the subendothelial space of Disse between hepatocytes and liver sinusoidal endothelial cells (LSECs). They are lipid storing cells with large lipid droplets (LDs) that contain triacylglycerols, cholesterol esters (CE) and mostly vitamin A in form of retinyl esters (12). As a result of activation, HSC lose their LDs, and transdifferentiate into a myofibroblast-like cells, that migrate to the site of injury and secrete ECM to produce a fibrous scar (13).

The most potent mitogen and chemoattractant for HSC is platelet-derived growth factor (PDGF). In the onset of liver injury, HSC rapidly enhance the production of PDGF and its receptor (PDGFR β) leading to the activation of mitogen-activated protein kinase (MAPK) and phosphatidylinositol 3-kinase (PI3K)/Akt signaling pathways (14). Activated HSC are characterized by a proliferative, contractile, inflammatory, chemotactic, and fibrogenic phenotype (**Figure 3**) (6). Alpha smooth muscle actin (α -SMA) is their most reliable marker. Despite HSC being the major source of liver myofibroblasts, other cell lineages including portal fibroblasts, circulating fibrocytes, mesenchymal stem cells, and mesothelial cells; may contribute to the myofibroblast population (13).

Kupffer cells (KC) are one of the first-line responders upon liver injury. In response to signals released by injured hepatocytes, such as DAMPs (extracellularly released intracellular components), they activate several signaling pathways ultimately leading to the production of proinflammatory cytokines and chemokines (such as tumor necrosis factor alpha (TNF α), interleukin 1 beta (IL-1 β), IL-6, C-X-C Motif chemokine ligand 2, and C-C Motif chemokine ligand 5), and growth factors (as transforming growth factor beta (TGF β), PDGF and connective tissue growth factor) amplifying tissue inflammation, recruiting monocytes and other inflammatory cell types and promoting fibrosis progression (15,16).

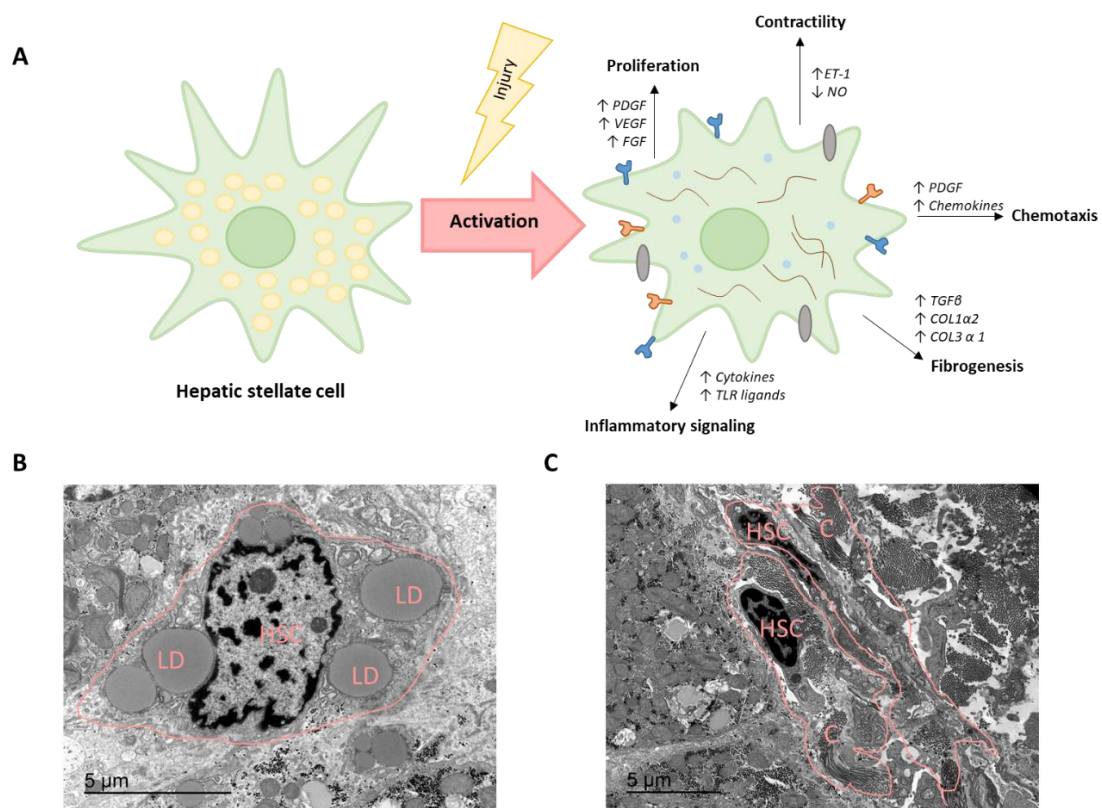


Figure 3. Activation of a HSC. A) Principal mechanisms responsible for HSC activation. B) TEM of a quiescent HSC with a cytoplasm full of lipid droplets (LD). C) TEM microphotography of an activated HSC surrounded by collagen (C) fibers.

Activated KC, macrophages and neutrophils are also a major source of ROS and reactive nitrogen species (RNS) during inflammation (17). Under physiological conditions, the aerobic cellular metabolism results in the production of ROS/RNS by the mitochondria, endoplasmic reticulum, and peroxisome. Hydrogen peroxide, hydroxyl radicals, and peroxynitrites are some examples. These molecules are naturally neutralized by enzymatic and non-enzymatic endogenous antioxidants; for instance, superoxide dismutase and

vitamin C (18). However, when the production of ROS/RNS surpasses the scavenging capacity of the antioxidants, oxidative stress is induced; directly damaging DNA, lipids, and proteins and contributing to exacerbated inflammation, necrosis, and apoptosis (19).

TGF β is the most profibrogenic cytokine and a driver of HSC activation. It is produced by KC, endothelial cells, hepatocytes, and HSCs (20). Once activated, TGF β binds to type II receptor, which in turn phosphorylates type I and induces downstream Smad and non-Smad signaling resulting in the transcription of fibrillar collagens such as collagen type I and type III, which are secreted in the space of Disse, replacing collagens type IV and VI (21). The mechanical rigidity caused by the accumulation of fibrillar collagens also leads to intrahepatic vasoconstriction and vascular resistance (22). Additionally, TGF β can also activate MAPK and PI3K/Akt signaling to further promote HSC activation (23).

In the healthy liver, ECM turnover is regulated by a balance between metalloproteinases (MMPs) and its potent inhibitors: tissue inhibitors of metalloproteinases (TIMPs) (24). Upon chronic injury, activated HSC increase the expression of MMP-13, MMP-3, MMP-2, MMP-9 and MMP-14 and at the same time, they express and secrete TIMPs, especially TIMP-1 and TIMP-2, which have been reported to downregulate the secretion and activity of some MMPs more than 20 fold (25,26). This imbalance between matrix production and degradation leads to the deposition of ECM, increasing liver stiffness. Furthermore, TIMP-1 acts as an antiapoptotic mediator, contributing to activated HSCs survival (27).

Besides, activated HSCs are involved in immunoregulation. They secrete cytokines, express toll like receptors, induce the infiltration of leukocytes, act as professional antigen presenting cells and produce neutrophil and mononuclear cells chemoattractants (28).

The sustained liver damage and subsequent release of inflammatory, growth and angiogenic factors also causes the loss of fenestrae, increases microvascular permeability and induces activation, proliferation, and migration of LSECs (20,29). Defenestrated LSECs increase endothelin 1 (ET-1) secretion and

decrease nitric oxide (NO) release, contributing to activated HSCs contractile phenotype (30,31). Furthermore, tissue inflammation and liver architectural remodeling predisposes to hypoxia, further stimulating angiogenesis (29). In turn, activated HSCs also contribute to angiogenesis through the production of vascular endothelial growth factor (VEGF) and angiopoietin-1 leading a feedforward cycle (21).

1.2.2 Fibrosis regression

It is known that hepatic fibrosis can potentially be halted and reversed after eliminating the cause of injury, although it may vary depending on the etiology (32). Compelling evidence supports that sustained viral response to hepatitis C virus or suppression of hepatitis B virus can induce fibrosis regression in these patients, decreasing the risk of progression to liver decompensation and the need for liver transplantation. Moreover, fibrosis resolution correlates with improved clinical outcomes (32–35). Even so, it is not known why a percentage of these patients with sustained viral response do not show any reversal (6). Thanks to the use of new oral direct-acting antivirals, fewer patients are expected to develop cirrhosis in the future due to hepatitis C virus related infections (36).

Two key events have been established at cellular level for fibrosis regression, 1) hepatic myofibroblasts should undergo senescence and apoptosis; and 2) macrophages need to switch to the antiinflammatory phenotype (22). Profibrogenic signaling promotes HSCs resistance to apoptosis and fibrosis resolution induces programmed cell death and senescence (35). At the same time, distinct proresolving macrophage populations display phagocytic and anti-inflammatory functions, secreting MMPs, such as MMP-9, able to degrade ECM as well as molecules that promote HSCs apoptosis (13,15). Despite some evidence suggest that cirrhosis can also regress, in case of such advanced pathology this remains controversial (37,38). The vascular changes, abnormal hepatocyte regeneration, portal hypertension and severe architectural distortion as well as the presence of a mature scar with cross-linked matrix could contribute to this resistance to recover (26). Despite many preclinical studies and clinical trials have been conducted, to date there is not any antifibrotic therapy approved by the European Medicines Agency or Food and Drug Administration, remaining the

liver transplantation the unique curative option for patients with advanced liver disease (6).

1.2.3 PTTG1/DLK1 axis

Pituitary tumor-transforming gene 1 (PTTG1), the index mammalian securin, was first isolated from rat pituitary tumor cells in 1997 (39). PTTG1 is a protein critical for the regulation of faithful sister chromatids separation during mitosis since it inhibits separase (40,41). In the beginning of the anaphase, PTTG1 is degraded through ubiquitination by the anaphase-promoting complex (42). Moreover, PTTG1 has transactivating activity controlling the expression of a myriad of genes (43).

Human *PTTG1* is located on the chromosome 5 (5q33.1). This gene has an enhancer element, three SP1/GC boxes, three AP1 binding sites, one AP2 binding site, and a cyclic AMP and insulin response elements (44). Several transcription factors have been reported as promoter activators and repressors including SP1 and Krüppel-like factor 6 (45,46). PTTG1 is a multi-domain protein consisting on a transactivation domain in the functional C-terminal region with a SH3 domain-binding and a PTTG-binding factor binding motifs. In the N-terminal regulatory region PTTG1 has a DNA binding domain, a destruction box required for ubiquitin-mediated proteolysis, a SH3 domain-binding motif, and a KEN box (Figure 4) (47–49).

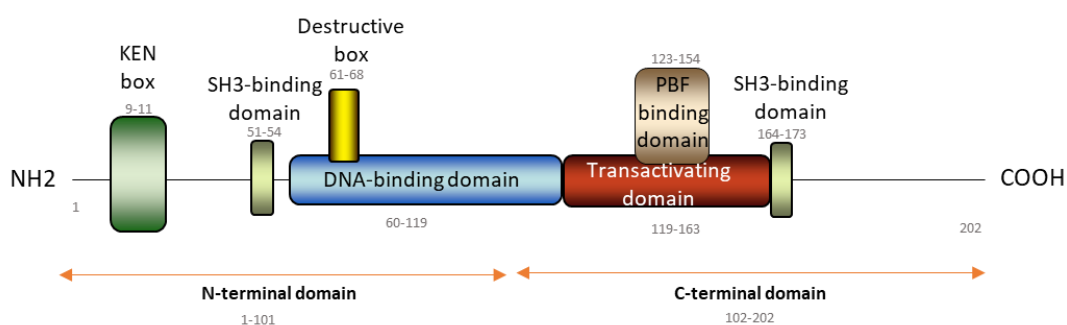


Figure 4. Schematic representation of the human PTTG1 protein in domains. Positions of the elements are shown by amino acid residue numbers. Adaptation from: Vlotides G, Eigler T, Melmed S. Pituitary tumor-transforming gene: physiology and implications for tumorigenesis. *Endocr Rev.* 200;28(2):165-86.

PTTG1 is a multi-faceted protein since it also plays a role on organ development, gene regulation, DNA repair, apoptosis, and metabolism (49,50). Despite it is mostly a cytosolic protein, it is also partially localized to in the

nucleus interacting with multitude of promoters (51). PTTG-binding factor facilitates PTTG1 translocation into the nucleus (43). Mice lacking PTTG1 are viable and fertile but exhibit aberrant cell cycle progression, premature centromere division, testicular and splenic hypoplasia, as well as thrombocytopenia and thymic hyperplasia (50). Furthermore, male mouse knock out (KO) for *PTTG1* also develop diabetes during late adulthood due to pancreatic a defective beta cell proliferation (52).

In healthy tissues, *PTTG1* expression is almost restricted to the embryo, testis, thymus, spleen, and ovary (53). In many malignancies *PTTG1* is overexpressed acting as an oncogene, for instance in pituitary adenoma (54), non-small cell lung cancer (55), breast cancer (56,57), colorectal cancer (58,59), thyroid cancer (60), ovarian cancer (61), glioma (62), and HCC (63). PTTG1 overexpression has been shown to promote cell transformation, proliferation, angiogenesis, migration, and invasion (40,57,64–67). Besides, PTTG1 levels have been correlated with tumor progression and associated with poor prognosis (62,65). PTTG1 has been found to induce expression of factors like VEGF and MMPs facilitating angiogenesis (49,59,68), to bind to c-myc promoter inducing cell proliferation (48), and to regulate PDGF induced migration and proliferation activating MAPK/extracellular signal-regulated kinase (ERK) and PI3K/AKT/mammalian target of rapamycin (mTOR) signaling pathways (69,70). Moreover, estrogens, extracellular calcium, insulin, and insulin growth factor 1 are some of the mediators found to regulate *PTTG1* expression (57,71,72).

In the adult liver, PTTG1 expression is very restricted (43). But it has been reported to be strongly induced in the fetal liver, during liver regeneration, and HCC (73,74). In HCC, PTTG1 positively correlates with alpha-fetoprotein (AFP) serum levels, portal vein tumor thrombosis, and lower 5-year survival rates (63,75). Moreover, PTTG1 promotes and regulates the expression of VEGF (75). Adenovirus (AD) mediated transfer of *PTTG1*-small interfering RNA (siRNA) induces p53 dependent apoptosis in various hepatoma cell lines and decreases tumor growth rate in xenograft nude mice (74). Other investigators proposed that PTTG1-mediated apoptosis and anti-proliferative effect are associated with the repression of AKT and the activation of p38 MAPK pathways (76). In this line, Huang *et al.* suggested that the long non-coding RNA pituitary tumor-

transforming 3, which parental gene is PTTG1, is augmented in human HCC enhancing PTTG1 expression and activating PI3K /AKT signaling; boosting tumor growth and invasion into adjacent tissue and metastases (77). The loss of Krüppel-like Factor 6, a tumor suppressor gene frequently inactivated in HCC, has also been associated to *PTTG1* upregulation in HCC. Lee *et al.* demonstrated that this suppressor gene directly interacts with PTTG1 promoter to transcriptionally repress it and promote cell proliferation (78). Finally, *Tnfa* has been shown to facilitate *Pttg1* expression, which in turn promotes hepatocellular proliferation inducing *c-myc* in experimental diethylnitrosamine (DEN)-induced HCC (79). Despite quite attention has been given to the role of PTTG1 on HCC development, few investigations have focused on preneoplastic stages such fibrosis. In biopsies from patients with cirrhosis induced by viral hepatitis, it was found that the viral protein HBx inhibits PTTG1 ubiquitination promoting its accumulation in the infected hepatocytes without affecting its mRNA levels (80). Moreover, it has been reported that the lack of *Pttg1* decreased HSC activation, and the expression of type I collagen, *Vegf*, *Tgfb* and *Tnfa* in mice with thioacetamide-induced liver fibrosis (81).

Espina *et al.* reported that delta like non-canonical notch ligand 1 (DLK1) was one of PTTG1 most abundant targets inhibiting adipogenesis *in vitro* (82). Both adipocytes dedifferentiation and myofibroblasts transdifferentiation share the need of adipogenic transcription regulation, in which DLK1 has been reported to be one of the master regulators (83).

DLK1, also named fetal antigen 1 or preadipocyte factor 1, is a single pass transmembrane protein and a non-canonical member of the delta-notch signaling pathway (84). Human DLK1 gene is located in the DLK1- type III iodothyronine deiodinase (DIO3) gene cluster. This cluster encodes for several protein coding genes, long non-coding RNAs, small nuclear RNAs, miRNAs and pseudogenes (85). DLK1 is maternally imprinted by hypomethylation of imprinting control regions and paternally expressed by hypermethylation of the same regions on chromosome 14 (14q32.2) (86). Several transcription factors such as Krüppel-like factor 6 or E2f1 regulate DLK1 promoter activity (87,88).

DLK1 protein consists in a signal peptide, six epidermal growth factor (EGF)-like tandem repeats, a juxtamembrane region with a TNF α converting enzyme (TACE)-mediated cleavage site, a transmembrane domain, and a short intracellular tail (**Figure 5**) (89). *Dlk1* has two alternative splicing isoforms in humans, one cleavable and one tethered in the membrane (90). DLK1 membrane-proximal cleavage by TACE results in the release of the EGF-like extracellular region, a soluble product of 50 kDa. The 50 kDa form has a similar function inhibiting adipocyte differentiation to that of the full-length membrane-associated one but since it is soluble, it can act in both autocrine and paracrine manners (91). Furthermore, the cleavage in the second EGF repeat generates a biologically inactive 25 kDa soluble form (90). Both membrane associated and large soluble forms are physiologically upregulated during embryogenesis in all three germinal layers controlling cell proliferation and differentiation (92). However, after birth DLK1 expression is highly restricted to few tissues and progenitor cells such as placenta, testes, ovaries, insulin-producing β cells in the pancreas, pituitary, and adrenal glands (93).

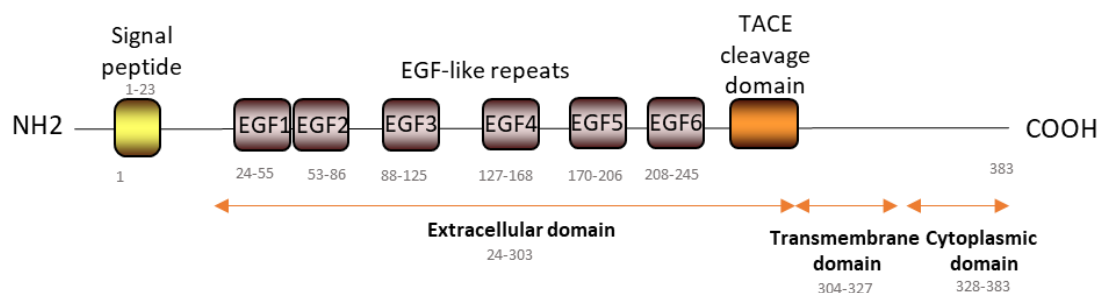


Figure 5. Schematic representation of the human DLK1 protein in domains. Positions of the elements are shown by amino acid residue numbers. Adaptation from: Montenegro L, Labarta JJ, Piovesan M, Canton APM, Corripio R, Soriano-Guillén L, et al. Novel Genetic and Biochemical Findings of DLK1 in Children with Central Precocious Puberty: A Brazilian-Spanish Study. *J Clin Endocrinol Metab* 2020 1;105(10):dgaa461.

DLK1 is involved in cellular differentiation: neurogenesis, osteogenesis and adipogenesis. DLK1 promotes the generation of neurons from ESC-derived neural progenitors (94) and stimulates osteoclastogenesis by inhibiting bone formation and stimulating bone resorption (95). Furthermore, DLK1 prevents the differentiation of preadipocytes into mature adipocytes, acting as a negative regulator of adipogenesis (96). Mice lacking *Dlk1* are obese, hyperlipidemic and present slow growth, blepharophimosis, and skeletal abnormalities (97). On the other side, mice overexpressing *Dlk1* exhibit improved glucose tolerance, reduced fat stores and decreased hepatic lipogenesis, due to an increase in growth

hormone production and stimulated muscle fatty acid oxidation (98). Jensen CH *et al.* further reported that augmented DLK1 circulating levels in humans are associated to increased body fat and that soluble DLK1 negatively modulates glucose uptake in skeletal muscle by regulating the expression of glucose transporter type 4. Finally, they also showed that *Dlk1* deficiency protects against diet-induced obesity and insulin resistance (99).

DLK1 is also overexpressed during tissue regeneration and several malignancies including neuroblastoma (100), glioma (101), HCC (102), prostate (103), and lung cancer (104). Under hypoxia, several hypoxia inducible factors have been reported to bind to the proximal 5' promoter region of DLK1 gene, which contains three putative hypoxia responsive elements, increasing DLK1 expression (105,106). Hypoxia has also been shown to promote TACE- proteolytic cleavage inducing the release of DLK1 extracellular form, altogether facilitating the maintenance of an undifferentiated phenotype, and inducing cellular tumorigenicity, stemness, and invasion (106,107).

Regarding CLDs, Zhu LN *et al.* reported that DLK1 is induced in the liver after partial hepatectomy. They also showed that KO for *Dlk1* activated HSCs decreased canonical Wnts expression and derepressed epigenetically peroxisome proliferator-activated receptor gamma mediating a quiescent phenotype (83). Besides, the administration of exogenous DLK1 resulted in improved glucose tolerance and decreased steatosis in a mouse model of leptin deficiency and diabetes, activating the 5' AMP-activated protein kinase pathway (108). In relation to HCC, Li H *et al.* reported that serum DLK1 correlated with tumor size and AFP levels, and higher DLK1 levels were associated to lower survival rates in HCC (109). AD-mediated *DLK1* knockdown in xenograft and DEN-induced mouse HCC resulted in reduced tumor size and inhibited tumor progression due to cell differentiation (110). Huang J *et al.* also showed that DLK1 upregulation in HCC could be consequence of genomic DNA methylation of the imprinted domain deregulation (111). Finally, Pan LR *et al.* showed that following liver injury hepatocytes express DLK1, and release two soluble forms of 25 and 50 kDa, being the larger one the responsible for HSCs activation via paracrine signaling. Likewise, they demonstrated that DLK1 induced HSC activation *in vitro* whereas *DLK1* KO inhibited it (112).

1.3 Liver cirrhosis and complications

Hepatic cirrhosis is an advanced stage of fibrosis that consists of the development of necroinflammation and pathological parenchymal regenerative nodules encapsulated by fibrotic septa with a severe distortion of the vasculature (1). Due to the elevated loss of parenchymal cells, quiescent hepatocytes are activated to recoup the liver. But since adult differentiated hepatocytes have low telomerase activity, it results in telomere shortening and cellular senescence (113). Eventually, progenitor cell population is activated to restore lost hepatocytes, namely ductular reaction (113). Hence, both regenerating nodules and ductular reactions are found in the cirrhotic liver.

The clinical course of advanced liver disease can be separated into compensated and decompensated stages. The first is an asymptomatic phase characterized by conserved quality of life, with a median survival of 9 to 12 years (114). The decompensated phase is characterized by the deterioration of the liver function and the onset of a clinical phenotype, frequently ascites, variceal bleeding, and jaundice; as well as the apparition of a systemic disease with multi-organ dysfunction (115,116). This decompensation can eventually progress to HCC or death and it is associated with the worsening of patient prognosis, with a median survival of around 2 years (117).

Portal hypertension is a major complication and a driving factor in the natural story of the disease (118). In accordance with Ohm's law ($\text{Pressure} = \text{blood flow} * \text{resistance}$), portal pressure is equal to the product of portal blood flow and intrahepatic venous resistance (119). Hepatic venous pressure gradient is a surrogate marker of portal pressure. It indicates portal hypertension when it is higher than 6 mmHg, however, it is considered clinically significant when higher than 10 mmHg (120). In most chronic diseases, increased intrahepatic vascular resistance in the cirrhotic liver is the primary cause of portal hypertension, since it induces congestion of portal venous flow and elevates portal pressure (121). The distorted architecture, capillarization of sinusoids, dysfunctional endothelium with an impaired production of vascular mediators and HSCs contraction are the main factors contributing to increase vascular intrahepatic resistance.

In turn, portal hypertension induces the formation of portosystemic collaterals to decompress the portal vein and shunt a part of the flow to the systemic circulation bypassing the liver (122). Moreover, large conductive systemic vessels dilate to increase the blood flow into the portal system, counterbalance the increased portal resistance, and augment the venous return to the heart (**Figure 6**) (123). But this only aggravates the portal hypertension and progressively results in an hyperdynamic circulation, leading to peripheral organ hypoperfusion (124,125).

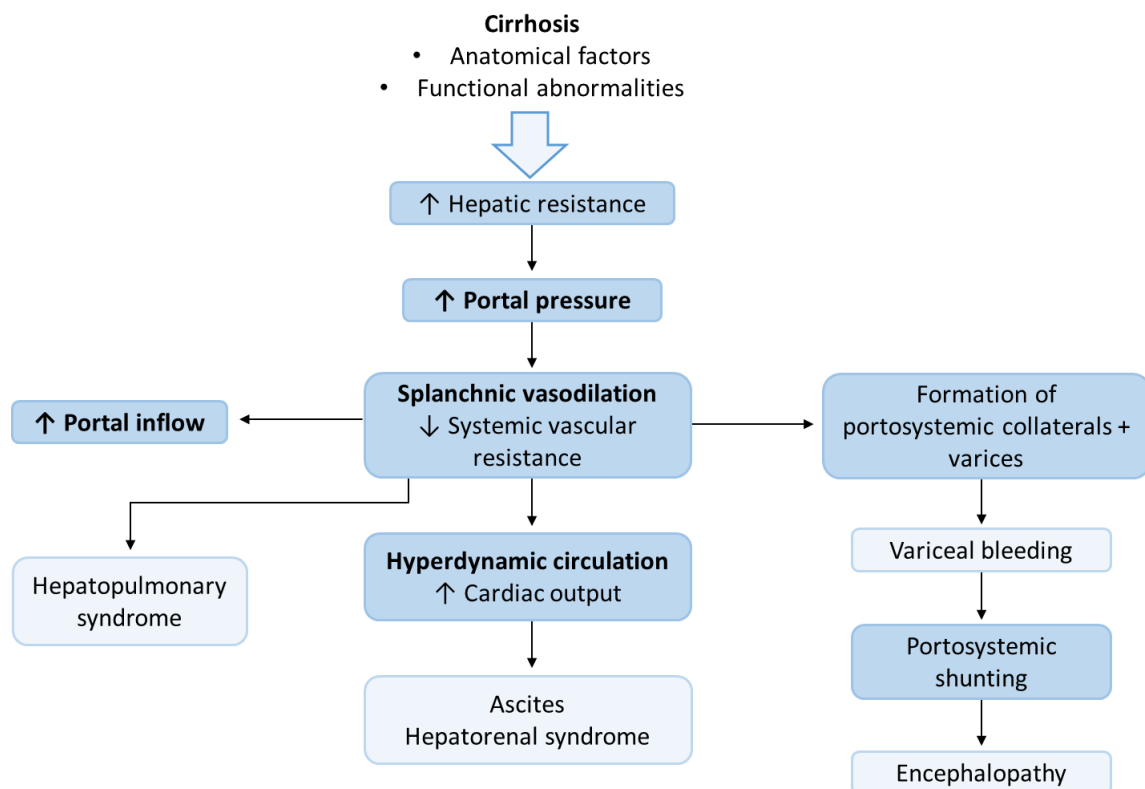


Figure 6. Pathophysiology of portal hypertension in cirrhosis. Adaption from: Tsochatzis EA, Bosch J, Burroughs AK. Liver cirrhosis. *Lancet*. 2014;383(9930):1749–61.

An increase of plasma volume and cardiac output (CO) initially maintains the arterial pressure. But as cirrhosis progresses, effective volemia decreases and arterial pressure diminishes (126). As a compensatory mechanism to maintain the arterial pressure, vasoconstrictors and anti-natriuretic factors including the sympathetic nervous and renin-angiotensin-aldosterone systems are stimulated. But their activation ultimately decreases kidney glomerular filtration, inducing tubular reabsorption of sodium and causing sodium retention and decreased free water clearance (124,127,128). Severe renal vasoconstriction is the hallmark of the hepatorenal syndrome, a serious complication of liver cirrhosis (129).

Portal hypertension is also associated to a pronounced escape of the intravascular fluid to the interstitial space (128). Ascites is the pathological accumulation of the excess of fluid in the peritoneal cavity and it is associated with poor survival (130). Other common complications include variceal bleeding, spontaneous bacterial peritonitis (bacterial infection in the ascites), jaundice, hepatic encephalopathy (neuropsychiatric abnormalities), acute-on-chronic liver failure, hepatic pulmonary syndrome, and cirrhotic cardiomyopathy (115,130,131).

Current clinical guidelines for the management of patients with decompensated cirrhosis recommend to initiate at the earliest aetiologic treatment, in addition to targeting the complications as they occur (115). For instance, non-selective beta blockers are used to prevent variceal bleeding because they are able to induce splanchnic vasoconstriction and decrease CO (118,132). Nevertheless, the ideal treatment for these patients would consist on the restoration of the main pathological alterations including liver architecture, inflammation, fibrosis, and circulation in order to induce disease regression. Unfortunately, this treatment does not exist and liver transplantation remains the only potential curative option for these patients.

1.3.1 Role of nitric oxide in liver cirrhosis

NO is a short-lived gas that diffuses across cellular membranes causing autocrine and paracrine effects (133). It has a variety of physiological functions including vascular vasodilation, neurotransmission, regulation of proliferation, platelet and leukocyte activation, and non-specific immune reactions (134). NO is endogenously synthesized by the enzyme nitric oxide synthase (NOS) as a byproduct of the conversion of arginine to citrulline in a complex set of redox reaction steps (133). During this process several cofactors and prosthetic groups are needed, including reduced nicotine adenine dinucleotide phosphate, flavin-adenine dinucleotide, flavin mononucleotide, calmodulin, tetrahydrobiopterin, and heme (135). NOS is a dimeric protein with a reductase and an oxidase domain (136). Three isoforms have been cloned in mammals: neuronal, inducible (iNOS/Nos2) and endothelial (eNOS/Nos3), but the two latter are the most important in the hepatic tissue (137). In the liver, HSCs, macrophages, vascular smooth muscle cells, and hepatocytes synthesize iNOS *de novo* after induction by

inflammatory mediators and independently of any hemodynamic or mechanic stimuli (136). iNOS-produced NO is independent of calcium and can modulate collagen synthesis, proliferation, and wound contraction (18). Depending on the stimulus and duration of iNOS expression, its effects can be protective or detrimental (138). In opposite, eNOS is a calcium-calmodulin-dependent constitutively expressed enzyme, which responds to endogen and exogen mediators as well as physical and receptor stimuli to regulate vessel reactivity (136,139). Phosphorylation at key residues including Ser617, Ser635 or Ser1177 is required for eNOS activation; whereas phosphorylation of Ser116 or Thr495 acts as an inhibitory sign (140). PI3K/AKT, cAMP-dependent protein kinase A, adenosine monophosphate-activated protein kinase, cGMP-dependent protein kinase G and calmodulin Kinase II-dependent pathway induce the phosphorylation at Ser1177, whereas cAMP-dependent protein kinase A induces Ser635 and Ser116 phosphorylation (**Figure 7**) (141).

Once synthesized, NO activates the enzyme guanylate cyclase inducing the formation of cyclic guanosine monophosphate (cGMP) and ultimately decreasing intracellular calcium concentration and leading to cell relaxation and vasodilation (136). Besides, NO has cGMP-independent effects. NO can react with oxygen and free radicals and induce the formation of RNS, for instance peroxynitrite (138). Besides, it can regulate cellular contractility by the postraslational modification S-nitrosylation of specific cysteine thiols (142). Nitrosylation may also protect NO from forming RNS. In turn, nitrosylation may facilitate further postraslational modifications such as acetylation, phosphorylation, and ubiquitination (18).

NO has also an important role in the pathogenesis of liver cirrhosis contributing to augment intrahepatic resistance and splanchnic vasodilation. Intrahepatic NO production is decreased, whereas it is overproduced in the splanchnic vasculature (143).

In the cirrhotic liver, overproduction of inflammatory mediators results in endothelial dysfunction. This is associated with a decreased intrahepatic production of NO and increased vasoconstrictors synthesis such as ET-1 and thromboxane A₂ (119,124,125). Cirrhotic livers show impaired Akt activation and

eNOS phosphorylation (143,144). Oxidative stress also contributes to decrease NO bioavailability in the cirrhotic liver by scavenging it. Additionally, apart from decreased NO concentration, cirrhotic HSC also show resistance to NO mediated relaxation (145).

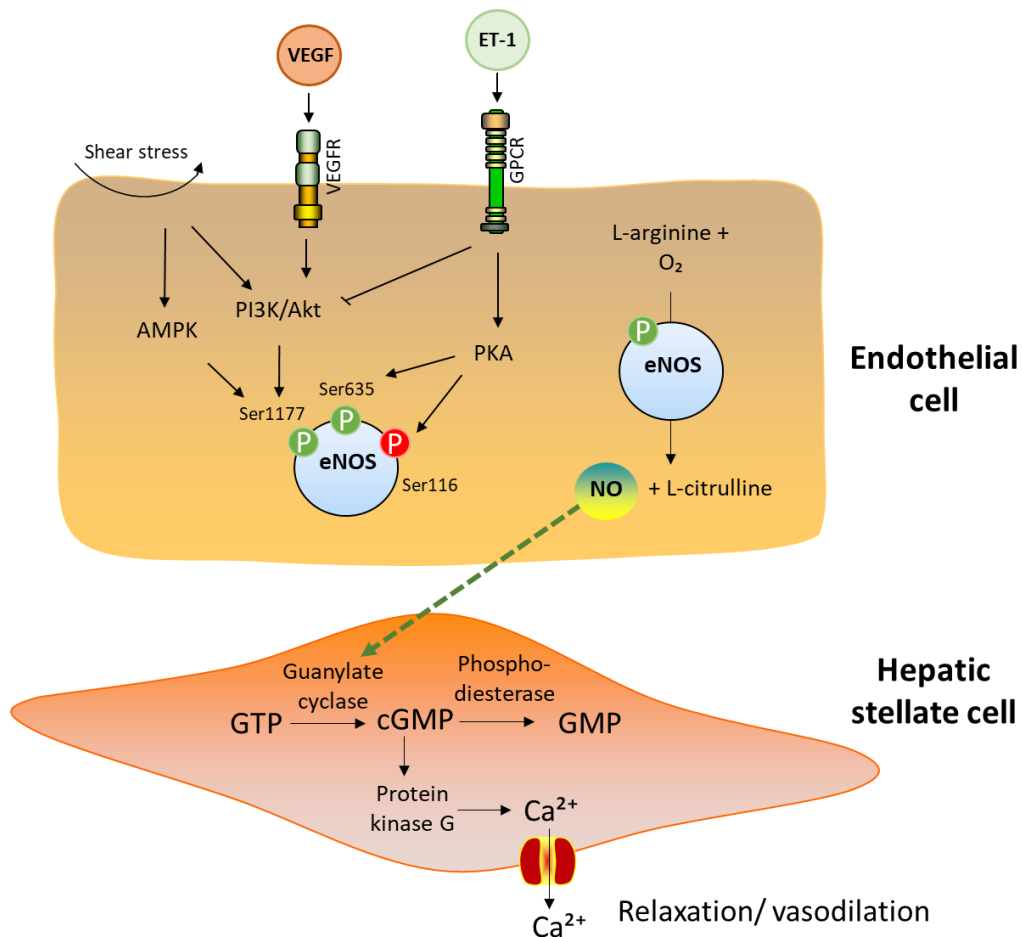


Figure 7. NO synthesis and effects in endothelial and HSCs. AMPK: 5' adenosine monophosphate-activated protein kinase, ET-1: endothelin 1, cGMP: Guanosine monophosphate, GPCR: G protein-coupled receptor, GTP: guanosine triphosphate, PKA: cAMP-dependent protein kinase A.

On the contrary, arterial production of NO is increased contributing to splanchnic and systemic vasodilation, and the resulting hyperdynamic syndrome (146). In fact, patients with liver cirrhosis show elevated concentrations of nitrites and nitrates in the serum (147). Multiple mechanisms have been reported to contribute to this vasodilation. Elevated intrahepatic resistance induces shear stress within the mesenteric arteries increasing eNOS transcription and phosphorylation by Akt (133). Moreover, mediators such as VEGF have been reported to promote calmodulin binding to eNOS and NO synthesis (148,149). Additionally, cirrhotic patients often show increased bacterial translocation from

the gut to extraintestinal sites due to intestinal bacterial overgrowth, impaired host defenses, and disruption of the gut mucosal barrier (150). These translocated bacteria directly induce the synthesis of tetrahydrobiopterin, a cofactor required for NOS-derived NO production. Besides, the production of proinflammatory cytokines activate iNOS (151). In fact, the liver of rats with decompensated cirrhosis shows upregulated iNOS expression in the mesenteric arteries (139). Finally, NO also acts as an angiogenic factor promoting vascular remodeling and angiogenesis ultimately inducing the formation of portosystemic collaterals (133).

1.4 Hepatocellular carcinoma

HCC is the most frequent primary liver malignancy accounting for 75- 80 % of liver cancer cases, which also include hepatoblastoma, angiosarcoma, and cholangiocarcinoma (152). In 2018, liver cancer was the 5th most diagnosed cancer and 2nd cause of cancer death worldwide among men, being 2 to 3 times lower in women (153). Incidence and etiology of HCC are dynamic and geographically heterogeneous due to differences in racial and ethnic groups and the prevalence of its principal risk factors (**Figure 8**) (154). In most cases, HCC arises in patients with previous liver diseases, being cirrhosis the strongest risk factor (155). Furthermore, other factors such as the severity of the underlying liver disease, genetic predisposition, and the cellular microenvironment, are involved in determining the development and progression of HCC (155). However, in some cases HCC develops in the absence of previous liver disease due to malignant transformation of adenomas (156).

The likelihood to detect a new nodule with ultrasonography is very high, especially when they are bigger than 10 mm (157). For this reason, this is the preferred technique used for the detection of individuals at high risk to develop HCC such as patients with hepatic cirrhosis (158). Other imaging techniques such as computed tomography or magnetic resonance imaging help to evaluate the lesion (159). AFP has been the most used serological marker to diagnose HCC because it correlates with tumor differentiation, size and volume, stage, and survival of patients (160). However, its use is not recommended as a surveilling

technique since it can be low in early tumor stages and cirrhotic patients could present elevated transitory AFP levels in the absence of HCC (157).

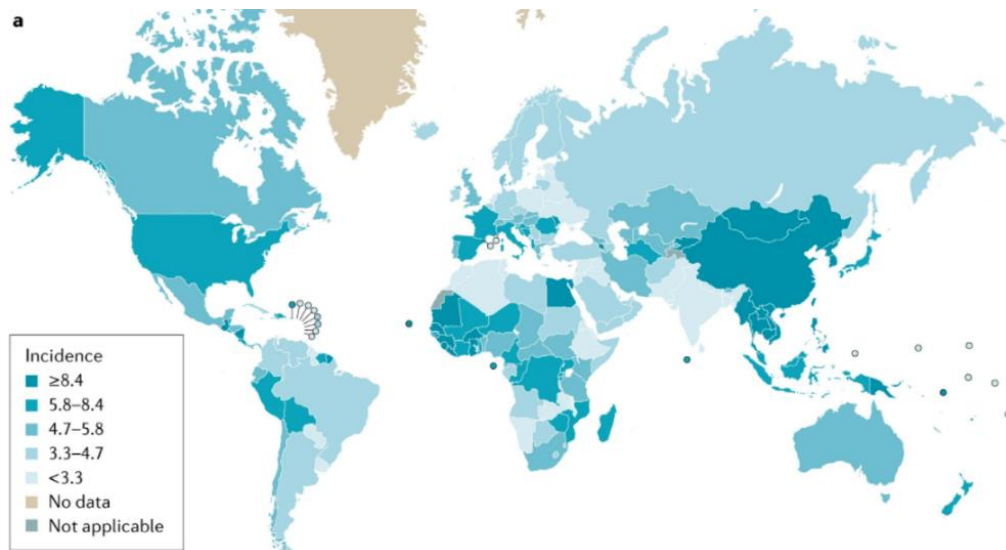


Figure 8. Incidence of primary liver cancer worldwide. Original from: Yang JD, Hainaut P, Gores GJ, Amadou A, Plymoth A, Roberts LR. A global view of hepatocellular carcinoma: trends, risk, prevention and management. *Nat Rev Gastroenterol Hepatol.* 2019;16(10):58.

The staging system mostly used in HCC to establish prognosis and determine treatment is the Barcelona Clinic Liver Cancer algorithm (BCLC) (**Figure 9**). This system stratifies patients according to tumor stage, degree of liver impairment, and presence of cancer related symptoms and pairs the prognostic evaluation with treatment indication (161). Treatment options for patients with HCC are limited and include surgical resection, liver transplantation, transarterial embolization, radiofrequency ablation, and systemic therapy. Treatments are based on the severity of the underlying liver disease, size and distribution of the hepatic tumors (162). Surgical resection is the preferred therapy for patients with localized HCC, non-cirrhotic and well-preserved hepatic functions. However, it is associated with a recurrence rate of ~65 % at 5 years (163). Patients who are not eligible for surgical resection, liver transplantation is the only potentially curative option and it is associated to ~60-80 % 5-year survival and ~50% 10-year survival (159). But most HCC cases are diagnosed in an advanced stage of the disease (BCLC stage B or C) when few therapeutic options are available. In the last decades, efforts have been made in order to develop numerous compounds that specifically target altered molecular signaling pathways in HCC, but very few have demonstrated to improve survival (161). Despite minimally enhancing patient survival, Sorafenib was the first

pharmacological therapy approved and is the standard of care for frontline therapy (159). It is a multikinase inhibitor that targets PDGF and VEGF receptors 1, 2, and 3; as well as the serine–threonine kinases Raf-1 and B-Raf, inhibiting angiogenesis and tumor growth (164).

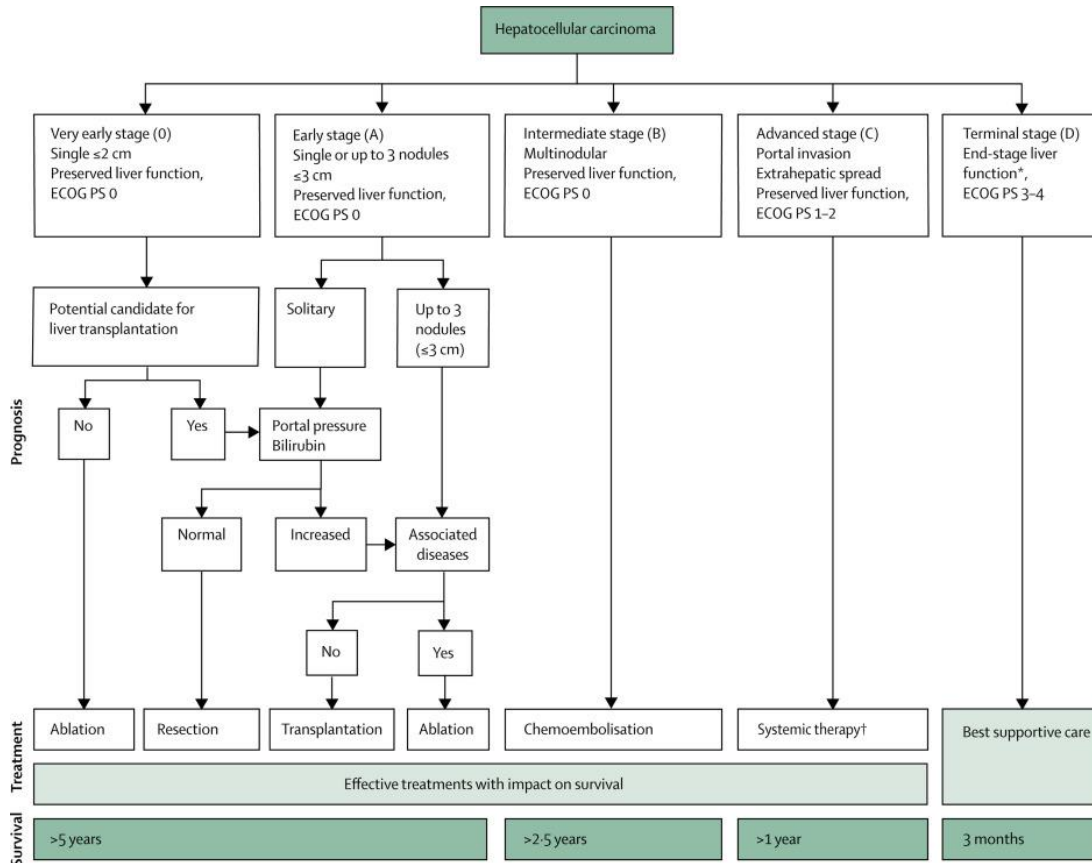


Figure 9. Barcelona Clinic Liver Cancer staging algorithm. Original figure from: Forner A, Reig M, Bruix J. Hepatocellular carcinoma. *Lancet*. 2018;391(10127):1301–14.

1.4.1 Genetic landscape

HCC is an inflammation-related cancer that arises from a non-resolved inflammation, perpetuation of the wound-healing response, and accumulation of multiple genetic and epigenetic alterations that directly affect critical cellular functions including proliferation, metabolism, adhesion, apoptosis, and survival (161,165).

Genetic instability, chromosomal aberrations, aberrant expression of regulating RNAs, somatic mutations and copy number variations in oncogene and tumor suppressor genes; are the most common drivers for neoplastic transformation (113,166). Additionally, some germline mutations, including

single-nucleotide polymorphisms have also been related to risk of HCC development, but more research is needed in this field (167,168).

HCC has a broad spectrum of mutations. Recently, 161 putative genetic alterations have been found, being just two to six the driver mutations (169). The most common genetic alterations are found in the promoter of the enzyme that prevents telomere shortening, namely telomerase reverse transcriptase (TERT) (**Figure 10**). In more than 90% of HCC cases, these mutations reactivate the absent telomerase in the senescent cirrhotic liver and induce uncontrolled cellular proliferation (170). The most common alterations include: TERT promoter mutations (40–60%), hepatitis B virus insertion in the TERT promoter (10–15%), and TERT amplification (5–6%) (168). Other common mutations implicate the following genes: tumoral protein 53 (15–40%), catenin beta 1 (10–35%), AT-rich interaction domain 1A (*ARID1A*, 5–17%), *ARID2* (3–18%), *AXIN1* (5–15%), ribosomal protein S6 kinase A3 (2–9%), nuclear factor erythroid 2-related factor 2 (3–6%), Kelch like ECH associated protein 1 (2–8%), retinoblastoma (3–8%) and *VEGFA* (5%), and fibroblast growth factor 19 (5–10%) (167,171). However, not all mutations found in the cirrhotic liver are related to malignant transformation and, in fact, some might be beneficial (167).

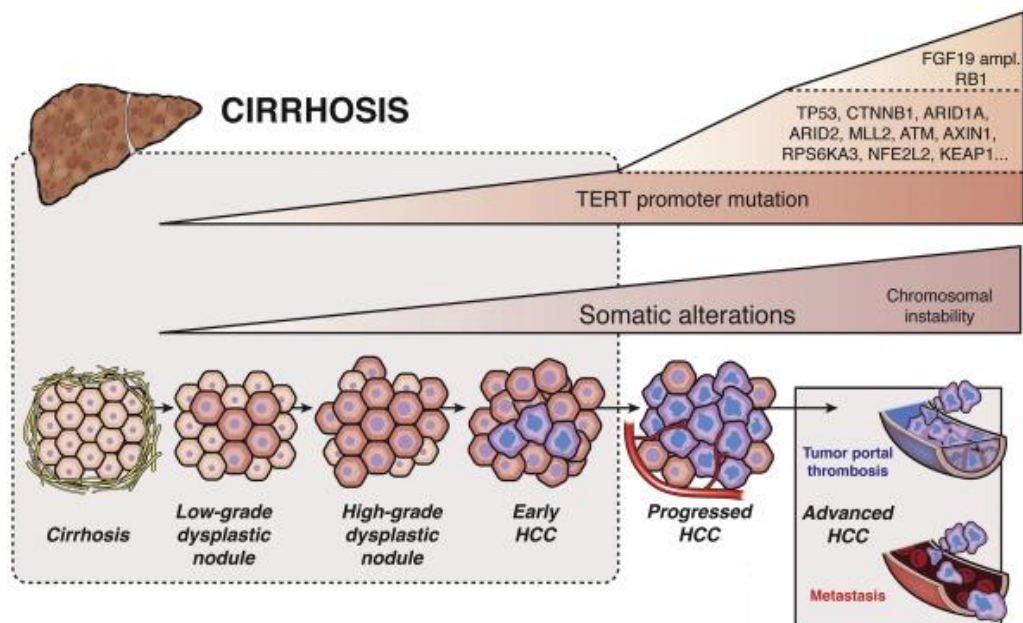


Figure 10. Mechanisms of malignant transformation in HCC. Original figure from: Zucman-Rossi J, Villanueva A, Nault JC, Llovet JM. Genetic Landscape and Biomarkers of Hepatocellular Carcinoma. *Gastroenterology*, 2015;149(5):1226-1239.e4.

Accumulating evidence also reveals that dysregulated genomic DNA methylation is one of the early events in HCC (172). In fact, hepatic tumors show global hypomethylation, which plays an important role in increasing genomic instability. Additionally, tumor cells present specific promoter aberrant hypermethylation resulting in the inactivation of tumor suppressor genes (173). Furthermore, non-coding RNAs, including long non-coding RNAs and microRNAs, dysregulation has been reported in HCC. These epigenetic dysregulations further contribute to treatment resistance.

Each HCC has unique molecular fingerprint and the assessment of molecular defects by next generation sequencing has led to the classification of HCC by mutational signatures with the aim to ultimately predict in the future treatment response to molecular therapies (174). Nevertheless, nowadays the most common mutational drivers remain undruggable (155).

1.4.2 Cellular and molecular mechanisms

Hepatocarcinogenesis is a highly complex long-standing multistep process in which a premalignant environment promotes the neoplastic transformation of hepatocytes and their survival activating anti-apoptotic signaling and inhibiting immune surveillance (175). Despite it has been extensively studied, the underlying precise molecular mechanisms involved in hepatocyte malignant transformation, tumor initiation, progression, and metastasis are not completely understood.

Sustained oxidative stress directly damages DNA, lipids, and proteins. ROS/RNS can oxidize purines and pyrimidines, trigger the formation of apurinic/aprimidinic DNA sites, and induce base modifications or single and double strand breaks, facilitating genomic instability and mutagenesis (176). The most abundant mutagenic adduct is 8-hydroxydeoxyguanine (177). Oxidative stress also induces peroxidation of polyunsaturated fatty acids (PUFAs), and subsequent formation of the reactive lipid electrophile 4-hydroxy-noenal to modulate various signaling processes (178). Moreover, proteins rich in cysteine, tyrosine, tryptophan, and histidine are also particularly sensible to oxidative damage, altering their structure and function (179). Changes in the cellular redox balance modulate signaling transduction activating MAPK and redox sensitive

kinases. The first family include ERK, the c-Jun NH₂-terminal kinase, and p38, which are involved in the regulation of processes including proliferation, differentiation, and apoptosis (176). The second one sense redox state using cysteine motifs to modulate cell cycle, proliferation, and survival pathways. It involves cytoplasmic mediators (thioredoxins), nuclear signaling factors (such as Redox factor-1) and transcription factors (for instance AP-1 and nuclear factor kappa beta).

In addition to oxidative stress, an immunosuppressive microenvironment plays a vital role facilitating tumor initiation and malignant transformation. Long term activation of the inflammatory response contributes to a phenotypic switch of macrophages from M1-like (pro-inflammatory, cytotoxic, anti-tumoral) to M2-like (anti-inflammatory, immunoregulatory, immunosuppressive) (180). Effector functions are downregulated, and macrophages are reeducated towards immune tolerance, producing predominantly immunosuppressive cytokines and chemokines such as IL-4, IL-10, TGF β , C-C Motif Chemokine Ligand 17 and 24 (181,182). M2 polarized macrophages are also involved in tissue remodeling, producing MMPs (1, 2, 3, 9 and 12), plasmin and urokinase-type plasminogen activator and its receptor; that modify the microenvironment degrading ECM and releasing sequestered growth factors, promoting angiogenesis and invasion, and generating bioactive cleavage products (175,183). Likewise, M2-like cells are involved in the production of mitogens that stimulate proliferation of tumor cells as well as other stromal cell types (175).

The remodeling of ECM alters the blood flow, which together with unrestrained tumor cells proliferation, results in insufficient oxygen supply of tumor cells and promotes a hypoxic microenvironment (**Figure 11**) (184). Under hypoxia, hypoxia inducible factor 1 α accumulates and induces the expression of proangiogenic factors such as VEGF, PDGF, fibroblast growth factor, and angiopoietins; that ultimately activate intracellular MAPK and PI3K/AKT signaling cascades to induce endothelial proliferation, migration and new blood vessels formation and branching (185,186). Angiogenesis directly contributes to metastasis and to high likelihood of HCC recurrence after surgical resection (187). Furthermore, hypoxia also upregulates genes involved in epithelial to mesenchymal transition (EMT), in which epithelial cells assume a mesenchymal

phenotype; characterized by migratory capacity, invasiveness, augmented production of ECM, and resistance to apoptosis (185,188).

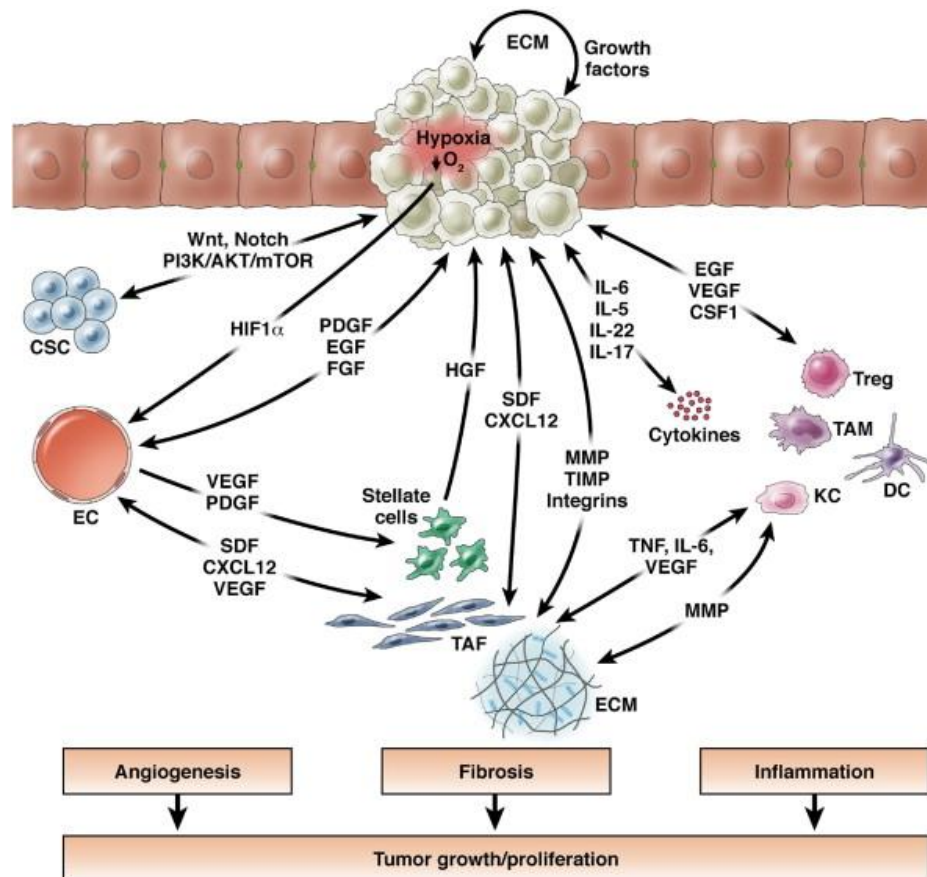


Figure 11. Mechanisms influencing tumor growth and progression. CSF-1: colony stimulating factor 1, FGF: fibroblast growth factor, Tregs: regulatory T cells, HGF: hepatocyte growth factor, EGFR: epidermal growth factor receptor, HIF-1: hypoxia-inducible factor 1, SDF-1: stromal cell-derived factor 1, DC: dendritic cells. Original figure from: Hernandez-Gea V, Toffanin S, Friedman SL, Llovet JM. Role of the microenvironment in the pathogenesis and treatment of hepatocellular carcinoma. *Gastroenterology*. 2013;144(3):512-27.

Furthermore, T cytotoxic cells are dysfunctional and display an exhausted and tolerant phenotype, characterized by impaired effector function and increased expression of inhibitory checkpoint molecules as programmed cell death protein 1, T cell immunoglobulin and mucin domain 3, and cytotoxic T lymphocyte-associated antigen 4 (180). At the same time, endothelial cells, monocytes, and KC increase the expression of their ligands (175). Besides, more immunosuppressive cells, secreting inhibitory cytokines and killing effector cells; are recruited. They include tumor-associated macrophages (TAMs), T regulatory cells (a subpopulation of CD4⁺ T lymphocytes), invariant natural killer T cells and myeloid-derived suppressor cells (175). TAMs are the major type of leucocytes localized in the stroma of HCC, triggering tumor cell proliferation, immune suppression, angiogenesis, EMT, invasion, and metastasis (181). They are mainly

M2 polarized, but its phenotype is plastic. Despite the prognostic value of elevated amounts of TAMs remains controversial in patients with HCC (189), the clue in predicting better or worse survival could be in the different types of infiltrated TAMs (190). Finally, antigen presenting cells also fail in their antigen associated processing (180). Altogether leads to a decreased immune system recognition of malignant cells and setting a proneoplastic promoting microenvironment.

Despite the theory of its origin is controversial (dedifferentiated hepatocytes, circulating bone marrow cells, or liver progenitor cells), several authors have demonstrated the presence of cancer stem cells in HCC (191). They are considered tumor initiators and have been reported to be responsible for the maintenance and propagation of the tumor thanks to their capacity to self-renew and differentiate into all cancer cell lineages present in the tumor (192). These cells strongly interact with the tumor microenvironment and their communication with immune cells and tumor associated fibroblasts is very important for the maintenance of stemness via activation of pathways like Wnt, Notch or STAT3, and inducing EMT and prometastatic signals (191).

2. GENE THERAPY

2.1 Overview

According to the European Medicines Agency, gene therapy consists of an advanced medicinal product, which contains a recombinant acid nucleic with the aim to regulate, repair, replace, add or delete a genetic sequence; being the recombinant acid nucleic or the product of its expression the one that directly produces the therapeutic, prophylactic, or diagnostic effect (193).

In brief, once the mutant gene responsible for the cause of the disease is identified, it must be cloned, namely transgene. This transgene is tailored for example to augment or suppress the expression; and then loaded in a vector able to deliver it to the target cell of the diseased patient and correct the defective gene (194). Gene therapy enables the generation of medicines for untreatable diseases by conventional treatments. Furthermore, the possibility of durable cure with a single application makes gene therapy very appealing (195).

On its early days, gene therapy was proposed for the treatment of monogenetic inherited diseases. However, to date many diseases have been targeted with this type of therapy. In early 2000, gene therapy suffered major setbacks. An 18-year-old patient died in a pilot study following adenoviral gene transfer for the treatment of ornithine transcarbamylase deficiency (196). Besides, some patients with X-linked severe combined immunodeficiency disease developed leukaemia after treating them with *ex vivo* retroviral mediated gene transfer (197). Since then, intense research has been done in the field to overcome these problems and during the last two decades its application has grown enormously, with beyond 1.800 ongoing clinical trials and more than 24 gene therapies approved for clinical use worldwide (195). Being the most numerous related to cancer therapy, followed by monogenic, infectious, and cardiovascular diseases (198). Worth highlighting, one of the most recent applications of gene therapy: the engineered chimeric antigen receptor T cells, which has revolutionized how cancer is treated and used to treat refractory hematologic malignancies (199). Shortly, this therapy consists on the delivery of a gene that encodes for a chimeric antigen receptor with a lentivirus into *ex vivo* patient's autologous cultured T cells in order to recognize *in vivo* a cancer-specific antigen (195).

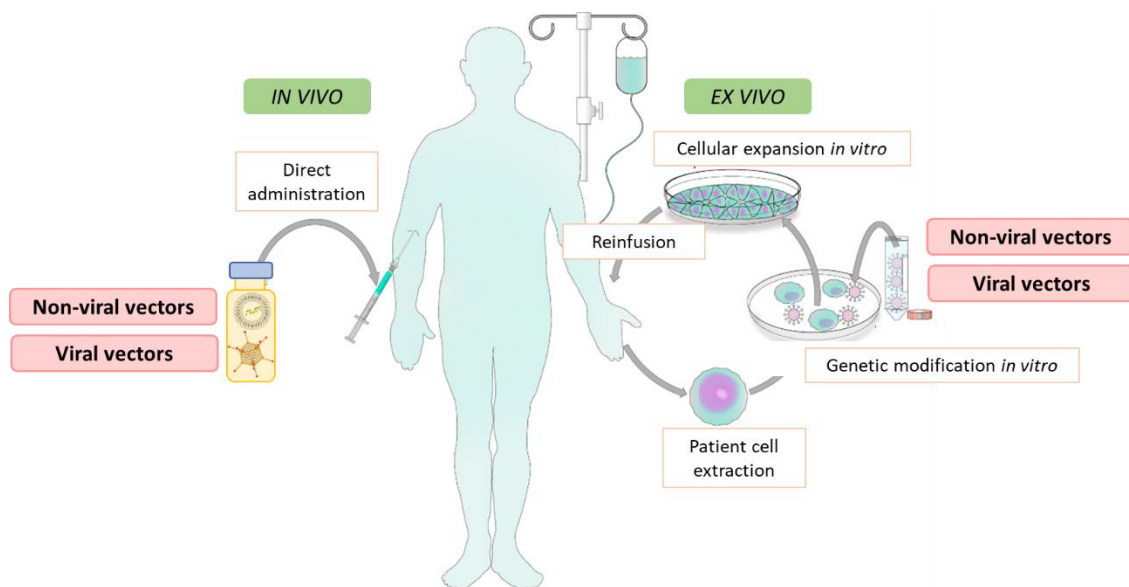


Figure 12. Different strategies used in gene therapy. Adaptation from: Bulcha JT, Wang Y, Ma H, Tai PWL, Gao G. Viral vector platforms within the gene therapy landscape. *Signal Transduct Target Ther.* 2021;6(1):53.

Two different strategies can be used to achieve gene therapy: *in vivo* and *ex vivo* gene delivery (**Figure 12**) (193). *In vivo* cell therapy consists of the delivery into the target cells via local or systemic administration. The most used vectors

adeno-associated viruses (AAVs) (195). A pair of examples where *in vivo* therapy has successfully been applied are Glybera for the treatment of familial lipoprotein lipase deficiency (200) and Luxturna for the treatment of retinal dystrophy (201). In contrast, for *ex vivo* gene therapy, the cells from the patient are collected, cultured, and modified prior the administration back to the recipient. In these cases, usually a normal copy of a specific defective gene is delivered with the use of lentiviruses (195). Two examples are Zynteglo approved for the treatment of β -thalassemia (202) or Tecartus for the treatment of mantle cell lymphoma (203).

Despite the rapid progress made in the field, with many clinical trials already done, some potential risks and ethical issues are still a matter of concern. Unlike traditional drugs, gene therapy is more complex, and its mechanisms of action are often difficult to understand and predict. It is very complicated to evaluate preclinical research and extrapolate animal data regarding factors such as on- and off-target effects, immunogenicity, and side effects. In Europe, the European Medicines Agency regulates advanced therapy medicinal products, including medicines based on genes, tissues, or cells, with the Regulation (EC) No 1394/2007; with specific guidelines for their clinical trial applications due to the complexity of the products (204). Furthermore, aside from safety, since gene editing can be potentially performed in both somatic and germline cells additional ethical questions are rising. Some would argue that germline gene therapy can potentially result in the elimination of inherited defects, which translates to a prophylactic medicine. But these effects would be irreversible and have a much wider impact than just the treated individual (205). Additionally, scientists are not able to predict long-term effects onto future generations such as mutagenicity (204). Even so, the current European legislation only allows the somatic gene therapy (198).

2.2 Types of vectors

As above-mentioned, optimal delivery and uptake of naked nucleic acids by the target cells is very inefficient and largely depends on factors such as protection of the genetic material from degradation, efficient target cell delivery, duration of expression, and size of the transgene (194,206). Different delivery vehicles can be used in gene therapy to overcome these issues: viral and non-viral vectors.

2.2.1 Viral vectors

Ideally, viral vectors take advantage of the viral infection pathway but elude the genes involved in viral replication and toxicity (207). This is performed by replacing the non-essential genes by a regulatory cassette which controls the stable or transient expression of the transgene and the transgene itself (199). Viral proteins related to replication of the vector and to the structure of the virus are maintained to create virus particles, in which replicated genomes are packaged (207). Viral vectors are highly efficient delivering nucleic acids in both dividing and non-dividing cells (208). A big range of viral vectors is available for transient short-term and permanent long-term expression, but the most used are lentiviruses, ADs and AAVs (**Table 1**) (198). Moreover, they are usually selected according to the cells they have tropism to.

Table 1. Main characteristics of the most used viral vectors.

	Lentivirus	Adenovirus	Adeno-associated virus
Genome	Single-stranded RNA	Double-stranded DNA	Single-stranded DNA
Envelope	Enveloped	Non-enveloped	Non-enveloped
Packaging capacity	~9 kb	~7,5 kb	~5 kb
Transduction efficiency	Moderate	High	Moderate
Genome integration	Yes	No	No
Expression	Stable	Transient	Transient/stable
Immunogenicity	Low	High	Very low
Gene therapy strategy	<i>Ex vivo</i>	<i>In vivo</i>	<i>In vivo</i>

Lentiviruses are enveloped single-stranded RNA retroviruses that infect non-dividing and dividing cells (209). These are integrating vectors that allow stable long-term expression (210). Moreover, they have a large cloning capacity of ~9 kb that can even contain multiple genes. Importantly, lentiviruses elicit quite weak immune responses. However, their large-scale manufacturing requires a complicated production (199). This type of viruses is frequently used in *ex vivo* replacement therapy (210)

ADs are non-enveloped double-stranded DNA viruses that infect non-dividing and dividing cells. They are characterized by great transduction efficiency,

epichromosomal persistence in the host cell, and a scalable production system (199). They have a quite big cloning capacity of ~9 kb. Different serotypes display different tissue tropisms, which can be very useful for gene therapy (210). Their major drawback is the pre-existing viral immunity in the general population, which can trigger strong immune responses when administered in humans (199).

AAVs are non-enveloped single-stranded DNA viruses which have not attributed to any human disease yet. These are non-integrative and lack the essential genes needed for replication and expression of its own genome; therefore AAVs need the machinery of another virus to complete their life cycle (199). The use of these vectors limits the long-term expression but decreases the risk of insertional mutagenesis (195). Their major limitations include the size transgene which cannot exceed ~5 kb, the host immune responses to capsid components and transgene products, and the difficulty to achieve scalable production. Recombinant AAV are the least immunogenic (211).

To sum up, viral vectors are very efficient transfecting host cells, but they also can potentially lead to immunogenicity, cytotoxicity, or insertional mutagenesis (194).

2.2.2 Non-viral vectors

To effectively deliver the genetic material, non-viral vectors need to prevent endonuclease degradation, immune-reactivity, non-specific interactions, and renal clearance. Moreover, they must reach target tissues and cells, allow cellular uptake, and successfully escape the endosome before undergoing degradation by a lysosome (**Figure 13**).

Non- viral gene delivery can be divided into physical and chemical approaches. The former attempt to force nucleic acids into the cytoplasm or nucleus, whereas the latter utilize engineered particles to target the cells and successfully transfect the genetic material (208). Physical methods include electroporation, sonoporation, laser irradiation, and microinjection, between many others. However, these methods will not be further discussed. The most commonly used chemical delivery approaches are lipoplexes (DNA/cationic lipid), polyplexes

(DNA/cationic polymer), peptiplexes (DNA/peptides), inorganic particles, or combinations.

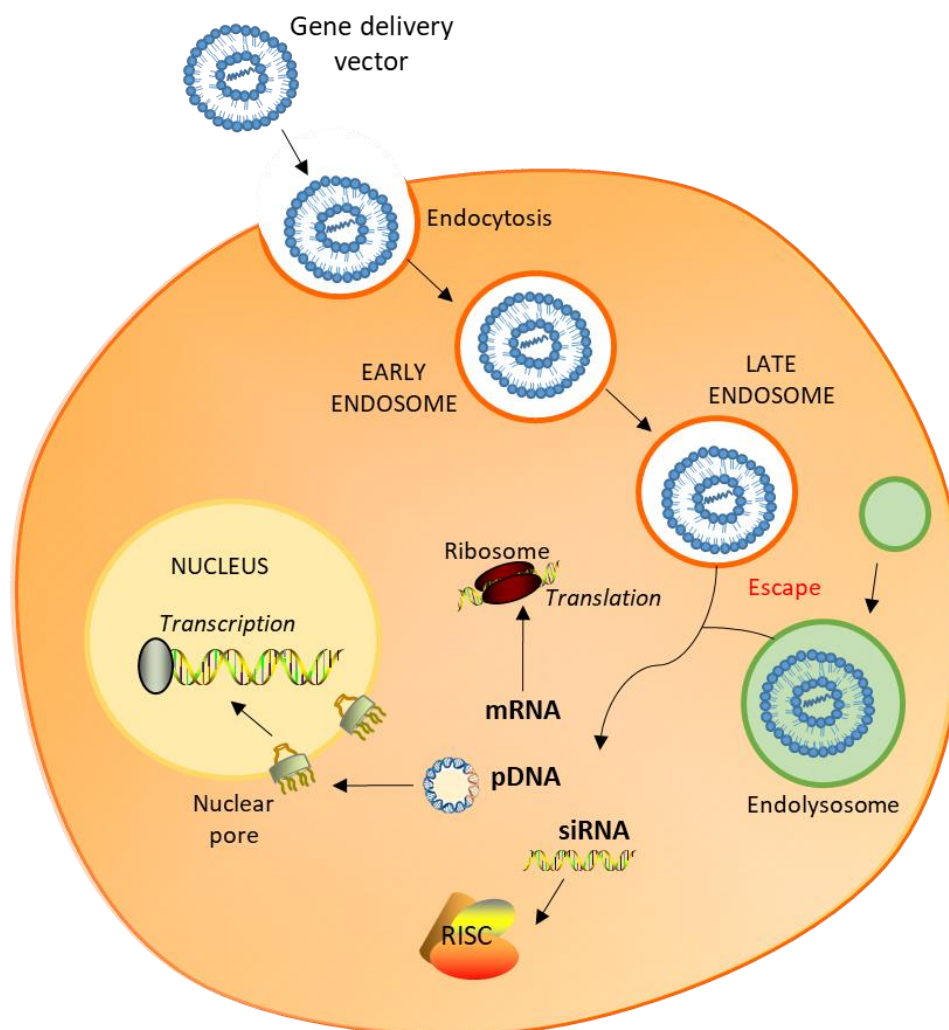


Figure 13. Schematic representation of processes of on-viral vectors gene therapy.

Cationic lipids are formed by a positively charged hydrophilic head and hydrophobic tail (194). The head binds with the negatively charged phosphate group in the genetic material via electrostatic interactions to form lipoplexes. Lipids are biocompatible, biodegradable, and can integrate hydrophilic and hydrophobic substances (212). Moreover, they show low toxicity and immunogenicity. Lipoplexes have structural flexibility and are easy to prepare at large scale. Nevertheless, their major challenge is to target a specific type of cells (213). Lipoplexes are commonly found as liposomes, lipid emulsions, or solid lipid nanoparticles (NPs) (212).

Cationic polymers can neutralize the negatively charged genetic material to form a polyplex and transport it to targeted cells (212). Polyplexes are more stable than lipoplexes (194). They can be categorized into non-biodegradable like polyethylenimine or biodegradable as poly(beta-amino ester) (pBAE). Biodegradable polymers are usually preferred due to lower cytotoxicity given that repeated administration is often necessary (212). Besides, polymers can be natural or synthetic. Natural polymers are very biocompatible, but their properties can vary batch to batch, whereas synthetic ones are well-characterized and their physiochemical properties can be tailored; but sometimes lack enough interaction with the cells (206).

Cationic peptides are short chains of 2–50 amino acid residues linked via peptide bonds rich in basic residues like arginine. They can directly interact with genetic material via conjugation or electrostatic forces to form peptiplexes (212). Cationic peptides are biocompatible and biodegradable. They are easy to synthesize, stable, and show efficient packaging and membrane transport (206). Moreover, peptides can be attached to poly- or lipoplexes to functionalize them and target specifically the vector. One example is cell-penetrating peptides (194).

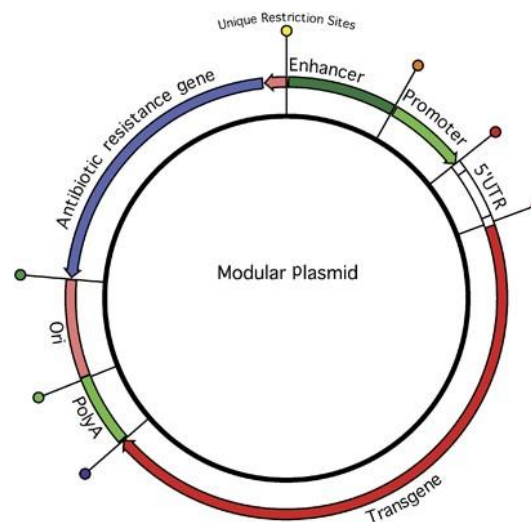
Finally, inorganic materials are also used as gene carriers. They are more stable than organic materials. Some examples include mesoporous silica NPs, carbon nanotubes, and quantum dots (212). Inorganic nanomaterials can be tailored to provide protection from nucleic acid degradation and efficient cellular targeting and nucleic acid release. These materials, with positively charged surface groups can conjugate genetic materials non-covalently or via electrostatic attractions (214).

In conclusion, non-viral vectors are less immunogenic, cytotoxic, and mutagenic than viral vectors. Moreover, they are more stable, can be tailored and have higher gene capacity, at the same time they are cheaper and easier to produce compared to viral vectors (194,209,212).

2.2.2.1 Genetic therapy technologies

The most common approaches in gene therapy are gene addition or inhibition. Gene addition involves the addition of a copy of the defective or inexistent gene. Plasmid DNA (pDNA) and single strand messenger (mRNA) are the genetic materials most used. In contrast, gene inhibition is performed to silence the expression of an altered gene, being siRNA the approach most used. However, microRNA and antisense oligonucleotides can be also employed. Finally, permanent correction of the mutated gene can be achieved using specific genome editing tools like CRISPR/Cas9 technology (215). However, this method will not be further discussed in this thesis.

Figure 14. Schematic representation of a pDNA design. The expression cassette: the mammalian or viral promoter sequences for gene expression; 5' untranslated region (5'UTR) including introns, reporter transgene or gene of interest and polyadenylation (polyA) sequence. The bacterial backbone contains a bacterial origin of replication (ori) and an antibiotic resistance gene or other selectable marker for plasmid amplification in bacteria. Ideally, modular regions would be separated by a unique restriction site for ease of manipulation. Original figure from: Progress and Prospects: Gill DR, Pringle IA, Hyde SC. The design and production of plasmid vectors. *Gene Ther.* 2009;16(2):165-71.



A plasmid is a simple circular double-stranded DNA molecule from <1.000 to >200.000 bp typically found in prokaryotes (216). pDNA is very simple with two main parts: 1) an expression cassette formed by regulatory sequences such as enhancers or promoters that regulate the expression in mammalian cells and a transgene of interest; and 2) a bacterial backbone generally with an antibiotic resistance gene and a prokaryotic promoter required to produce the pDNA in bacteria (**Figure 14**) (217). Therefore, the manipulation of the regulatory elements enables to impact the gene transfer. Furthermore, plasmids have very large packaging capacity and can include multiple expression cassettes (216). Once in the target cell, pDNA needs to be translated in the nucleus (218). On non-dividing cells, the nuclear pore complex can be used to transport pDNA into the nucleus without energy expenditure. Furthermore, to improve nucleus delivery peptides with nuclear localization signals can be employed (219). The use of pDNA is very safe because it is weakly immunogenic and does not integrate to the

genomic DNA, therefore, there is no potential risk of oncogenesis (216). It can be handled at room temperature but generally shows poor transfer efficiency. Modifications such as the removal of CpG dinucleotides and good promoter selection can enable sustained transgene expression (217). Furthermore, good delivery vectors are needed to assure correct cell targeting and efficient gene transfer.

mRNA is single stranded RNA molecule of 300 to 5.000 kDa, up to 15 kb. It usually contains a cap, 5' and 3' untranslated regions and a poly(A)-tail and the encoded gene of interest (218). Oppositely to pDNA, mRNA lacks CpG motifs, which reduces its immunogenicity (219). In the target cell, mRNA needs to reach the cytoplasm to be translated by the host machinery in the corresponding proteins (218). It cannot integrate into the genome, therefore there is no risk of insertional mutations (219). Moreover, mRNA transfection is very efficient and facile due to the small size of the molecule and avoidance of a specific promoter selection (220). However, mRNA is highly unstable due to the presence of a hydroxyl group on the second carbon atom of the sugar moiety that prevents stable double β -helix structure formation (219). Additionally, it can be easily degraded by ubiquitously present nucleases, and it cannot cross cellular membranes due to its anionic nature. For all these reasons, mRNA efficient delivery and transfection relies on the use of a good vector.

siRNAs are double stranded DNA molecules of ~20-25 nucleotides long with 5'-phosphorylation and a 2 nucleotide overhang on the 3' end of each guide strand (antisense) and passenger strand (sense), which ultimately post-transcriptionally inhibit the expression of a gene (221). Once administered intravenously, siRNAs are unstable, highly susceptible to nuclease degradation and likely to induce immune responses through the interaction with toll-like receptors (222). Moreover, they are highly anionic molecules that cannot diffuse across cellular membranes. Finally, if they can be internalized, siRNAs also need to be released from endosomes to reach the RNA interference machinery of the cell. Therefore, the delivery of siRNAs is a major challenge and choosing a good vector is very important. Besides, to improve chemical stability and efficacy as well as increase cell specificity, reduce immunogenicity and decrease off target effects, siRNA can be chemically modified (222).

Once internalized, long double-stranded RNA is cleaved by an enzyme of the RNase III family called Dicer, into two double stranded siRNA, generally bearing a 2-nucleotide overhang on the 3' end of each guide strand (antisense) and passenger strand (sense) (223,224). Next, the siRNA binds to the multi-protein RNA-induced silencing complex (RISC), consisting of argonaute-2, dicer and transactivating response RNA binding-protein. The passenger strand is cleaved from the 5' end of the guide strand which will be degraded, while the guide is integrated to the activated RISC complex. This activated complex binds to the target mRNA and initiates endonucleolytic cleavage through the action of argonaute-2, resulting in post-transcriptional gene silencing (**Figure 15**) (206,224).

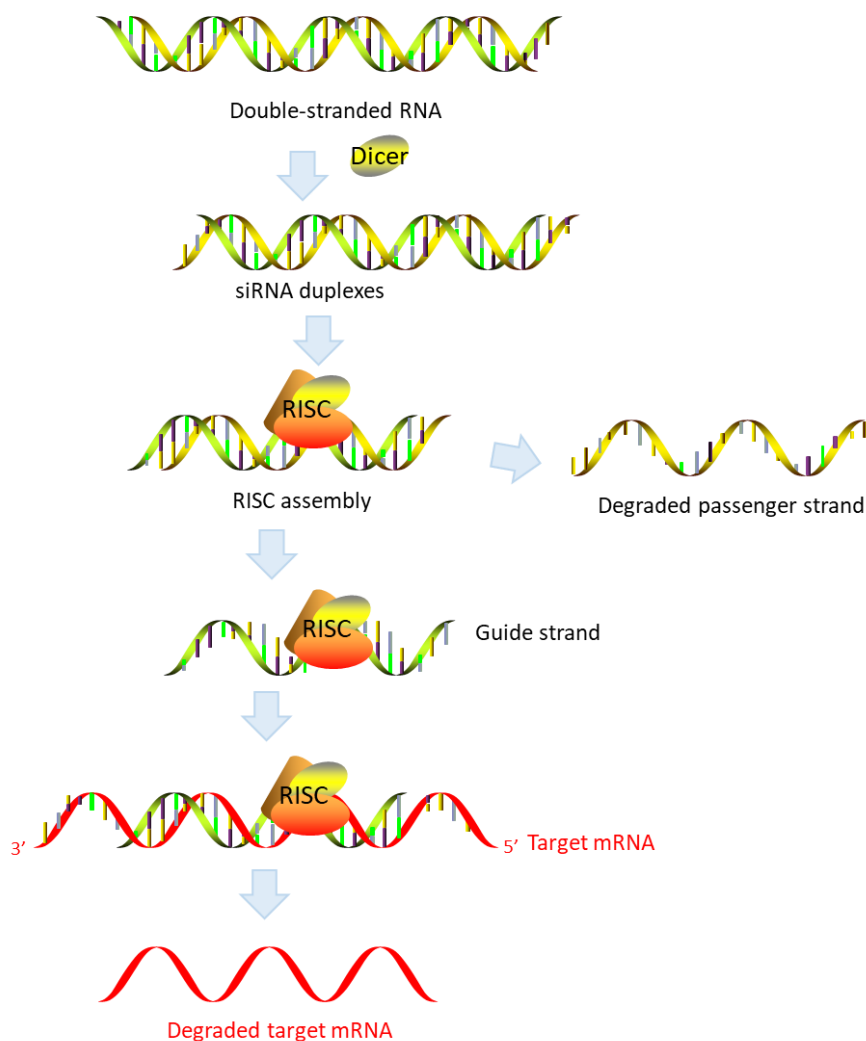


Figure 15. Schematic siRNA-mediated gene silencing.

2.3 Gene therapy in liver fibrosis

Gene therapy has been proved beneficial in a variety of diseases. Therefore, it might also be beneficial in liver fibrosis, which treatment remains an unmet need since to date, no drug has been approved for this condition. Genes involved in HSC activation and proliferation as well as in collagen synthesis or ECM remodeling are the most common targeted genes. These include for instance TGF β , PDGF, and TIMPs. However, most of these genes are not specifically upregulated in fibrogenesis and are involved in other critical processes. For this reason, their inhibition might result in harmful effects (225). Selecting a relevant therapeutic gene is of major importance for an effective fibrosis resolution and very challenging at the same time.

As above mentioned, gene delivery can be performed using two strategies. In the case of liver diseases, *ex vivo* gene delivery would involve the isolation of cells from a resected lobe, their genetic modification *in vitro*, and the transplantation back to the patient. This strategy is very selective and eliminates off-target effects as well as potential toxicities. But the main limitations include the low proliferative and repopulating capacity of primary hepatocytes. By contrast, since the liver receives one fifth of the CO and the fenestrations of the hepatic endothelium allow molecules smaller than 100-200 nm to reach hepatocytes; *in vivo* gene delivery represents a more appealing approach (226). It has been reported that vector transduction in non-parenchymal liver cells, predominantly LSECs and KCs, inversely correlates with parenchymal cells uptake. Moreover, transgene expression in hepatocytes directly correlates with the diameter of the fenestrae and interventions that increase it, induce enhanced genetic material uptake by hepatocytes (227). Nevertheless, during liver fibrosis targeted cell delivery is more complicated due to sinusoids capillarization and exuberant collagen deposition. Furthermore, issues directly related to gene therapy itself, such as genetic material instability, renal excretion, non-specific tissue accumulation, poor uptake, and release from endosomes into the cytoplasm; even complicate more an efficient genetic material delivery (228).

To overcome these issues, viral and non-viral vectors have been tailored to specifically target the liver and specific cell types like hepatocytes. Some

strategies include the use of vectors with liver tropism as AAV serotype 2 (229) or hepatocyte-specific expression cassettes that restrict gene expression to hepatocytes (230). The physical properties such as chemical structure, size and charge of non-viral vectors can be modified, as well as surface markers or molecules can be added to direct them to certain liver cells (231). For instance, these vectors have been functionalized with molecules such as vitamin A (232), transferrin (233), or mannose (231); peptides such as PDGFR β binding peptide (234) or the peptide sequence RGD (arginine-glycine-aspartic acid) (231); and receptors as asialoglycoprotein receptor (235) to enhance uptake.

Undoubtedly, an increasing number of publications have reported successful liver-targeted gene therapies in experimental models. Nevertheless, more effort needs to be dedicated on translating the results into the clinic. Being the innate and adaptive immune responses, hepatic toxicity, and large-scale vector production; the major challenges (213).

3. NANOPARTICLES

3.1 Overview

NPs are defined as a wide class of materials that typically are roughly 1 to 100 nm, but often used up to 300-500 nm (236,237). Due to their large ratio of surface area to volume compared to bulk materials, NPs possess unique physical and chemical properties.

Over the last years, the field of biomedicine has gained much interest in NPs. Nanomedicine is the discipline devoted the use of nanomaterials for medical applications, including diagnosis and treatment of diseases at the molecular level (238). For instance, NPs have been used as sensitive contrast agents, to transport diagnostic or therapeutic agents or to detect molecular changes in a highly sensitive manner (238). Organic (like polymers and liposomes), inorganic (as quantum dots and iron oxide) and carbon-based NPs (as graphene quantum dots or carbon nanotubes) are the most used NPs in biomedicine (191).

Nanomaterials must be non-toxic, biocompatible, water dispersible, non-immunogenic, and stable in physiological media (191). Due to their small size,

NPs can easily enter to the body through different routes, but their effective delivery is still challenging and largely depends on: 1) physiochemical properties of the NPs such as size, shape, composition, charge, and polydispersity (PDI) (**Figure 16**); 2) biological factors like type of target organ, biomolecular milieu, proteins and pH, and 3) the interplay and interactions between both (239,240). NPs can be tailored modifying its optical, magnetic, electronic, and biologic characteristics to overcome these issues (238). In some cases, coating the NP with several agents or biomolecular ligands can further improve biocompatibility, prevent opsonizing proteins to adhere to the NP, reduce rapid metabolism and clearance, or provide selective targeting.

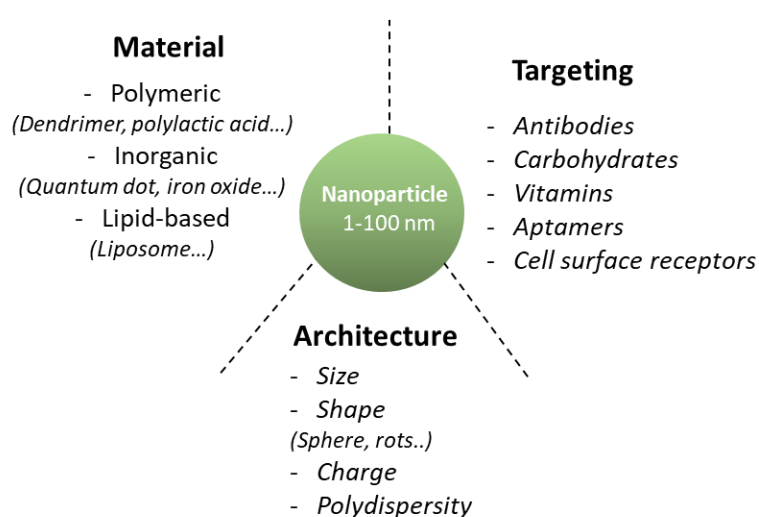


Figure 16. Design of a nanoparticle.

Although, NPs can be administered by inhalation, ingestion, dermal or injection in humans, in the present work we will just consider intravenous administration. Following the intravenous administration, an array of plasma proteins attaches to the surface of the NP, commonly referred as protein corona. The assembly of this coating provides a new biological identity to the NP, and directly affects its colloidal stability, interactions, biodistribution, toxicity, and clearance (241). Some of these attached proteins can be opsonins, for instance component fragments and apolipoproteins. These opsonins are recognized by surface receptors of the reticuloendothelial system and make the NP susceptible of mononuclear phagocytic clearance (242). It has been reported that NPs < 6 nm may be directly eliminated through the kidney, whereas NPs > 6 nm tend to be sequestered by the liver and spleen (243). Since the liver via both the hepatic

artery and the portal vein receives approximately 21 % of the heart CO and the blood flow in the hepatic sinusoids is lower than in the systemic circulation; preferential NPs hepatic retention is favored (244). Once in the hepatic sinusoids, KCs recognize NPs as foreign materials and internalize them, especially ones that are aggregated, with larger diameters, negatively charged and hydrophobic (243). Smaller but negatively charged NPs are likely to escape from KCs uptake and be removed from circulation by LSEC, which further can deliver the NPs through fenestrae or via transcytosis to hepatocytes (231,237). Furthermore, NPs smaller than the sinusoid fenestrations (50- 200 nm in diameter) can diffuse into the space of Disse and undergo rapid uptake by hepatocytes, which have high affinity for positively charged NPs (237,245). These NPs will ultimately be cleared through hepatobiliary excretion (243). In the spleen, NPs are mostly internalized by splenic macrophages, whereas larger NPs are susceptible to be retained in the red pulp, increasing the particle removal by splenic filtration as increases NPs size (242,246).

3.2 Cerium oxide nanoparticles

3.2.1 Characteristics

Cerium is a rare earth element in the lanthanide series of the periodic table, being the most reactive of them due to its electropositive nature (247–249). At the nanoscale level, cerium can be bound to oxygen acquiring a fluorite crystalline lattice structure which exhibits oxygen vacancies that arise with the loss of oxygen and/or its electrons (250). Both Ce^{3+} and Ce^{4+} cerium valence states can coexist on the surface of the nanoparticle and thanks to the redox-cycling between the cerium states, cerium oxide NPs (CeO_2 NPs/nanoceria) can behave as strong antioxidants (**Figure 17**) (251).

Due to its unique characteristics, nanoceria can behave as an oxidant or reducing element in response to physical parameters such as the presence of other ions, temperature, and oxygen partial pressure. Furthermore, the increased surface area to volume ratio that exists in a NP of ~ 5 nm diameter enables CeO_2 NPs to auto-regenerate its antioxidant activity (252). Indeed, because of its ability to catalyze redox reactions, nanoceria has been widely used for decades in industrial processes ranging from chemical mechanical polishing and

planarization (253), corrosion protection (254), solid oxide fuel cells, as catalytic convertor for removing toxic gases (255), coating for metals and alloys to diesel fuel oxidation catalysis (256).

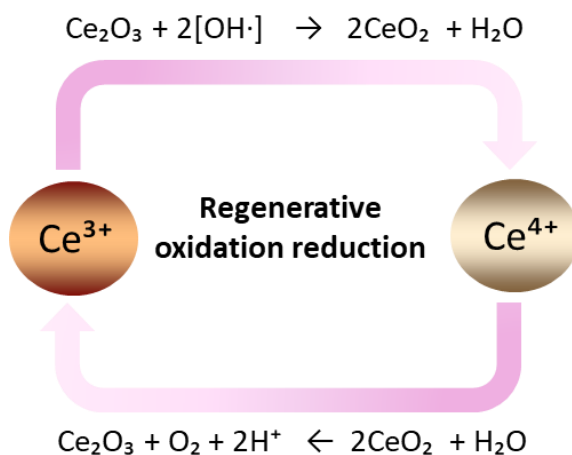


Figure 17. Oxidation and reduction states of cerium. Adaptation from: Xu C, Qu X. Cerium oxide nanoparticle: a remarkably versatile rare earth nanomaterial for biological applications. *NPG Asia Materials*, 2014; 6, e90.

CeO₂NPs have also been reported to display multi-enzyme mimetic properties, including superoxide dismutase, catalase, oxidase, peroxidase, and phosphatase (251,257). Furthermore, nanoceria has shown antibacterial activity (175). For all these reasons, in spite that some toxic effects of nanoceria particles have been described when they are inhaled (258) or administered in huge amounts (248,259), several groups explored whether the antioxidant properties of nanoceria could be of benefit in biomedical purposes. CeO₂NPs have been evaluated as promising treatments in a variety of illnesses such as diabetes (260), retinal diseases (252), chronic inflammation (261), cardiomyopathy (262), neurodegenerative diseases (250), and cancer (263), between many others. Although positive results were obtained, the use of these NPs as a therapeutic tool still is a matter of concern. The synthesis method, type of stabilizing agent used, the Ce³⁺/Ce⁴⁺ surface ratio, aggregation, corrosion, and interaction with extracellular matrix proteins critically modify CeO₂NPs physicochemical properties and fate (249,257).

3.2.2 Applications in liver diseases

Since nanoceria possess strong antioxidant and anti-inflammatory properties and as abovementioned, liver diseases are characterized by sustained inflammation and oxidative stress; it is compressible that several authors have

studied the potential of CeO₂NPs to treat liver diseases (**Figure 18**). In fact, experimental evidence suggests that CeO₂NPs have the potential to be hepatoprotective and attenuate the progression of several hepatic diseases including liver fibrosis and fatty liver disease (264).

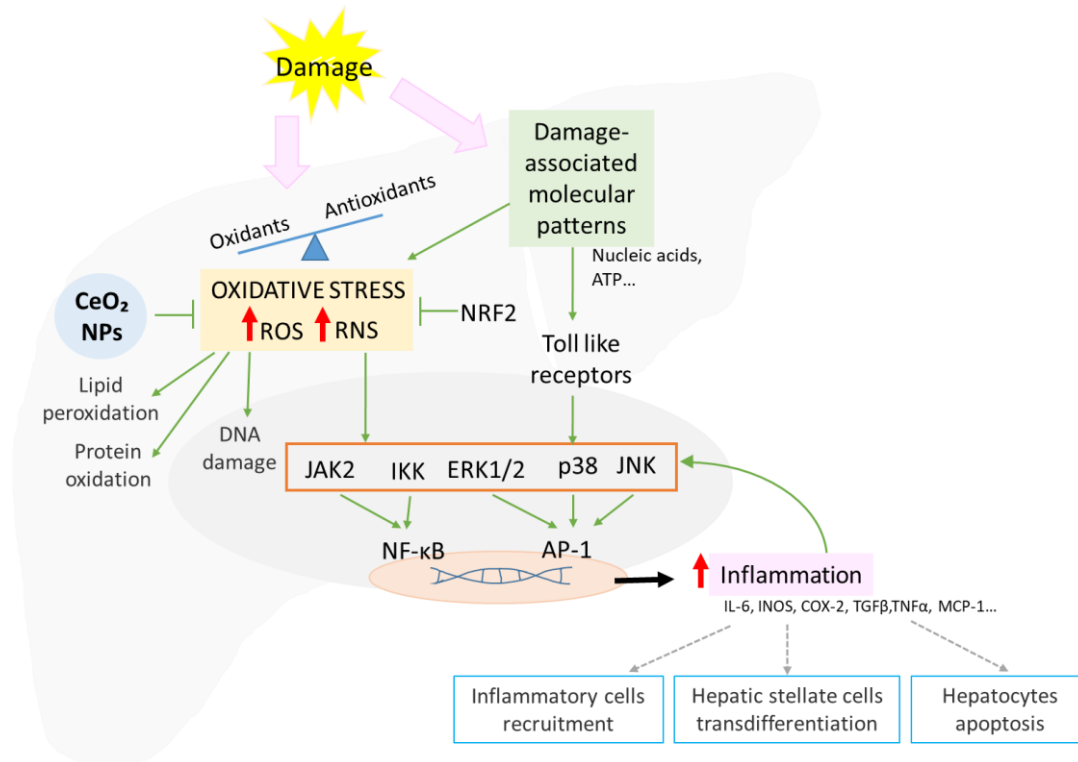


Figure 18. Schematic representation of the signaling pathways involved in oxidative stress-mediated inflammation and CeO₂NP effects. Original from: Casals G, Perramón M, Casals E, Portolés I, Fernández-Varo G, Morales-Ruiz M, Puentes V, Jiménez W. Cerium Oxide Nanoparticles: A New Therapeutic Tool in Liver Diseases. *Antioxidants* (Basel). 2021; 10(5): 660.

After systemic administration in rats, CeO₂NPs mostly accumulate in the liver and spleen for at least 8 weeks; with trace amounts in lungs and kidney, and no presence in heart or brain (265–269). Being feces the principal route of elimination (265,268). Besides, Ni D *et al.* calculated that the half-life of these NPs was 2h, being already uptaken by the liver and spleen 3h largely by the LSECs and KC after mice intravenous injection (270). Furthermore, Parra-Robert *et al.* recently demonstrated by TEM that immortalized human HepG2 hepatocytes can successfully internalize CeO₂NPs, which are found in membrane compartments or free in the cytoplasm (271).

In a rat model of carbon tetrachloride (CCl₄)-induced fibrosis, CeO₂NPs treatment improved hepatic function, portal hypertension and fat deposition; at the same time it diminished the expression of markers of oxidative stress, such as

heat shock protein family a member 5 and *activating transcription factor 3*, and inflammation like *Il-1 β* and *iNos* (265). Besides, nanoceria downregulated the elevated *Il-6* transcript expression both in the portal vein of cirrhotic rats *in vivo* and in immortalized portal endothelial cells *in vitro*. Furthermore, the secretome of these treated cells induced macrophage polarization (272). In agreement, CeO₂NPs protected from prooxidant and proinflammatory cytotoxicity and reduced the expression of inflammation-related genes including *iNOS*, *neutrophil cytosol factor 2*, *myeloperoxidase*, and *prostaglandin endoperoxide synthase 1* in H₂O₂ challenged HepG2 cells. The phosphoproteomic analysis of these cells revealed that nanoceria interfered with *mTOR*, *MAPK kinase /ERK*, *casein kinase 2 alpha 1*, and *protein kinase A* signaling (273).

Besides, after hepatectomy liver regeneration has shown to be stimulated by CeO₂NPs. Additionally, nanoceria treatment after acetaminophen-induced liver injury decreased oxidative stress markers, stimulated hepatocyte proliferation, and activated nuclear factor kappa beta signaling pathway (266). Likewise, concomitant CeO₂NPs administration with the widely used chemotherapeutic agent doxorubicin resulted hepatoprotective by diminishing serum lipid peroxidation and transaminases, as well as, preserving the hepatic histologic architecture compared to doxorubicin alone (274).

Moreover, nanoceria has shown promising powerful anti-steatotic and anti-inflammatory effects in both *in vitro* and *in vivo* experimental models of NAFLD. CeO₂NPs significantly reduced total saturated fatty acids and unsaturated fatty acids longer than 18 carbon atoms in immortalized human hepatic HepG2 cells exposed to oleic and palmitic acids. This effect was accompanied by changes in the elongase and desaturase activities induced by fatty acid challenge (271). Eilenberger *et al.* cultured spheroid HepG2 cells and exposed them to palmitic and oleic acids. The treatment of these spheroids with a mixture of zinc salt of mefenamic acid, hydroxypropyl- β -cyclodextrin, and CeO₂NPs in a ratio of 1:6:1 resulted in decreased TNF- α and IL-8 secretion (275). Furthermore, nanoceria treatment diminished total liver lipids and triglycerides as well as visceral adipose tissue mass in rats with monosodium glutamate-induced obesity. Additionally, CeO₂NPs decreased the serum levels of proinflammatory cytokines IL-1 β and IL-12B p40 while they restored the anti-inflammatory IL-4 (276). Interestingly,

Carvajal *et al.* showed in a methionine/choline-deficient diet rat model of diet-induced NAFLD that CeO₂NPs treatment significantly decreased hepatic LD size and lipid peroxidation. Besides, the liver of these rats decreased the total amount of triglycerides and CE derived fatty acids, evaluated by mass spectrometry, as well as lipid signaling evaluated by transcriptomic analysis (277). Additionally, CeO₂NPs have also shown to restore normal serum lipid profile, alleviate hepatic lipid peroxidation, and protect liver architecture in fipronil-induced NAFLD model (278). Finally, the therapeutic effect of CeO₂NPs and CeO₂ embedded inside a mesoporous silica was evaluated in a NAFLD experimental genetic model of obese Zucker rats. The treatment with both types of CeO₂NPs resulted in significant decrease of triglycerides, low density lipoprotein cholesterol, circulating palmitic acid, and total fatty acids in the serum. Furthermore, the treatments downregulated the hepatic PI3K/AKT/mTOR pathway (279).

Finally, only few studies have investigated the utility of CeO₂NPs for the prevention of acute liver injury. Ibrahim HG *et al.*, evaluated the effects of eight days CeO₂NPs administration before a single administration of DEN in mice. Nanoceria pretreatment decreased serum ALT and hepatic lipid peroxidation, at the same time it augmented the activity of myeloperoxidase, NO levels, and the expression of antioxidant enzymes including catalase, glutathione, and glutathione s-transferase compared to DEN alone treated mice (280). Finally, nanoceria has shown to be useful for the prevention of ischemia reperfusion injury in mice by scavenging ROS and protecting cells from oxidative damage, preventing superoxide dismutase depletion, alleviating tissue injury, decreasing neutrophil infiltration, and reversing the level of proinflammatory cytokines to normal ranges (270).

3.3 Poly(beta-amino ester) nanoparticles

3.3.1 Characteristics

pBAE are a family of degradable and biocompatible polyesters bearing cationic side chains. Base polymers were synthesized for the first time by David Lynn and Langer via one-pot Michael addition reaction (281). In short, they can be synthesized by adding amines and diacrylates to a solvent, such as dimethyl sulfoxide, and stirred at different temperatures for different times depending on

the desired PDI and viscosity. Primary amines possess two reaction sites that can conjugate with two acrylate sites to form linear polymers. When the amino carry two secondary amino groups, one site can react with one acrylate (282). Next, the base polymer and amine-containing end-cap monomer are separately dissolved in tetrahydrofuran and then mixed (**Figure 19**). Finally, linear polymers are purified by precipitation with diethyl ether, vacuum dried, and can be stored at -20°C (283,284). The physiochemical properties, such as charge and PDI, are highly tunable and are subjected to the monomers used in the polymerization (282). For this reason, there are different pBAE libraries and have been reported more than 2.500 different linear pBAE (284). Highly branched pBAE can also be obtained by using triacrylates (282).

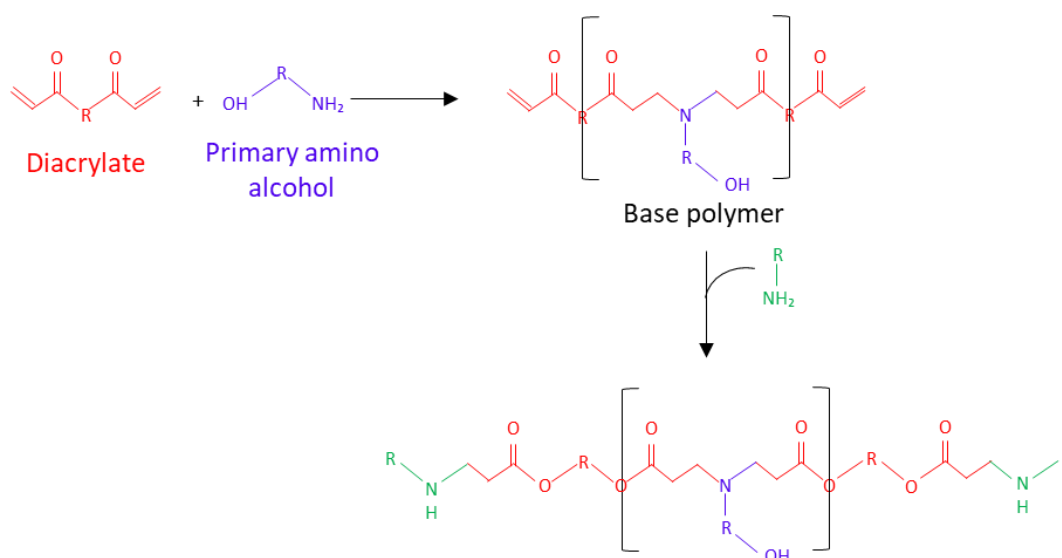


Figure 19. Schematic representation of the synthesis of a linear pBAE. Adaptation from: Iqbal S, Qu Y, Dong Z, Zhao J, Rauf Khan A, Rehman S, et al. Poly (β -amino esters) based potential drug delivery and targeting polymer; an overview and perspectives (review). *Eur Polym J.* 2020;141:110097.

The addition of a nucleic acid is critical for the formation of pBAE NPs since both interact electrostatically and self-assemble in non-toxic nanoscale polyplexes, which stabilize the DNA and slow the fast pBAE degradation (281,285). The ratio between the nucleic acid and pBAE, reported as mass ratio of polymer to nucleic acid (w/w), is of major importance for the generation of small and stable NPs and efficient gene material delivery (286).

pBAE polyplexes are internalized by cells via endocytosis. They are pH sensitive and escape from endosomal degradation through proton sponge mechanism (284,287). In short, during endosomal maturation hydrogen ions are

accumulated inside the endosome. To restore the equilibrium potential chloride and water diffuse into the endosome, but ultimately it leads to osmotic swelling and endosomal membrane disruption and release all the contents into the cytoplasm (288). It has been reported that the presence of tertiary amines in pBAE improves the buffering capacity and facilitates endosomal escape (286). Furthermore, pBAE are significantly less toxic compared to other cationic polymers like poly(ethylenimine) and poly(lysine); and under physiological conditions they are degraded via hydrolysis of their backbone esters (289).

Functionalization with several molecules or moieties for specific cell targeting has been reported. Antigen presenting cells targeting has been achieved by the addition of mannose (290) or terminal oligopeptides (291). Besides, endothelial cell delivery has been performed coating pBAE NPs with polyglutamic acid conjugated to an RGD peptide (292) or VHPK peptides that target vascular cell adhesion molecule 1 protein (293). Finally, cluster of differentiation 3 antibody-functionalized polyglutamic acid has been used for selectively target T lymphocytes (294).

Furthermore, therapeutics can be conjugated via disulfide bond, which are stable extracellularly but are rapidly degraded by glutathione and thiredoxin reductases once in the cytoplasm (284). Accordingly, pBAE NPs have extensively been studied as drug/protein carriers and transfection vectors. For instance, gene therapy delivery has been studied to target the lung (295,296), cartilage (297), brain malignant tumors (298,299), breast cancer (300), or human papillomavirus-related cervical malignancy (301). Moreover, other applications include the delivery of systemic immunotherapy in melanoma and colorectal carcinoma experimental models (302), or doxorubicin into tumor cells (293). But there is still a long way to go before to be able to use some of these approaches in the clinical setting.

3.3.2 Applications in liver diseases

As abovementioned, pBAE NPs are promising delivery vectors for a variety of diseases and the liver is not an exception. In 2017, Zamboni CG *et al.* formulated a library of different pGFP- pBAE polyplexes and evaluated which one had the most efficient cellular uptake and gene delivery in several HCC cell lines. Once

selected, they were administered *in vivo* to nude mice with HCC. The polyplexes already reached the tumor 6h after intravenous injection (283). Moreover, Vaughan HJ *et al.* demonstrated that locally administered tumor necrosis factor-related apoptosis-inducing ligand plasmid conjugated to pBAE NPs slowed tumor growth *in vivo* (303). Finally, the addition of targeting moieties has shown to enhance liver accumulation following intravenous administration. Fornaguera *et al.* showed that engineered end-oligopeptides pBAE NPs with retinol moiety strongly accumulated in the spleen and secondly in the liver of mice; being the antigen presenting cells the liver cell type with highest transfection (291).

HYPOTHESES

Liver fibrosis is a wound healing response that attempts to limit the consequences from chronic damage to the liver. It is characterized by a dysregulation of extracellular matrix (ECM) synthesis and degradation, leading to excessive ECM accumulation. The pathophysiology of the disease is complex and involves an interplay of cells, mediators, and pathways; being hepatic stellate cells (HSC) the major effectors. Significant efforts have been dedicated to unravel the mechanisms under the disease; and despite it has been shown to be potentially reversible with the removal of the etiologic agent, there is absence of effective specific treatments to treat this pathology. Besides if fibrosis progresses, it can lead to life-threatening conditions including cirrhosis and eventually, hepatocellular carcinoma (HCC).

Pituitary tumor-transforming gene 1 (PTTG1) is a multi-faceted protein strongly expressed in the fetal liver and during HCC, whereas it is almost absent in the adult liver. In adipose tissue, delta like non-canonical notch ligand 1 (DLK1) has shown to be one of the most abundant PTTG1 targets. Furthermore, in the liver, DLK1 has been shown to be involved in HSC activation.

Taking altogether into account, the **first work hypothesis** is the following: *PTTG1/DLK1 pathway could be a key mediator governing the fibrogenic process, and therefore, its inhibition could be a successful approach to attenuate experimental liver fibrosis progression.*

Hepatocarcinogenesis is an extremely complex process in which a premalignant environment promotes the transformation and survival of hepatocytes while inhibiting immune surveillance. Accumulating evidence indicates that oxidative stress plays a major role in liver carcinogenesis and tumor progression not only by directly damaging lipids and proteins and amplifying inflammation; but also driving genomic damage and instability. Besides, oxidative stress is of major importance in regulating processes such as proliferation, apoptosis, and senescence. In line, antioxidants have shown to display promising hepatoprotective effects in both experimental and human chronic liver diseases.

Furthermore, during the last decades, nanomedicine has been on the spotlight because of the highly tunable properties of NPs, making them suitable for the diagnosis and treatment of diseases. Cerium oxide NPs (CeO₂NPs) behave as strong auto-regenerative antioxidants thanks to their oxygen vacancies and increased surface area to volume ratio. In fact, CeO₂NPs have been shown to display beneficial antioxidant, anti-inflammatory and anti-steatotic effects for the treatment of experimental liver diseases including fibrosis and non-alcoholic steatohepatitis.

In this regard, the **second work hypothesis** is the following: *CeO₂NPs could be a beneficial therapeutic approach to target experimental HCC-associated oxidative stress and mitigate tumor progression.*

Increased intrahepatic resistance due both architectural and functional abnormalities is the major contributor to portal hypertension, a hallmark syndrome of advanced liver disease. Portal hypertension is concomitant of other hemodynamic alterations including systemic arterial hypotension and high cardiac output. Numerous studies have demonstrated that a deficit in intrahepatic nitric oxide (NO) bioavailability has an important role in the pathogenesis of portal hypertension by strongly contributing to increase hepatic resistance. NO is a gaseous mediator with a strong vasodilator effect. At systemic level, NO is key in the development of the arterial hypotension, which in conjunction with an elevated cardiac output results in the hyperdynamic circulation present in patients with decompensated cirrhosis.

It may be assumed that to a good strategy to compensate diminished hepatic NO production would be to administrate nitrates. However, orally administered nitrates have only been proved beneficial reducing portal hypertension and variceal bleeding in combination with beta-blockers, which act as splanchnic vasoconstrictors (304,305).

For that matter, the **third work hypothesis** is the following: *Liver-targeted functionalized pBAE NPs containing an NO donor could ameliorate portal hemodynamics and liver function in experimental cirrhosis.*

OBJECTIVES

The **first objective** of this doctoral thesis was *to evaluate the role of PTTG1/DLK1 pathway in the development of experimental hepatic fibrosis and to elucidate the potential therapeutic effects of its interference*. In this regard, the study was aimed:

1. To assess the temporal relationship between *Pttg1* and *Dlk1* activation and fibrosis progression in rats with experimental liver cirrhosis.
2. To determine whether *PTTG1* is overexpressed in human cirrhosis.
3. To assess whether lacking *Pttg1* gene modifies collagen deposition and the expression of fibrosis-related genes in CCl₄-treated mice.
4. To elucidate the effect of non-targeted *Pttg1* interference in the development of experimental liver fibrosis.

The **second objective** of this doctoral thesis was *to investigate therapeutic value of CeO₂NPs in experimentally induced rat HCC*. In this regard, the study was aimed:

1. To analyze the biodistribution of intravenous administered CeO₂NPs in rats with experimental DEN-induced HCC.
2. To assess tumor progression in rats with experimental HCC treated with CeO₂NPs.
3. To investigate the signaling mechanisms of action of CeO₂NPs at lipidome, genome and phosphoproteome levels.
4. To evaluate the effect of CeO₂NPs treatment on survival of rats with experimental HCC.
5. To unveil the cellular and subcellular uptake of CeO₂NPs by isolated human livers and a human-derived liver cancer cell line.

The **third objective** of this doctoral thesis was *to investigate potential effects on portal hemodynamics and liver function of functionalized liver-specific nanoparticles containing a NO donor in experimental cirrhosis*. In this regard, the study was aimed:

1. To characterize the properties of retinol functionalized pBAE NPs as carriers for liver-targeted NO donor therapy.
2. To investigate organ and vascular biodistribution after intravenous administration of NO donor retinol pBAE NPs in rats with experimental cirrhosis.
3. To evaluate the potential effects of liver-targeted NO donor pBAE NPs on portal and systemic hemodynamics, as well as, on serum markers of liver function in rats with decompensated cirrhosis.
4. To assess the potential impact of NO donor retinol pBAE NPs on hepatic fibrogenesis and inflammatory pathways in rats with decompensated cirrhosis.






MATERIALS, METHODS, AND
RESULTS

ARTICLE 1: The pituitary tumor-transforming gene 1 / delta like homolog 1 pathway plays a key role in liver fibrogenesis

The **first objective** of this doctoral thesis was to evaluate the role of PTTG1/DLK1 pathway in the development of experimental hepatic fibrosis and to elucidate the potential therapeutic effects of its interference.

Perramón M, Carvajal S, Reichenbach V, Fernández-Varo G, Boix L, Macias L, Melgar-Lesmes P, Bruix J, Melmed S, Lamas S, Jiménez W. The pituitary tumour-transforming gene 1/delta-like homologue 1 pathway plays a key role in liver fibrogenesis. Liver Int. 2022 Mar;42(3):651-662.

The pituitary tumour-transforming gene 1/delta-like homologue 1 pathway plays a key role in liver fibrogenesis

Meritxell Perramón^{1,2}  | Silvia Carvajal^{1,2} | Vedrana Reichenbach^{1,2} |
Guillermo Fernández-Varo^{1,2} | Loreto Boix^{2,3,4}  | Laura Macias-Muñoz^{1,2} |
Pedro Melgar-Lesmes^{1,2,5,6}  | Jordi Bruix^{2,3,4} | Shlomo Melmed⁷  | Santiago Lamas⁸ |
Wladimiro Jiménez^{1,2,5} 

¹Biochemistry and Molecular Genetics Service, Hospital Clínic Universitari, Barcelona, Spain

²Institut d'Investigacions Biomèdiques August Pi i Sunyer (IDIBAPS), Centro de Investigación Biomédica en Red de Enfermedades Hepáticas y Digestivas (CIBERehD), Barcelona, Spain

³Department of Medicine, University of Barcelona, Barcelona, Spain

⁴Barcelona-Clínic Liver Cancer Group, Hospital Clínic Universitari, Barcelona, Spain

⁵Department of Biomedicine, University of Barcelona, Barcelona, Spain

⁶Institute for Medical Engineering and Science, Massachusetts Institute of Technology, Cambridge, MA, USA

⁷Department of Medicine, Cedars-Sinai Research Institute, University of California School of Medicine, Los Angeles, CA, USA

⁸Centro de Biología Molecular Severo Ochoa (CSIC-UAM), Madrid, Spain

Correspondence

Wladimiro Jiménez, Hospital Clínic Universitari, Villarroel 170, Barcelona 08036, Spain.
Email: wjimenez@clinic.cat

Funding information

This work was supported by grants to WJ SAF2015-64126-R and RTI2018-094734-B-C21, to SL SAF2015-66107-R and to PML RYC2018-023971-I funded by MCIN/AEI/ 10.13039/501100011033 and by the "European Union NextGenerationEU/PRTR". Grant 2017 SGR858 funded by Agència de Gestió d'Ajuts Universitaris i de Recerca. The Centro de Investigación Biomédica en Red de Enfermedades Hepáticas y Digestivas (CIBERehd) is funded by the Instituto de Salud Carlos III.

Abstract

Background and Aims: *PTTG1* is almost undetectable in adult livers but is highly expressed in hepatocarcinoma. While little is known about its involvement in liver fibrosis, *PTTG1* expression is associated with *DLK1*. We assessed the role of the *PTTG1/DLK1* pathway in fibrosis progression and the potential therapeutic effect of *PTTG1* silencing in fibrosis.

Methods: *Pttg1* and *Dlk1* were studied in liver and isolated cell populations of control and fibrotic rats and in human liver biopsies. The fibrotic molecular signature was analysed in *Pttg1*^{-/-} and *Pttg1*^{+/-} fibrotic mice. Finally, *Pttg1* silencing was evaluated in rats as a novel antifibrotic therapy.

ABBREVIATIONS: Acta2, α -SMA, alpha 2-smooth muscle actin; Agt, angiotensinogen; All, angiotensin II; Akt1, AKT serine/threonine kinase 1; ANOVA, one-way analysis of variance; Bcl2, B-cell lymphoma 2; bwt, body weight; C⁻ siRNA, negative control siRNA; Cav1, Caveolin 1; Ccl11, C-C motif chemokine ligand 11; Ccl3, C-C motif chemokine ligand 3; CCl₄, carbon tetrachloride; Ccr2, C-C motif chemokine receptor 2; Col1a2, collagen type I Alpha 2 Chain; Col3a1, collagen type III Alpha 1 Chain; Ctgf, cellular communication network factor 2; Cxcr4, C-X-C motif chemokine receptor 4; ddPCR, droplet digital PCR; DLK1, delta-like homologue 1; EC, endothelial cell; ECM, extracellular matrix; Edn1, endothelin 1; Egf, epidermal growth factor; FasL, tumour necrosis factor receptor superfamily, member 6 ligand; Grem1, gremlin 1; HCC, hepatocellular carcinoma; HDAC, histone deacetylases; HEP, hepatocytes; HIF1, hypoxia-inducible factor 1; HSC, hepatic stellate cells; Ifng, interferon Gamma; Il, interleukin; Il13ra2, interleukin 13 receptor subunit alpha 2; Ilk, integrin linked kinase; Inhbe, inhibin subunit beta E; Itga2, integrin subunit alpha 2; Itgb, integrin subunit beta; KO, knock out; Lox, lysyl oxidase; MAP, mean arterial pressure; MMPs, matrix metalloproteinases; Myc, MYC proto-oncogene, BHLH, transcription factor; Pdgf, platelet-derived growth factor; Plat, plasminogen activator, tissue type; Plau, plasminogen activator, urokinase; PP, portal pressure; *Pttg1* siRNA, *PTTG1* pre-designed siRNA; *PTTG1*, pituitary tumour-transforming gene 1; RT-PCR, real-time PCR; siRNA, small interference RNA; Smad3, SMAD family member 3; Smad6, SMAD family member 6; Smad7, SMAD family member 7; Stat6, signal transducer and activator of transcription 6; TACE, tumour necrosis factor-alpha converting enzyme; Tgfb, transforming growth factor-beta receptor; TGF β , transforming growth factor-beta; Thbs, thrombospondin; TIMPs, tissue inhibitor of matrix metalloproteinases; TNF α , tumour necrosis factor-alpha; WT, wild type.

This is an open access article under the terms of the Creative Commons Attribution License, which permits use, distribution and reproduction in any medium, provided the original work is properly cited.

© 2022 The Authors. *Liver International* published by John Wiley & Sons Ltd.

Results: *Pttg1* and *Dlk1* mRNA selectively increased in fibrotic rats paralleling fibrosis progression. Serum DLK1 concentrations correlated with hepatic collagen content and systemic and portal haemodynamics. Human cirrhotic livers showed greater *PTTG1* and *DLK1* transcript abundance than non-cirrhotic, and reduced collagen was observed in *Pttg1 Pttg1^{-/-}* mice. The liver fibrotic molecular signature revealed lower expression of genes related to extracellular matrix remodeling including *Mmp8* and *9* and *Timp4* and greater *eotaxin* and *Mmp13* than fibrotic *Pttg1^{+/+}* mice. Finally, interfering *Pttg1* resulted in reduced liver fibrotic area, lower α -*Sma* and decreased portal pressure than fibrotic animals. Furthermore, *Pttg1* silencing decreased the transcription of *Dlk1*, *collagens I* and *III*, *Pdgfr β* , *Tgfr β* , *Timp1*, *Timp2* and *Mmp2*.

Conclusions: *Pttg1/Dlk1* are selectively overexpressed in the cirrhotic liver and participate in ECM turnover regulation. *Pttg1* disruption decreases *Dlk1* transcription and attenuates collagen deposition. *PTTG1/DLK1* signalling is a novel pathway for targeting the progression of liver fibrosis.

KEYWORDS

extracellular matrix, fibrosis, gene therapy, liver, siRNA

Lay Summary

PTTG1 and *DLK1* transcription are increased in rats and patients with hepatic cirrhosis. *PTTG1* is involved in fibrotic extracellular matrix remodeling and its silencing decreases portal hypertension and alleviates fibrosis progression.

1 | INTRODUCTION

Cirrhosis is a major determinant of morbidity and mortality and predisposes to hepatic failure and liver cancer. Halting the progression of fibrosis to cirrhosis is considered as a foremost goal in patients with liver disease. Anti-inflammatory agents, arresting hepatic stellate cells (HSC) activation substances, renin-angiotensin system inhibitors, cannabinoid receptor antagonists, hepatoprotective peptides, transforming growth factor- β (TGF β) or platelet-derived growth factor (PDGF) antagonists and chemokine receptor antagonists are among the numerous candidates assessed to limit or reverse liver fibrogenesis.¹⁻⁴ However, most of these compounds have shown limited efficacy and/or adverse side effects, and consequently, an antifibrogenic pharmacological treatment for liver fibrosis is currently lacking.

The pituitary tumour-transforming gene (*PTTG1*) is the index mammalian securin.⁵ *PTTG1* is overexpressed in a variety of cell lines including hepatocellular carcinoma (HCC).⁶ It encodes a multifunctional protein involved in the regulation of faithful chromatid segregation during mitosis, DNA repair, apoptosis, metabolism and gene transcription.⁷ Interestingly, *PTTG1* modulates extracellular

matrix (ECM) turnover regulating several matrix metalloproteinases (MMPs).^{8,9} Despite overexpression of *PTTG1* in liver biopsies from patients with HCC, very little data are available on its expression in preneoplastic conditions such as advanced liver fibrosis and cirrhosis. This is particularly striking as several factors induce *PTTG1* expression, including estrogens, fibroblast growth factor, insulin, insulin growth factor-1 and hepatocyte growth factor^{7,10} all increased under conditions of chronic liver injury.¹¹⁻¹⁴ Moreover, microenvironmental hypoxia occurring in damaged hepatic tissue could also regulate *PTTG1* expression through the hypoxia-inducible factor 1.¹⁵ *PTTG1* also acts to regulate growth factors, angiogenesis and exhibits transforming activity *in vitro* and *in vivo*.^{16,17} Furthermore, hepatic *PTTG1* expression is upregulated after partial hepatectomy and has been proposed as a new marker of proliferation in liver regeneration.¹⁸ These findings support the exploration of whether *PTTG1* could contribute to the activation of fibroproliferative processes in liver disease. In addition, delta-like homologue 1 (*DLK1*) was identified as one of the most abundantly expressed *PTTG1* targets.¹⁹ The *DLK1* gene encodes a single-pass transmembrane protein that belongs to a family of epidermal growth factor (EGF) repeat-containing proteins.²⁰ *DLK1* is a non-canonical ligand of Notch receptors that mediate a metabolic shift from lipid storage to peripheral lipid oxidation in adipocytes, participate in differentiation processes and behave as a growth factor.²¹ It consists of six EGF-like tandem repeats, a juxtamembrane region with a tumour necrosis factor-alpha converting enzyme (TACE)-mediated cleavage site, a transmembrane domain and a short intracellular tail.²² *DLK1* can act as both transmembrane and soluble protein. *DLK1* membrane-proximal cleavage by TACE results in the release of the EGF-like

extracellular region, a large soluble product of 50 kDa. This form has a similar function inhibiting adipocyte differentiation to that of the full-length membrane-associated protein, but since it is soluble it can act in an autocrine and paracrine manner. Moreover, both *PTTG1* and *DLK1* genes show concomitant expression in human fetal liver, placenta and different carcinomas, including pituitary adenoma, breast adenocarcinoma and neuroblastoma.¹⁹ Given this background, we aimed to explore the hypothesis that *PTTG1/DLK1* signalling should play a central role in the activation of the fibrogenic process in liver disease.

2 | MATERIALS AND METHODS

2.1 | Induction of hepatic cirrhosis in rats

This study was performed in control ($n = 32$) and male Wistar rats with different degrees of fibrosis ($n = 77$) (Charles-River, Saint Aubin Les Elseuf, France). Fibrosis was induced by repetitive carbon tetrachloride (CCl_4) inhalation.²³ The rats were fed ad libitum with standard chow and water containing phenobarbital (0.3 g/L), as drinking fluid. Animals were exposed to a CCl_4 atmosphere twice a week, starting with 0.5 minutes for three sessions. Afterwards, the duration was increased to 1, 2, 3, 4 and 5 minutes until the end of the investigation. To induce variable degrees of hepatic fibrosis CCl_4 -treated rats were studied at the 8th, 13th, 16th and 19th week after starting the fibrosis induction protocol. Control rats were studied following similar periods of phenobarbital administration. When scheduled, animals were anaesthetised and a haemodynamic study was performed. Afterwards, a blood sample was obtained and animals were sacrificed by isoflurane overdose (Forane, Abbott Laboratories S.A., Madrid, Spain). Organ samples were snap-frozen or fixed in 10% buffered formalin.

2.2 | Induction of fibrosis in mice

This study was performed in fibrotic and control male *Pttg1* wild-type (*Pttg1*^{+/+}) and knock out (*Pttg1*^{-/-}) mice. *Pttg1*^{-/-} mice with C57BL/6 genetic background were provided by Dr Shlomo Melmed and the origin of these mice has been described previously.²⁴ Fibrosis was induced in *Pttg1*^{+/+} ($n = 4$) and *Pttg1*^{-/-} ($n = 7$) by i.p. injection of CCl_4 (1 ml CCl_4 /kg of body weight [bwt], previously diluted 1:8 vol/vol in corn oil) three times a week for 4 weeks. All animals were kept under constant temperature and humidity in 12 hours controlled dark/light cycle, and they were fed ad libitum on a standard pellet diet.

2.3 | In vivo *Pttg1* interference

A group of fibrotic rats randomly received i.v. *Pttg1* small-interfering RNA (siRNA, assay ID s133880, 0.25 mg/kg/dose bwt, $n = 6$) or scrambled siRNA (Ambion in vivo negative control No. 1, $n = 6$) as the

negative control (C^- siRNA) every 10 days from the 9th to the 13th week after starting the fibrosis induction protocol. In vivo transfection was performed using InvivoFectamine 3.0 kit (Invitrogen, Life Technologies Corporation, Carlsbad, CA, USA) following the manufacturer's instructions. Six control rats were also included. Rats were studied in the 14th week.

2.4 | Statistical analysis

Quantitative data were analysed using GraphPad Prism 5 (GraphPad Software Inc., San Diego, CA) and statistical analysis of the results was performed by unpaired Student's *t* test, one-way analysis of variance (ANOVA) with Newman-Keuls post hoc test or Kruskal-Wallis test with Dunn post hoc test when appropriate. Correlations between the variables studied were analysed with Pearson two-tailed test. Results are expressed as mean \pm SE and considered significant with $P < 0.05$.

Additional materials and methods are provided in the Supplementary material section.

3 | RESULTS

3.1 | Fibrosis quantification and staging

The liver of rats treated with CCl_4 showed macroscopic finely granulated surfaces. According to the time of CCl_4 exposure, we observed progressive ECM accumulation, evolving from a light deposition, mainly in the portal area, to numerous and thicker septa in those animals submitted to longer CCl_4 exposure periods. Most animals exposed to the toxin for the longest periods of time developed cirrhosis. Consequently, rats were staged according to the percentage of fibrotic area with respect to the total area of the liver biopsy: mild and moderate fibrosis was defined when the percentage of fibrotic area $<6\%$ ($n = 6$), severe fibrosis $6\%–11\%$, ($n = 8$) and cirrhosis $>11\%$ ($n = 11$). Control rats ($n = 13$) displayed no appreciable alterations in liver histology. Figure 1A shows representative Sirius red staining from a control liver, a liver with mild/moderate fibrosis, a liver with severe fibrosis and a cirrhotic liver. Fibrotic/cirrhotic rats had important alterations in liver function tests, which were more pronounced in cirrhosis (Table S1).

3.2 | Hepatic *Pttg1* and *Dlk1* mRNAs parallel the intensity of liver fibrosis and selectively occurs in this organ

Progression of liver fibrosis was associated with a concomitant increase in *Pttg1* mRNA expression (Figure 1B). *Pttg1* expression significantly increased in rats with severe fibrosis and reached maximum levels in rats with cirrhosis. Interestingly, *Pttg1* transcript was selectively detected in the liver of cirrhotic animals, but not in the

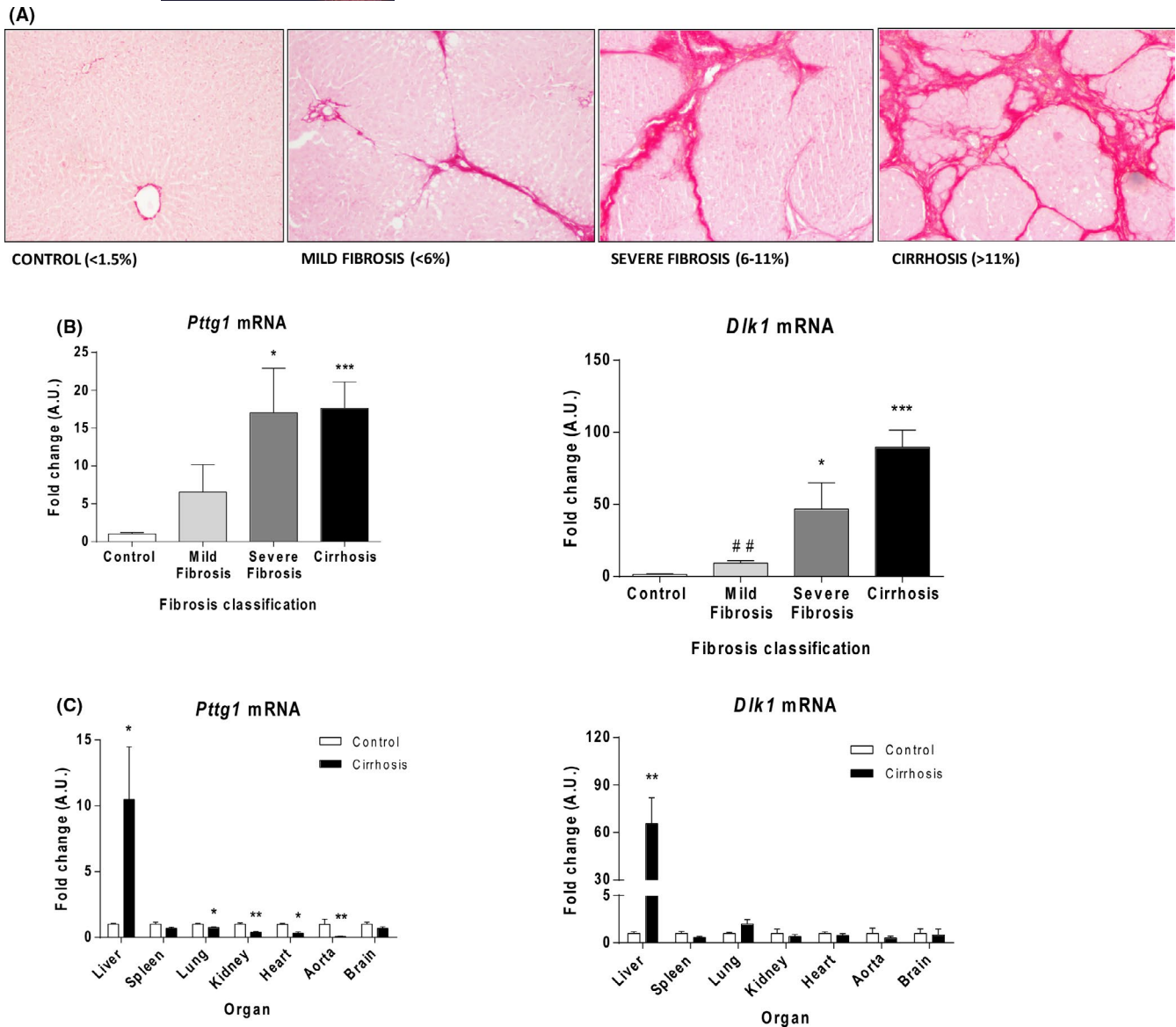


FIGURE 1 Expression of *Pttg1* and *Dlk1* in experimental liver fibrosis. A, Staging of CCl₄-treated rats based on liver-collagen content. Sirius red staining of representative liver sections (×100). B, Hepatic *Pttg1* and *Dlk1* mRNA of control (n = 13) and CCl₄-treated rats with mild/moderate fibrosis (n = 6), severe fibrosis (n = 8) and cirrhosis (n = 11). C, *Pttg1* and *Dlk1* mRNA in organs from control (n = 5) and cirrhotic rats (n = 5). Results are expressed as mean ± SE. *P < 0.05, **P < 0.01, ***P < 0.001 vs control; ##P < 0.01 vs cirrhosis. One-way ANOVA with Newman-Keuls post hoc test or Kruskal-Wallis test with Dunn post hoc test

spleen, lungs, kidneys, heart, aorta or brain (Figure 1C). *Pttg1* mRNA abundance was also assessed by droplet digital PCR (ddPCR). Results were in line with those obtained in real-time PCR (RT-PCR) experiments. The liver of cirrhotic rats showed a much higher abundance of *Pttg1* transcripts (411 ± 67 copies/μl) than that found in control livers (20 ± 2 copies/μl, P < 0.001). In contrast, with the exception of heart (7 ± 1 vs 28 ± 2 copies/μl, P < 0.05) no differences were found between spleen (614 ± 94 vs 947 ± 172 copies/μl), kidney (27 ± 4 vs 38 ± 5 copies/μl), lung (74 ± 8 vs 87 ± 5 copies/μl) aorta (4 ± 1 vs 27 ± 12 copies/μl) and brain (17 ± 3 vs 21 ± 1 copies/μl) of cirrhotic and control rats. The pattern expression of *Pttg1* was paralleled by a similar profile for *Dlk1* mRNA (Figure 1B). *Dlk1* mRNA abundance progressively increased, the lowest levels observed in rats with mild/

moderate fibrosis, the highest in cirrhotic rats. Indeed, *Dlk1* activation was selectively detected in the cirrhotic liver but not in other assessed organs (Figure 1C).

3.3 | *Pttg1* and *Dlk1* are mainly expressed in hepatic parenchymal tissue

To identify the cellular source of altered expression of both *Pttg1* and *Dlk1* in hepatic tissue, we isolated primary cells from the liver of cirrhotic and control rats. Both, *Pttg1* and *Dlk1* exhibited low or almost negligible mRNA expression in different control cell types (Figure 2A). By contrast, marked *Pttg1* mRNA abundance was

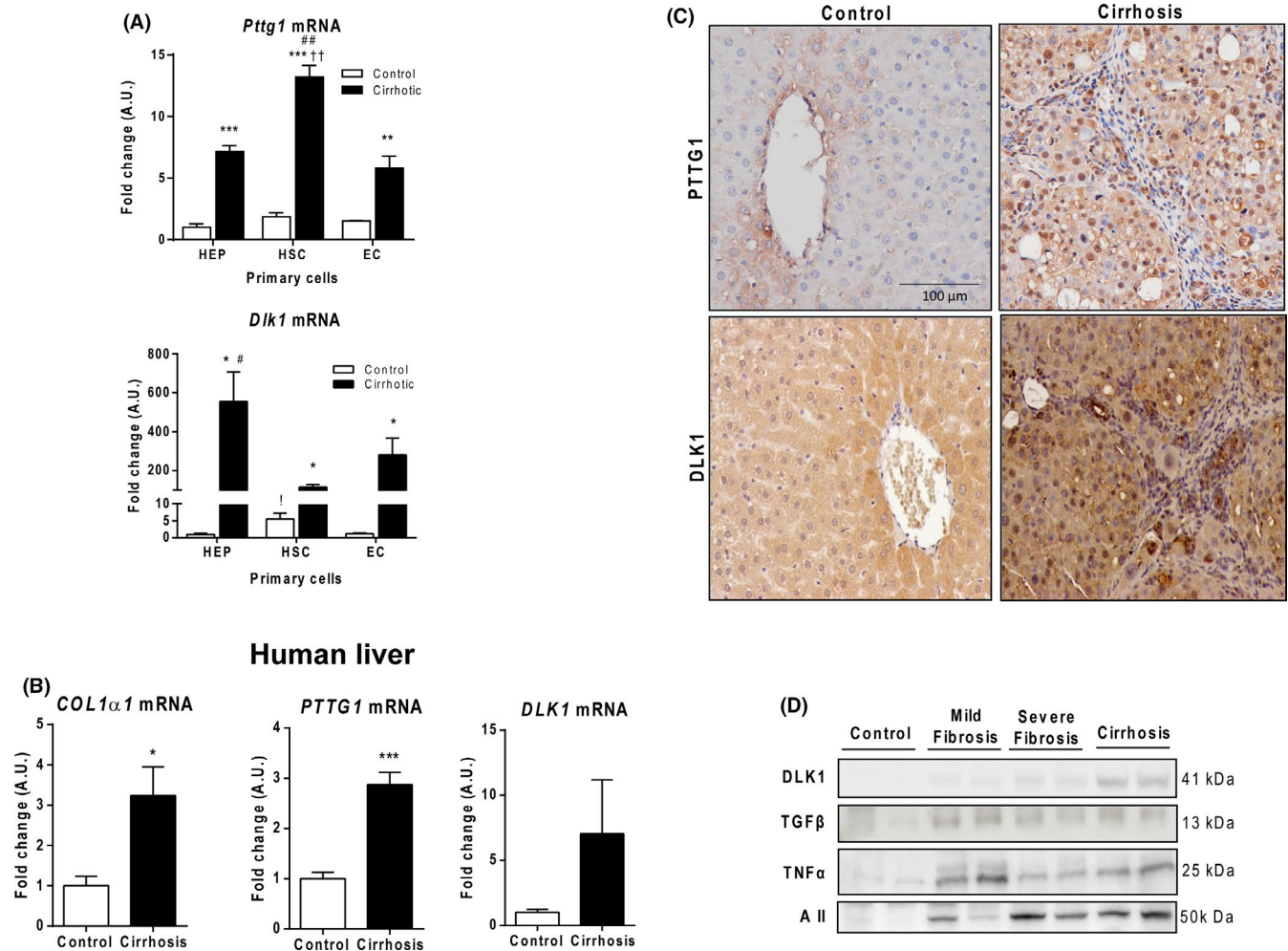


FIGURE 2 *Pttg1* and *Dlk1* expression. A, *Pttg1* and *Dlk1* mRNA in hepatocytes (HEP), stellate cells (HSC) and endothelial cells (EC) from control ($n = 2$) and cirrhotic rat livers ($n = 2$). Results are expressed as mean \pm S.E. * $P < 0.05$, ** $P < 0.01$ vs control, †† $P < 0.01$ vs cirrhotic HEP; # $P < 0.05$, ## $P < 0.01$ vs cirrhotic EC. ! $P < 0.05$ vs control HEP. B, *COL1 α 1*, *PTTG1* and *DLK1* mRNA in liver from cirrhotic ($n = 12$) and non-cirrhotic patients ($n = 7$). * $P < 0.05$, *** $P < 0.001$ vs control. C, Immunolocalization of *PTTG1* and *DLK1* in rat control and cirrhotic liver (200 \times). D, Western blots for rat hepatic *DLK1*, *TGF β* , *TNF α* and angiotensin II (AII)

observed in three types of liver cells isolated in cirrhotic rats, the highest abundance being found in HSC (Figure 2A). This was paralleled by striking activation of *Dlk1* mRNA but was largely observed in hepatocytes (HEP) (Figure 2A). In an attempt to further delineate the relative contribution of HEP and HSC to the acute increase in *Pttg1* and *Dlk1* in cirrhotic liver, we next measured the absolute concentration of these transcripts in the isolated cells. In line with the RT-PCR results, the absolute *Pttg1* mRNA values were similar in both types of cells (HEP: 125 ± 7 copies/ μ l, HSC: 131 ± 3 copies/ μ l), whereas *Dlk1* mRNA values were lower in HSC (80 ± 11 copies/ μ l) than in HEP (154 ± 9 copies/ μ l). Overactivation of the *PTTG1*/*DLK1* axis in human cirrhosis was further confirmed. Paralleling the increased abundance of collagen I alpha 1 (*COL1 α 1*) messenger, higher expression of both *PTTG1* and *DLK1* mRNA was observed in samples derived from cirrhotic patients in comparison to non-cirrhotic biopsies. Next, we performed histological immunolocalization of *PTTG1* and *DLK1* in the liver of cirrhotic and control rats. Both proteins were almost undetectable in control samples. However, in cirrhotic

livers, they were clearly identified either in the parenchymal area or close to the portal tracts and fibrous septa (Figure 2C). Additionally, *DLK1* expression clearly differs from that of other well established profibrogenic substances, since *DLK1* hepatic protein content only exhibited a clear relationship with fibrosis intensity (Figure 2D).

3.4 | Serum *DLK1* values rise in parallel with liver fibrosis and correlate with hemodynamics

Advanced progression of liver fibrosis was associated with a parallel increase in circulating levels of *DLK1*, showing a significant increase in rats with cirrhosis (53.13 ± 5.66 ng/ml, $P < 0.001$) (Figure 3A). A close direct relationship between *DLK1* and hepatic collagen content was found in CCl_4 -treated rats ($r = 0.74$; $P < 0.001$) (Figure 3B). Animals with cirrhosis showed frank hypotension (mean arterial pressure [MAP]: 87 ± 13 mm Hg, $P < 0.001$) as compared with control rats (MAP: 123 ± 2 mm Hg).

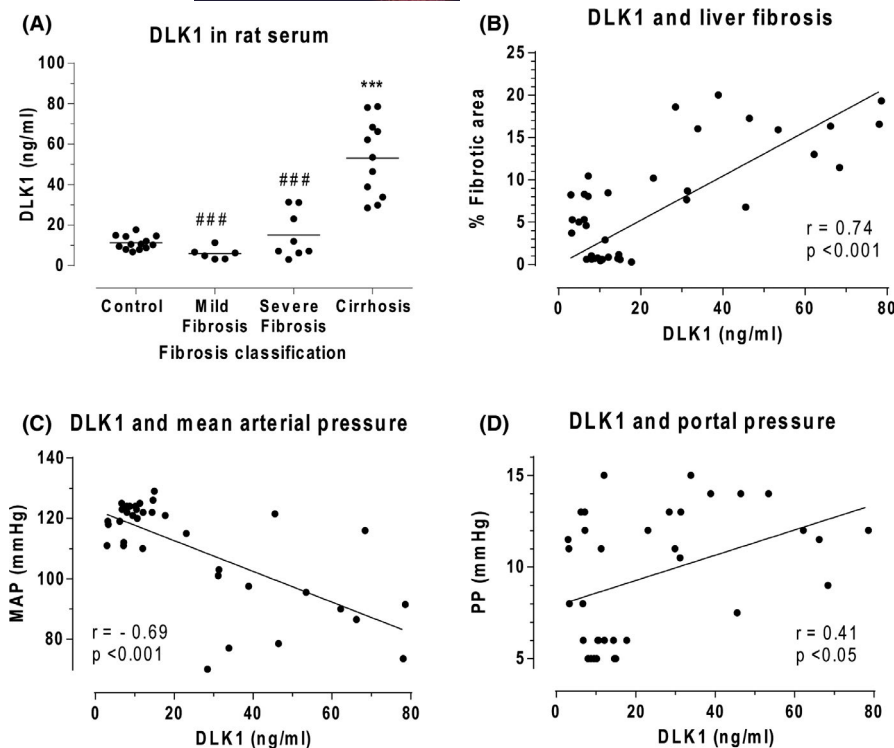


FIGURE 3 DLK1 serum levels in rats with experimental fibrosis. A, Serum concentrations of DLK1 in control ($n = 13$), mild/moderate fibrosis ($n = 6$), severe fibrosis ($n = 8$) and cirrhotic ($n = 11$) rats. Each point represents single DLK1 value in serum. Horizontal lines indicate the mean value for each group. *** $P < 0.001$ vs control; ### $P < 0.001$ vs cirrhotic. One-way ANOVA with Newman-Keuls post hoc test. Correlation of DLK1 serum levels with (B) histological quantification of liver fibrosis ($r = 0.74$; $P < 0.001$); C mean arterial pressure ($r = -0.69$; $P < 0.001$); and D, portal pressure ($r = 0.43$; $P < 0.01$) in control ($n = 13$) and CCl_4 -treated ($n = 25$) rats. Pearson two-tailed test

MAP inversely correlated with serum DLK1 in CCl_4 -treated rats ($r = -0.69$, $P < 0.001$) (Figure 3C). Furthermore, serum concentration of DLK1 also depicted a direct relationship with the degree of portal hypertension in fibrotic/cirrhotic animals ($r = 0.41$, $P < 0.05$) (Figure 3D).

3.5 | Fibrosis is significantly attenuated in $\text{Pttg1}^{-/-}$ mice

CCl_4 -treated $\text{Pttg1}^{+/+}$ mice had mild/moderate fibrosis mainly characterized by perivenular and periportal deposition with incipient development of the portal and venular septa, ending blindly in the parenchyma; whereas $\text{Pttg1}^{-/-}$ mice displayed thinner septa and more preserved hepatic parenchyma (Figure 4A) than $\text{Pttg1}^{+/+}$ animals. These findings were confirmed by morphometric analysis in which $\text{Pttg1}^{-/-}$ mice showed a significantly reduced percentage of fibrosis area than sections of $\text{Pttg1}^{+/+}$ mice (Figure 4B). This attenuation in liver fibrosis was also associated with an almost 50% reduction in *Dlk1* mRNA expression. In fact, whereas fibrotic $\text{Pttg1}^{+/+}$ mice showed a 55.7 ± 5.0 -fold change increase in *Dlk1* mRNA overcontrol $\text{Pttg1}^{-/-}$ mice, these figures were of a 30.9 ± 7.5 -fold change increase in $\text{Pttg1}^{-/-}$ fibrotic mice.

3.6 | Expression pattern of fibrogenesis-related genes in $\text{Pttg1}^{-/-}$ mice

Further insight on the effects of $\text{Pttg1}^{-/-}$ in the liver of CCl_4 -treated mice was obtained by determining the mRNA expression of 86 genes

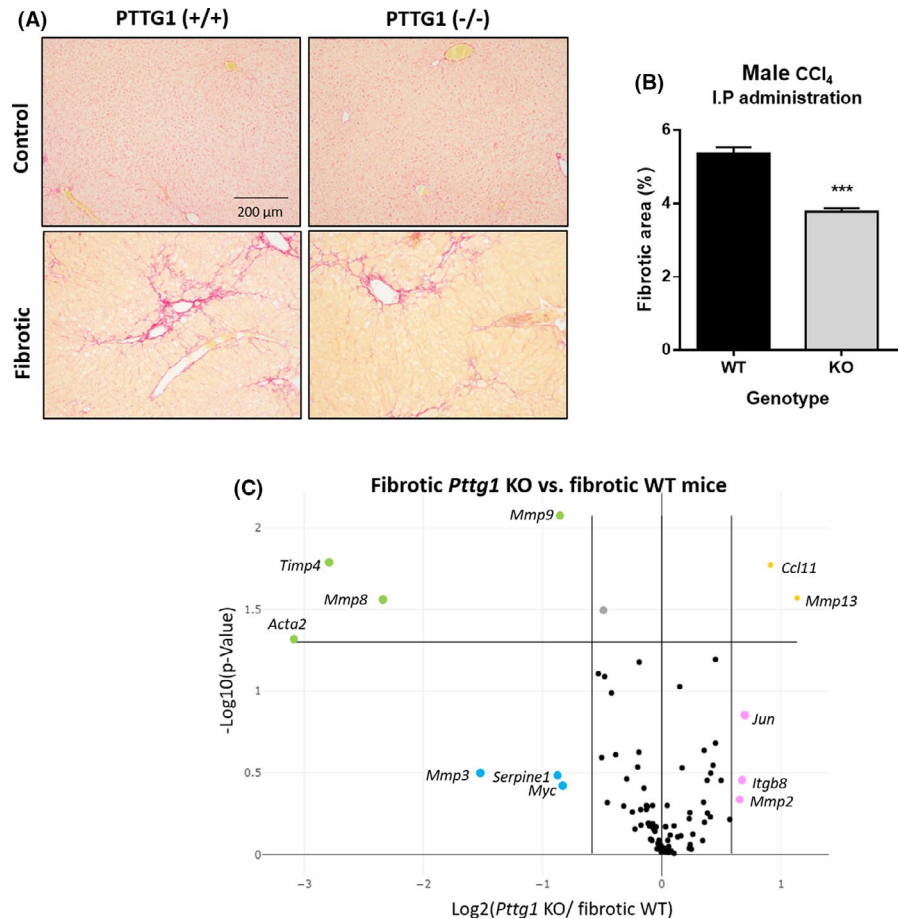
involved in the fibrogenic process. Table 1 shows all the genes showing a 1.5-fold or greater change in expression between the liver of $\text{Pttg1}^{+/+}$ control or CCl_4 -treated mice. Regardless of the moderate hepatic collagen deposition observed in $\text{Pttg1}^{+/+}$ mice treated with CCl_4 , these animals showed a clear fibrotic molecular signature. Actually, 24 genes were significantly upregulated, including *Acta2* and *Grem1* which encode proteins involved in HSC activation and epithelial to mesenchymal transition,²⁵ genes related to ECM and adhesion molecules (*Col1a2*, *Col3a1*, *Mmp1a*, *Mmp9* and *Plau*) and several genes related to inflammation (*Il1 α* , *Il1 β* , *Ilk*, *Il10*, *Tnf*, *Ccl3* and *Cxcr4*), growth (*Agt*) and signal transduction (*Inhbe*, *Smad3*, *Stat6*, *Smad6*, *Tgfb1*, *Tgfb1r1*, *Tgfb2*, *Thbs1* and *Thbs2*) compared to control $\text{Pttg1}^{+/+}$ mice.

A 1.5-fold or greater change in expression with $P < 0.05$ was considered statistically significant in comparing fibrotic $\text{Pttg1}^{+/+}$ vs $\text{Pttg1}^{-/-}$ mice. In addition to reducing the mRNA expression of *Acta2* (gene encoding α -smooth muscle actin protein), the lack of *Pttg1* inhibited the expression of several genes involved in ECM turnover including *Mmp8*, *Mmp9* and *Timp4* (Figure 4C). We also observed a significant increase in *Ccl11* and *Mmp13*. The former encodes eotaxin a chemokine that has been described to be upregulated in senescent HSC²⁶ whereas the latter encodes for a metalloprotease involved in the degradation of a fibrotic liver matrix.²⁷

3.7 | Assessment of *Pttg1* siRNA in cultured rat hepatocytes and fibrotic rats

To investigate the efficacy and duration of gene silencing in cultured rat hepatocytes, we transfected CC-1 cells. Following treatment,

FIGURE 4 Hepatic fibrosis in *Pttg1*^{-/-} mice. A, Sirius red staining from healthy and fibrotic *Pttg1*^{+/+} and *Pttg1*^{-/-} mice (100×). B, Fiber content in *Pttg1*^{+/+} (n = 4) and *Pttg1*^{-/-} (n = 7) mice. ****P* ≤ 0.001 vs *Pttg1*^{+/+}, unpaired t-test. C, Volcano plot of the differentially expressed genes in a pair-wise comparison of *Pttg1*^{+/+} (n = 4) and *Pttg1*^{-/-} (n = 4) mice. Significance was set to a *P* value based on a Student's t-test of 0.05 ($-\log_{10} [P\text{-value}] \geq 1.30$), the biological cut-off was set to a fold regulation of ± 1.5 fold ($-1 \geq \log_{1.5} [\text{FC of fibrotic } Pttg1 \text{ KO/fibrotic WT}] \geq 1$). According with these two criteria, the top 12 differentially expressed genes are labeled with their corresponding gene ID. Insignificant (black), statistically but not biologically significant down-regulated (grey), biologically but not statistically downregulated (blue) and upregulated (pink), and both biologically and statistically significant downregulated (green) up regulated (yellow) genes in fibrotic *Pttg1*^{+/+} mice



Pttg1 mRNA was significantly lower than that in the siRNA C⁻ group at 24, 48 and 72 hours (Figure 5A). These results indicate that *Pttg1* siRNA effectively suppresses *Pttg1* expression in rat-cultured hepatocytes. *Pttg1* siRNA was also effective at silencing the enhanced expression of *Pttg1* mRNA in fibrotic rats (Figure 5B). In fact, whereas fibrotic rats treated with scrambled siRNA displayed approximately 15 times higher levels of *Pttg1* mRNA than control animals, an abundance of this transcript in the liver of fibrotic rats receiving *Pttg1* siRNA was not different from that found in healthy animals. In addition to silencing hepatic *Pttg1* mRNA, administration of *Pttg1* siRNA also inhibited hepatic *Dlk1* mRNA expression in fibrotic rats (Figure 5B).

3.8 | Effect of *Pttg1* siRNA on liver histology, portal pressure and profibrogenic genes in fibrotic rats

Fibrotic rats treated with C⁻ siRNA showed initial stages of the characteristic pattern of perivenular and periportal deposition of connecting tissue with development of portal-to-portal septa and evidence of architectural distortion resulting in micronodular fibrosis (Figure 6A). However, biopsies obtained from fibrotic rats treated with *Pttg1* siRNA displayed less remarkable architectural alterations,

with thinner septa, and more preserved hepatic parenchyma. This was confirmed by morphometric analysis of Sirius red-stained sections (Figure 6B). This abrogation of fibrosis was consistently observed in all animals exposed to *Pttg1* silencing. Similar results were found when staining alpha 2 smooth muscle actin (α -SMA). We detected α -SMA as linear staining in the portal tracts and fibrous septa of both groups of fibrotic rats (Figure 6A). Staining was more diffuse in rats receiving *Pttg1* siRNA than in C⁻ siRNA. In line, *Pttg1* siRNA also showed significantly reduced portal hypertension than fibrotic animals receiving C⁻ siRNA (Figure 6B). Furthermore, *Pttg1*-silenced animals significantly decreased hepatic mRNA expression of *Tnfa* compared to fibrotic rats.

As anticipated, *Col1a2* and *Col3a1* mRNA was significantly increased in fibrotic rats treated with C⁻ siRNA. Consistently, we also observed activation of key genes involved in profibrogenic mechanisms, such as *Tgfb β 1* and *Pdgfr β* (Figure 6C), and an altered balance of MMPs and TIMPs, specifically, increased transcription of *Mmp2*, *Mmp9*, *Timp1* and *Timp2* (Figure 6D). In line with previous results, administration of *Pttg1* siRNA resulted in a significantly lower abundance of *Col1a2*, *Col3a1*, *Mmp2*, *Timp1* and *Timp2* transcripts (Figure 6C,D). Furthermore, *Tgfb β 1* and *Pdgfr β* expression appeared also markedly attenuated, indicating that *Pttg1* silencing effectively abrogates profibrogenic activity in CCl₄-induced fibrosis.

3.9 | Effect of *Pttg1* siRNA on serum markers of liver function

Pttg1 siRNA treatment was associated with a tendency towards normalization of most systemic indicators of liver function (Table 2). Actually, aspartate aminotransferase, lactate dehydrogenase, gamma-glutamyl transferase, total bilirubin and triglycerides were

TABLE 1 Hepatic mRNA expression of genes involved in pathogenic mechanisms of liver fibrosis showing 1.5-fold or greater regulation between control *Pttg1*^{+/+} (n = 4) and fibrotic *Pttg1*^{+/+} (n = 4) mice

Gene symbol	Fold regulation	Gene symbol	Fold regulation
Fibrosis			
<i>Acta2</i>	1.92**	<i>Bcl2</i>	2.35
<i>Grem1</i>	-2.35*	<i>Fasl</i>	1.78
Extracellular matrix and cell adhesion molecules			
<i>Col1a2</i>	4.72***	<i>Mmp9</i>	4.44**
<i>Col3a1</i>	3.79***	<i>Mmp13</i>	5.59
<i>Lox</i>	2.95	<i>Mmp14</i>	2.42
<i>Itga2</i>	2.38	<i>Plat</i>	7.52
<i>Itgb3</i>	1.57	<i>Plau</i>	4.50*
<i>Itgb5</i>	1.57	<i>Serpine1</i>	9.35
<i>Mmp1a</i>	4.54**	<i>Timp1</i>	2.84
<i>Mmp2</i>	8.51	<i>Timp2</i>	2.06
<i>Mmp3</i>	1.55	<i>Timp3</i>	1.86
<i>Mmp8</i>	4.55	<i>Timp4</i>	1.96
Inflammatory cytokines and chemokines			
<i>Ccl3</i>	7.58*	<i>Il1a</i>	2.98**
<i>Ccl11</i>	-1.75	<i>Il1b</i>	2.69*
<i>Ccr2</i>	4.35	<i>Il4</i>	-1.56
<i>Cxcr4</i>	3.44*	<i>Il5</i>	-1.61
<i>Ifng</i>	2.38	<i>Ilk</i>	1.53***
<i>Il10</i>	4.43*	<i>Tnf</i>	4.64*
<i>Il13ra2</i>	1.82		
Growth factors			
<i>Agt</i>	1.60**	<i>Egf</i>	1.73
<i>Ctgf</i>	-1.65	<i>Pdgfa</i>	1.72
<i>Edn1</i>	1.52	<i>Pdgfb</i>	2.43
Signal transduction			
<i>Cav1</i>	1.51	<i>Tgfb1</i>	2.04**
<i>Inhbe</i>	2.85	<i>Tgfb2</i>	2.67
<i>Myc</i>	2.69	<i>Tgfb3</i>	2.69
<i>Smad3</i>	1.83*	<i>Tgfb1</i>	1.79*
<i>Smad6</i>	2.17*	<i>Tgfb2</i>	2.37*
<i>Smad7</i>	1.91	<i>Thbs1</i>	3.01*
<i>Stat6</i>	1.69*	<i>Thbs2</i>	2.98*
Epithelial-to-mesenchymal transition			
<i>Akt1</i>	1.63		

Abbreviations: *mRNA* determined by *Acta2*, Alpha 2 smooth muscle actin; *Agt*, angiotensinogen; *Akt1*, AKT serine/threonine kinase 1; *Bcl2*, B-cell lymphoma 2; *Cav1*, caveolin 1; *Ccl3*, C-C Motif chemokine ligand 3; *Ccl11*, C-C motif chemokine ligand 11; *Ccr2*, C-C motif chemokine receptor 2; *Col1a2*, collagen type I Alpha 2 Chain; *Col3a1*, collagen type III Alpha 1 Chain; *Ctgf*, cellular communication network factor 2; *Cxcr4*, C-X-C motif chemokine receptor 4; *Edn1*, Endothelin 1; *Egf*, epidermal growth factor; *Fasl*, tumour necrosis factor receptor superfamily, member 6 Ligand; *Grem1*, Gremlin 1; *Ifng*, interferon gamma; *Il1a*, Interleukin 1 Alpha; *Il1b*, Interleukin 1 Beta; *Il4*, Interleukin 4; *Il5*, Interleukin 5; *Il10*, Interleukin 10; *Il13ra2*, Interleukin 13 Receptor Subunit Alpha 2; *Ilk*, Integrin Linked Kinase; *Inhbe*, Inhibin Subunit Beta E; *Itga2*, Integrin Subunit Alpha 2; *Itgb3*, Integrin Subunit Beta 3; *Itgb5*, Integrin Subunit Beta 5; *Lox*, Lysyl Oxidase; *Mmp1a*, Matrix Metalloproteinase 1a; *Mmp2*, matrix metalloproteinase 2; *Mmp3*, matrix metalloproteinase 3; *Mmp8*, matrix metalloproteinase 8; *Mmp9*, matrix metalloproteinase 9; *Mmp13*, matrix metalloproteinase 13; *Mmp14*, matrix metalloproteinase 14; *Myc*, MYC proto-oncogene, BHLH transcription factor; *Pdgfa*, platelet-derived growth factor subunit A; *Pdgfb*, platelet-derived growth factor subunit B; *Plat*, plasminogen activator, tissue type; *Plau*, plasminogen activator, Urokinase; *Serpine1*, serpin family E member 1; *Smad3*, SMAD family member 3; *Smad6*, SMAD family member 6; *Smad7*, SMAD family member 7; *Stat6*, signal transducer and activator of transcription 6; *Tgfb1*, transforming growth factor-beta 1; *Tgfb2*, transforming growth factor-beta 2; *Tgfb3*, transforming growth factor-beta 3; *Tgfb1*, transforming growth factor-beta receptor 1; *Tgfb2*, transforming growth factor-beta receptor 2; *Thbs1*, thrombospondin 1; *Thbs2*, thrombospondin 2; *Timp1*, tissue inhibitor of metalloproteinase 1; *Timp2*, tissue inhibitor of metalloproteinase 2; *Timp3*, tissue inhibitor of metalloproteinase 3; *Timp4*, tissue inhibitor of metalloproteinase 4; *Tnf*, tumour necrosis factor.

P* < 0.05; *P* < 0.01; ****P* < 0.001 vs control WT mice. Unpaired Student's *t* test.

found to be near normal. Overall, these results support the protective effects on hepatic function resulting from *Pttg1* mRNA silencing in rats with experimental fibrosis.

4 | DISCUSSION

This investigation aimed to explore whether *PTTG1/DLK1* signalling contributes to the activation of the fibroproliferative process in liver disease. In agreement with previous studies, *Pttg1* mRNA was almost undetectable in healthy animals. In contrast, *Pttg1* mRNA levels were markedly overexpressed in the liver of rats with hepatic fibrosis, reaching maximal abundance in cirrhotic rats. Moreover, only hepatic tissue of cirrhotic rats showed a significantly increased abundance of *Pttg1* mRNA with respect to control animals. Paralleling *Pttg1* results, *Dlk1* mRNA expression markedly increased in fibrotic rats, with a close correlation with collagen deposition. *Dlk1* transcript was also selectively overexpressed only in the liver. In addition, liver *DLK1* protein levels mirrored expression patterns of the cognate transcript. The lowest abundance was found in rats with mild fibrosis and the highest in cirrhotic rats. This clearly differs from the behaviour of other profibrogenic factors. Cell fractionation experiments showed increased *Pttg1* and *Dlk1* mRNA in HEP, HSCs and endothelial cells (ECs) in liver tissue of cirrhotic rats compared to controls. Furthermore, *PTTG1* and *DLK1* protein

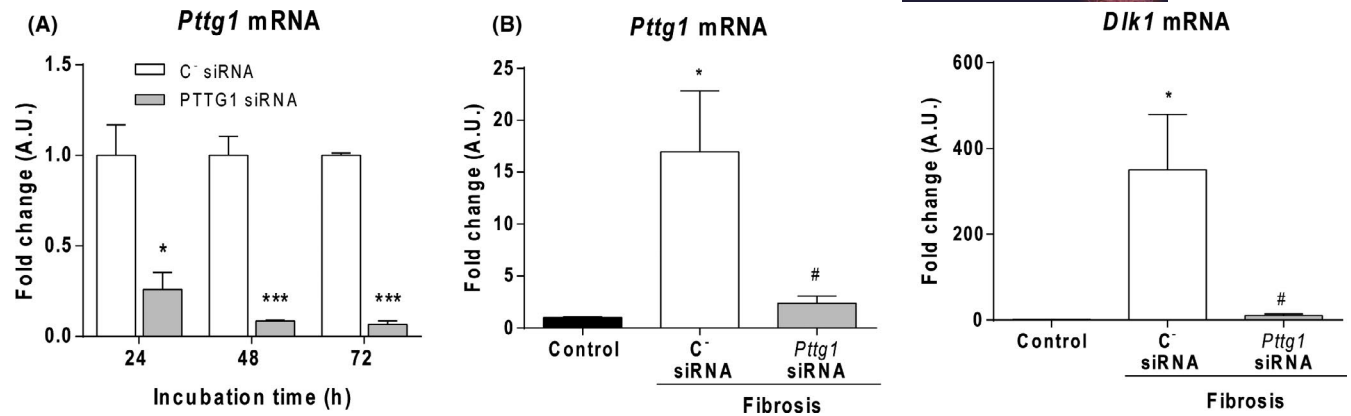


FIGURE 5 Effect of *Pttg1* siRNA on *Pttg1* and *Dlk1* expression. A, mRNA expression of *Pttg1* in CC-1 cells transfected with C⁻ siRNA or *Pttg1* siRNA for 24, 48 and 72 h. Results are expressed as mean \pm SE. * $P < 0.05$, *** $P < 0.001$ vs C⁻ siRNA. One-way ANOVA with Newman-Keuls post hoc test. B, mRNA expression of *Pttg1* and *Dlk1* in liver tissue of control ($n = 6$) and fibrotic rats treated with C⁻ siRNA ($n = 6$) or *Pttg1* siRNA ($n = 6$). * $P < 0.05$ vs C⁻ siRNA; # $P < 0.05$ vs *Pttg1* siRNA. Kruskal-Wallis test with Dunn post hoc test

staining in cirrhotic rats resulted in an intense, although topologically undefined, positive signal in the hepatic parenchyma, being more pronounced close to the portal tracts. Finally, on exploring the expression of *PTTG1/DLK1* in the human liver we also observed that, whereas control livers showed negligible *PTTG1* or *DLK1* mRNA expression, samples from cirrhotic patients markedly overexpressed *PTTG1* mRNA. To our knowledge, this is the first investigation demonstrating *PTTG1* mRNA induction in human cirrhosis. In parallel, *DLK1* was also increased in human samples in line with previous investigations showing that *DLK1* is frequently upregulated in human HCC but rarely detected in adjacent non-cancerous liver tissue.²⁸ Overall, our findings indicate that the *PTTG1/DLK1* pathway is relevant in the pathogenesis of liver fibrosis. This contention was further supported by results obtained in *Pttg1* KO mice. Previous investigations performed in thioacetamide-induced fibrosis showed significantly weaker macromorphological signs of bridging fibrosis in *Pttg1*^{-/-} in comparison to *Pttg1*^{+/+} mice.²⁹ This finding was further confirmed in the current study in CCl₄-treated mice, indicating that the lack of *Pttg1* attenuates the development of murine liver fibrosis. Subsequent gene expression analysis pointed toward disruption of ECM turnover as a major driver of this phenomenon. In fact, stringent analysis of alterations in gene expression induced by *Pttg1*^{-/-} in fibrotic animals, considering only those genes showing both statistically and biologically significant downregulation, revealed a group of genes all involved in fibrogenesis including *Mmp9*, *Mmp8*, *Timp4* and *Acta2*. Of interest, this occurred in the setting of diminished *Myc* mRNA expression, which encodes a nuclear phosphoprotein that regulates the transcription of numerous genes involved in the cell cycle, cell growth, differentiation, apoptosis, transformation, genomic stability and angiogenesis.³⁰ Moreover, *Pttg1* is a powerful activator of *Myc*,³¹ which suggest that this gene could play a central role in *PTTG1* induced fibrosis signalling pathway.

Our findings suggest that RNA-based therapy targeting *Pttg1*, such as siRNA, may prevent the development of liver fibrosis. siRNA-*Pttg1*-treated rats displayed significantly weaker macromorphological

signs of liver fibrosis, a decrease in portal hypertension and a lesser amount of activated HSC. These results suggest that a reduction in the proportion of activated HSC is involved in the inhibition of liver fibrogenesis. Amelioration in portal pressure is most likely a consequence of the antifibrotic effect induced by *Pttg1* siRNA administration. These results are also supported by a lower abundance of liver *Col1a2* and *Col3a1* mRNAs and some other markers of active fibrosis such as *Tgfb β 1* and *Pdgfr β* . It has been reported that interference of *PTTG1* in ovarian epithelial tumour cells resulted in diminished expression and release of TGF β , whereas increased expression of *Pttg1* mRNA mirrored *Tgfb β* mRNA expression.³² In our study *Pttg1* mRNA interference tended towards lower levels of *Tgfb β 1*, although without statistical significance. This is consistent with previous reports in fibrotic *Pttg1* null mice in which hepatic *Tgfb β* mRNA was significantly lower than in the liver of WT mice.²⁹

Pttg1 mRNA interference in fibrotic rats also downregulated hepatic expression of the PDGF receptor, *Pdgfr β* . Specific blockade of the intrahepatic PDGFR β pathway with adenoviral vectors in CCl₄-induced fibrosis rats³³ or systemic PDGF antagonism in bile duct ligated rats led to significantly reduced hepatic fibrosis.³⁴ Considering that PDGF is the most potent pro-proliferative cytokine for HSCs^{35,36} reduced fibrosis observed after *Pttg1* mRNA interference treatment likely is a consequence of blockade of HSC proliferation and inhibition of chemotaxis, which thereby decreases the number of cells able to synthesize ECM proteins.

Administration of *Pttg1* siRNA to fibrotic rats also affects the regulation of ECM remodelling. In experimental and human cirrhosis, fibrosis appears to be the result of not only excessive ECM synthesis but also reduced degradation.^{37,38} Fibrotic rats receiving C⁻ siRNA presented a marked induction of *Col1a2* and *Col3a1* gene expression as well as a significant upregulation of *Mmp2* and *Mmp9* which can be the result of a compensatory mechanism designed to eliminate the excess of scar tissue. In our study, treatment with *Pttg1* siRNA was also associated with a significant increase in the MMPs/TIMPs ratio. This could be due to preferential *Timp1* and *Timp2* inhibition,

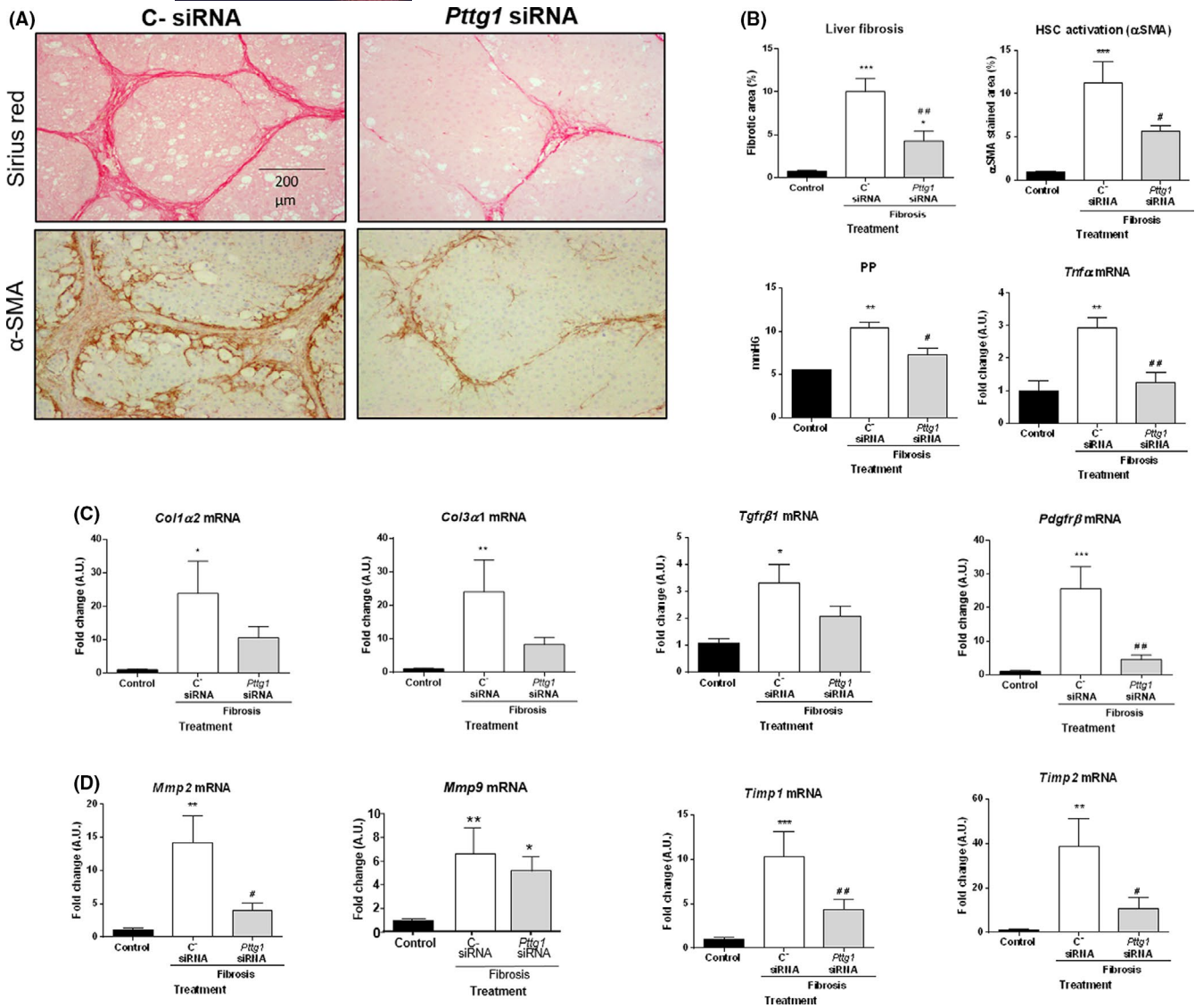


FIGURE 6 Effect of *Pttg1* blockade on fibrosis progression. Control (n = 6) and fibrotic rats receiving C-siRNA (n = 6) or *Pttg1* siRNA (n = 6). A, Sirius red and α -SMA stainings (100x). B, Quantitative measurement of relative fibrosis and α -SMA positive area, portal pressure and *Tnf α* mRNA. C, Hepatic messenger expression of *Col1 α 2*, *Col3 α 1*, *Tgfr β 1* and *Pdgfr β* . D, Hepatic *Mmp2*, *Mmp9*, *Timp1* and *Timp2* mRNA expression. Results are given as mean \pm SE. * P < 0.05, ** P < 0.01, *** P < 0.001 vs control; # P < 0.05, ## P < 0.01 vs C-siRNA treated rats. One-way ANOVA with Newman-Keuls post hoc test or the Kruskal-Wallis test with Dunn post hoc test

thereby supporting the concept that PTTG1 activity is a regulator of the ECM degradation pattern in the injured liver mainly by controlling TIMPs activity.

Interestingly, we also observed a tendency towards normalization of most surrogate liver function serum markers. However, this was not the case with transaminases. This finding, previously documented in null *Pttg1* fibrotic mice,²⁹ indicates that *Pttg1* mRNA interference has no effect on CCl₄-induced hepatotoxicity and further supports the concept that *Pttg1* deficiency directly interferes with fibrosis.

Several potential mechanisms mediate the effects of *Pttg1* knock-down on hepatic fibrosis. First, the *Pttg1* blockade prevents hepatic *Dlk1* overexpression. *Pttg1* acts as a post-transcriptional regulator of *Dlk1*,¹⁹ and *Dlk1* inhibition results in reduced HSC activation and

associated fibrosis.³⁹ The decrease of *Dlk1* expression mediated by *Pttg1* downregulation was associated with a significant reduction in activation of HSC, suggesting that PTTG1/DLK1 pathway plays a pivotal role in the hepatic fibroproliferative process. On the other hand, both *Pttg1* and *Dlk1* share common regulatory mechanisms in which histone deacetylases (HDAC) are involved. Actually, HDAC1 expression has been shown to be responsible for the proliferation of corticotroph cells via *Pttg1*,⁴⁰ whereas HDAC3 activity represses *Dlk1* expression in preadipocytes and NIH 3 T3 cells.⁴¹ Second, *Pttg1* is involved in the regulation of ECM turnover key proteins. Experimental evidence indicates that *Pttg1* is a major regulator of *Mmp2* by inducing its secretion and expression.⁹ MMP2 plays an important role in remodelling basement membranes as it degrades several components including collagen IV, laminin and fibronectin.³⁸ The present study shows that *Mmp2*

TABLE 2 Serum markers of liver function in control rats and fibrotic rats treated with C⁻ or Pttg1 siRNAs

	Fibrosis		
	Control (n = 6)	C ⁻ siRNA (n = 6)	Pttg1 siRNA (n = 6)
Alanine transaminase (U/L)	43 ± 6	1069 ± 356 [*]	1226 ± 385 [*]
Aspartate transaminase (U/L)	56 ± 11	2342 ± 561 ^{**}	924 ± 235
Lactate dehydrogenase (U/L)	356 ± 27	1197 ± 224 [*]	349 ± 49
Gamma-glutamyl transferase (U/L)	0.03 ± 0.03	5.38 ± 1.68 ^{**}	2.40 ± 1.10
Total bilirubin (mg/dL)	0.00 ± 0.00	1.08 ± 0.32 ^{***}	0.22 ± 0.12
Total proteins (g/L)	49.7 ± 2.2	41.0 ± 3.0 [*]	44.5 ± 1.8
Albumin (g/L)	27.6 ± 1.8	23.9 ± 1.9	27.0 ± 2.1
Total cholesterol (mg/dL)	55.4 ± 9.9	68.29 ± 8.39	50.80 ± 6.43
Triglycerides (mg/dL)	4.34 ± 1.03	57.5 ± 12.7 ^{**}	33.0 ± 7.7
Glucose (mg/dL)	207 ± 36	73 ± 23 [*]	91 ± 21

One-way ANOVA with the Newman-Keuls post hoc test or the Kruskal-Wallis test with the Dunn post hoc test when appropriate. Results are given as mean ± SE.

P* < 0.05; *P* < 0.01; ****P* < 0.001 vs control.

expression increases in liver fibrosis, however, Pttg1 interference may have an antifibrogenic effect also by reducing Mmp2 expression and, consequently, by blocking degradation of normal perisinusoidal matrix and promoting activation of quiescent HSC.⁴² In this study, we also observed that Pttg1 blocking reduced TIMPs expression. Timp1 and Timp2 are mainly expressed in activated HSC, thus, Timp1 and Timp2 expression could be reduced as a result of diminished HSC activation in these animals. TIMPs also stimulate fibroblast proliferation.⁴³ Thus, Timp1 and Timp2 downregulation could also contribute to decreased proliferation of activated HSC. A graphical model summarizing the proposed mechanism underlying PTTG1-induced promotion of liver fibrosis is provided in the supplementary information section.

In conclusion, this investigation shows that serial administration of Pttg1 siRNA exerts antifibrotic effects when administered during induction of hepatic damage. Pttg1 gene silencing normalizes expression of Dlk1, arrests activation of HSC, diminishes expression of ECM-related genes and finally decreases hepatic collagen deposition and reduces portal hypertension. Thus, the PTTG1/DLK1 axis may represent a valuable target for the prevention and treatment of liver fibrosis.

CONFLICT OF INTEREST

The authors declare no competing interests. Dr Bruix consults for, advises, and is on the speakers' bureau and received grants from Bayer-Shering and BTG. He consults for and advises MSD. He consults for and is on the speakers' bureau for Sirtex. He consults for and received grants from Arqule and Ipsen. He consults for Novartis, Bristol-Myers Squibb, Eisai, Kowa, Terumo, Gilead, Bio Alliance, Roche, AbbVie, Merck, AstraZeneca, Incyte, Quirem, Adaptimmune and Lilly.

ETHICAL APPROVAL

All animal procedures and human samples were approved by the Investigation and Ethics Committee of the Hospital Clinic and Animal Experimentation Committee of the University of Barcelona (Barcelona,

Spain). Human samples have consented for research in accordance with ethical guidelines of the 1975 Declaration of Helsinki.

DATA AVAILABILITY STATEMENT

The data that support the findings of this study are available from the corresponding author upon reasonable request.

ORCID

Meritxell Perramón  <https://orcid.org/0000-0002-1944-8337>

Loreto Boix  <https://orcid.org/0000-0002-6015-3901>

Pedro Melgar-Lesmes  <https://orcid.org/0000-0002-2009-5911>

Shlomo Melmed  <https://orcid.org/0000-0002-2355-3447>

Wladimiro Jiménez  <https://orcid.org/0000-0002-9376-0214>

REFERENCES

- Neef M, Ledermann M, Saegesser H, et al. Oral imatinib treatment reduces early fibrogenesis but does not prevent progression in the long term. *J Hepatol.* 2006;44(1):167-175.
- Teixeira-Clerc F, Julien B, Grenard B, et al. CB1 cannabinoid receptor antagonism: a new strategy for the treatment of liver fibrosis. *Nat Med.* 2006;12(6):671-676.
- Bataller R, Sancho-Bru P, Ginés P, Brenner DA. Liver fibrogenesis: a new role for the renin-angiotensin system. *Antioxid Redox Signal.* 2005;7:1346-1355.
- Krenkel O, Puengel T, Govaere O, et al. Therapeutic inhibition of inflammatory monocyte recruitment reduces steatohepatitis and liver fibrosis. *Hepatology.* 2018;67(4):1270-1283.
- Pei L, Melmed S. Isolation and characterization of a pituitary tumor-transforming gene (PTTG). *Mol Endocrinol.* 1997;11(4):433-441.
- Cho-Rok J, Yoo J, Jang YJ, et al. Adenovirus-mediated transfer of siRNA against PTTG1 inhibits liver cancer cell growth in vitro and in vivo. *Hepatology.* 2006;43(5):1042-1052.
- Vlotides G, Chen YH, Eigler T, Ren SG, Melmed S. Fibroblast growth factor-2 autocrine regulation in pituitary Folliculostellate TtT/GF cells. *Endocrinology.* 2009;150(7):3252-3258.
- Li H, Yin C, Zhang B, et al. PTTG1 promotes migration and invasion of human non-small cell lung cancer cells and is modulated by miR-186. *Carcinogenesis.* 2013;34(9):2145-2155.

9. Yan H, Wang W, Dou C, Tian F, Qi S. Securin promotes migration and invasion via matrix metalloproteinases in glioma cells. *Oncol Lett*. 2015;9(6):2395-2901.
10. Chen PY, Yen JH, Kao RH, Chen JH. Down-regulation of the oncogene PTTG1 via the KLF6 tumor suppressor during induction of myeloid differentiation. *PLoS One*. 2013;8:e71282.
11. Zimmermann EM, Sartor RB, McCall RD, Pardo M, Bender D, Lund PK. Insulin-like growth factor 1 and interleukin 1 messenger RNA in a rat model of granulomatous enterocolitis and hepatitis. *Gastroenterology*. 1993;105(2):399-409.
12. Jin-no K, Tanimizu M, Hyodo I, Kurimoto F, Yamashita T. Plasma level of basic fibroblast growth factor increases with progression of chronic liver disease. *J Gastroenterol*. 1997;32(1):119-121.
13. Rosmorduc O, Wendum D, Corpechot C, et al. Hepatocellular hypoxia-induced vascular endothelial growth factor expression and angiogenesis in experimental biliary cirrhosis. *Am J Pathol*. 1999;155(4):1065-1073.
14. Sinclair M, Gow PJ, Angus PW, et al. High circulating oestrone and low testosterone correlate with adverse clinical outcomes in men with advanced liver disease. *Liver Int*. 2016;36(11):1619-1627.
15. Koi M, Boland CR. Tumor hypoxia and genetic alterations in sporadic cancers. *J Obstet Gynaecol Res*. 2011;37(2):85-98.
16. Abbud RA, Takumi I, Barker EM, et al. Early multipotential pituitary focal hyperplasia in the α -subunit of glycoprotein hormone-driven pituitary tumor-transforming gene transgenic mice. *Mol Endocrinol*. 2005;19(5):1383-1391.
17. Ishikawa H, Heaney AP, Yu R, Horwitz GA, Melmed S. Human pituitary tumor-transforming gene induces angiogenesis. *J Clin Endocrinol Metab*. 2001;86(2):867-874.
18. Akino K, Akita S, Mizuguchi T, et al. A novel molecular marker of pituitary tumor transforming gene involves in a rat liver regeneration. *J Surg Res*. 2005;129(1):142-146.
19. Espina AG, Méndez-Vidal C, Moreno-Mateos MA, et al. Induction of Dlk1 by PTTG1 inhibits adipocyte differentiation and correlates with malignant transformation. *Mol Biol Cell*. 2009;20(14):3353-3362.
20. Smas CM, Chen L, Sul HS. Cleavage of membrane-associated pref-1 generates a soluble inhibitor of adipocyte differentiation. *Mol Cell Biol*. 1997;17:977-988.
21. Rodríguez P, Higuera MA, González-Rajal A, et al. The non-canonical NOTCH ligand DLK1 exhibits a novel vascular role as a strong inhibitor of angiogenesis. *Cardiovasc Res*. 2012;93(2):232-241.
22. Falix FA, Tjon-A-Loi MRS, Gaemers IC, Aronson DC, Lamers WH. DLK1 protein expression during mouse development provides new insights into its function. *ISRN Developmental Biology*. 2013;2013:1-10. <https://doi.org/10.1155/2013/628962>
23. Clària J, Jiménez W. Experimental models of cirrhosis and ascites. In: Arroyo V, Ginés P, Rodés J, Schrier RW, eds. *Ascites and Renal Dysfunction in Liver Disease: Pathogenesis Diagnosis and Treatment*. 2nd edition. Blackwell Science Inc; 2005:215-226.
24. Wang Z, Yu R, Melmed S. Mice lacking pituitary tumor transforming gene show testicular and splenic hypoplasia, thymic hyperplasia, thrombocytopenia, aberrant cell cycle progression, and premature centromere division. *Mol Endocrinol*. 2001;15(11):1870-1879.
25. Karagiannis GS, Musrap N, Saraon P, et al. Bone morphogenetic protein antagonist gremlin-1 regulates colon cancer progression. *Biol Chem*. 2015;396(2):163-183.
26. Tacke F, Trautwein C, Yagmur E, et al. Up-regulated eotaxin plasma levels in chronic liver disease patients indicate hepatic inflammation, advanced fibrosis and adverse clinical course. *J Gastroenterol Hepatol*. 2007;22(8):1256-1256, 1264.
27. Hemmann S, Graf J, Roderfeld M, Roeb E. Expression of MMPs and TIMPs in liver fibrosis – a systematic review with special emphasis on anti-fibrotic strategies. *J Hepatol*. 2007;46(5):955-975.
28. Huang J, Zhang X, Zhang M, et al. Up-regulation of DLK1 as an imprinted gene could contribute to human hepatocellular carcinoma. *Carcinogenesis*. 2006;28(5):1094-1103. <https://doi.org/10.1093/carcin/bgl215>
29. Buko V, Belonovskaya E, Naruta E, et al. Pituitary tumor transforming gene as a novel regulatory factor of liver fibrosis. *Life Sci*. 2015;132:34-40.
30. Chakravorty D, Jana T, Das Mandal S, Seth A, Bhattacharya A, Saha S. MYCbase: a database of functional sites and biochemical properties of Myc in both normal and cancer cells. *BMC Bioinform*. 2017;18:224.
31. Pei L. Identification of c-myc as a down-stream target for pituitary tumor-transforming gene. *J Biol Chem*. 2001;276(11):8484-8491.
32. Shah PP, Kakar SS. Pituitary tumor transforming gene induces epithelial to mesenchymal transition by regulation of twist, snail, slug, and E-cadherin. *Cancer Lett*. 2011;311(1):66-76.
33. Reichenbach V, Fernández-Varo G, Casals G, et al. Adenoviral dominant-negative soluble PDGFR β improves hepatic collagen, systemic hemodynamics, and portal pressure in fibrotic rats. *J Hepatol*. 2012;57(5):967-973.
34. Borkham-Kamphorst E, Herrmann J, Stoll D, Treptau J, Gressner AM, Weiskirchen R. Dominant-negative soluble PDGF-b receptor inhibits hepatic stellate cell activation and attenuates liver fibrosis. *Lab Invest*. 2004;84(6):766-777.
35. Pinzani M. PDGF and signal transduction in hepatic stellate cells. *Front Biosci* 2002; 7:1720-1726.16.
36. Friedman SL. Mechanisms of hepatic fibrogenesis. *Gastroenterology*. 2008;134(6):1655-1669.
37. Arthur MJP. Fibrogenesis II. Metalloproteinases and their inhibitors in liver fibrosis. *American Journal of Physiology-Gastrointestinal and Liver Physiology*. 2000;279(2):G245-G249. <https://doi.org/10.1152/ajpgi.2000.279.2.g245>
38. Murphy G, Cockett MI, Ward RV, Docherty AJP. Matrix metalloproteinase degradation of elastin, type I collagen and proteoglycans. *Biochem J*. 1991;277:277-279.
39. Pan RL, Wang P, Xiang LX, Shao JZ. Delta-like 1 serves as a new target and contributor to liver fibrosis down-regulated by mesenchymal stem cell transplantation. *J Biol Chem*. 2011;286(14):12340-12348.
40. Hagiwara R, Kageyama K, Niioka K, Takayasu S, Tasso M, Daimon M. Involvement of histone deacetylase 1/2 in adrenocorticotrophic hormone synthesis and proliferation of corticotroph tumor AtT-20 cells. *Peptides*. 2021;136:170441.
41. Li D, Yea S, Li S, et al. Krüppel-like factor-6 promotes preadipocyte differentiation through histone deacetylase 3-dependent repression of DLK1. *Journal of Biological Chemistry*. 2005;280(29):26941-26952. <https://doi.org/10.1074/jbc.m500463200>
42. Alcolado R, Arthur MJP, Iredale JP. Pathogenesis of liver fibrosis. *Clin Sci*. 1997;92(2):103-112.
43. Madtes DK, Elston AL, Kaback LA, Clark JG. Selective induction of tissue inhibitor of metalloproteinase-1 in bleomycin-induced pulmonary fibrosis. *Am J Respir Cell Mol Biol*. 2001;24(5):599-607.

SUPPORTING INFORMATION

Additional supporting information may be found in the online version of the article at the publisher's website.

How to cite this article: Perramón M, Carvajal S, Reichenbach V, . The pituitary tumour-transforming gene 1/ delta-like homologue 1 pathway plays a key role in liver fibrogenesis. *Liver Int*. 2022;00:1-12. doi: [10.1111/liv.15165](https://doi.org/10.1111/liv.15165)

**THE PITUITARY TUMOR-TRANSFORMING GENE 1 (PTTG1) / DELTA LIKE
HOMOLOG 1 (DLK1) PATHWAY PLAYS A KEY ROLE IN LIVER
FIBROGENESIS**

Meritxell Perramón, Silvia Carvajal, Vedrana Reichenbach, Guillermo Fernández-Varo, Loreto Boix, Laura Macias-Muñoz, Pedro Melgar-Lesmes, Jordi Bruix, Shlomo Melmed, Santiago Lamas, Wladimiro Jiménez

Table of contents

Supplementary Materials & methods.....	2
Supplementary graphical model	13
Supplementary Table 1	15
References	16

Supplementary Materials & methods

Mouse genotyping. Mouse genomic DNA was isolated from ear biopsies using a specific kit (Extract-N-Amp™ Tissue PCR Kit; Sigma-Aldrich, Darmstadt, Germany). PCR was performed using the primer pairs to amplify the *Pttg1* gene (primer forward: 5'-GTGCTACTTCCATTTGTCACGTCC-3' and primer reverse: 5'-TTAGCTGTGAGCTCGTCCGGTG-3') and other primer pairs in order to verify the disruption of the *Pttg1* gene (primer forward: 5'-TAGGCTTTTCGGCAACTCTGTTGAC-3' and primer reverse: 5'-TTCTGGGGACTGAATTCAGG-3'). The PCR conditions were as follows: 38 cycles at 94 °C for 30 s, 58 °C for 1 min, and 72°C for 1 min 40 s. PCR products were electrophoresed in 1.5 % agarose 1x TAE (40 mM Tris, 20 mM acetic acid and 1 mM ethylenediaminetetraacetic acid) gels. For visualization, gels were stained with 1xSYBR® Safe DNA Gel Stain (Life Technologies) and digital images were captured in ImageQuant™ LAS 4000 to distinguish the WT (220 bp) and *Pttg1* KO (700 bp) mice.

Messenger expression of *Dlk1* and fibrosis gene expression PCR array in the liver of *Pttg1* KO mice. Total RNA of control WT (n=4), fibrotic WT (n=4), and fibrotic *Pttg1* KO (n=4) mice was extracted using a RNA extraction column kit (RNAeasy, Qiagen, Venlo, The Netherlands). RNA concentrations were determined by spectrophotometric analysis (ND-100 spectrophotometer; Thermo Fisher Scientific, Waltham, MA, USA). First strand cDNA was synthesized from 500 ng of total RNA using a RT² First Strand Kit (Qiagen). Primers and probes for gene expression assays (Applied Biosystems) were selected as follows: *Dlk1* (Taqman assay reference from Applied Biosystems: Mm00494477_m1) and *Hprt* used as an endogenous standard

(Mm03024075_m1). Expression assays were designed using the Taqman Gene Expression assay software (Applied Biosystems). RT-PCR was analyzed in duplicate and performed with a Lightcycler-480 II (Roche Diagnostics). Real-time PCR arrays were performed using the RT² Profiler™ PCR Array Mouse Fibrosis (Qiagen). All procedures were performed according to the manufacturer's protocol. This PCR array combines the quantitative performance of SYBR Green-based Real-time PCR with the multiple gene profiling capabilities of microarrays to profile the expression of 86 key genes involved in fibrogenic processes. PCR array plates were processed in a Light Cycler 480 (Roche Diagnostics) using automated baseline and threshold cycle detection. Gene expression was normalized to internal controls to determine the fold change in gene expression between test and control samples. The relative quantity of the product was expressed as fold-induction of the target gene compared with the reference gene according to the formula $2^{-\Delta\Delta CT}$. Data were interpreted using the SABiosciences web-based PCR array data analysis tool (<http://pcrdataanalysis.sabiosciences.com/pcr/arrayanalysis.php>).

Hemodynamic measurements. Rats were anesthetized with Inactin® (100 mg/kg bwt, Sigma-Aldrich Chemie GmbH, Steinherim, Germany) and prepared with a PE-50 polyvinyl catheter in the left femoral artery. A blood sample (1 ml) was obtained from each animal to analyze standard biochemistry tests. A midline abdominal incision (2 cm) was made and the portal vein was cannulated through an ileocolic vein with a PE-50 catheter to measure PP. After verifying free blood reflux, the catheter was fixed to the mesentery with cyanoacrylate glue. Hemodynamic parameters were recorded in a multichannel system (PowerLab®, ADInstruments, Sydney, Australia). Hemodynamic

parameters were allowed to equilibrate for 30 min and values of MAP and PP were recorded over two time periods of 10 min. Each value represents the average of 2 measurements.

Fibrosis quantification. Liver sections (4 μm) were stained in 0.1 % Sirius red F3B (Sigma-Aldrich, St. Louis, MO, USA) in saturated picric acid (Sigma-Aldrich). Sirius red selectively binds collagen proteins and was used to stain collagen fibrils in the liver of CCl_4 -treated rats (1). The relative fibrotic area, expressed as a percentage of total liver area, was assessed by analyzing 32 fields of Sirius red-stained liver sections per animal as previously described (2). Each field was acquired at 100X magnification with an E600 microscope (Nikon, Tokyo, Japan) and a RT-Slider Spot digital camera (Diagnostic Instruments, Sterling Heights, MI, USA). Results were analyzed using imaging software (ImageJ, NIH). To evaluate the relative fibrosis area, the collagen area measured was divided by the net field area and then multiplied by 100. Subtraction of the vascular luminal area from the total field area yielded the net fibrosis area.

Liver cell fractionation. Primary hepatocytes, liver endothelial cells (EC), and HSCs were freshly isolated from the livers of control (n= 2) and cirrhotic (n= 2) adult male Wistar rats. Animals were euthanized by isoflurane overdose and the liver was perfused through the portal vein using a peristaltic pump at a flow rate of 14 ml/min, first with pre-warmed washing buffer (1 % HEPES- Hanks' balanced salt solution, 1 mM EGTA) and then, with a pre-warmed perfusion buffer (1 % HEPES- HBSS, 2.5 mM CaCl_2 , 0.5 mg/ml collagenase). In order to allow outflow of the solutions, the cava vein was cut. After perfusion, the liver was excised, cut and placed in a pre-warmed digestion

solution (1 % HEPES- HBSS, 2.5 mM CaCl₂, 0.05 mg/ml collagenase, 0.03 mg/ml DNase) for 5 min in a water bath at 37 °C. Digested tissue was filtered through a 100 µm cell strainer to eliminate undigested tissue remnants and cell suspension was centrifuged at 70 g for 1 min at 4 °C. The supernatant contained non-parenchymal cells (NPC), whereas hepatocytes were found in the pellet. HSCs were purified from the NPC fraction after 14 % Nycodenz gradient (Sigma-Aldrich). Following centrifugation at 2500 rpm without brake for 15 min at room temperature, two interphases were obtained. The upper interphase was enriched in HSC and the lower interphase contained polymorphonuclear cells and EC. The lower interphase was seeded in petri dishes and incubated for 35 min in a humid 5 % CO₂ atmosphere in order to enhance EC purity by selective adherence time of PMN.

Immunodetection of α-SMA, PTTG1 and DLK1. Liver sections from fibrotic rats underwent microwave antigen retrieval to unmask antigens hidden by cross-linkage occurring during tissue fixation. Endogenous peroxidase activity was blocked by hydrogen peroxide pretreatment for 10 min and with 5 % goat serum for 45 min. The sections were then stained with mouse anti-α-SMA (1:1200; Dako Denmark A/S, Glostrup, Denmark), rabbit anti-DLK1 (1/250 Abcam, Milton, Cambridge, UK), or rabbit anti-PTTG1 (1/100 Invitrogen, Waltham, Massachusetts, USA) and the first was incubated for 1 h at room temperature and the two latter were incubated overnight at 4 °C. The LSAB 2 System-HRP (Dako Denmark A/S) was used for antigen detection and antigen visualization was achieved with streptavidin peroxidase and counterstained with hematoxylin. As negative controls, immunostaining was performed without the first antibody. The area of positive staining was visualized using a digital

microscope (Eclipse E600; Nikon, Tokyo, Japan) in 16 random fields per animal. The percentage of immunostained α -SMA/fields areas of digital photomicrographs was then quantified.

Western Blot Analysis of DLK1, TGF β , TNF α and All. Hepatic tissue from fibrotic and control rats was individually homogenized as described previously (2). To detect DLK1, TGF β , TNF α and All, 40 μ g of total denatured proteins were loaded on a 10 % (DLK1) and 12 % (TGF β , TNF α and All) SDS-polyacrylamide gel (Mini-PROTEAN III; Bio-Rad Laboratories, Hercules, CA). Gels were transferred for 2 h at 4 °C to nitrocellulose membranes of 0.45 μ m for DLK1, All and TNF α , and to 0.2 μ m for TGF β , which were stained with Ponceau S Red as a control for protein loading. Thereafter, membranes were blocked with 5 % non-fat milk for TGF β and All and with 5 % and 1 % bovine serum albumin for TNF α and DLK1, respectively, in TTBS buffer at room temperature for 2 h. Then, they were incubated overnight at 4 °C with rabbit monoclonal anti-DLK1 (1:1000 dilution; Abcam, Cambridge, UK), polyclonal anti-TGF β , (1:1000 dilution; Abcam, Cambridge, UK), polyclonal anti-All (1/500 Santa Cruz, Dallas, TX) or polyclonal anti-TNF α antibodies (1/1000 dilution; Cell Signaling Technology, Danvers, MA), followed by incubation with a donkey anti-rabbit horseradish peroxidase-conjugated secondary antibody (1:2000; Amersham Biosciences, GE Healthcare, Piscataway, NJ, USA). The bands were visualized by chemiluminescence (Luminata Forte Western HRP substrate; EMD Millipore, Billerica, MA, USA).

Antibody	Catalog number	Brand
Anti-DLK	ab21682	Abcam

Anti-All	sc-20718	Santa Cruz Biotechnology INC
Anti-TNF alpha	3707	Cell Signaling Technology
Anti-TGF beta	ab66043	Abcam

Messenger expression of PTTG1, DLK1 and COL1 α 1 in human liver tissue. To assess whether *PTTG1* mRNA is over expressed in human fibrotic liver, this parameter as well as *COL1 α 1* and *DLK1* mRNA were assessed in a group of 12 samples obtained by liver resection from patients with cirrhosis associated with hepatitis C virus infection. In addition, we analyzed liver biopsies from 7 non-cirrhotic patients. Non-cirrhotic samples were obtained from fragments of colon metastatic resections before vascular clamping. Patients provided written informed consent for medical research according to the principles of the Declaration of Helsinki. Total RNA was extracted as previously described and 1 μ g of total RNA was reverse transcribed using a complementary DNA synthesis kit (High-Capacity cDNA Reverse Transcription Kit, Applied Biosystems, Foster City, CA). The primers and probes for human *PTTG1* (*probe#22* left: 5'-GCCTCTCATGATCCTTGACG-3', right: 5'-GCTTGAAGGAGACTGCAACA-3'), *DLK1* (*probe#68* left: 5'-GACGGGGAGCTCTGTGATAG-3', right: 5'-TCATAGAGGCCATCGTCCA-3'), *COL1 α 1* (*probe#* left: 5'-AATCCTCGAGCACCTGA-3' right: 5'-CCCCTGGAAAGAATGGAGAT-3'), and hypoxanthine-guanine phosphoribosyltransferase (*HPRT*), used as an endogenous standard (*probe#73* left: 5'-TGACCTTGATTTATTTTGCATACC-3', right: 5'-CGAGCAAGACGTTTCAGTCCT-3') were designed according to human *PTTG1*,

DLK1, *COL1 α 1* and *HPRT* sequences (GenBank NM_001282382.1, NM_003836.6, NM_000088.4. and NM_000194.2, respectively).

Cell culture and treatments. CC-1 cells, an adult rat hepatocyte cell line (3), were a generous gift from Dr. J. Clària. Cells were grown at 37 °C in a 5 % CO₂ atmosphere in Eagle's minimum essential medium media supplemented with 2 mM of glutamine, 1 % nonessential amino acids, penicillin (50 U/ml), streptomycin (50 µg/ml), 20 mM HEPES and 10 % fetal bovine serum. Cells were plated (1 x 10⁵ per well) in 24-well plates (MilliporeSigma, Massachusetts, USA) and grown until 70 % confluence. The medium was replaced by serum free medium 24 h before transfection.

In vitro *Pttg1* interference. CC-1 cells were transfected with a final concentration of 20 nM of Silencer Select PTTG1 Pre-Designed siRNA (*Pttg1* siRNA), Silencer Select GAPDH positive control siRNA (C⁺siRNA) or Silencer Select Negative control No 1 siRNA (C⁻ siRNA). Transfections were performed using Lipofectamine RNAiMAX Reagent according to the manufacturer's instructions (Life Technologies, Grand Island, NY, USA). Cells were incubated in Opti-MEM Reduced Serum Media (Invitrogen Life Technology) with or without Silencer Select siRNA- Lipofectamine RNAiMAX complexes for 24, 48 and 72 h. All transfections were performed in duplicate. The efficacy of gene silencing was assessed by quantitative real-time PCR analysis. *Pttg1* siRNA is a 21 bp duplex deoxyribonucleotide with a sense strand corresponding to nucleotides 392 to 410 of the reported rat *Pttg1* mRNA sequence. All siRNAs were designed and synthesized by Ambion (Life Technologies LTD, Leicestershire UK).

mRNA expression of Dlk1 and Pttg1 in isolated and cultured cell lines. Total RNA from HEP, HSC, EC, and CC-1 cells was extracted using TRIzol (TRI Reagent; Sigma-Aldrich, St. Louis, MO, USA). One microgram of total RNA was reverse transcribed as previously described. Specific primers and probes used for the different genes studied were designed to include intron spanning using the Universal Probe Library Assay Design Center through the ProbeFinder v2.45 software (Roche Diagnostics, Indianapolis, IN. <https://www.roche-applied-science.com/sis/rtpcr/upl/index.jsp>). *Pttg1* (probe#68; left: 5'-AGTCTACTAAGACACAAGGCTCTGC-3', right 5'-CAGGCAGGTCAAACCTCTCA-3'), *Dlk1* (probe#76; left: 5'-CCTGTGTGAGAAGTGCCTA-3'), *Hprt* (probe#95; left: 5'-GACCGGTTCTGTCATGTCG-3' right: 5'-ACCTGGTTCATCATCACTAATCAC-3') was used as the reference gene. The primers were designed according to rat sequences (GenBank NM_022391.3, NM_053744.1, NM_012583.2 respectively). Real time quantitative PCR was analyzed in duplicate and performed with the Light Cycler 480 (Roche Diagnostics). Ten µl volume reactions of diluted 1:8 cDNA, 200 nM primer dilution, 100 nM pre-validated 9-mer probe (Universal ProbeLibrary, Roche Diagnostics) and FastStart TaqMan Probe Master (Roche Diagnostics) were used in each PCR reaction. The fluorescence signal was captured during each of the 45 cycles (denaturizing 10 s at 95 °C, annealing 20 s at 60 °C and extension 1 s at 72 °C). *Hprt* was used as a reference gene for normalization and water was used as a negative control. Relative quantification was calculated using the comparative threshold cycle, which is inversely related to the abundance of mRNA transcripts in the initial sample. The mean CT of duplicate measurements was used to calculate

Δ CT as the difference in CT for target and reference. The relative quantity of product was expressed as the fold-induction of the target gene compared with the reference gene according to the formula $2^{-\Delta\Delta CT}$, where $\Delta\Delta CT$ represents Δ CT values normalized with the mean Δ CT of control samples

Droplet digital PCR (ddPCR) analysis. The total number of transcripts of two candidate genes *Pttg1* (assay ID: dRnoCPE5168832, Bio-Rad, Hercules, California, USA) and *Dlk1* (assay ID: dRnoCPE5166190) and a reference gene *Hprt1* (assay ID: dRnoCPE5167187) of isolated primary cirrhotic cells were quantified using the ddPCR platform (QX200; Bio-Rad). In addition, *Pttg1* and *Hprt1* absolute transcripts were also evaluated in organs (liver, spleen, lung, kidney, heart, aorta, and brain) from control and cirrhotic rats. The total 20 μ l reaction mixture included 10 μ l of 2x ddPCR Supermix for probes (no dUTP), 1 μ l of 20x target primer/probes (FAM), 1 μ l of 20x reference primer/probes (HEX), 1 μ l of cDNA from 25 ng RNA, and 7 μ l of RNase/DNase free water. Each ddPCR reaction mixture and 70 μ l of droplet generation oil were carefully loaded to a DG8 cartridge, which was covered with Droplet Generator Gasket (Bio-Rad) and transferred into the QX200 Droplet Generator (Bio-Rad) to generate a maximum of 20,000 droplets from each sample. Then, 40 μ l of droplets were transferred to a 96-well PCR plate for amplification using the C1000 Touch PCR thermal cycler (Bio-Rad). Each reaction was performed in duplicate. The PCR conditions were as follows: enzyme activation (95°C, 10 min), 40 cycles of denaturation (94 °C, 30 sec) and annealing (55°C, 1 min), enzyme deactivation (98°C, 10 min), and final hold (4°C). The temperature ramping rate was 2°C/sec. Following PCR, the plates were directly analyzed with the QX200 Droplet Reader (Bio-Rad). The data were processed using

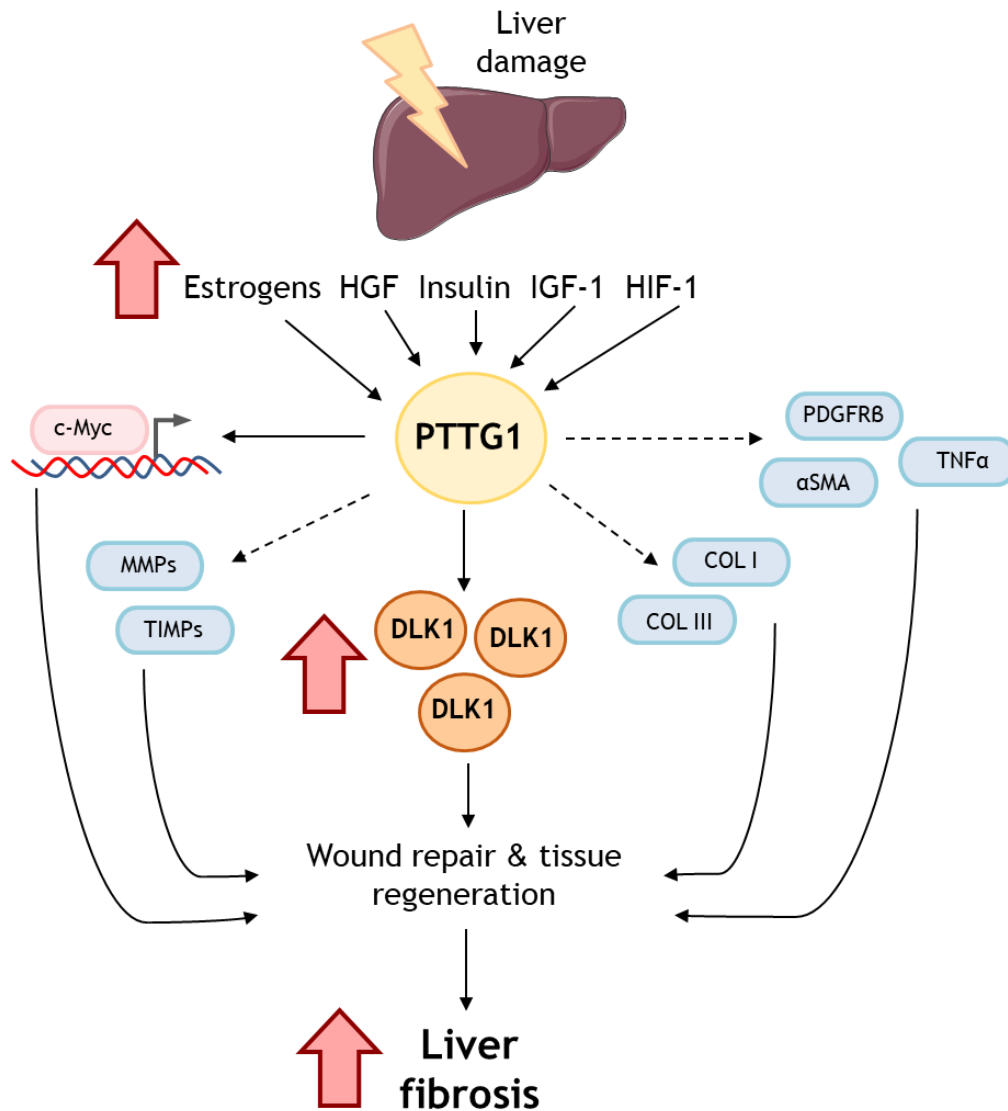
Quanta Soft Analysis Pro 1.0.596 (Bio-Rad). Samples with >10,000 droplets were considered for further analysis. The individual threshold for each sample was automatically calculated by the software. QuantaSoft software provides concentration results in copies of target per μ l.

Hepatic messenger expression of fibrosis related genes. Liver samples from treated and untreated animals were also fixed in 10 % buffered formalin for further hematoxylin and eosin and immunostaining analysis. Total RNA was extracted using a commercially available kit (RNAeasy, Qiagen, Germany) and reverse transcribed. A group of selected fibrosis-related genes was analyzed, including: *Pttg1*, *Dlk1*, *Pdgfr β* (probe#69; left: 5'-GCGGAAGCGCATCTATATCT-3', right 5'-GCGGAAGCGCATCTATATCT-3'), *Tgf β 1*(probe#53; left 5'-AAGGCCAAATATTCCCAACA- 3', right 5'-ATTTTGGCCATCACTCTCAAG-3'), *Col1 α 1* (probe#95; left 5'-AGACCTGGCGAGAGAGGAGT-3', right 5'-ATCCAGACCGTTGTGTCCTC-3'), Collagen III α 1 (*Col3 α 1*) (probe#49; left: 5'-TCCCCTGGAATCTGTGAATC-3', right 5'-TGAGTCGAATTGGGGAGAAT-3'), tissue inhibitor of matrix metalloproteinases type 1 (*Timp1*) (probe#95; left 5'-CATGGAGAGCCTCTGTGGAT-3', right 5'-TGTGCAAATTTCCGTTTCCTT-3'), tissue inhibitor of matrix metalloproteinases type 2 (*Timp2*) (probe#73; left 5'-GACAAGGACATCGAATTTATCTACAC-3', right 5'-CCATCTCCTTCCGCCTTC-3'), *Mmp2* (probe#60; left 5'-CTCCACTACGCTTTTCTCGAAT-3', right 5'-TGGGTATCCATCTCCATGCT-3') and matrix *Mmp9* (probe#53; left: 5'-CCTGAAAACCTCCAACCTCA-3', right: 5'-GAGTGTAACCATAGCGGTACAGG-3'). *Hprt*) was used as the reference gene. Primers were designed according to rat sequences (GenBank NM_022391.3, NM_053744.1, NM_031525.1,

NM_012775.2, NM_053356.1, NM_032085.1, NM_053819.1, NM_021989.2, NM_031054.2, NM_031055.1 and NM_012583.2 respectively). Real Time quantitative PCR was performed as described above.

DLK1 quantification and other measurements. Serum DLK1 levels were determined by an enzyme-linked immunosorbent assay (ELISA Kit for Rat DLK1, USCN Life Science Inc., Wuhan, China) that measures the serum levels of the 50 kDa larger soluble form of the DLK1 protein. The assay was conducted according to the manufacturer's instructions and determined at a wavelength of 450 nm (FLUOstar OPTIMA; BMG LABTECH, Ortenberg, Germany). Standard parameters of liver and renal function were measured in the BS-200E Chemistry Analyzer (Mindray Medical International Ltd, Shenzhen, China).

Supplementary graphical model.



Proposed mechanism underlying PTTG1-induced promotion of liver fibrosis. Liver injury increases the synthesis of mediators such as estrogens, hepatocyte growth factor (HGF), insulin, insulin growth factor 1 (IGF-1), and hypoxia inducible factor 1 (HIF-1), which, in turn, induce the expression of *Pttg1*. *Pttg1* acts as a transcriptional activator of c-myc. Furthermore, *Pttg1* has an indirect effect on increasing the expression of metalloproteinases (MMPs), tissue inhibitors of metalloproteinases (TIMPs), collagens I (COL I) and III (COL III), platelet derived growth factor receptor beta (PDGFR β), tumor necrosis

factor alpha (TNF α), and alpha-smooth muscle actin (α SMA). Importantly, *Pttg1* increases *Dlk1* expression, which is involved in wound repair and tissue regeneration. Activation of these mechanisms finally results in accentuation of liver fibrosis. Continuous arrows indicate a direct effect, whereas discontinuous arrows denote an indirect effect.

Supplementary Table 1: Body weight, standard liver function tests and serum electrolyte values in the rats included in the study.

	Control (n=13)	Mild Fibrosis (n=6)	Severe Fibrosis (n=8)	Cirrhosis (n=11)
Fibrotic area (%)		< 6%	6 - 11%	> 11%
Body weight (g)	489 + 8	432 + 14 *	373 + 56 *	396 + 13
Alanine Transaminase (U/l)	44 + 3	280 + 107 **	618 + 240 ***	749 + 415 ***
Aspartate Transaminase (U/L)	87 + 5	195 + 50 ##	571 + 204 #	1454 + 366 ***
Total bilirubin (mg/dl)	0.00 + 0.00	0.05 + 0.02 ##	0.34 + 0.20 *	2.03 + 0.33 ***
Total proteins (g/l)	63.9 + 1.7	59.2 + 5.8	56.1 + 2.2 #	42.4 + 2.1 ***
Albumin (g/l)	37.1 + 0.6	31.8 + 1.1	33.2 + 1.3 #	23.2 + 1.2 ***
Gamma-glutamyltransferase (U/l)	0.11 + 0.06	0.53 + 0.18 #	4.51 + 1.90 **	12.71 + 2.02 ***
Creatinine (mg/dl)	0.56 + 0.01	0.50 + 0.06 #	0.48 + 0.03 #	0.69 + 0.06
Na⁺ (mEq/l)	143.0 + 1.1	142.4 + 1.2	142.9 + 0.9	146.0 + 2.1
K⁺ (mEq/l)	5.41 + 0.12	4.99 + 0.27 #,+	4.27 + 0.17 ***	4.19 + 0.15 ***

*p<0.05, *p<0.01, ***p<0.001 compared with control group; #p<0.05, ##p<0.01 compared with cirrhotic group; p< 0.05 compared with severe fibrosis. One-way ANOVA with the Newman-Keuls post hoc test and Kruskal-Wallis test with the Dunn post hoc test when appropriate. Results are given as means ± S.E.

Supplementary references





1. Jiménez W, Parés A, Caballería J, Heredia D, Bruguera M, Torres M, *et al.* Measurement of fibrosis in needle liver biopsies: evaluation of a colorimetric method. *Hepatology*.1985; 5(5):815-818.
2. Muñoz-Luque J, Ros J, Fernández-Varo G, Tugues S, Morales-Ruiz M, Álvarez CE, *et al.* Regression of fibrosis after chronic stimulation of cannabinoid CB2 receptor in cirrhotic rats. *J Pharmacol Exp Ther*.2008; 324(2):475-483.
3. López-Parra M, Titos E, Horrillo R, Ferré N, González-Pérez A, Martínez-Clemente M, *et al.* Regulatory effects of arachidonate 5-lipoxygenase on hepatic microsomal TG transfer protein activity and VLDL-triglyceride and apoB secretion in obese mice. *J of Lipid Res*.2008; 49(12):2513-2523.

ARTICLE 2: Bespoken Nanoceria: An Effective Treatment in Experimental Hepatocellular Carcinoma

The **second objective** of this doctoral thesis was to investigate therapeutic value of CeO₂NPs in experimentally induced rat HCC.

Fernández-Varo G, Perramón M, Carvajal S, Oró D, Casals E, Boix L, Oller L, Macías-Muñoz L, Marfà S, Casals G, Morales-Ruiz M, Casado P, Cutillas PR, Bruix J, Navasa M, Fuster J, Garcia-Valdecasas JC, Pavel MC, Puentes V, Jiménez W. Hepatology. 2020;72(4):1267–82.

Bespoken Nanoceria: An Effective Treatment in Experimental Hepatocellular Carcinoma

Guillermo Fernández-Varo ^{1,2}, Meritxell Perramón ¹, Silvia Carvajal,¹ Denise Oró,¹ Eudald Casals,³ Loreto Boix,⁴ Laura Oller,¹ Laura Macías-Muñoz,¹ Santi Marfà,¹ Gregori Casals,^{1,5} Manuel Morales-Ruiz,^{1,2,5} Pedro Casado ⁶, Pedro R. Cutillas,⁶ Jordi Bruix,⁴ Miquel Navasa,⁷ Josep Fuster,⁷ Juan Carlos Garcia-Valdecasas,⁷ Mihai C. Pavel,⁷ Víctor Puentes,⁸⁻¹⁰ and Wladimiro Jiménez ^{1,2}

BACKGROUND AND AIMS: Despite the availability of new-generation drugs, hepatocellular carcinoma (HCC) is still the third most frequent cause of cancer-related deaths worldwide. Cerium oxide nanoparticles (CeO₂NPs) have emerged as an antioxidant agent in experimental liver disease because of their antioxidant, anti-inflammatory, and antisteatotic properties. In the present study, we aimed to elucidate the potential of CeO₂NPs as therapeutic agents in HCC.

APPROACH AND RESULTS: HCC was induced in 110 Wistar rats by intraperitoneal administration of diethylnitrosamine for 16 weeks. Animals were treated with vehicle or CeO₂NPs at weeks 16 and 17. At the eighteenth week, nanoceria biodistribution was assessed by mass spectrometry (MS). The effect of CeO₂NPs on tumor progression and animal survival was investigated. Hepatic tissue MS-based phosphoproteomics as well as analysis of principal lipid components were performed. The intracellular uptake of CeO₂NPs by human *ex vivo* perfused livers and human hepatocytes was analyzed. Nanoceria was mainly accumulated in the liver, where it reduced macrophage infiltration and inflammatory gene expression. Nanoceria treatment increased liver apoptotic activity, while proliferation was attenuated. Phosphoproteomic analysis revealed that CeO₂NPs affected the phosphorylation

of proteins mainly related to cell adhesion and RNA splicing. CeO₂NPs decreased phosphatidylcholine-derived arachidonic acid and reverted the HCC-induced increase of linoleic acid in several lipid components. Furthermore, CeO₂NPs reduced serum alpha-protein levels and improved the survival of HCC rats. Nanoceria uptake by *ex vivo* perfused human livers and *in vitro* human hepatocytes was also demonstrated.

CONCLUSIONS: These data indicate that CeO₂NPs partially revert the cellular mechanisms involved in tumor progression and significantly increase survival in HCC rats, suggesting that they could be effective in patients with HCC. (HEPATOLOGY 2020;72:1267-1282).

Hepatocellular carcinoma (HCC) is the third leading cause of death by cancer worldwide.⁽¹⁾ HCC commonly arises in patients with underlying chronic liver disease and is considered a typical inflammation-associated tumor.⁽²⁾ The appearance of cirrhosis greatly favors the onset of HCC through mechanisms not yet well known that began to be elucidated in recent years.⁽³⁾ In the last decade, complex

Abbreviations: AA, arachidonic acid; AFP, alpha-fetoprotein; CD, cluster of differentiation; CE, cholesterol ester; CeO₂NP, cerium oxide nanoparticle; DEN, diethylnitrosamine; Δ-6D, Δ-6 desaturase; EDX, energy-dispersive X-ray spectroscopy; ERK, extracellular signal-regulated kinase; FA, fatty acid; HAADF, high-angle annular dark-field; HCC, hepatocellular carcinoma; ICP-MS, inductively coupled plasma-mass spectrometry; Itgb4, integrin beta 4; LA, linoleic acid; MAPK, mitogen-activated protein kinase; MS, mass spectrometry; NEFA, nonesterified FA; NMP, normothermic machine perfusion; NP, nanoparticle; PC, phosphatidylcholine; PE, phosphatidylethanolamine; P-ERK, phosphorylated ERK; PUFA, polyunsaturated FA; ROS, reactive oxygen species; STEM, scanning transmission electron microscope; TEM, transmission electron microscopy; TG, triglycerides; TMAOH, tetramethylammonium hydroxide; TUNEL, terminal deoxynucleotidyl transferase-mediated deoxyuridine triphosphate nick-end labeling.

Received August 26, 2019; accepted December 20, 2019.

Additional Supporting Information may be found at onlinelibrary.wiley.com/doi/10.1002/hep.31139/supplinfo.

Supported by Dirección General de Investigación Científica y Técnica, Ministerio de Ciencia, Innovación y Universidades (SAF15-64126-R and RTI2018-094734-B-C21, to W.J.; SAF2016-75358-R, to M.M.-R.), Agència de Gestió d'Ajuts Universitaris i de Recerca (SGR 2017/2019, to W.J.), Instituto de Salud Carlos III (FIS PI15-00077 and FIS PI19-00774, to G.C. and G.F.-V.; PI18/00763, to J.B. and L.B.), AECC (PI044031, to J.B. and L.B.), and WCR (AICR) (16-0026, to J.B. and L.B.). Co-funded by European Regional Development Fund/ European Social Fund (ERDF/ESF) "A way to make Europe"/ "Investing in your future". Cofinanced by Agència de Gestió d'Ajuts Universitaris i de Recerca and ERDF/ESF "A way to make Europe"/ "Investing in your future" under the Operational Program of Catalonia 2014-2020 (grant 2018 PROD 00187). The Centro de Investigación Biomédica en Red de Enfermedades Hepáticas y Digestivas (CIBERehd) is funded by the Instituto de Salud Carlos III.

genetic alterations, epigenetic chromosomal aberrations, and cellular signaling pathways triggering tumor development, progression, and metastasis have been characterized.⁽⁴⁾ The current systemic treatments of HCC are based on molecularly targeted therapies. Sorafenib, a multikinase inhibitor, was the first compound for first-line treatment of patients with advanced-stage HCC.⁽⁵⁾ However, clinical trials have found only modest improvement in overall survival,⁽⁶⁾ and the emergence of resistance episodes reveals the need to develop effective therapies for HCC.⁽⁷⁾ Although the available drugs improve clinical outcomes, the median overall survival continues to be approximately 1 year.^(8,9)

Of particular importance is the role of reactive oxygen species (ROS) in the onset and progression of HCC.⁽¹⁰⁾ Mechanistic studies show that ROS induce alterations in DNA and modify key cellular processes such as cell proliferation and apoptosis.⁽¹¹⁾ Thus, it has been hypothesized that HCC develops because chronic oxidative stress exerts a selective pressure that favors the outgrowth of cells from progenitor clones that are more resistant to oxidative damage.⁽¹²⁾

Antioxidant agents have demonstrated their efficacy in chronic liver diseases equilibrating hepatic ROS metabolism, thereby improving liver functionality.⁽¹³⁾

Recently, cerium oxide nanoparticles (CeO₂NPs) have emerged as an antioxidant and anti-inflammatory agent. Superoxide dismutase activity⁽¹⁴⁾ (conversion of superoxide anion into hydrogen peroxide and finally oxygen), catalase activity^(15,16) (hydrogen peroxide into oxygen and water), and peroxidase activity⁽¹⁷⁾ (hydrogen peroxide into hydroxyl radicals), among others, have been attributed to CeO₂NPs. Consequently, the wide spectrum of antioxidant enzyme-mimetic activities of CeO₂NPs has been explored in the treatment of many diseases related to the overproduction of ROS. Thus, the ability of CeO₂NPs to modulate oxidative stress in diseases ranging from retinal degeneration,⁽¹⁸⁾ neurodegenerative diseases,⁽¹⁹⁾ diabetes,⁽²⁰⁾ ischemia,⁽²¹⁾ cardiopathies,⁽²²⁾ gastrointestinal inflammation,⁽²³⁾ and especially cancer has been described.⁽²⁴⁻²⁷⁾ As well, the therapeutic possibilities of CeO₂NPs have been shown in the case of experimental liver disease.⁽²⁸⁻³²⁾

© 2020 The Authors. HEPATOLOGY published by Wiley Periodicals, Inc., on behalf of American Association for the Study of Liver Diseases. This is an open access article under the terms of the Creative Commons Attribution-NonCommercial License, which permits use, distribution and reproduction in any medium, provided the original work is properly cited and is not used for commercial purposes.

View this article online at wileyonlinelibrary.com.

DOI 10.1002/hep.31139

Potential conflict of interest: Dr. Bruix consults for, advises, is on the speakers' bureau of, and received grants from Bayer-Shering and BTG. He consults for and advises MSD. He consults for and is on the speakers' bureau for Sirtex. He consults for and received grants from Arqule and Ipsen. He consults for Novartis, Bristol-Myers Squibb, Eisai, Kowa, Terumo, Gilead, Bio Alliance, Roche, AbbVie, Merck, AstraZeneca, Incyte, Quirem, Adaptimmune, and Lilly.

ARTICLE INFORMATION:

From the ¹Service of Biochemistry and Molecular Genetics, Hospital Clinic Universitari, Centro de Investigación Biomédica en Red de Enfermedades Hepáticas y Digestivas (CIBERehd), Institut d'Investigacions Biomèdiques August Pi i Sunyer (IDIBAPS), Barcelona, Spain; ²Departament of Biomedicine, University of Barcelona, Barcelona, Spain; ³School of Biotechnology and Health Sciences, Wuyi University, Jiangmen, China; ⁴Barcelona-Clinic Liver Cancer Group, Liver Unit, Hospital Clinic de Barcelona, CIBERehd, IDIBAPS, University of Barcelona, Barcelona, Spain; ⁵Working Group for the Biochemical Assessment of Hepatic Disease-SEQC^{ML}, Barcelona, Spain; ⁶Centre for Haemato-Oncology, Barts Cancer Institute, Queen Mary University of London, London, UK; ⁷Liver Surgery and Transplant Unit, Digestive and Metabolic Diseases Institute, Hospital Clínic de Barcelona, CIBERehd, IDIBAPS, University of Barcelona, Barcelona, Spain; ⁸Institut Català de Recerca i Estudis Avançats (ICREA), Barcelona, Spain; ⁹Institut Català de Nanociència i Nanotecnologia (ICN2), Bellaterra, Spain; ¹⁰Vall d'Hebron Institute of Research (VHIR), Barcelona, Spain.

ADDRESS CORRESPONDENCE AND REPRINT REQUESTS TO:

Wladimiro Jiménez, Ph.D.
Servicio de Bioquímica y Genética Molecular
Hospital Clinic Universitario
Villarroel 170
Barcelona 08036, Spain
E-mail: wjimenez@clinic.cat
Tel.: +34 93 2275400 ext. 3091

or
Victor Puentes, Ph.D.
Institut Català de Nanociència i Nanotecnologia, Campus UAB
Barcelona 08193, Spain
E-mail: victor.puentes@icn2.cat
Tel.: +34 93 7374622

We considered the potential therapeutic value of CeO₂NPs in an experimental model of HCC in rats by chronic administration of diethylnitrosamine (DEN). We assessed the impact of CeO₂NPs on tumor progression and survival, the accumulation in isolated human liver, and their intracellular adsorption by human liver-derived cancer cells.

Material and Methods

SYNTHESIS AND CHARACTERIZATION OF RAT SERUM ALBUMIN STABILIZED CeO₂NPs

CeO₂NPs of 4–5 nm were synthesized by the chemical precipitation of cerium (III) nitrate hexahydrate (Sigma-Aldrich, St. Louis, MO) in a basic aqueous solution.^(14,15,17,28) Cerium (III), 10 mM, was dissolved in 100 mL of Milli-Q water at room temperature. To this, 3 mL of tetramethylammonium hydroxide (TMAOH) solution (1 M) was added slowly at room temperature under vigorous stirring (final concentration of 10 mM), and the mixture was allowed to age under mild stirring overnight. During the first minutes, the solution is colorless, and then it turns progressively brownish. Afterward, nanoparticles (NPs) were purified by centrifugation (10,000g, 10 minutes, at room temperature), and the resultant pellet was resuspended in 100 mL aqueous solution of 1 mM TMAOH. The xlenol orange test and inductively coupled plasma-mass spectrometry (ICP-MS) indicated a full conversion of Ce to CeO₂NPs. Thus, the final CeO₂ concentration for this synthesis was determined to be 1.72 mg/mL (6.7•10¹⁵ NPs/mL) and then diluted to the 1 mg/mL employed solution. Further details on CeO₂NPs synthesis and characterization can be found in the Supporting Information.

CeO₂NPs ADMINISTRATION

CeO₂NPs or vehicle were dispersed in saline solution and intravenously given as a bolus (500 µL) through the tail vein. CeO₂NPs (0.1 mg/kg body weight) or vehicle (saline solution containing TMAOH ammonium salts 0.8 mM) were injected twice a week for 2 consecutive weeks starting at the sixteenth week after beginning DEN administration.

HCC INDUCTION IN RATS

Experimental studies were performed in 118 male Wistar rats weighing 200 g (Charles-River, Saint Aubin les Elseuf, France). HCC was chemically induced in 110 rats by an intraperitoneal administration of DEN (50 mg/kg body weight; Sigma-Aldrich) once a week for 16 weeks, and eight healthy rats were included as a control group.

ACCUMULATION OF Ce IN ISOLATED HUMAN LIVERS

To assess whether the human liver parallels the kinetic adsorption pattern shown by CeO₂NPs in the rat liver, human livers from three donors, designated subjects H1, H2, and H3, were used in the present study. Livers were procured in the Hospital Clinic (Barcelona, Spain), rejected for transplantation, and approved for research.

CeO₂NPs ADSORPTION BY HUMAN HEPATOCYTE CANCER CELLS

To investigate whether human hepatocytes are able to intracellularly take up CeO₂NPs, subsequent studies were performed in HepG2 cells, a human cell line derived from a liver HCC (ATCC, Manassas, VA).

ETHICAL APPROVAL

The study was approved and performed according to the criteria of the Investigation and Ethics Committee of the Hospital Clínic Universitari (Barcelona, Spain). Animals received humane care according to the criteria outlined in the “Guide for the Care and Use of Laboratory Animals”. The study of the human livers was conducted in the Hospital Clínic de Barcelona, which is part of the European Union-funded Consortium for Organ Preservation in Europe (<http://www.ope-eu.com>).

For further information, please refer to the Supporting Information.

Results

CHARACTERIZATION OF CeO₂NPs

A description of the characterization of the CeO₂NPs used in this study has been published.⁽³²⁾ High-resolution transmission electron microscopic

(TEM) analysis indicated that the NPs had a spherical morphology and were predominantly within the size range of 4–20 nm. The X-ray diffraction pattern showed pure CeO₂NPs with the typical peak broadening characteristic of nanosized particles. Initially, the employed NPs are positively charged, and the colloidal stability is mediated by electrostatic repulsion (zeta potential +43.0 ± 1.3 mV, conductivity 0.303 ± 0.006 mS/cm, and pH 4.3). Albumin conjugation in the surface of the CeO₂NPs has been characterized by the increase in dynamic light scattering (from 5 to 20 nm) and decrease in zeta potential (from +42.8 to -10 mV, which is the average zeta potential value of proteins in serum) (Supporting Fig. S1). Indeed, the solubility of CeO₂NPs in physiological media is challenging, and a strong tendency to aggregate and sediment impedes their medical use even more, modifying their protective effects toward the proinflammatory (<https://www.frontiersin.org/articles/10.3389/fimmu.2017.00970/full>). To evaluate the electronic structure of the CeO₂NPs and the influence on Ce valence state due to the presence of rat serum albumin, we performed X-ray photoelectron spectroscopy measurements. Ce three-dimensional spectra of all samples are shown in Supporting Fig. S2, where it can be clearly observed that the Ce³⁺/Ce⁴⁺ ratio is not affected by the presence of bovine serum albumin in the CeO₂NPs surface.

THE RAT MODEL OF DEN-INDUCED LIVER INJURY EXHIBITS CHARACTERISTICS OF MULTIFOCAL HCC

Macroscopic examination of the liver specimens and histological examination confirmed the development of multifocal HCC nodules with a dysmorphic or dyschromic appearance (Fig. 1A) that was markedly attenuated in the animals receiving CeO₂NPs. Interestingly, DEN-injured rats treated with CeO₂NPs showed a significantly lower liver/body weight ratio (Fig. 1B).

LIVER AND SPLEEN ARE THE MAJOR TARGETS OF CeO₂NPs IN HCC RATS

Following intravenous CeO₂NPs administration, tissue Ce accumulation was analyzed by ICP-MS. Two weeks after the last administration of CeO₂NPs 90.0% and 7.7% of the total dose of Ce collected was located

in the liver and the spleen, respectively, whereas these figures were 77.3% and 21.7% 3 weeks after the completion of the CeO₂NPs dosing schedule (Fig. 1C).

SERUM BIOCHEMICAL PARAMETERS AND CIRCULATING LEVELS OF ALPHA-FETOPROTEIN

HCC rats showed significant alterations of liver function tests such as decreased levels of albumin and glucose, higher levels of total bilirubin and total cholesterol, and increased activity of markers of hepatocyte injury such as aspartate aminotransferase, alanine aminotransferase, and gamma-glutamyl transferase. We did not observe significant differences between HCC rats receiving or not receiving CeO₂NPs (Supporting Table S2). However, nanoceria administration did significantly reduce the circulating levels of alpha-fetoprotein (AFP), a tumor-associated marker for HCC (Fig. 1B).

EFFECT OF CeO₂NPs ON COLLAGEN CONTENT AND CELLULAR APOPTOSIS IN LIVER TISSUE

Long-term administration of DEN promoted incipient formation of fibrotic septa and periportal accumulation of collagen as a consequence of continuous hepatic injury. However, no significant differences in hepatic collagen content were noted between treated and nontreated rats with HCC (Fig. 2A).

The terminal deoxynucleotidyl transferase-mediated deoxyuridine triphosphate nick-end labeling (TUNEL) assay showed a significant increase in positive cells in the liver sections of DEN-injured rats treated with CeO₂NPs (Fig. 2B). We also observed a significantly increased protein expression of activated caspase-3 in HCC rats treated with CeO₂NPs (Fig. 2C). These results indicate that treatment with CeO₂NPs results in acceleration of apoptosis, thereby inhibiting HCC growth.

CeO₂NPs DECREASE MACROPHAGE INFILTRATION AND REDUCE INFLAMMATORY GENE OVEREXPRESSION IN LIVER TISSUE

Macrophage infiltration measured by positive cluster of differentiation 68 (CD68) staining was

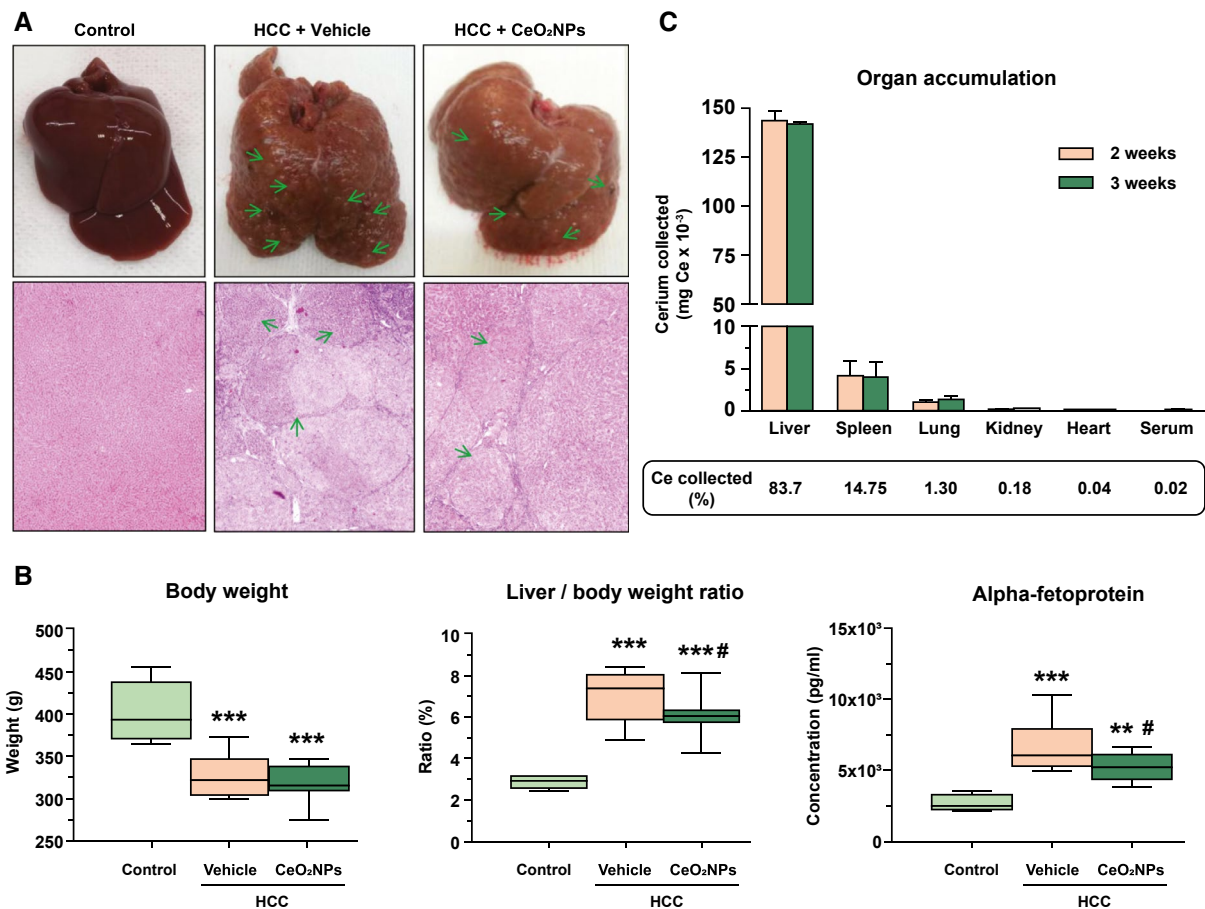


FIG. 1. DEN-induced model of HCC and biodistribution of CeO₂NPs. (A) Representative photographs of the liver and hematoxylin and eosin staining (magnification, 40) from control and DEN-injured rats. DEN was administered for 16 weeks, followed by a 2-week washout period. Green arrows point at nodules present in HCC rats. (B) Body weight, liver/body weight ratio, and serum levels of AFP in control rats and HCC rats. Serum samples were collected 1 week after the last dose of CeO₂NPs. (C) ICP-MS quantification of cerium. Major organs and serum from HCC rats receiving CeO₂NPs collected at two different time points: 2 (n = 3) and 3 (n = 4) weeks after the last administration of CeO₂NPs. This corresponds to the nineteenth and twentieth weeks after starting DEN administration. ***P* < 0.01 and ****P* < 0.001 versus control; #*P* < 0.05 versus HCC + vehicle. One-way analysis of variance and Newman-Keuls *post hoc* test.

observed in intratumoral and peritumoral areas, being significantly lower in HCC rats receiving CeO₂NPs (Fig. 3A). mRNA expression of inflammatory, macrophage phenotype, cell growth and differentiation genes was analyzed in liver biopsies of control and HCC rats. Chronic administration of DEN induced higher gene expression of macrophage M1 markers, such as interleukin 1 beta, tumor necrosis factor alpha, inducible nitric oxide synthase, and cyclooxygenase-2 (Supporting Table S3). Interestingly, administration of CeO₂NPs significantly down-regulated M1 genes involved in proinflammatory function.

CeO₂NPs DECREASE HEPATIC CELLULAR PROLIFERATION

We assessed the effect of CeO₂NPs on cell proliferation and the phosphorylation levels of proteins involved in tumor progression. Immunohistochemistry revealed abundant cellular proliferation in liver sections from DEN-injured animals. The cell proliferation rate, measured as the percent of Ki67-positive hepatocyte nuclei, was markedly lower in CeO₂NPs-treated rats (Fig. 3B). To ascertain the potential effect of CeO₂NPs on interfering with the Ras/mitogen-activated protein kinase (MAPK) signaling pathway,

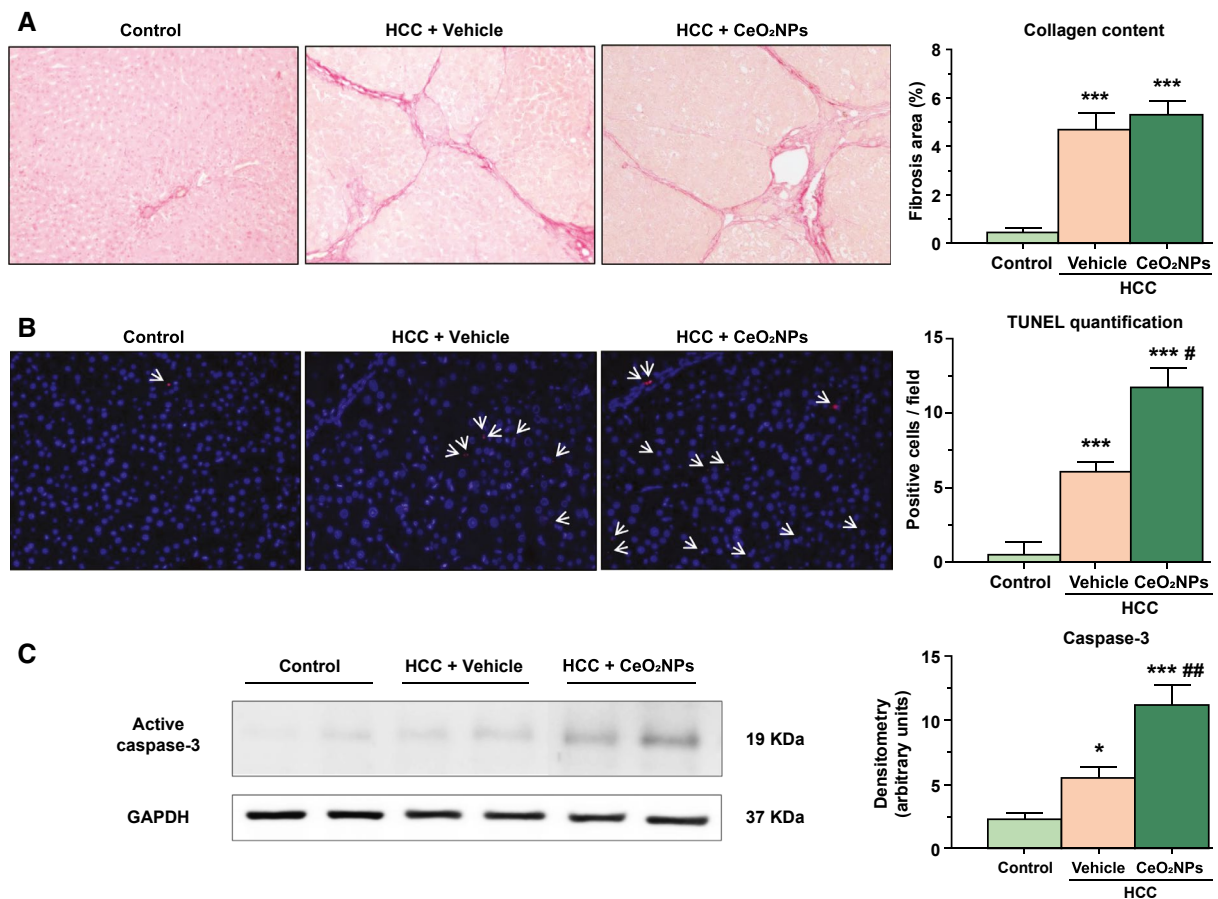


FIG. 2. Effect of CeO₂NPs on hepatic fibrosis and cellular apoptosis. (A) Sirius red staining of representative liver sections obtained from control and DEN-injured rats (magnification, 100). (B) Representative TUNEL assay in liver sections of control rats and HCC rats (magnification, 200). White arrows point to apoptotic (red) cells. (C) Representative western blot for activated caspase-3 in liver tissue of control rats and HCC rats. **P* < 0.05 and ****P* < 0.001 versus control group; #*P* < 0.05 and ##*P* < 0.01 versus HCC + vehicle. One-way analysis of variance and Newman-Keuls *post hoc* test, Kruskal-Wallis test, and Dunn's *post hoc* test, with unpaired Student *t* test when appropriate. Abbreviation: GAPDH, glyceraldehyde 3-phosphate dehydrogenase.

we assessed protein expression of total extracellular signal-regulated kinase 1/2 (ERK1/2) and phosphorylated ERK1/2 (P-ERK1/2) in liver samples of HCC rats by western blot. It was of note that CeO₂NPs treatment resulted in a significant reduction of P-ERK1/2 (Fig. 3C). These results suggest that the antiproliferative action of CeO₂NPs is related to interference with the Ras/MAPK signaling pathway in HCC rats.

EFFECT OF CeO₂NPs ON ALTERED CELL SIGNALING PATHWAYS IN LIVER TISSUE

To investigate the effects of CeO₂NPs on kinase-driven signaling pathways, we evaluated the

phosphoproteome profile by mass spectrometry (MS). We identified and quantified a total of 5,048 phosphopeptides in six independent biological replicates that were run twice. Principal component analysis showed that CeO₂NPs-treated samples separate from vehicle-treated samples in principal component 1 (Fig. 4A). At arbitrary threshold values of ±0.8-fold change (log₂) and *P* < 0.05, the phosphorylation of 349 peptides was increased, while the phosphorylation of 133 was decreased after CeO₂NPs treatment (Fig. 4B; Supporting Table S4). This set of regulated phosphopeptides included 20 phosphorylation sites in kinases, of which 11 were increased and nine were decreased (Fig. 4C). Gene ontology analysis showed that cell-cell adhesion and RNA splicing were enriched in the set of genes

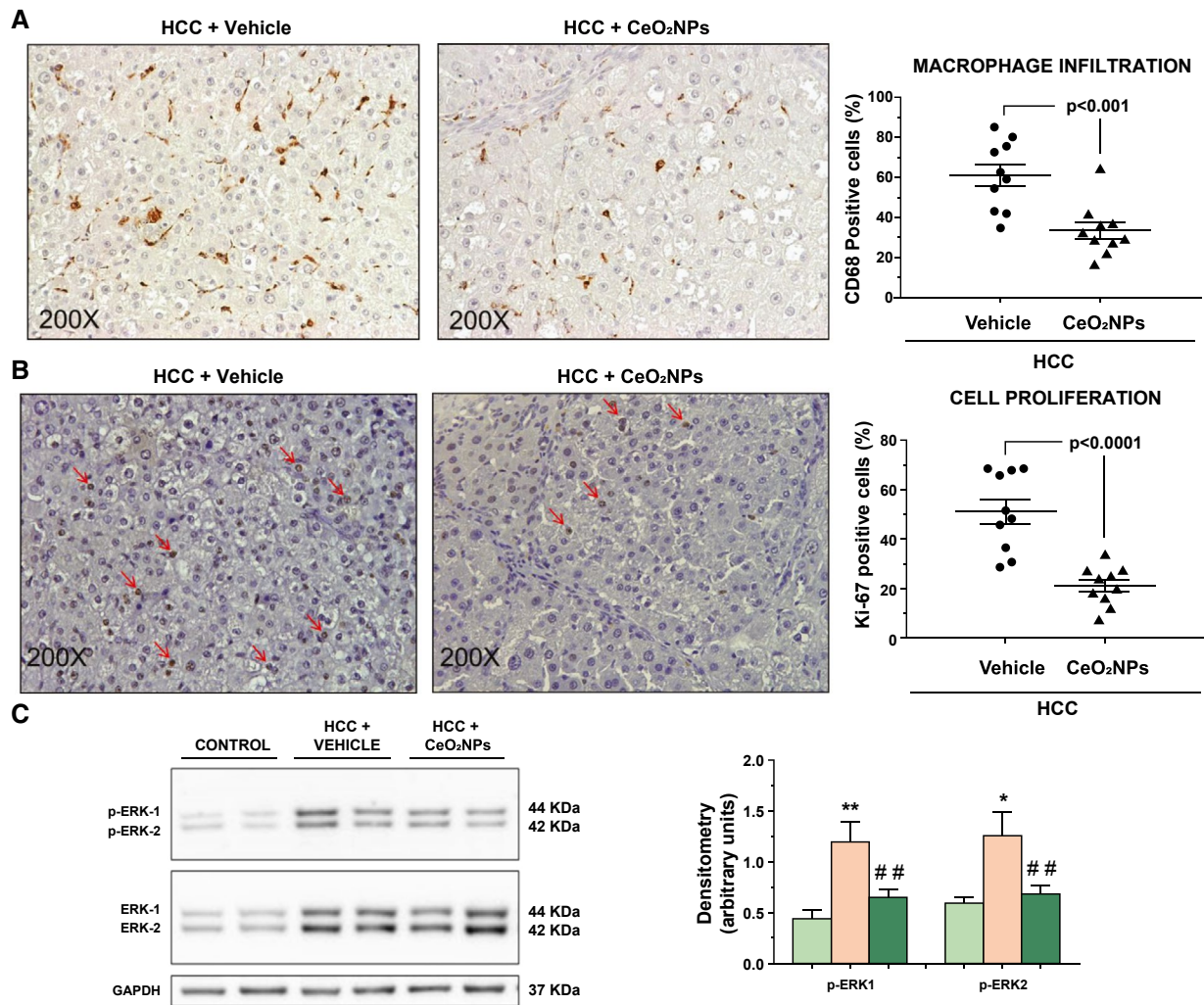


FIG. 3. Effect of CeO₂NPs on infiltrating cells, cellular proliferation, and levels of P-ERK1/2 in tumoral tissue. (A) CD68 immunostaining of representative liver sections from HCC rats (magnification, 200). (B) Ki67 immunostaining of representative liver sections from HCC rats (magnification, 200). Red arrows mark nuclei positive for Ki67 staining. (C) Representative western blots of total ERK1/2 and P-ERK1/2 in liver homogenates of control rats and HCC rats. Forty micrograms of protein extracts were loaded per lane. * $P < 0.05$ and ** $P < 0.01$ versus control; # $P < 0.01$ versus HCC + vehicle. One-way analysis of variance and Newman-Keuls *post hoc* test, with unpaired Student *t* test when appropriate. Abbreviation: GAPDH, glyceraldehyde 3-phosphate dehydrogenase.

that code for the regulated phosphopeptides (Fig. 4D). The set of regulated phosphopeptides linked to cell–cell adhesion included 43 sites in 27 proteins that presented an increased phosphorylation after CeO₂NPs treatment and 16 sites in 11 proteins that presented a decreased phosphorylation after NP treatment (Fig. 4E). In addition, proteins linked to cell–matrix adhesion including CD44 and integrin beta 4 (Itgb4) showed a decreased phosphorylation

after CeO₂NPs treatment (Fig. 4F). Finally, the set of regulated phosphopeptides linked to RNA splicing included 36 sites in 18 proteins that presented increased phosphorylation and four sites in three proteins that showed decreased phosphorylation (Fig. 4G). These data suggest that CeO₂NPs have a global effect on the phosphorylation pattern of liver cells from rats with HCC that mainly affects proteins related to cell adhesion and RNA splicing.

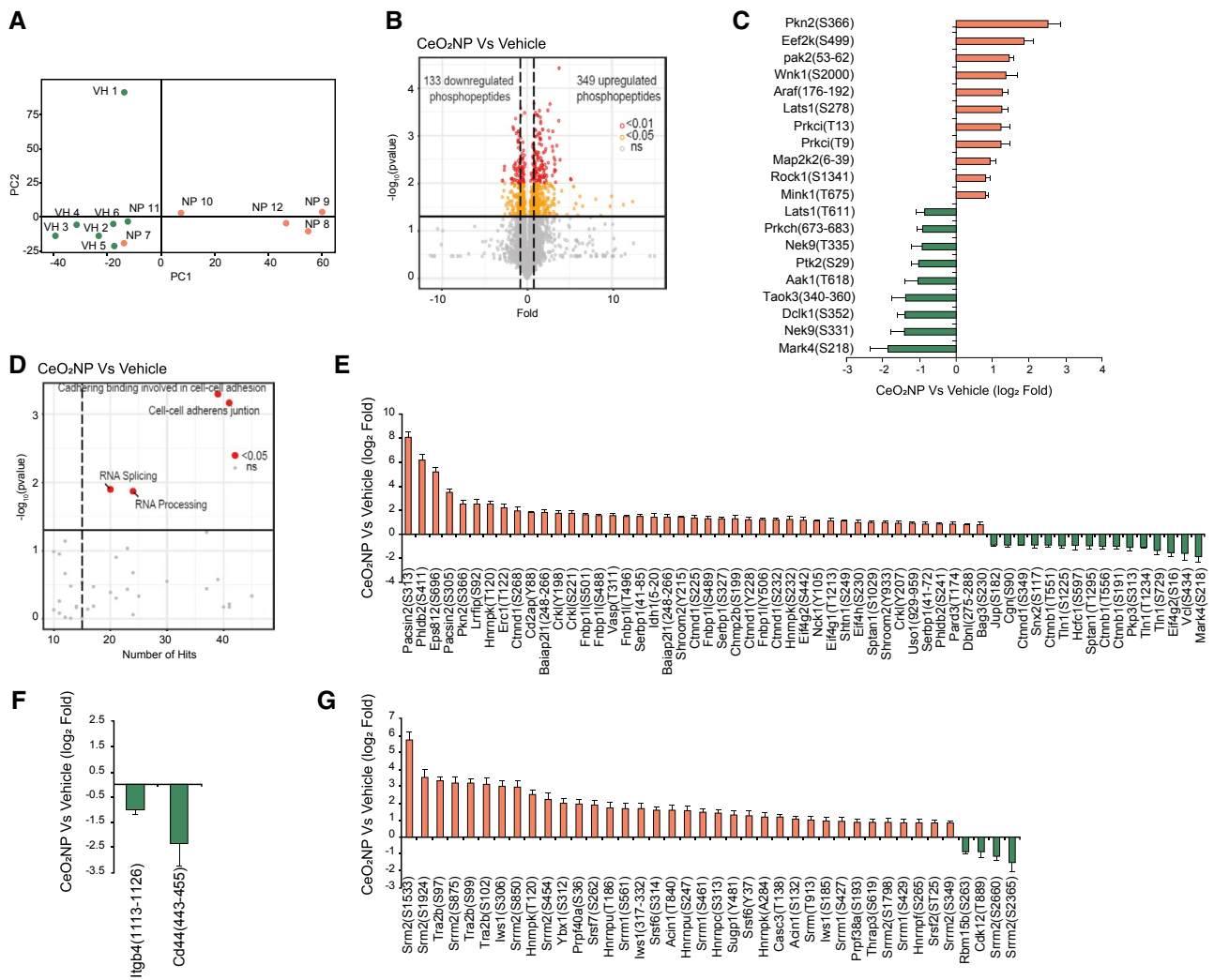


FIG. 4. Effect of CeO₂NPs on the phosphoproteome of livers from rats with HCC. (A) Principal component analysis showing the global effect of CeO₂NPs on the phosphoproteome of hepatic cells from HCC rats. Blue dots (VH) indicate biological replicates treated with vehicle, while red dots (NP) indicate replicates treated with CeO₂NPs. (B) Volcano plot showing phosphopeptides regulated by CeO₂NPs. Peptides were considered regulated when $P < 0.05$ (1.3 in $-\log_{10}$ scale) and fold change in \log_2 scale >0.8 (increased) or <-0.8 (decreased). Statistical significance was assessed using an unpaired two-tailed Student t test. (C) Chart showing phosphorylation sites in kinases regulated by CeO₂NPs treatment. (D) Volcano plot showing gene ontologies enriched in proteins whose phosphorylation was regulated by CeO₂NPs. Statistical significance of the enrichment was assessed using a modified Fisher's exact test. (E) Phosphorylation sites linked to cell-cell adhesion and regulated by CeO₂NPs treatment. (F) Effect of CeO₂NPs treatment over the phosphorylation of CD44 and Itgb4. (G) Phosphorylation sites linked to RNA splicing and regulated by CeO₂NPs treatment.

EFFECT OF CeO₂NPs ON HEPATIC LIPID METABOLISM

Analysis of total fatty acids (FAs) of principal lipid components in hepatic tissue of HCC animals indicates a dysregulation of FA metabolism mainly occurring in cholesterol ester (CE)- and nonesterified FA (NEFA)- derived FAs (Supporting Table S5). The most important effects induced by CeO₂NPs were found in

phosphatidylcholine (PC)-derived FAs, which are by far the most abundant lipid component in the liver. In fact, we observed a significant decrease in polyunsaturated FAs (PUFAs), which was exclusively due to a marked diminution in arachidonic acid (AA; C20:4n6; Fig. 5A). We also observed significant changes in C14:0, C16:1, and C17:0, although the differences were quantitatively much less important. Moreover, in NEFA-derived, triglyceride (TG)-derived, and CE-derived FAs, we

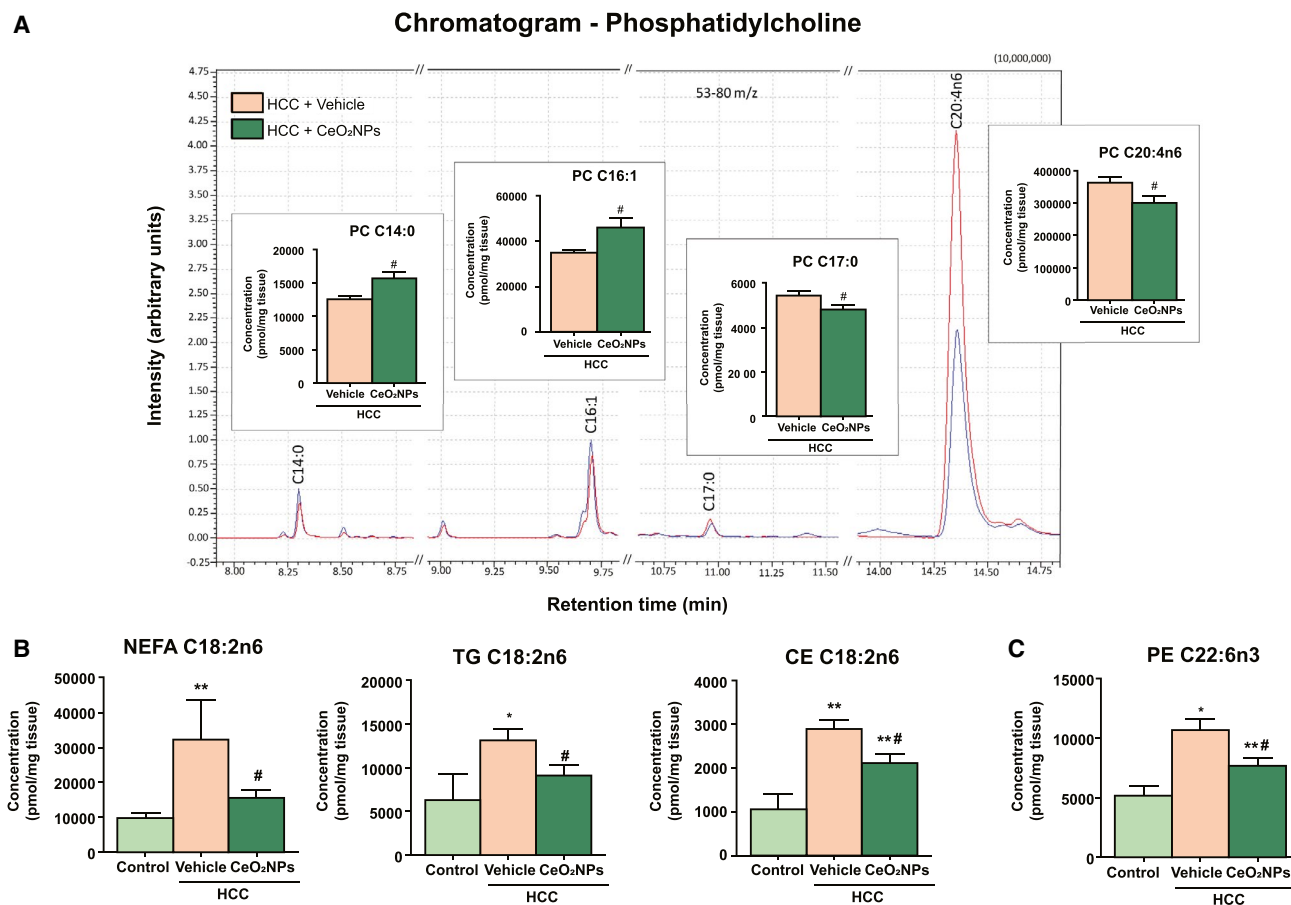


FIG. 5. Representative chromatogram of PC-derived FAs in rats with HCC. (A) Superposition of a representative gas chromatography MS total ion current chromatograms showing the analysis of PC-derived FAs obtained from HCC rats treated with vehicle (red) or CeO₂NPs (blue). The represented peaks are the FAs which showed significant differences between groups. Gas chromatography peaks are labeled with the corresponding FA identification. For each peak there is a graph with the quantification of the FA. (B) Effect of nanoceria treatment in linoleic FAs in different lipid components (NEFA, TG, and CE). (C) Effect of CeO₂NPs in PE-derived docosahexaenoic acid (C22:6n3). * $P < 0.05$ and ** $P < 0.01$ versus control; # $P < 0.05$ versus HCC + vehicle. Unpaired Student t test and Mann-Whitney test when appropriate.

observed that HCC rats showed significantly increased liver content of linoleic acid (LA; C18:2n6) than healthy rats, a phenomenon that was reversed in HCC animals treated with CeO₂NPs (Fig. 5B). Of note, on analyzing phosphatidylethanolamine (PE)-derived FAs, we observed that CeO₂NPs administration was associated with a significant reduction in the very long chain PUFA docosahexaenoic acid (C22:6n3) (Fig. 5C).

CeO₂NPs IMPROVE SURVIVAL IN DEN-INJURED RATS

To assess how the above changes translate into clinical outcome, we investigated the impact of these

NPs on the survival of two groups of HCC rats. The median survival reached by CeO₂NPs-treated rats was significantly higher than that in rats receiving vehicle ($P < 0.05$) (Fig. 6A). Next, we were interested in comparing the effect of CeO₂NPs to that of sorafenib. Four groups of rats receiving vehicle, CeO₂NPs, sorafenib, and CeO₂NPs plus sorafenib were investigated. The median survival was markedly lower in HCC rats receiving vehicle (15.5 days, $P < 0.05$) than in those animals receiving CeO₂NPs (31 days), sorafenib (33.5 days), or CeO₂NPs plus sorafenib (33.5 days) (Fig. 6B). The combined therapy showed the longest survival, although differences did not reach statistical significance.

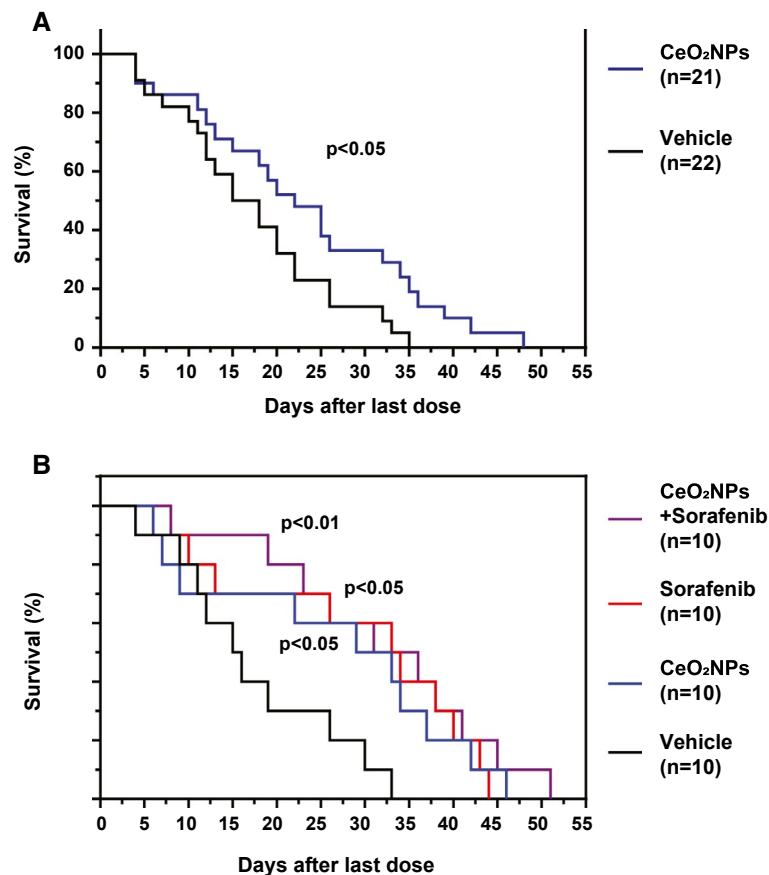


FIG. 6. Effect of CeO₂NPs on survival. (A) HCC rats randomly received two weekly doses of CeO₂NPs or vehicle through the tail vein at the sixteenth and seventeenth weeks, and their survival was analyzed. (B) HCC rats were randomly distributed into four groups receiving vehicle, CeO₂NPs, sorafenib, or the combination CeO₂NPs and sorafenib. Sorafenib was delivered daily by intragastric administration (10 mg/kg) for 14 days. $P < 0.05$ and $P < 0.01$ versus HCC + vehicle, log-rank (Mantel-Cox) test.

CeO₂NPs RETENTION BY HUMAN LIVER

To determine whether CeO₂NPs can be internalized by the human liver, three experimentally viable human livers, declined for transplantation, were perfused with CeO₂NPs under normothermic machine perfusion (NMP) (Supporting Information). Liver function tests and hemodynamic parameters were monitored during perfusion (data not shown) to ensure organ viability and proper device functioning.

To study the cellular uptake and intracellular localization of CeO₂NPs in human livers, ICP-MS and TEM imaging were performed. The concentration of Ce in the serum leaving the liver through the hepatic veins reached the highest levels 15 minutes after NPs administration (Fig. 7A). At 30 minutes of perfusion, the amount of Ce in the perfusate was reduced by at

least 50% when compared to the previous time point and further decreased at 60 minutes. In the case of donor H3, at 60 minutes of NMP, the Ce concentration in the perfusate was still around 45% due to the fact that in this particular organ the injected dose of NPs was almost 100 times higher than in H1 and H2 livers.

Ce subcellular location was examined using conventional bright and enhanced dark field TEM. Liver tissue from all donors was morphologically well preserved, and the cells presented a viable morphology. Liver biopsies obtained from donor H3 were examined under conventional TEM and energy-dispersive X-ray spectroscopy (EDX). In conventional TEM, CeO₂NPs appeared as small, dense, black structures in the form of agglomerates of different sizes inside blood vessels, the space of Disse, endothelial cells, and some blood circulating cells (Fig. 7B). CeO₂NPs

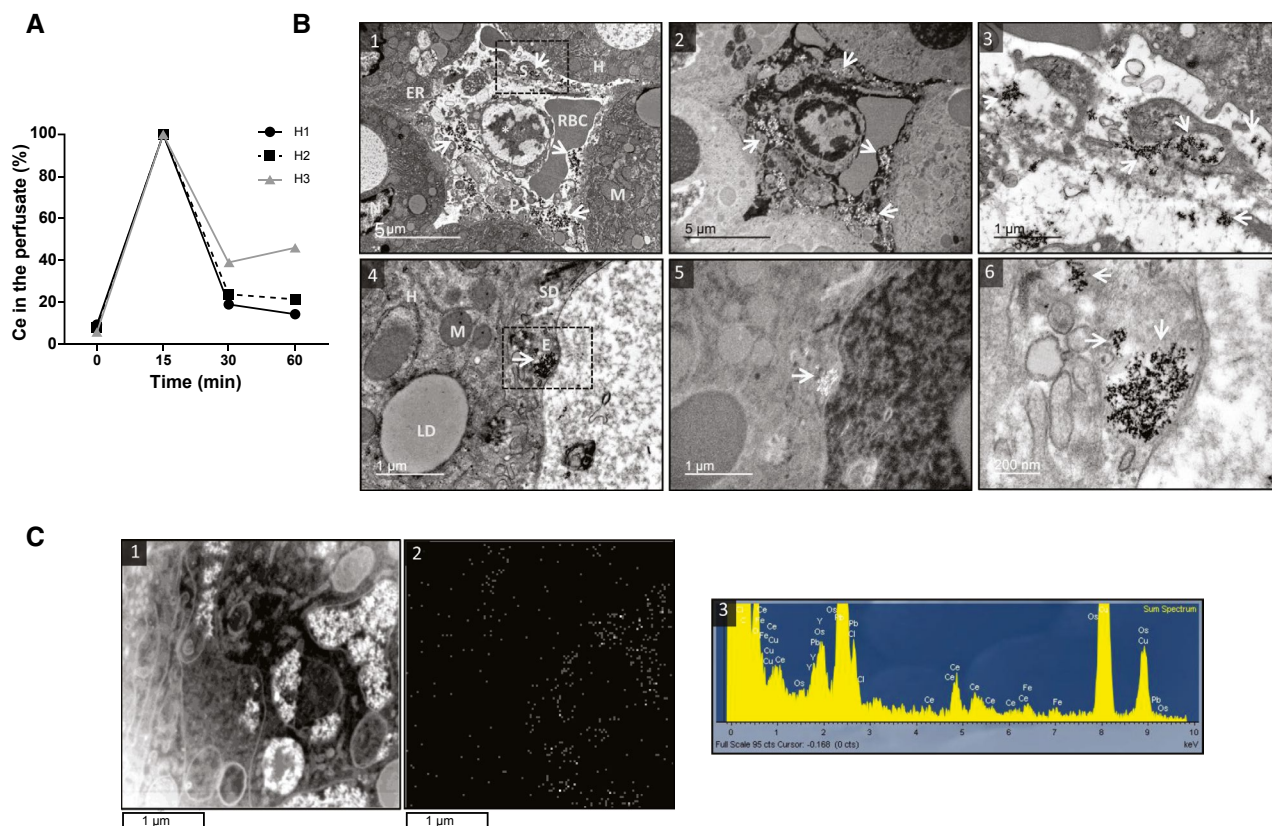


FIG. 7. Accumulation of Ce in isolated human livers. (A) Amount of Ce in the perfusate 0, 15, 30, and 60 minutes after NP administration. ICP-MS data are expressed as percent of Ce present in the perfusate compared to the highest Ce amount present in the serum of each liver. (B) Assessment of CeO_2 NPs subcellular location in human hepatic tissue after 1 hour of NP infusion; (1,2,3) TEM image of a blood vessel containing NPs surrounded by hepatocytes. In bright field (1), aggregates of CeO_2 NPs (white arrows) appear as dark, electron-dense spots. In dark field (2), nanoparticles are seen bright. (3) Magnified view of the boxed area depicting the nanoparticles in the space of Disse. (4,5) TEM image of a hepatocyte in the proximity of an endothelial cell containing CeO_2 NPs, bright and dark field, respectively. (6) High-magnification micrograph of the boxed area showing in detail the NPs inside the endothelial cell. *Apoptotic cell. (C) (1) STEM-HAADF image of endosome-like vesicles of an endothelial cell. (2) STEM-EDX element-distribution map showing the spatial distribution of Ce in the region outlined. Four adjacent pixel/spectra binned for each point. (3) EDX sum spectrum ($Y = \text{counts}$, $X = \text{keV}$) showing the average elemental composition of the image. Abbreviations: E, endothelial cell; ER, endoplasmic reticulum; H, hepatocyte; LD, lipid droplet; M, mitochondria; N, nucleus; P, platelet; RBC, red blood cell; S, sinusoid; SD, space of Disse.

were observed both free and within intracellular, single-membrane, endosome-like organelles. In dark field TEM, given its high atomic number relative to the elements typically found in organic tissues, Ce is expected to appear as very bright dots, as shown in Fig. 7B. The presence of Ce was further confirmed using high-angle annular dark-field scanning transmission electron microscopy (HAADF-STEM), which provides structural and chemical information with atomic resolution. Figure 7C shows a representative region in the set of analyzed images. The elemental map (central panel) shows the spatial distribution of Ce in the region outlined in the left panel, and the

EDX spectrum (right panel) confirms the elemental composition. In addition to Os from the postfixation, Cu from the TEM grid, and Pb from the staining, Ce is the only element detected by using EDX analysis.

CeO_2 NPs ADSORPTION BY HUMAN HEPATOCYTE CANCER CELLS

To assess whether human hepatocytes can internalize CeO_2 NPs, HepG2 cells, a human derived cell cancer line, were exposed to CeO_2 NPs ($10 \mu\text{g/mL}$) for 24 hours and subjected to TEM analysis. NPs were

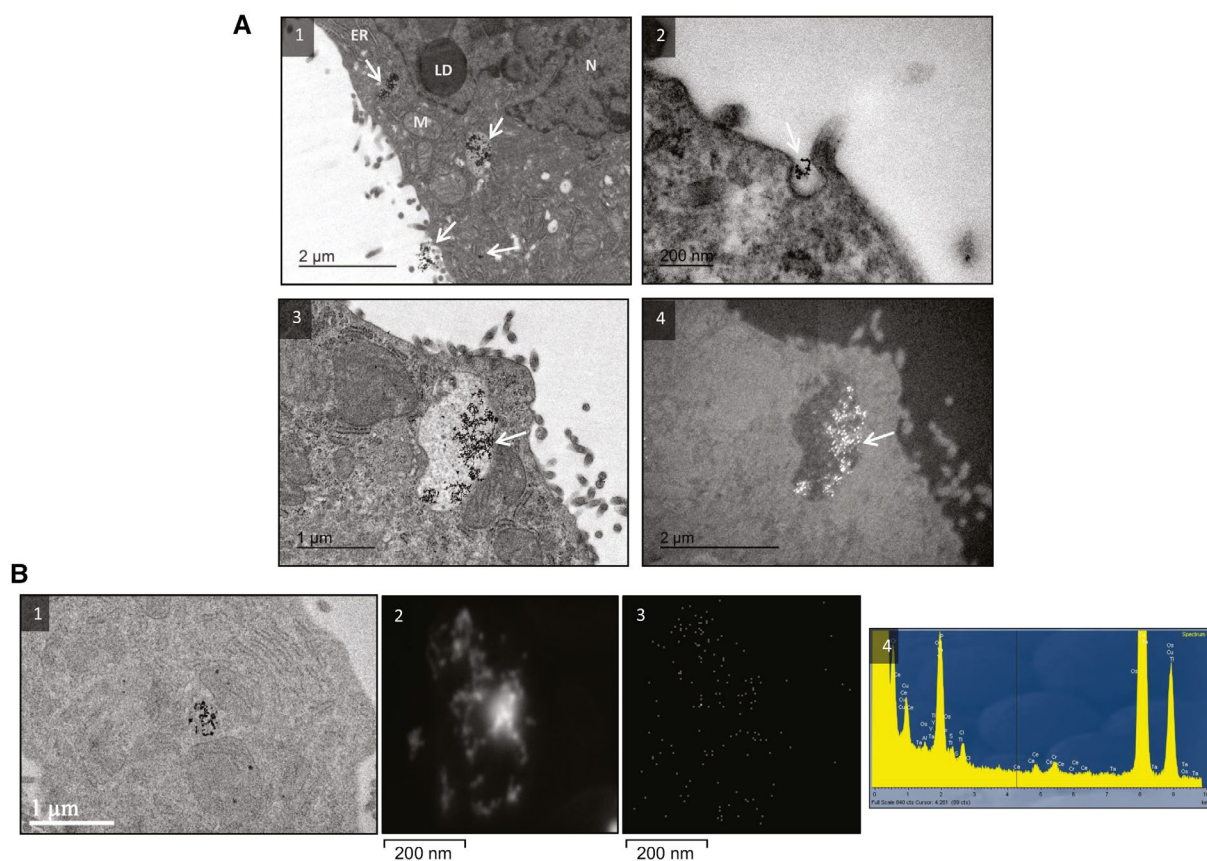


FIG. 8. CeO₂NPs adsorption in human hepatocyte cancer cells. (A) TEMs of HepG2 cells showing the uptake of NPs: (1) hepatocyte exposed to CeO₂NPs (white arrows) for 24 hours, with some NPs adhering to the cell membrane, others confined to vesicles, and a few free in the cytoplasm; (2) formation of pseudopodia with NPs in the center; (3,4) vesicle loaded with CeO₂NPs in bright and dark fields, respectively. (B) (1) TEM image displaying NPs in the cytoplasm of a hepatocyte; (2) STEM-HAADF image from the NPs; (3) Ce elemental mapping with four adjacent pixel/spectra binned for each point; (4) EDX sum spectrum (Y = counts, X = keV) showing the average elemental composition of the image. Abbreviations: ER, endoplasmic reticulum; LD, lipid droplet; M, mitochondria; N, nucleus.

strongly attached to the outer leaflet of the plasmatic membrane, free in the cytoplasm, and mostly inside numerous endosome-like bodies of diverse morphology (Fig. 8A). The mitochondria, the endoplasmic reticulum, and the nucleus of these hepatocytes appeared normal. To verify that the electron-dense granules were indeed CeO₂NPs, we performed dark field microscopy followed by HAADF-STEM. In both dark field TEM and STEM, NPs appeared as bright spots. The Ce elemental map and EDX spectrum confirmed the presence of Ce in the preparations (Fig. 8B).

Discussion

The ability of nanocerium to catalyze redox reactions has been widely used in petrochemical

industries and catalytic exhaust converters for decades.⁽³³⁾ The use of these NPs as a therapeutic tool is still a matter of concern. This is mainly due to the tendency of CeO₂NPs to evolve when in contact with physiological media.⁽³⁴⁾ Variability in the response and loss of antioxidant activity are the outcomes of these alterations. In the current investigation, some of these difficulties have been overcome by preparing albumin-coated CeO₂NPs with high monodispersity and high stability in the physiological media. This coating prevents the development of large NP aggregates and protein corona formation, resulting in a stable colloidal solution with sustained and more intense effects.

Unfortunately, HCC is still rather orphan in terms of highly effective systemic treatment. In this context, oxidative stress, mainly contributed by ROS, has

been implicated in the pathogenesis of several diseases including cancer. It is well known that ROS can drive the initial development and progression of cancer as well as down-regulate antioxidant enzymes that normally combat free radical production.⁽¹⁰⁾ Consequently, many antioxidant compounds, enzymes, and inhibitors of reduced nicotinamide adenine dinucleotide phosphate oxidase have been studied for treating chronic inflammation and cancer. However, results to date have been suboptimal, mainly due to their low systemic bioavailability and insufficient levels at the target sites.

Here we consider that CeO₂NPs could be an NP-based therapy platform in HCC, which would be able to induce ROS degradation and tumor recession by virtue of their great self-regenerating antioxidant capacity. Because the antioxidant effect of CeO₂NPs is catalytic and consequently permanent, this would represent a clear competitive advantage over other antioxidant therapies needing permanent application. In addition, CeO₂NPs are only active as a catalyst when there is an excess of ROS; otherwise, they are inert and appear innocuous.

The carcinogenic effect of DEN is due to an enhancement of hepatocyte proliferation mainly in the centrilobular hepatocytes. DEN is bioactivated following hydroxylation by the cytochrome P450 (CYP) system; then, the hydroxylated DEN is oxidized by CYP2E1 to reactive products in rat liver liposomes. DEN-treated rats displayed macroscopically distorted liver, with altered liver weight and anomalous microscopic architecture of the liver parenchyma showing diffuse dysplasia and fibrotic tracts. This prompted us to assess whether the HCC liver, as indeed occurs in the normal liver, is also a main target for CeO₂NPs. Our results further confirm that, even in a liver with intense tumorigenic activity, CeO₂NPs maintain their high selective targeting on the hepatic tissue.

Parameters indicating altered tissue growth or proliferation and ongoing proinflammatory processes were significantly less activated in rats receiving CeO₂NPs. Treated rats showed increased liver/body weight ratio, decreased macrophage infiltration, and lower amount of Ki67-positive cells. Ki67 is a nuclear antigen extensively used as a proliferation marker and as a prognostic indicator for cancer. We also observed decreased serum concentration of AFP, the main serological biomarker of dedifferentiation

of hepatocytes that is associated with the development of HCC. This occurred in the frame of attenuated macrophage M1 proinflammatory gene expression in the liver tissue of HCC-treated rats. Tumor-associated macrophages are well known for their trophic abilities and for providing immunosuppressive tumor microenvironment and therefore facilitating tumor progression.⁽³⁵⁾ In that sense, lowering macrophage numbers in liver tissue by means of chemotaxis inhibition or cell death could partially explain the antitumor effects of nanoceria.

Evidence supports that CeO₂NPs have a specific antitumorigenic effect in HCC rats. First, following NPs administration, we observed increased liver apoptotic activity. This is consistent with previous studies describing that after exposure to antioxidant cuprous oxide NPs, lung melanoma cells activate caspase-3 and caspase-9, inducing apoptosis of tumor cells.⁽³⁶⁾ On the other hand, CeO₂NPs also resulted in decreased levels of P-ERK1/2, an essential component of the Ras/Raf/MAPK kinase/ERK signaling pathway. This is among the principal routes controlling cell survival, differentiation, proliferation, growth, angiogenesis, regulation of glucose and lipid metabolism, and inflammation.⁽³⁷⁾

The impact of CeO₂NPs on cell phosphorylation in HCC has not been systematically investigated using untargeted MS-based proteomics. Our initial principal component analysis suggests a global effect of CeO₂NPs over protein phosphorylation in the liver of HCC rats that significantly affected 9.5% of all detected phosphorylation sites. The effect of CeO₂NPs comprised both increased and decreased phosphorylation. The administration of CeO₂NPs affected kinases involved in signaling pathways related to apoptosis, cell proliferation, migration, and survival such as p21 (RAC1) activated kinase 2, eukaryotic elongation factor 2 kinase, protein tyrosine kinase 2/focal adhesion kinase 2, and NIMA-related kinase 9. Interestingly, a gene ontology analysis showed an enrichment of proteins linked to RNA splicing and cell-cell adhesion in the subset of proteins whose phosphorylation were significantly regulated after CeO₂NPs treatment. Splicing is a process frequently deregulated in cancer cells because it can regulate the function of key proteins involved in apoptosis, proliferation, angiogenesis, and migration.⁽³⁸⁾ In this regard, CeO₂NPs treatment that reduced cell proliferation caused both an increase and a decrease in the phosphorylation of proteins involved in splicing. Cell adhesion is also a

process heavily deregulated in cancer cells with multiple proteins involved in cell–cell adhesion considered as tumor suppression or oncogenes.⁽³⁹⁾ Our gene ontology analysis indicates that CeO₂NPs produce a large effect on the phosphorylation pattern of proteins involved in cell–cell adhesion with proteins presenting both overphosphorylation and downphosphorylation, suggesting an alteration in this biological process. We observed a reduced phosphorylation of two other cell surface proteins involved in cell adhesion, CD44 and Itgb4.

A hallmark of cancer cells is dysregulation of FA metabolism to support proliferation.⁽⁴⁰⁾ Accordingly, total serum TG and cholesterol were found to be significantly decreased in HCC rats. Highly proliferative cancer cells have strong lipid and cholesterol avidity; consequently, these cells either increase the uptake of exogenous lipids or overactivate their endogenous synthesis.⁽⁴¹⁾ Excessive lipids and cholesterol in cancer cells are stored in lipid droplets as cholesteryl esters,⁽³⁷⁾ which is in agreement with our findings of increased CE-derived FAs in hepatic HCC tissue. The analysis of principal lipid components also revealed an increase in NEFA probably due to an increased generation to support tumor growth.

The most important effects induced by CeO₂NPs are found in PC-derived FAs. The decrease in PC-PUFAs resulting from CeO₂NPs administration was mostly due to a decrease in AA.⁽⁴²⁾ Phospholipases A₂, C, and D can mediate the release of esterified AA from cellular phospholipids, a process which already seems incremented in HCC. Free AA can be metabolized through enzymatic reactions or act as a second messenger in signal transduction pathways⁽⁴³⁾; some of these pathways were demonstrated to be significantly up-regulated in our HCC rats. After nanoceria treatment, the decrease in esterified PC-AA was more pronounced. This phenomenon seems to be related to the increase of apoptosis in these rats because free AA is able to promote the activation of sphingomyelinase and the apoptotic process.⁽⁴⁴⁾

CeO₂NPs treatment reversed the increase in NEFA-derived, TG-derived, and CE-derived LA in HCC rats. LA, one of the most abundant FAs in all lipid components, has been reported to change the metabolism of intrahepatic CD4⁺ T cells, leading them to apoptosis and, thus, contributing to HCC development.⁽⁴⁴⁾ Neoplastic hepatocyte lesions have been associated with changes in the PUFA profile,

which are likely due to an abnormal essential FA metabolism involving Δ -6 desaturase (Δ -6D).⁽⁴³⁾ The activity and expression of this desaturase are regulated by the intracellular redox state.⁽⁴⁵⁾ This suggests that the restoration of normal hepatic levels of LA in the HCC rats treated with CeO₂NPs could result from the reactivation of Δ -6D activity due to the reduction in oxidative stress.

The translation of the antitumorigenic effects induced by CeO₂NPs into a clinically significant improvement was assessed by investigating the effect of CeO₂NPs on survival. Treated HCC rats showed a clear amelioration in this parameter. To date, tyrosine kinase inhibitors, such as sorafenib, lenvatinib, cabozatinib, or regorafenib, as well as the antiangiogenic antibody ramucirumab, are considered effective therapies in patients with advanced HCC.⁽⁴⁶⁾ The effect of CeO₂NPs on overall survival was similar to that observed with sorafenib, which indicates that these NPs are at least as effective as sorafenib under the conditions studied. The combination of both treatments did not result in an additional improvement in survival in comparison to each treatment administered alone. CeO₂NPs and sorafenib likely interfere with common signaling pathways, such as angiogenesis through vascular endothelial growth factor signaling, which would explain why the combination of both compounds did not result in any additional effect. The effects of CeO₂NPs on the ERK1/2 signaling pathway, the modulation of the phosphorylation state of a high number of peptides, and their manifestations on cell proliferation and apoptosis mirror some of the abundant data reported on sorafenib effects.⁽⁴⁷⁾

For a comprehensive understanding of whether the behavior of CeO₂NPs in the human liver resembles that observed in rats with HCC, we administered nanoceria to human livers under *ex vivo* normothermic perfusion. The *ex vivo* experiments confirmed that CeO₂NPs have high avidity for human liver because they accumulate in the target tissue readily after administration. The NPs were found both free and within intracellular, single-membrane, endosome-like organelles. The elemental analysis combined with the STEM helped us to confirm their presence and distinguish them from endogenous structures and artifacts in the tissue. Moreover, *in vitro* experiments with the HepG2 cell line confirmed the uptake and retention of

CeO₂NPs by human hepatocyte cancer cells mostly in endosome-like bodies.

In conclusion, these results indicate that the anti-oxidant properties of CeO₂NPs partially revert cell mechanisms involved in tumor progression and significantly increase survival in HCC rats, indicating that this inorganic nanomaterial represents an effective treatment in experimental HCC. These findings suggest that CeO₂NPs alone or in combination with the current molecular targeted therapies could be effective at stopping or attenuating the tumoral progression in patients with HCC.

Acknowledgment: We thank the Scientific and Technology Centers of the University of Barcelona (CCiT-UB) for their contribution to the ultrastructural examination and the subcellular location of CeO₂NPs in human liver samples and HepG2 human hepatocytes.

Author Contributions: Contributions to conception and design by G.F.V., V.P. and W.J. Acquisition of data by G.F.V., M.P., S.C., D.O., E.C., L.B., L.O., L.M.M., S.M., G.C., P.C., M.C.P., and W.J. Data analysis and interpretation by G.F.V., M.P., E.C., M.M.R., P.C., P.R.C., V.P. and W.J. Drafting the article by G.F.V., M.P., V.P. and W.J. Revising it critically for important intellectual content by J.B., P.C., P.R.C., M.N., J.F., and J.C.G.V. Final approval of the version to be published by V.P. and W.J.

REFERENCES

- Bray F, Ferlay J, Soerjomataram I, Siegel R, Torre L, Jemal A. Global cancer statistics 2018: GLOBOCAN estimates of incidence and mortality worldwide for 36 cancers in 185 countries. *CA Cancer J Clin* 2018;68:394-424.
- European Association for the Study of the Liver. EASL clinical practice guidelines: management of hepatocellular carcinoma. *J Hepatol* 2018;69:182-236.
- Zhang DY, Friedman SL. Fibrosis-dependent mechanisms of hepatocarcinogenesis. *HEPATOLOGY* 2012;56:769-775.
- Guichard C, Amaddeo G, Imbeaud S, Ladeiro Y, Pelletier L, Maad IB, et al. Integrated analysis of somatic mutations and focal copy-number changes identifies key genes and pathways in hepatocellular carcinoma. *Nat Genet* 2012;44:694-698.
- Llovet JM, Ricci S, Mazzaferro V, Hilgard P, Gane E, Blanc JF, et al. Investigators study group. Sorafenib in advanced hepatocellular carcinoma. *N Engl J Med* 2008;359:378-390.
- Cheng AL, Kang YK, Chen Z, Tsao CJ, Qin S, Kim JS, et al. Efficacy and safety of sorafenib in patients in the Asia-Pacific region with advanced hepatocellular carcinoma: a phase III randomised, double-blind, placebo-controlled trial. *Lancet Oncol* 2009;10:25-34.
- van Malenstein H, Dekervel J, Verslype C, Van Cutsem E, Windmolders P, Nevens F, et al. Long-term exposure to sorafenib of liver cancer cells induces resistance with epithelial-to-mesenchymal transition, increased invasion and risk of rebound growth. *Cancer Lett* 2013;329:74-83.
- Bruix J, Qin S, Merle P, Granito A, Huang YH, Bodoky G, et al.; RESORCE Investigators. Regorafenib for patients with hepatocellular carcinoma who progressed on sorafenib treatment (RESORCE): a randomised, double-blind, placebo-controlled, phase 3 trial. *Lancet* 2017;389:56-66.
- Forner A, Reig M, Bruix J. Hepatocellular carcinoma. *Lancet* 2018;391:1301-1314.
- Waris G, Ahsan H. Reactive oxygen species: role in the development of cancer and various chronic conditions. *J Carcinog* 2006;5:14.
- Calvisi DF, Conner EA, Ladu S, Lemmer ER, Factor VM, Thorgeirsson SS. Activation of the canonical Wnt/beta-catenin pathway confers growth advantages in c-Myc/E2F1 transgenic mouse model of liver cancer. *J Hepatol* 2005;42:842-849.
- Roskams T, Yang SQ, Koteish A, Durnez A, DeVos R, Huang X, et al. Oxidative stress and oval cell accumulation in mice and humans with alcoholic and nonalcoholic fatty liver disease. *Am J Pathol* 2003;163:1301-1311.
- Laviña B, Gracia-Sancho J, Rodríguez-Vilarrupla A, Chu Y, Heistad DD, Bosch J, et al. Superoxide dismutase gene transfer reduces portal pressure in CCl₄ cirrhotic rats with portal hypertension. *Gut* 2009;58:118-125.
- Heckert EG, Karakoti AS, Seal S, Self WT. The role of cerium redox state in the SOD mimetic activity of nanoceria. *Biomaterials* 2008;29:2705-2709.
- Pirmohamed T, Dowding JM, Singh S, Wasserman B, Heckert E, Karakoti AS, et al. Nanoceria exhibit redox state-dependent catalase mimetic activity. *Chem Commun (Camb)* 2010;46:2736-2738.
- Cafun JD, Kvashnina KO, Casals E, Puentes VF, Glatzel P. Absence of Ce³⁺ sites in chemically active colloidal ceria nanoparticles. *ACS Nano* 2013;7:10726-10732.
- Heckert EG, Seal S, Self WT. Fenton-like reaction catalyzed by the rare earth inner transition metal cerium. *Environ Sci Technol* 2008;42:5014-5019.
- Chen J, Patil S, Seal S, McGinnis JF. Rare earth nanoparticles prevent retinal degeneration induced by intracellular peroxides. *Nat Nanotechnol* 2006;1:142-150.
- Schubert D, Dargusch R, Raitano J, Chan SW. Cerium and yttrium oxide nanoparticles are neuroprotective. *Biochem Biophys Res Commun* 2006;342:86-91.
- Pourkhalili N, Hosseini A, Nili-Ahmadabadi A, Hassani S, Pakzad M, Baeri M, et al. Biochemical and cellular evidence of the benefit of a combination of cerium oxide nanoparticles and selenium to diabetic rats. *World J Diabetes* 2011;2:204-210.
- Kim CK, Kim T, Choi IY, Soh M, Kim D, Kim YJ, et al. Ceria nanoparticles that can protect against ischemic stroke. *Angew Chem Int Ed Engl* 2012;51:11039-11043.
- Niu J, Azfer A, Rogers LM, Wang X, Kolattukudy PE. Cardioprotective effects of cerium oxide nanoparticles in a transgenic murine model of cardiomyopathy. *Cardiovasc Res* 2007;73:549-559.
- Colon J, Hsieh N, Ferguson A, Kupelian P, Seal S, Jenkins DW, et al. Cerium oxide nanoparticles protect gastrointestinal epithelium from radiation-induced damage by reduction of reactive oxygen species and upregulation of superoxide dismutase 2. *Nanomedicine* 2010;6:698-705.
- Li H, Liu C, Zeng YP, Hao YH, Huang JW, Yang ZY, et al. Nanoceria-mediated drug delivery for targeted photodynamic therapy on drug-resistant breast cancer. *ACS Appl Mater Interfaces* 2016;8:31510-31523.
- Nourmohammadi E, Khoshdel-Sarkarizi H, Nedacina R, Sadeghnia HR, Hasanzadeh L, Darroudi M, et al. Evaluation of anticancer effects of cerium oxide nanoparticles on mouse fibrosarcoma cell line. *J Cell Physiol* 2019;234:4987-4996.

- 26) Tarnuzzer RW, Colon J, Patil S, Seal S. Vacancy engineered ceria nanostructures for protection from radiation-induced cellular damage. *Nano Lett* 2005;5:2573-2577.
- 27) Patel P, Kansara K, Singh R, Shukla RK, Singh S, Dhawan A, et al. Cellular internalization and antioxidant activity of cerium oxide nanoparticles in human monocytic leukemia cells. *Int J Nanomed* 2018;13:39-41.
- 28) Oró D, Yudina T, Fernández-Varo G, Casals E, Reichenbach V, Casals G, et al. Cerium oxide nanoparticles reduce steatosis, portal hypertension and display anti-inflammatory properties in rats with liver fibrosis. *J Hepatol* 2016;64:691-698.
- 29) Adebayo OA, Akinloye O, Adaramoye OA. Cerium oxide nanoparticles attenuate oxidative stress and inflammation in the liver of diethylnitrosamine-treated mice. *Biol Trace Elem Res* 2020;193:214-225.
- 30) Córdoba-Jover B, Arce-Cerezo A, Ribera J, Pauta M, Oró D, Casals G, et al. Cerium oxide nanoparticles improve liver regeneration after acetaminophen-induced liver injury and partial hepatectomy in rats. *J Nanobiotechnology* 2019;17:112.
- 31) Carvajal S, Perramón M, Oró D, Casals E, Fernández-Varo G, Casals G, et al. Cerium oxide nanoparticles display antilipogenic effect in rats with non-alcoholic fatty liver disease. *Sci Rep* 2019;9:12848.
- 32) Casals E, Gusta MF, Piella J, Casals G, Jiménez W, Puentes V. Intrinsic and extrinsic properties affecting innate immune responses to nanoparticles: the case of cerium oxide. *Front Immunol* 2017;8:970.
- 33) Reed K, Cormack A, Kulkarni A, Mayton M, Sayle D, Klaessig F, et al. Exploring the properties and applications of nanoceria: is there still plenty of room at the bottom? *Environ Sci Nano* 2014;1:390-405.
- 34) Casals E, Gonzalez E, Puentes VF. Reactivity of inorganic nanoparticles in biological environments: insights into nanotoxicity mechanisms. *J Phys D Appl Phys* 2012;45:44.
- 35) Krenkel O, Tacke F. Liver macrophages in tissue homeostasis and disease. *Nat Rev Immunol* 2017;17:306-321.
- 36) Wang Y, Yang F, Zhang HX, Zi XY, Pan XH, Chen F, et al. Cuprous oxide nanoparticles inhibit the growth and metastasis of melanoma by targeting mitochondria. *Cell Death Dis* 2013;29:e783.
- 37) Asati V, Mahapatra DK, Bharti SK. PI3K/Akt/mTOR and Ras/Raf/MEK/ERK signaling pathways inhibitors as anticancer agents: structural and pharmacological perspectives. *Eur J Med Chem* 2016;109:314-341.
- 38) Czuby A, Piekliko-Witkowska A. Protein kinases that phosphorylate splicing factors: roles in cancer development, progression and possible therapeutic options. *Int J Biochem Cell Biol* 2017;91:102-115.
- 39) Fearnley GW, Young KA, Edgar JR, Antrobus R, Hay IM, Liang WC, et al. The homophilic receptor PTPRK selectively dephosphorylates multiple junctional regulators to promote cell-cell adhesion. *eLife* 2019;8:e44597.
- 40) Röhrig F, Schulze A. The multifaceted roles of fatty acid synthesis in cancer. *Nat Rev Cancer* 2016;16:732-749.
- 41) Bechmann LP, Hannivoort RA, Gerken G, Hotamisligil GS, Trauner M, Canbay A. The interaction of hepatic lipid and glucose metabolism in liver diseases. *J Hepatol* 2012;56:952-964.
- 42) Hanna VS, Hafez EAA. Synopsis of arachidonic acid metabolism: a review. *J Adv Res* 2018;11:23-32.
- 43) Abel S, Smuts CM, de Villiers C, Gelderblom WC. Changes in essential fatty acid patterns associated with normal liver regeneration and the progression of hepatocyte nodules in rat hepatocarcinogenesis. *Carcinogenesis* 2001;22:795-804.
- 44) Brown ZJ, Fu Q, Ma C, Kruhlik M, Zhang H, Luo J, et al. Carnitine palmitoyltransferase gene upregulation by linoleic acid induces CD4⁺ T cell apoptosis promoting HCC development. *Cell Death Dis* 2018;9:620.
- 45) Valenzuela R, Echeverria F, Ortiz M, Rincón-Cervera MÁ, Espinosa A, Hernandez-Rodas MC, et al. Hydroxytyrosol prevents reduction in liver activity of Δ -5 and Δ -6 desaturases, oxidative stress, and depletion in long chain polyunsaturated fatty acid content in different tissues of high-fat diet fed mice. *Lipids Health Dis* 2017;16:64.
- 46) Bruix J, Reig M, Sherman M. Evidence-based diagnosis, staging, and treatment of patients with hepatocellular carcinoma. *Gastroenterology* 2016;150:835-853.
- 47) Wilhelm SM, Adnane L, Newell P, Villanueva A, Llovet JM, Lynch M. Preclinical overview of sorafenib, a multikinase inhibitor that targets both Raf and VEGF and PDGF receptor tyrosine kinase signaling. *Mol Cancer Ther* 2008;7:3129-3140.

Author names in bold designate shared co-first authorship.

Supporting Information

Additional Supporting Information may be found at onlinelibrary.wiley.com/doi/10.1002/hep.31139/supinfo.

BESPOKEN NANOCERIA: A NEW EFFECTIVE TREATMENT IN EXPERIMENTAL HEPATOCELLULAR CARCINOMA

Guillermo Fernández-Varo^{1,7}, Meritxell Perramón¹, Silvia Carvajal¹, Denise Oró¹, Eudald Casals², Loreto Boix³, Laura Oller¹, Laura Macías-Muñoz¹, Santi Marfà¹, Gregori Casals^{1,8}, Manuel Morales-Ruiz^{1,7,8}, Pedro Casado⁴, Pedro R. Cutillas⁴, Jordi Bruix³, Miquel Navasa⁵, Josep Fuster⁵, Juan Carlos Garcia-Valdecasas⁵, Mihai C. Pavel⁵, Víctor Puntès⁶, Wladimiro Jiménez^{1,7}.

Supplementary Materials & methods

Supplementary Fig. 1

Supplementary Fig. 2

Supplementary Table 1

Supplementary Table 2

Supplementary Table 3

Supplementary Table 5

Supplementary References

Supplementary Materials & methods

Synthesis and characterization of rat serum albumin (RSA) stabilized CeO₂NPs: As-synthesized CeO₂NPs were conjugated with RSA to increase their biocompatibility and solubility in physiological media. Albumin was added 100-fold the amount needed to cover CeO₂NPs surface to ensure complete coverage. 10 mg of RSA were dissolved in 1 ml of PB 50 mM without stirring and kept in the fridge until its complete dissolution. Then 10 ml of CeO₂NPs were added dropwise to the protein solution while applying a mild stirring. The sample was kept in the fridge during 24 hours to allow the complete adsorption of RSA molecules onto the NPs surface. Both the synthesis and conjugation of NPs were performed under sterile conditions. CeO₂NPs were kept at 4 °C until administration to animals.

The surface charge of the NPs was characterized in a Z-sizer (Malvern, Worcestershire, UK) while the crystal size was characterized by high-resolution (HR-TEM) in the Tecnai G2 F20 at 200 kV (FEI, Oregon, USA). The crystal structure was analyzed by HR-TEM (Tecnai 200 kV and XRD 8Xpert Pannalytical, MA, USA), and the light interaction by UV-VIS spectroscopy (Shimatzu, Kyoto, Japan). Size distribution was computer analyzed by Image J (National Institutes of Health, Bethesda, MD, USA).

X-ray Photoelectron Spectroscopy (XPS): X-ray Photoelectron Spectroscopy (XPS) was performed on a SPECS system equipped with a monochromatic Al source operating at 300 W and a Phoibos 150 MCD-9 detector. Binding energy (BE) values were referred to the C 1s peak at 285.0 eV. Data processing was performed with the CasaXPS software. Cerium 3d spectra were analyzed using six peaks for Ce⁴⁺ (V, V'', V''', U, U'' and U'''),

corresponding to three pairs of spin-orbit doublets, and four peaks (two doublets) for Ce^{3+} (V_0 , V' , U_0 and U'), based on the peak positions reported by Mullins et al. (1), where U and V refer to the $3d_{3/2}$ and $3d_{5/2}$ spin-orbit components, respectively.

Organ accumulation of Ce in HCC rats: To determine the main target organs of CeO_2NPs , 7 DEN-injured rats were included in the study. The animals were randomly euthanized at the 14th (n=3) and 21st (n=4) day after the last administration of CeO_2NPs . Next, blood samples were collected and the organs were dissected and kept at $-80\text{ }^\circ\text{C}$ for Ce content quantification.

Effect of CeO_2NPs on tumor progression: This protocol included 20 rats with HCC receiving CeO_2NPs (n=10) or vehicle (n=10). The animals were euthanized with an overdose of isoflurane (5%) 2 weeks after the last administration of DEN, to avoid the local effects of acute necrosis. The liver from each animal was dissected, weighed and macroscopically examined. Thereafter, liver specimens were snap frozen and stored at $-80\text{ }^\circ\text{C}$ for further mRNA and protein expression analysis. Liver samples were also fixed in 10% buffered formalin for further hematoxylin and eosin (H&E), sirius red and immunostaining analysis. Serum samples were frozen at $-20\text{ }^\circ\text{C}$ until further determination of standard parameters of liver function and serum concentration of α -fetoprotein (AFP) and cytokines.

Effect of CeO_2NPs on survival in HCC rats: To investigate whether nanoceria administration is able to improve survival in experimental HCC, 43 DEN-treated rats randomly received CeO_2NPs (n=21) or vehicle (n=22). Thereafter animals were kept in their cages until the appearance of signs of deterioration that indicated distress such as severe piloerection, secretion of the

Harderian gland, ascites, jaundice, hemorrhage, weight loss of more than 20 % of the body weight or abnormal posture and behavior. At this point, rats were euthanized with an isoflurane overdose. In addition, the effect of CeO₂NPs on overall survival was compared to the well-established antitumoral agent sorafenib. With this purpose, 40 DEN-injured rats randomly received two intravenous weekly doses of CeO₂NPs (n=10) or vehicle (TMAOH, n=10) for two weeks or a daily intragastric administration of sorafenib (10 mg/kg, n=10) for 14 days or the combined administration of CeO₂NPs plus sorafenib (n=10). Survival was evaluated as indicated above.

Histological examination and quantification of fibrosis and apoptosis in liver tissue: Liver sections (4 μm) were stained with H&E and digital images were acquired at 40X magnification with a microscope (Eclipse E600; Nikon, Tokyo, Japan) coupled to a digital camera (RT-Slider Spot; Diagnostic Instruments, Sterling Heights, MI, USA).

Fibrosis measurement was performed using in 0.1% Sirius red F3B (Sigma-Aldrich, St. Louis, MO, USA) in saturated picric acid (Sigma-Aldrich, St. Louis, MO, USA). Relative fibrosis area (expressed as a percentage of total liver area) was assessed by analyzing 32 fields of Sirius red-stained liver sections per animal. Each field was acquired at 100X magnification as described above and the results were analyzed using imaging software (ImageJ, National Institutes of Health, Bethesda, MD, USA). To evaluate the relative fibrosis area, the collagen area measured was divided by the net field area and then multiplied by 100. Subtraction of vascular luminal area from the total field area yielded the final calculation of the net fibrosis area. The amount

of fibrosis measured in each animal was analyzed, and the average value was presented as a percentage.

To determine the degree of hepatic apoptosis we used the terminal deoxynucleotidyl transferase dUTP nick-end labeling (TUNEL) assay (2) using the fluorescein-FragEL DNA fragmentation detection kit (In Situ Cell Death Detection Kit, TMR red, Roche) according to the manufacturer's protocol. To quantify and compare the rates of cell death between both groups, a semiquantitative scoring method was used. For each sample, the number of TUNEL-positive cells was counted per 200X high-power field. At least eight representative fields were evaluated for each experimental group, from which an average value was calculated.

Immunodetection of CD68 and Ki67: Liver sections from fibrotic rats underwent microwave antigen retrieval to unmask antigens hidden by cross-linkage occurring during tissue fixation. Endogenous peroxidase activity was blocked by hydrogen peroxide pretreatment for 10 min and with 5% goat serum for 45 min. Infiltrating macrophages/monocytes in the liver tissue and hepatocyte proliferation were assessed by CD68 and Ki67 immunostaining, respectively, using an immunoperoxidase method. The sections were stained with mouse anti-CD68 (1:150; AbD Serotec, Oxford, UK) or with rat anti-Ki67 (1:100; Abcam plc, Cambridge, UK) antibodies and incubated for 1.5 and 1h, respectively, at RT. The LSAB 2 System-HRP (Dako Denmark A/S) was used for antigen detection, and antigen visualization was achieved with streptavidin peroxidase and counterstained with hematoxylin. Stainings were visualized using a digital microscope at 200X high-power field. Macrophages (CD68-positive cells) were quantified by counting 20 random fields per each section

and the area of Ki67-positive staining was assessed 10 random fields per animal.

Hepatic messenger expression of inflammatory, macrophage phenotype and cell growth related genes: Total RNA was extracted from the middle liver lobe of control and DEN-injured rats using a commercially available kit (RNAeasy; QIAGEN, Hilden, Germany). The RNA concentration was determined by spectrophotometric analysis (ND-100 spectrophotometer; Thermo Fischer Scientific, Waltham, MA, USA). One microgram of total RNA was reverse-transcribed using a cDNA synthesis kit (High-Capacity cDNA Reverse Transcription Kit; Applied Biosystems, Foster City, CA, USA). Specific primers and probes used for the different genes studied were designed to include intron spanning using the Universal Probe Library Assay Design Center through ProbeFinder version 2.5 software (Roche Diagnostics, Indianapolis, IN, USA; <http://lifescience.roche.com/shop/es/mx/overviews/brand/universal-probe-library>). A panel of selected genes dealing with inflammation, macrophage phenotype, cell growth and differentiation was analyzed. The panel included the following: Interleukin 1 β (IL1- β) (probe 76: left 5'-CAGGAAGGCAGTGCTCACTCA-3' and right 5'-TCCCACGAGTCACAGAGGA-3'), Tumor Necrosis Factor α (TNF α) (probe 68: left 5'-CGTAGCCCACGTCGTAGC-3' and right 5'-GGTTGTCTTTGAGATCCATGC-3'), Interleukin 6 (IL-6) (probe 20: left 5'-CCCTTCAGGAACAGCTATGAA-3' and right 5'-ACAACATCAGTCCCAAGAAGG-3'), inducible Nitric Oxide Synthase (iNOS) (probe 95: left 5'-AAAATGGTTTCCCCCAGTTC-3' and right 5'-CAGCTTGTCCAGGGATTCTG-3') and Cyclooxygenase 2 (COX-2) (probe 125: left 5'-GATGCTATCTTTGGGGAGACC-3' and right 5'-

CCATAAGGCCTTTCAAGGAGA-3'), Cluster of Differentiation 163 (CD163) (probe 73: left 5'-ATGGGGAAGGCACAACACTG-3' and right 5'-TCAGATCCGCTCCGTCTAA-3') Arginase 1 (ARG-1) (probe 66: left 5'-TGGGAAAAGCCAATGAACA-3' and right 5'-TGCTTCCAATTGCCATACTG-3'), Peroxisome Proliferator-Activated Receptor γ (PPAR γ) (probe 125: left 5'-CCCAATGGTTGCTGATTACA-3' and right 5'-GGACGCAGGCTCTACTTTGA-3') and Vascular Endothelial Growth Factor A (VEGFA) (probe 66: left 5'-CCTGTGTGCCCTAATGC-3' and right 5'-AGGTTTGATCCGCATGATCT-3'), Hypoxanthine-Guanine Phosphoribosyltransferase (HPRT) (probe 95: left 5'-ACCTGGTTCATCATCACTAATCAC-3' and right 5'-GACCGTTCTGTCATGTCG-3') was used as the reference gene. Primers were designed according to rat sequences (GenBank codes NM_031512.2, NM_012675.2, NM_012589.1, NM_012611.3, NM_017232.3, NM_001107887.1, NM_017134.2, NM_013124.3, NM_031836.3, and NM_012583.2). Real-time quantitative polymerase chain reaction (RT-PCR) was analyzed in duplicate and performed with the LightCycler 480 (Roche Diagnostics). A 10 μ l volume reaction of diluted 1:8 cDNA, 200 nM primer dilution, 100 nM prevalidated 9-mer probe (Universal ProbeLibrary) and FastStart TaqMan Probe Master (Roche Diagnostics) were used in each PCR. A fluorescence signal was captured during each of the 45 cycles (denaturing for 10 s at 95 °C, annealing for 20 s at 60 °C, and extension for 1 s at 72 °C). Water was used as a negative control. Relative quantification was calculated using the comparative threshold cycle (Ct), which is inversely related to the abundance of mRNA transcripts in the initial sample. The mean Ct of duplicate measurements was used to calculate Δ Ct as the difference in Ct for target and

reference. The relative quantity of product was expressed as fold induction of the target gene compared with the reference gene according to the formula $2^{-\Delta\Delta CT}$, where $\Delta\Delta CT$ represents ΔCT values normalized with the mean ΔCT of control samples.

Western blot analysis of caspase-3, and ERK1/2: Hepatic tissue from control and DEN-injured rats was individually homogenized as described previously (3). To detect activated caspase-3, 40 μ g of total denatured proteins were loaded on a 12% SDS-polyacrylamide gel (Mini-PROTEAN III; Bio-Rad Laboratories, Hercules, CA, USA). Gels were transferred to nitrocellulose membranes of 0.2 μ m at RT for 2 h, were stained with Ponceau S red as control for protein loading and blocked with 1% bovine serum albumin in TTBS buffer at RT for 2h. Membranes were then incubated with rabbit polyclonal anti-activated caspase-3 (1:300 dilution; Abcam, Cambridge, UK) at 4 °C for 48 h. Next, membranes were incubated with a donkey anti-rabbit horseradish peroxidase-conjugated (HRP) secondary antibody (1:2000; Amersham Biosciences, GE Healthcare, Piscataway, NJ, USA) at RT for 1 h. The bands were visualized by chemiluminescence (Luminata Forte Western HRP substrate; EMD Millipore, Billerica, MA, USA). To detect total and phospho-ERK1/2, 40 μ g of total denatured proteins were loaded on a 10% SDS-polyacrylamide gel (Mini-PROTEAN III; Bio-Rad Laboratories, Hercules, CA, USA), respectively. Gels were transferred to nitrocellulose membranes of 0.45 μ m overnight at 4 °C and the membranes were stained with Ponceau S red as control for protein loading and were then blocked with 5% defatted milk in TTBS buffer at RT for 2h. Membranes were then incubated with rabbit polyclonal anti-total-ERK1/2 and anti-phospho-ERK1/2 (1:1000 dilution; Cell Signaling Technology, Beverly, MA)

with 5% defatted milk in TTBS buffer at RT for 2h. Membranes were incubated with a donkey anti-rabbit horseradish peroxidase-conjugated (HRP) secondary antibody (1:2000; Amersham Biosciences, GE Healthcare, Piscataway, NJ, USA) at RT for 1h. Bands were visualized by chemiluminescence (Luminata Forte Western HRP substrate; EMD Millipore, Billerica, MA, USA).

Hepatic lipid profiling by mass spectrometry analysis: Liver tissue (50 mg) was homogenized in chloroform: methanol (2:1, v/v, Scharlab, Barcelona, Spain, 372978 and PanReact AppliChem, Darmstadt, Germany, 1310911611, respectively) containing 0.005 % butylated hydroxytoluene (Sigma Aldrich, Saint Louis, USA, W218405). Glyceryl trinonadecanoate (TG (19:0/19:0/19:0) Sigma Aldrich, Madrid, Spain), cholesteryl heptadecanoate (CE (17:0)), 1,2-dinonadecanoyl-sn-glycero-3-phosphocholine (PC (19:0/19:0)), 1,2-dipentadecanoyl-sn-glycero-3-phosphoethanolamine (PE (15:0/15:0)) and nonadecanoate were used as internal standards. Separation of triglycerides (TG), cholesterol esters (CE), phosphatidylcholines (PC) phosphatidylethanolamines (PE) and non-esterified fatty acids (NEFA) from total lipid liver extracts dissolved in chloroform was performed by solid-phase extraction (SPE) using aminopropyl silica columns as described previously (4,5). First, the CE and TG fractions were eluted with chloroform. Thereafter, PC were eluted with chloroform: methanol (3:2, v/v), PE were eluted with methanol and finally, NEFA were eluted in chloroform: methanol: acetic acid (100:2:2, v/v). In order to isolate CE and TG, the first fraction was evaporated under nitrogen stream, dissolved in hexane (Merck Millipore, Darmstadt, Germany, 104374) and transferred to a fresh preconditioned aminopropyl silica column preconditioned with hexane. Then CE were eluted with hexane, and TG

were eluted with hexane: chloroform: ethylacetate (100:5:5, v/v). All solvent fractions containing isolated lipids were dried under nitrogen stream and transesterified (FAME) with 0.5 M NaOH and boron trifluoride (Sigma Aldrich, Saint Louis, USA, B1252) in methanol.

Gas chromatography mass spectrometry (GC–MS) analyses of FAME were performed on a Shimadzu GC-MS QP2010 Ultra instrument (Kyoto, Japan). Final extracts were injected in splitless mode (valve opened at 1 min) into the gas chromatograph interfaced with a mass selective detector. Chromatographic separation was achieved on a Sapines-5MS+ capillary column (30 m × 0.25 mm internal diameter × 0.25 μm film thickness) from Teknokroma (Barcelona, Spain) with helium as a carrier gas at a constant velocity of 50 cm/s. The temperature program began at 50 °C, was maintained at this temperature for 3 min, then elevated at a 80 °C min⁻¹ rate to 240 °C, followed by an increase at a 2 °C min⁻¹ rate until 290 °C that were maintained for 2 min. The ion source and transfer line temperatures were set at 250 °C and 280 °C, respectively. The mass detector was operated in scan mode. Identification of the FAME in the sample extracts was achieved by mass spectrum and GC retention time comparison with reference standards (Sigma). Results are expressed as pmol or nmol of FA/mg of liver tissue, when appropriate.

Hepatic phosphoproteome analysis: Large-scale phosphoproteomics was used to gain further insight into the main kinase signaling pathways affected by nanoceria treatment. Thousands of phosphorylation sites were simultaneously quantified to estimate changes in kinase activity induced by CeO₂NPs in hepatic tissue of rats with HCC. Liver biopsies from DEN-injured

rats treated with CeO₂NPs (n=6) or receiving vehicle (n=6) were collected and kept at -80 °C. Hepatic tissues were solubilized in urea buffer (8 M Urea in 20 mM HEPES pH 8.0) supplemented with phosphatase inhibitors (1 mM Na₃VO₄, 1 mM NaF, 1mM Na₄P₂O₇ and 1 mM sodium β-glycerophosphate), further homogenized by sonication (30 cycles of 30 s on 30 s off; Diagenode Bioruptor® Plus, Liege, Belgium) and centrifuged to remove insoluble material. Protein amount was quantified by BCA (Thermo Fisher Scientific). For tryptic digestion, protein extracts (500 µg) were subjected to cysteine alkylation by sequential incubation with 10 mM dithiothreitol (DDT) and 16.6 mM iodoacetamide (IAM) for 1 h and 30 min, respectively, at 25 °C and agitation. Then urea concentration was reduced to 2 M by the addition of 20 mM HEPES (pH: 8.0), 100 µl of equilibrated trypsin beads [(50 % slurry of TLCK-trypsin (Thermo-Fisher Scientific; Cat. #20230)] were added and samples were incubated overnight at 37 °C. Trypsin beads were equilibrated by 3 washes with 20 mM HEPES (pH: 8.0). Trypsin beads were removed by centrifugation and resulting peptide solutions were desalted with C-18-Oasis cartridges as indicated by the manufacturer. Briefly, oasis cartridges were conditioned with 1 ml acetonitrile (ACN) and equilibrated with 2.5 ml of wash solution [0.1% trifluoroacetic acid (TFA), 2% ACN]. Peptides were loaded in the cartridges and washed with 1 ml of wash solution. Finally, peptides were eluted with 0.5 ml of glycolic acid buffer 1 (1 M glycolic acid, 5% TFA, 50% ACN). Enrichment of phosphorylated peptides was performed with TiO₂; eluents were normalized to 1 ml with glycolic acid buffer 2 (1 M glycolic acid, 5% TFA, 80% ACN) and incubated with 50 µl of TiO₂ beads buffer (50% bead slurry in 1 % TFA) for 5 min at room temperature. TiO₂ beads were packed by centrifugation in empty

spin columns (Gygen Corporation; Cat. TT2EMT) previously equilibrated by centrifugation with 200 μ l of ACN. TiO₂ loaded spin tips were sequentially washed with 100 μ l of glycolic acid buffer 2, ammonium acetate buffer (100 mM ammonium acetate in 25% ACN) and 10% ACN by RT centrifugation for 3 min at 1,500 g. For phosphopeptide elution, beads were incubated for 1 min at room temperature with 50 μ l of 5% NH₄OH in 10% ACN and centrifuged. This step was repeated three times (n=4). Finally, samples were snap frozen, dried in a SpeedVac, and pellets were stored at -80 °C. Phosphopeptide pellets were resuspended in 9 μ l of reconstitution buffer (20 fmol/ μ l enolase in 3% ACN, 0.1 % TFA) and 5.0 μ l were loaded onto an liquid chromatography tandem mass spectrometry system (LC-MS/MS) consisting on a Dionex UltiMate 3000 RSLC directly coupled to an Orbitrap Q-Exactive Plus mass spectrometer (Thermo Fisher Scientific). Phosphopeptides were loaded in a μ -pre-column (Acclaim™ PepMap™ 100 C18 LC; Cat 160454) and separated in an analytical column (Acclaim™ PepMap™ 100 C18 LC; Cat. 164569) using a gradient that run from 3% to 23% B over 120 min. Solvent A consisted of 3% ACN: 0.1 % FA, and solvent B consisted of 100 % ACN; 0.1 % FA. The UPLC system delivered a flow of 2 μ l/ min (loading) and 300 nl/min (gradient elution). The Q-Exactive Plus acquired full scan survey spectra (m/z 375-1,500) with a 70,000 FWHM resolution followed by data-dependent acquisition in which the 20 most intense ions were selected for HCD (higher energy collisional dissociation) and MS/MS scanning (200-2,000 m/z) with a resolution of 17,500 FWHM. Peptide identification was performed by matching of the MS/MS data to the SwissProt database restricted to rat entries with the Mascot search engine (6). Pescal software (7,8) was used to include all phosphopeptides identified with a mascot

expectancy of <0.05 (~2% false discovery rate) in a database of sites quantifiable by MS. Pescal software calculated peak areas for the extracted ions chromatograms of phosphorylated peptides in this database across all the samples compared.

Gene ontology analysis: David Bioinformatics Resources (V6.8; david.ncifcrf.gov) was used to determine the gene ontologies (GOs) enriched in the set of genes that code for the proteins whose phosphorylation is affected by CeO₂NPs treatment. Thus, genes that code for proteins that present at least 1 phosphorylation site significantly regulated by CeO₂NPs treatment were tested for enrichment using the set of genes that code for all the identified proteins as background. The software used a modified Fisher's Exact Test and GOs that presented a p value <0.05 were considered as enriched.

Accumulation of Ce in isolated human livers: Livers were donated after brain death (DBD; H1) or circulatory death (DCD; H2 and H3) (Maastricht category II). Two of the donors (H1 and H2) were male subjects and one (H3) female. They were aged 86, 62, and 57, respectively. The livers were evaluated during 6 h (n=2, H1 and H2) or 1 h (n=1, H3) of normothermic machine perfusion (NMP) using the OrganOx metra (OrganOx Ltd., Oxford, UK). During the retrieval procedure, the device was set-up as previously described (9). A sterile disposable set was installed on to the device and primed with 500 ml gelofusine (B. Braun Ltd) and three units of donor-matched packed red blood cells from the blood bank. Antibiotics were given at the outset. During the perfusion, heparin, insulin, prostacyclin, bile salts and fat-free parenteral nutrition were infused. Following retrieval of the donor organ by senior surgeons, the back table preparation of the graft was performed at 4 °C,

followed by cannulation of the hepatic artery, portal vein, inferior vena cava and bile duct. Then, the liver was connected to a NMP device and perfusion commenced. Sodium bicarbonate was added to normalize the pH. CeO₂NPs were administered in the perfusate reservoir at time point 0 h. Donors H1 and H2 were administered 20 ml of CeO₂NPs (1 mg/ml), while donor H3 received 92.5 ml of CeO₂NPs (20 mg/ml). During the perfusion, the NMP provided automated pumping, oxygen/air delivery, and heat exchange to control the perfusate within physiological limits of PO_2 and PCO_2 , temperature (37 °C), mean arterial pressure (65–75 mmHg), and inferior vena cava pressure (0–2 mmHg). Samples of the perfusate were collected at different time points (0, 15, 30, 60, 90, 180, and 360 min) for further biochemical analysis and Ce concentration determination. Wedge liver biopsies were taken at the end of NMP and were used for both ultrastructural analysis and Ce concentration determination. The tissue was either fixed or snap-frozen and stored at –80 °C. Ultrastructural analysis was performed using transmission electron microscopy (TEM). Briefly, human liver samples obtained after NMP were fixed in 2% paraformaldehyde and 2.5% glutaraldehyde in phosphate buffer (0.1 M; pH 7.4). After 90 min postfixation with osmium tetroxide and gradual dehydration using acetone, samples were embedded in Spur's resin. Thin sections (approximately 70 nm) were cut, placed on copper grids and then stained with uranyl acetate and lead citrate. The sections were examined and digital photomicrographs taken in a TEM JEOL 1010 operated at 80 kV and equipped with a Gatan Orius CCD camera. Additionally, in order to portrait the structure with atomic resolution and Z-contrast, High Angle Annular Dark Field (HAADF)

Scanning Transmission Electron Microscope (STEM) imaging was performed on JEOL J2100 operating at 200 Kv.

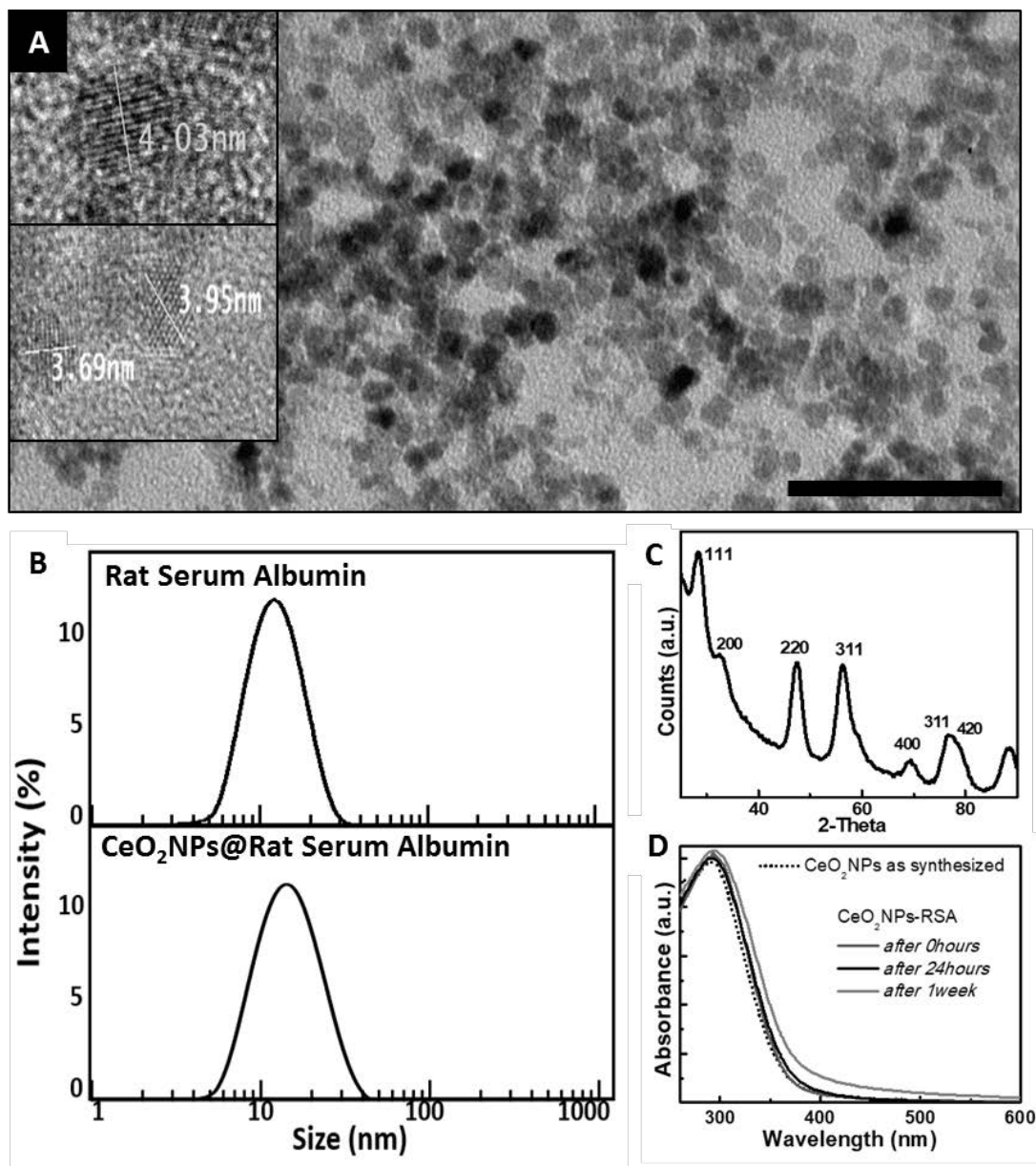
CeO₂NPs adsorption by human hepatocyte cancer cells: This immortalized, stable cell line can be repeatedly frozen, thawed and propagated. Cells were grown to confluence for 24 h in Dulbecco's Modified Eagle Medium (DMEM), supplemented with 50 U/ml penicillin, 50 µg/ml streptomycin, and 10% fetal calf serum (FCS), in a humidified atmosphere in 21% O₂ and 5% CO₂ at 37 °C. Thereafter, cells were switched to serum-free medium for 24h. For cell treatment, old medium was removed and replaced with fresh serum-free medium containing CeO₂NPs (10 µg/ml). Cells were incubated for 24h and then harvested for further TEM imaging as above described.

Other measurements and statistical analysis: Ce concentration in the liver was measured in tissue samples diluted with an aqueous solution of HNO₃ 2% w/w (Trace Metal Basis; Sigma-Aldrich) and analyzed for cerium concentration by inductively coupled plasma mass spectrometry (ICP-MS, Agilent 7500; Agilent Technologies, California, USA). The quantification was done by interpolation in a standard curve obtained from a commercial 1000 ppm Ce standard (Sigma-Aldrich). Standard serum biochemistry parameters were measured in the BS-200E Chemistry Analyzer (Mindray Medical International Ltd, Shenzhen, China) and serum levels of AFP were measured by an ELISA kit (Cusabio, China) following the instructions of the manufacturer. Luminex Magpix-based assay (Luminex corporation, Austin, TX, USA) was used to simultaneously determine the serum concentration of 16 different cytokines including EGF, VEGF, TNF-α, IL-17A, IL-13, IL-12p70, IL-10, IL-6, IL-5, IL-4, IL-2, IL-1β, IL-1α, IFN-γ, GM-CSF and G-CSF (Milliplex MAP Kit, EMD Millipore,

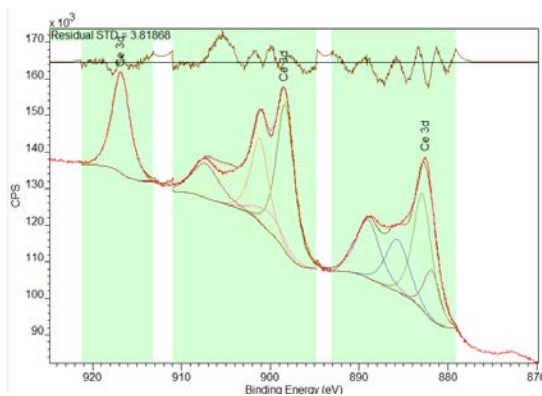
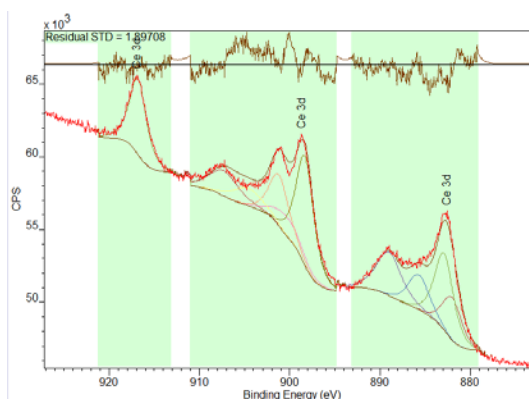
Billerica, MA). xPONENT Multiplex Assay Acquisition and Analysis Software was used to analyze the data.

Quantitative data were analyzed using GraphPad Prism 6 (GraphPad Software Inc., San Diego, CA), and statistical analyses of the results were performed by one-way analysis of variance (ANOVA) and Newman-Keuls post hoc test, Kruskal-Wallis test and Dunn's post hoc test, Log-rank (Mantel-Cox) test, unpaired Student's t-test and Mann-Whitney test when appropriate. Results are expressed as mean \pm SE and considered significant $p \leq 0.05$.

Ethical Approval: Approval was obtained from national research ethic committee and medical device regulatory body, in particular the Comité Ético de Investigación Clínica of the Hospital Clínic de Barcelona. All relevant ethical regulations relating to the conduct of the study were followed. Whole livers from DBD and DCD (Maastricht category II) donors at least 16 years of age were eligible. Specific donor consent was not required for trial inclusion. No organs were procured from prisoners. No patient identifiable data were collected.



Supplementary Fig. 1: Characterization of the CeO₂NPs. (A) TEM image of the as-synthesized NPs (scale bar is 50 nm) and High Resolution TEM of single particles showing pure CeO₂ atomic planes (insets); **(B)** DLS measurements of RSA and CeO₂NPs@RSA after purification; **(C)** X-ray diffractogram of the synthesized CeO₂NCs; **(D)** UV-VIS spectra of albuminized CeO₂NPs in DMEM+FBS at different times points.

CeO₂NPs before exposure to RSACeO₂NPs after exposure to RSA

Sample	% Ce(III)
CeO ₂ NPs-TMAOH	15
CeO ₂ NPs-RSA	16

Supplementary Fig. 2: XPS spectra of CeO₂-TMAOH (Before exposure to RSA) and CeO₂-RSA NPs after exposure and conjugation, and the corresponding Ce(III) quantification.

Supplementary Table 1: NPs characteristics.

NP characteristics	Value
Z-Potential after synthesis	+43 mV
Z-Potential after albuminization	- 14 mV
DLS after albuminization	12 nm
TEM size distribution	4± 1 nm

Supplementary Table 2: Body weight, standard liver and renal function test and serum markers of inflammation, cell growth and differentiation in control rats and in rats with HCC treated with CeO₂NPs or receiving vehicle.

	HCC		
	Control (n=8)	Vehicle (n=10)	CeO ₂ NPs (n=10)
Body weight (g)	401±12	328±8 ***	322±6 ***
Alanine transaminase (U/l)	35±2	110±17 **	110±13 **
Aspartate transaminase (U/l)	76±6	168±13 ***	185±11 ***
Lactate dehydrogenase (U/l)	398±58	474±58	553±63
Total bilirubin (mg/dl)	0.00±0.00	1.21±0.16 **	1.87±0.30 ***
Total proteins (g/l)	62.0±2.0	55.3±2.5	54.3±2.1
Albumin (g/l)	34.2±0.5	29.4±1.1 *	28.3±1.1 **
GGT (U/l)	0.09±0.03	67.1±7.1 ***	62.7±7.5 ***
Serum creatinine (mg/dl)	0.54±0.02	0.54±0.02	0.51±0.02
Serum sodium (mEq/l)	143.3±1.7	140.2±1.2	141.4±0.6
Serum potassium (mEq/l)	4.60±0.10	4.23±0.14	4.37±0.16
Total triglycerides (mg/dl)	149.8±43.3	96.5±10.3	85.9±6.6
Total cholesterol (mg/dl)	83.8±6.2	126.6±7.7 *	128.7±7.8 *
Glucose (mg/dl)	195.6±12.1	85.5±3.6 ***	90.8±3.0 ***
IL-1β (pg/ml)	14.8±2.5	101.0±39.2 **	76.4±14.2 **
IL-2 (pg/ml)	20.6±3.9	191.6±85.1*	16.9±1.07#
VEGF (pg/ml)	9.1±0.9	87.2±41.7 *	13.3±2.1

* p<0.05, ** p<0.01 and *** p<0.001 vs Control group; # p<0.05 vs HCC+ Vehicle group (one-way ANOVA and Newman-Keuls post hoc test, Kruskal-Wallis test and Dunn's post hoc test, and Mann-Whitney test when appropriate).

Supplementary Table 3: Messenger expression of genes involved in inflammation, macrophage phenotype, cell growth and differentiation in the liver of control and rats with DEN induced HCC that were exposed to CeO₂NPs or Vehicle.

	HCC		
	Control (n= 6)	Vehicle (n=10)	CeO ₂ NPs (n=10)
<u>Inflammation</u>			
<i>IL-1β</i>	1.00 \pm 0.11	1.65 \pm 0.12**	1.24 \pm 0.08##
<i>TNFα</i>	1.00 \pm 0.05	2.33 \pm 0.16***	1.94 \pm 0.14*** #
<i>IL-6</i>	1.00 \pm 0.35	1.73 \pm 0.32	1.24 \pm 0.16
<i>iNOS</i>	1.00 \pm 0.32	9.39 \pm 1.80***	5.57 \pm 0.86* #
<i>COX-2</i>	1.00 \pm 0.34	7.99 \pm 0.66***	5.99 \pm 0.32*** ##
<u>Macrophage phenotype</u>			
<i>CD163</i>	1.00 \pm 0.11	0.94 \pm 0.10	0.76 \pm 0.10
<i>ARG-1</i>	1.00 \pm 0.09	0.37 \pm 0.02***	0.37 \pm 0.03***
<u>Cell growth and differentiation</u>			
<i>PPARγ</i>	1.00 \pm 0.21	0.39 \pm 0.03***	0.35 \pm 0.02***
<i>VEGF</i>	1.00 \pm 0.07	0.44 \pm 0.02***	0.45 \pm 0.02***

Fold over HPRT. IL-1 β : Interleukin 1 β ; TNF α : Tumor Necrosis Factor α ; IL-6: Interleukin 6; iNOS: inducible Nitric Oxide Synthase; COX-2: Cyclooxygenase 2; CD163: Cluster of Differentiation 163; ARG-1: Arginase 1; PPAR γ : Peroxisome proliferator-activated receptor γ ; VEGF: Vascular endothelial growth factor. *p<0.05, **p<0.01 and ***p<0.001 vs Control group; #p<0.05 and ##p<0.01 vs HCC+ Vehicle group (one-way ANOVA and Newman-Keuls post hoc test).

Supplementary Table 5: Total FAs of principal lipid components in the hepatic tissue of control and HCC non-treated (vehicle) and treated (CeO₂NPs) rats (nmol/mg tissue).

	Control (n=7)	HCC	
		Vehicle (n=10)	CeO ₂ NPs (n=10)
Phosphatidylcholine	2003.0 ± 185.6	1792.0 ± 35.9	1687.0 ± 60.2
Non-esterified fatty acids	97.8 ± 23.8	192.0 ± 43.9*	113.6 ± 15.4
Phosphatidylethanolamine	88.9 ± 5.4	104.4 ± 7.2	99.8 ± 5.2
Cholesterol Esters	6.5 ± 0.9	10.4 ± 0.5**	9.2 ± 0.5*

Values are expressed as mean ± standard error. *p<0.05, **p<0.01 vs control rats (Unpaired Student's t-test).

Supplementary References

1. Mullins, D. R., Overbury, S. H. & Huntley, D. R. Electron spectroscopy of single crystal and polycrystalline cerium oxide surfaces. *Surf. Sci.* 1998, 307-319.
2. Gavrieli Y, Sherman Y, Ben Sasson SA. Identification of programmed cell death in situ via specific labeling of nuclear DNA fragmentation. *J Cell Biol* 1992;119:493-501.
3. Reichenbach V, Fernández-Varo G, Casals G, Oró D, Ros J, Melgar-Lesmes P, et al. Adenoviral dominant-negative soluble PDGFR β improves hepatic collagen, systemic hemodynamics, and portal pressure in fibrotic rats. *J Hepatol* 2012;57(5):967-973.
4. Burdge GC, Wright P, Jones AE, Wootton SA. A method for separation of phosphatidylcholine, triacylglycerol, non-esterified fatty acids and cholesterol esters from plasma by solid-phase extraction. *Br J Nutr* 2000;84(5):781-787.
5. Fisk HL, West AL, Childs CE, Burdge GC, Calder PC. The use of gas chromatography to analyze compositional changes of fatty acids in rat liver tissue during pregnancy. *J Vis Exp* 2014;85.
6. Perkins DN, Pappin DJ, Creasy DM, Cottrell JS. Probability-based protein identification by searching sequence database using mass spectrometry data. *Electrophoresis* 1999;20:3551-3567.
7. Casado P, Cutillas PR. A self-validating quantitative mass spectrometry method for assessing the accuracy of high-content phosphoproteomic experiments. *Mol Cell Proteomics* 2011;10(1):M110.003079.

8. Cutillas PR, Venhaesebroeck B. Quantitative profile of five murine core proteomes using label-free functional proteomics. *Mol Cell Proteomics* 2007;6:1560-1573.
9. Ravikumar R, Jassem W, Mergental H, Heaton N, Mirza D, Perera MT, et al. Liver Transplantation After Ex Vivo Normothermic Machine Preservation: A Phase 1 (First-in-Man) Clinical Trial. *Am J Transplant* 2016;16(6):1779-1787.

UNPUBLISHED MANUSCRIPT: Liver-targeted nanoparticles delivering nitric oxide reduce portal hypertension in cirrhotic rats

The **third objective** of this doctoral thesis was to investigate potential effects on portal hemodynamics and liver function of functionalized liver-specific nanoparticles containing a NO donor in experimental cirrhosis.

Perramón M, Navalón-López M, Fernández-Varo G, Moreno-Lanceta A, Fornaguera C, Melgar-Lesmes P, Borrós S, Jiménez W. Liver-targeted nanoparticles delivering nitric oxide reduce portal hypertension in cirrhotic rats.

LIVER-TARGETED NANOPARTICLES DELIVERING NITRIC OXIDE REDUCE PORTAL HYPERTENSION IN CIRRHOTIC RATS

Meritxell Perramón¹, María Navalón-López², Guillermo Fernández-Varo¹,
Alazne Moreno-Lanceta¹, Cristina Fornaguera², Pedro Melgar-Lesmes^{1,3,4},
Salvador Borrós², Wladimiro Jiménez^{1,3}

¹Biochemistry and Molecular Genetics Service of Hospital Clínic Universitari, Institut d'Investigacions Biomèdiques August Pi i Sunyer (IDIBAPS), Centro de Investigación Biomédica en Red de Enfermedades Hepáticas y Digestivas (CIBERehd), Barcelona, Spain. ²Grup d'Enginyeria de Materials (Gemat), Institut Químic de Sarrià (IQS), Ramon Llull University (URL), Barcelona, Spain. ³Department of Biomedicine, University of Barcelona, Barcelona, Spain. ⁴Institute for Medical Engineering and Science, Massachusetts Institute of Technology, Cambridge, USA.

Corresponding author: Dr. Wladimiro Jiménez. Hospital Clínic Universitari, Villarroel 170, Barcelona 08036, SPAIN. Email: wjimenez@clinic.cat, Phone: (+3493)2275400 ext 5518, Fax: (+3493)2275697

Electronic word count: 4346

Number of figures and tables: 6 figures, 1 table

FINANCIAL SUPPORT

This work was supported by the grant RTI2018-094734-B-C21 to WJ and RTI2018-094734-B-C22 to SB funded by MCIN/AEI/ 10.13039/501100011033 and by the European Union NextGenerationEU/PRTR. The Centro de Investigación Biomédica en Red de Enfermedades Hepáticas y Digestivas (CIBERehd) is funded by the Instituto de Salud Carlos III.

CONFLICT OF INTEREST

The authors declare no competing interests.

LIST OF ABBREVIATIONS

Ace2, angiotensin converting enzyme 2; Acta2, smooth muscle actin alpha 2; AST, aspartate transaminase; Bdkrb1, bradykinin B1; BDL, bile-duct ligation; cGMP, cyclic guanosine monophosphate; CO, cardiac output; Col1a2, collagen 1 alpha 2; Col3a1, collagen 3 alpha 1; CT, control; Cox2, cyclooxygenase 2; DLS, dynamic light scattering; ECM, extracellular matrix; Et1, endothelin; HSC, hepatic stellate cells; Il6, interleukin 6; i.v., intravenously; LDH, lactate dehydrogenase; MAP, mean arterial pressure; Mmp, metalloproteinase; NO, nitric oxide; NOS, nitric oxide synthase; NPs, nanoparticles; pBAE, poly(beta-amino ester); PDI, polydispersity index; PP, portal pressure; Ptgs2, Prostaglandin-endoperoxide synthase 2; RT-PCR, real-time quantitative PCR; Sphk1, Sphingosine kinase 1; Timp, tissue inhibitor of metalloproteinases; Tnfa, tumor necrosis factor alpha.

ABSTRACT

Background and Aims: Nitric oxide (NO) is a small vasodilator highly diffusible gas, with a key role in the pathogenesis of portal hypertension in advanced liver disease. Here, we assessed the potential therapeutic effect of a NO donor targeted to the liver by poly(beta-amino ester) nanoparticles (pBAE NPs) in experimental decompensated cirrhosis. **Methods:** NO donor pBAE NPs with retinol (ret) moiety were synthesized. Cy5 and mCherry plasmid were added to assess biodistribution following *in vivo* administration. Besides, hemodynamic

study was performed in another group of cirrhotic rats treated with control or NO donor ret pBAE NPs (30 mg/ kg of body weight) and hepatic fibrogenesis and inflammation were evaluated. **Results:** The administration of ret pBAE NPs resulted in an avid uptake and transfection of the cirrhotic liver and spleen. No NPs were found in the brain, lung, heart or in the general circulation. Liver-targeted NO donor NPs significantly decreased the serum levels of the enzymes aspartate aminotransferase and lactate dehydrogenase in cirrhotic rats. Noteworthy, the treatment with ret pBAE NPs containing a NO donor resulted in significantly ($p < 0.05$) decreased portal hypertension (10.17 ± 0.95 mmHg) in comparison to control NPs (13.4 ± 0.54 mmHg) in cirrhotic rats with ascites. No effect was found in systemic hemodynamics including mean arterial pressure, cardiac output and splanchnic perfusion pressure. Remarkably, liver-targeted NO donor NPs statistically and biologically diminished the transcription of genes related to vascular reactivity. Finally, the liver specific NO donor decreased the activation of hepatic stellate cells and the mRNA expression of endothelin 1, inducible nitric oxide synthase, tissue inhibitor of metalloproteinases 1, tumor necrosis factor alpha and interleukin 6. **Conclusion:** Liver-specific NO donor NPs effectively target the liver and could be therapeutically useful to mitigate the inflammation and portal hypertension characteristic of decompensated cirrhosis.

INTRODUCTION

Portal hypertension is a characteristic syndrome of patients with advanced liver disease and develops concomitantly with systemic arterial hypotension and hyperkinetic circulation (1). An important factor contributing to the increase in portal pressure is the elevation of the intrahepatic vascular resistance (2, 3). A deficit in the intrahepatic bioavailability of the endogenous vasodilator nitric oxide (NO) has been claimed as one of the most relevant contributory factors involved in the pathogenesis of this phenomenon. In the past years several strategies have been proposed to improve NO availability in the hepatic tissue, however suboptimal results were obtained with most of these therapeutics approaches. This lack of efficacy is mainly due to the remarkable dissimilarity of NO metabolism between the hepatic and systemic vasculatures. Actually, at difference to what occurs in the liver circulation, the systemic vessels of cirrhotic patients are characterized by increased production and activity of NO which in turn leads to arteriolar vasodilation and arterial hypotension. Therefore, any non-targeted strategy attempting to deliver NO into the liver also results in the unwanted accentuation of the systemic circulatory dysfunction already present in decompensated liver disease (3,4).

The current investigation was aimed to assess whether this problem could be overcome by selectively delivering NO to the hepatic vascular bed. Furthermore, we also hypothesized that liver function could also benefit from NO administration because of the properties of this mediator beyond its vasodilator activity, including anti-inflammatory and regenerative properties. Accordingly, we developed a new liver-targeted nanoformulation combining poly(beta-amino ester) polymer (pBAE) with an NO donor (organic nitrates). Thereafter, we

evaluated whether this pBAE nanoparticles (NPs) may ameliorate portal hypertension and other indicators of liver function without affecting systemic hemodynamics in experimental cirrhosis.

METHODS

Synthesis of retinol (ret) pBAE NPs. To selectively deliver NO to the liver, organic nitrites were selected as NO releasing moieties, pBAE NPs as delivery vehicles and ret as a targeting molecule. Briefly, NO donor ret pBAE NPs were formulated according the following combinations of polymers: K retinol (ret, 5 %), H (40 %) and K72-NO (55 %). The so-called K72-NO polymer is a nitrooxy-terminated organic acids based on C32-CK3 polymer. Control (CT) NPs were formulated with Kret (5%), H (40%), and K (55%) lacking the K72-NO. Additionally, equal volumes of mCherry protein plasmid (mCherry, 0.5 $\mu\text{g}/\mu\text{l}$) was added over the polymer combination (50 $\mu\text{g}/\mu\text{l}$ in 12.5×10^{-3} M sodium acetate buffer solution), mixed by pipetting and incubated for 30 min at room temperature. Thereafter, the mixture was precipitated in the same volume of diethyl pyrocarbonate water to form NPs, which were further added over a HEPES (20×10^{-3} M) + sucrose (4 % w/w) solution. To track the polymer in biodistribution studies, Cy5 was added (5 %) in the H polymer formulation.

Kret, and KH polymers were synthesized as described previously by Fonaguera *et al.* (5). K72-NO polymer was obtained by reacting N-bromaliphatic carboxylic acid (1 eq) and AgNO_3 (1.05 eq) in acetonitrile for 24 h in the dark to obtain the organic aldehyde AgBr. It was filtered and extracted using ethyl acetate through water addition to the reaction and then evaporated. C32 backbone

polymer was synthesized by reacting butanediol diacrylate (1eq) and 5-aminopentanol (1.08 eq) at 90 °C for 24h (24). C32 (1 eq), dicyclohexylcarbodiimide (1.05 eq) and n-nitrooxyaliphatic carboxylic acid (1 eq) and the catalyst 4-dimethylaminopyridine (0.05 eq) were reacted in tetrahydrofuran in ice for 30 min and at room temperature for the following 48 h. The product was filtered and ether was used to purify the polymer, which was reacted with CK3 (Ontores Lts, Shanghai, China) in dimethyl sulfoxide overnight. The product (K72-NO) was purified through the precipitation of diethyl ether–acetone mixture and was stored at -20 °C until use.

All reagents were purchased in Sigma-Aldrich (Darmstadt, Germany). K72-NO polymer was characterized by ¹H-NMR (400 MHz, CD₃OD, TMS) (ppm): = 4.48 (t. –CH₂-NO₃), 4.33 (br, NH₂-(CH₂)₄-CH-), 4.12 (t, CH₂-CH₂-O-), 3.57 (br, NH₂-CH-CH₂-S-), 2.95 (br, CH₂-CH₂-N-, NH₂-CH₂-(CH₂)₃-CH-), 2.83 (dd, -CH₂-S-CH₂), 2.67 (br, -N-CH₂-CH₂-C(=O)-O), 2.35 (t. HOOC-CH₂-), 1,82 (m. -OOC-CH₂-CH₂-), 1.74 (br, -O-CH₂- CH₂-CH₂-CH₂-O), 1.51 (m. –CH₂-CH₂-CH₂-NO₃).

Physicochemical characterization of ret pBAE NPs. CT and NO donor ret pBAE NPs characterization of hydrodynamic average size (nm), surface charge (mV) and polydispersity index (PDI) was obtained using a ZetaSizer Nano ZS (Malvern Instruments Ltd, Malvern, UK). Results are given as means ± S.E. for, at least, in triplicate.

Induction of experimental liver cirrhosis. Liver cirrhosis was induced as described previously (6) in a group of male Wistar rats (Charles-River, Saint Aubin les Elseuf, France) with chronic carbon tetrachloride (CCl₄) inhalation, until at least one week after the establishment of ascites. Animals were kept under

constant temperature and humidity in 12 h controlled dark/light cycle, and fed *ad libitum* with standard pellet and water containing phenobarbital (0.3 g/L). All animal procedures were approved by the Investigation and Ethics Committee of the Hospital Clinic and Animal Experimentation Committee of the University of Barcelona (Barcelona, Spain).

Biodistribution study. Two rats received intravenously (i.v.) Cy5 mCherry ret pBAE NPs or NPs lacking ret and were euthanized by isoflurane overdose (Forane, Abbott Laboratories S.A., Madrid, Spain) 3 h after the administration. Organ and arteries biopsies were fixed in 4 % paraformaldehyde, embedded in Tissue Teck O.C.T (Sakura Finetek, Tokio, Japón) and snap-frozen in isopentane. After obtaining cryosections, nuclei were stained with Vectashield Mounting Medium with DAPI (Vectorlabs, USA). Coverslip was placed on top of the specimen and photographs were taken using and Leica TCS-SPE confocal fluorescence microscope at 40x (Leica, Nussloch, Germany).

Hemodynamic study. Another group of cirrhotic rats with ascites were anesthetized with Inactin® (50 mg/kg body weight, Sigma-Aldrich Chemie GmbH, Steinherim, Germany). Following a stabilization period, mean arterial pressure (MAP) and basal cardiac output (CO) were measured. Next, rats randomly received thru the femoral vein 30 mg/kg body weight of CT (n = 5) or NO donor (n = 9) mCherry ret pBAE NPs. Two hours later, MAP, CO and portal pressure (PP) were measured. Splanchnic perfusion pressure (SPP) was estimated as MAP - PP. Rats were euthanized by isoflurane overdose and serum and liver samples were collected. Biopsies were snap frozen or fixed with 10 % buffered formalin for further paraffin embedding.

Hepatic messenger expression of a panel of fibrogenesis and inflammation-related genes. RNA extraction column kit (RNAeasy, Qiagen, Venlo, The Netherlands) was used to extract liver total RNA of CT (n = 5) or NO donor (n = 9) mCherry ret pBAE NPs-treated rats. RNA concentration was assessed by spectrophotometric analysis (ND-100 spectrophotometer; Thermo Fisher Scientific, Waltham, MA, USA) and 1 µg of total RNA was reverse transcribed using a complementary DNA synthesis kit (High-Capacity cDNA Reverse Transcription Kit, Applied Biosystems, Foster City, CA). Primers and probes used were designed using the Universal Probe Library Assay Design Center through the ProbeFinder v2.45 software (Roche Diagnostics, Indianapolis, IN.) and real-time quantitative PCR (RT-PCR) was performed as previously described (7). Collagen I $\alpha 2$ (*Col1 $\alpha 2$* , NM_053356.1, probe 95; left 5'-AGACCTGGCGAGAGAGGAGT-3', right 5'-ATCCAGACCGTTGTGTCCTC-3'), *Col3 $\alpha 1$* (NM_032085.1, probe 49; left: 5'-TCCCCTGGAATCTGTGAATC-3', right 5'-TGAGTCGAATTGGGGAGAAT-3'), tissue inhibitor of matrix metalloproteinases type 1 (*Timp1*) (NM_053819.1, probe 95; left 5'-CATGGAGAGCCTCTGTGGAT-3', right 5'-TGTGCAAATTTCCGTTTCCTT-3'), *Timp2* (NM_021989.2, probe 73; left 5'-GACAAGGACATCGAATTTATCTACAC-3', right 5'-CCATCTCCTTCCGCCTTC-3'), metalloproteinase 2 (*Mmp2*, NM_031054.2, probe 60; left 5'-CTCCACTACGCTTTTCTCGAAT-3', right 5'-TGGGTATCCATCTCCATGCT-3'), *Mmp9* (NM_031055.1, probe 53; left: 5'-CCTGAAAACCTCCAACCTCA-3', right: 5'-GAGTGTAACCATAGCGGTACAGG-3'), endothelin 1 (*Et1*, NM_012548.2, probe 22; left 5'-CAAGCTGGGAAAGAAGTGTATCTA-3' and right 5'-GTTGCTGATGGCCTCCAA-3'), cyclooxygenase 2 (*Cox2*, NM_017232.3, probe

125; left 5'-GATGCTATCTTTGGGGAGACC-3' and right 5'-CCATAAGGCCTTTCAAGGAGA-3'), tumor necrosis factor alpha (*Tnfa*, NM_012675.3, probe 68; left 5'-CGTAGCCCACGTCGTAGC-3' and right 5'-GGTTGTCTTTGAGATCCATGC-3'), interleukin 6 (*Il6*, NM_012589.1, probe 20; left 5'-CCCTTCAGGAACAGCTATGAA-3' and right 5'-ACAACATCAGTCCCAAGAAGG-3'), nitric oxide synthase 2 (*Nos2*, NM_012611.3, probe 95; left 5'-AAAATGGTTTCCCCCAGTTC-3' and right 5'-CAGCTTGTCCAGGGATTCTG-3'), *Nos3* (NM_021838.2, probe 76; left 5'-CTAGACACCCGGACAACCTC-3' and right 5'-GGTGGTCCACAATGGTCACT-3') and as the reference gene hypoxanthine-guanine phosphoribosyltransferase (NM_012583.2, probe 95; left: 5'-GACCGGTTCTGTTCATGTCG-3' right: 5'-ACCTGGTTCATCATCACTAATCAC-3').

RT2 Profiler PCR Array. Total liver RNA (500 ng) was reversetranscribed using a RT² First Strand Kit (Qiagen, Venlo, Netherlands). Real-time PCR array was performed using the RT² Profiler™ PCR Array Rat hypertension (Qiagen) according to the manufacturer's protocol.

Other analysis. Sirius red and α SMA staining were performed as previously described (7). Standard serum parameters of liver and renal function were measured using the BS-200E Chemistry Analyzer (Mindray Medical International Ltd, Shenzhen, China).

Statistical analysis. Data were analyzed using GraphPad Prism 6 (GraphPad Software Inc., San Diego, USA). Unpaired t-test or Mann Whitney test were performed when appropriate. Results were shown as mean \pm S.E. and considered significant when $p < 0.05$.

RESULTS

The cirrhotic liver is the main target of pBAE polyplexes with ret moiety after *in vivo* administration. First, in order to investigate NPs organ biodistribution, Cy5 mCherry ret pBAE NPs were administered i.v. to a cirrhotic rat with ascites. Organ samples were collected 3 h after administration and evaluated with fluorescent confocal microscopy. The presence of Cy5 fluorescent signal indicates the presence of the polymer, whereas mCherry fluorescent signal demonstrates effective cellular transfection.

The liver and spleen were the main targets of ret targeted NPs. Positive Cy5 and mCherry transfection were found in the cirrhotic liver and both co-localized close to fibrotic tracts (Figure 1). Besides, the spleen displayed a generalized Cy5 and mCherry positivity. Cy5 was also detected in the kidney, but no efficient transfection was observed. Importantly, the lung, the heart and the brain did not uptake NPs. Furthermore, no signal was detected in the general circulation (Figure 2 A and Supplementary figure 1).

Finally, the specific hepatic targeting of engineered pBAE NPs was not observed when ret was absent from the construct (Figure 2 B). Therefore, the hepatic targeting selectivity of the NPs was related to ret moiety.

Synthesis and characterization of NO donor ret pBAE NPs physicochemical properties. NO donor ret pBAE were synthesized as represented in Figure 3A. CT NPs had an hydrodynamic size of 147.8 ± 1.51 nm, PDI of 0.11 ± 0.003 and Z-potential of 38.47 ± 0.49 mV. As expected, the addition of the NO donor to the NPs increased their size to 234 ± 2.38 nm and their PDI to 0.21 ± 0.02 ; whereas it slightly decreased the Z-potential to 33.37 ± 0.96 mV

(Figure 3 B). Figure 3 C consists in a graphic representing the difference in the Z-average between both types of NPs.

Serum biochemical parameters of cirrhotic rats treated with CT or NO donor containing ret pBAE NPs. A group of cirrhotic rats with ascites was treated with CT (n = 5) or NO donor (n = 9) ret pBAE NPs. Both experimental groups showed similar body weight and amount of ascites (Table 1). Cirrhotic rats treated with CT NPs showed a marked alteration in serum liver function tests, including augmented levels of transaminases and decreased total proteins and albumin. Remarkably, the treatment with liver-targeted NO donor ret pBAE NPs significantly decreased aspartate transaminase (AST) and lactate dehydrogenase (LDH) quantity to almost a half (Table 1).

Liver-targeted NO donor polyplexes significantly ameliorate PP without affecting systemic hemodynamics. In order to evaluate the potential effect of the NO containing NPs in portal and systemic circulations, an hemodynamic study was performed for 2 h. Basal MAP was equal in both experimental groups (CT: 90 ± 2.55 vs NO donor: 85.89 ± 3.33 mm Hg) and it was maintained after 2 h of study (101.4 ± 4.95 vs 93.56 ± 3.44 mmHg) (Figure 4 A). Likewise, the measurement of CO at the end of the study revealed no differences between both treatment groups (394.2 ± 45.15 L/min vs 309.3 ± 37.96 L/min, Figure 4 B) neither in the SPP (93.6 ± 6.53 vs 83.39 ± 3.71 , Figure 4 C). Noteworthy, the measurement of PP at the end of the study revealed a significant decrease ($p < 0.05$) in cirrhotic animals with ascites treated with NO donor NPs (10.17 ± 0.95 mm Hg) in comparison to CT NPs (13.4 ± 0.54 mm Hg) (Figure 4 D).

Liver-targeted NO ret NPs modulate vascular reactivity gene expresison. Further knowledge on the hepatic effect of NO donor ret pBAE NPs in cirrhotic rats with ascites was gained using a commercially available PCR array. This array assessed the expression of 84 genes involved in biological pathways regulating blood vessel constriction and dilation. Only genes with ± 1.5 -fold change in hepatic expression and a $p < 0.05$ between NO donor and CT ret pBAE NPs in cirrhotic rats were considered biologically and statistically significant. Volcano plot of the data is presented in Figure 4 E. Actually, 4 genes were both biologically and significantly downregulated including: bradykinin B1 (*Bdkrb1*), angiotensin converting enzyme 2 (*Ace2*), prostaglandin-endoperoxide synthase 2 (*Ptgs2*, *Cox2*) and sphingosine kinase 1 (*Sphk1*).

Bdkrb1 encodes an inducible G-protein-coupled receptor that promotes tissue inflammation (8). *Ace2* is an enzyme that catalyzes the conversion of angiotensin II to Ang-(1-7) leading to vasodilation and cell proliferation inhibition (9). *Ptgs2* encodes for the protein cyclooxygenase 2 (COX2), an inducible enzyme involved in the production of prostaglandins implicated in the inflammatory response (10). *Sphk1* catalyzes the phosphorylation of sphingosine to form sphingosine 1-phosphate inducing inflammation, proliferation and apoptosis inhibition (11).

NO donor containing ret pBAE NPs did no modify extracellular matrix (ECM) remodeling. Sirius red staining showed that all decompensated cirrhotic rats displayed the characteristic perisinusoidal and marked bridging fibrosis, in addition to portal–portal septa surrounding liver nodules. The morphometric analysis revealed no significant differences between both experimental groups (Figure 5 A). The assessment of the mRNA expression of a panel of fibrosis

related-genes, including *Col1a2*, *Col3a1*, *Timp2*, *Mmp2* and *Mmp9* further confirmed no effect on ECM remodeling regulation (Figure 5 B). Strikingly, *Timp1* was significantly downregulated in the liver of NO donor ret pBAE NPs treated rats in comparison to CT NPs treated ones.

Liver-targeted NO donor NPs induce a reduction in hepatic stellate cell (HSC) activation and proinflammatory gene expression. Interestingly, the administration of liver-targeted NO donor NPs resulted in a significant reduction in the hepatic staining of α SMA, the most used marker for activated HSC (Figure 6 A). Moreover, the analysis of the mRNA expression of a panel of proinflammatory genes revealed a significant downregulation of *Et1*, *Nos2*, *Cox2*, *Tnfa*, and *Il6* (Figure 6 B). The constitutively expressed gene *Nos3* was not affected by the treatment

DISCUSSION

Patients with decompensated liver cirrhosis have a very elevated mortality risk mostly due to complications associated to portal hypertension. This study was addressed to design and evaluate the therapeutic potential of a nanoformulation containing an NO donor that selectively targets the liver aimed to ameliorate the hemodynamic parameters disturbed in decompensated cirrhosis.

NO donors are a family of compounds specifically designed to release NO or NO-related species. Different chemical groups with different pharmacokinetic and dynamic properties have been described including NONOates and organic nitrates (12). Although positive outcomes in experimental fibrosis/cirrhosis, to

date none has proven efficacy in any clinical trial partially due to their non-specific *in vivo* distribution (13, 14). In this regard, a liver-targeted nanoformulation could be beneficial to selectively deliver NO donors for the treatment of portal hypertension in cirrhosis.

Poly(beta-amino ester) (pBAE) are a family of biocompatible polymers synthesized from an acrylate and an amine by Michael addition (15). pBAE are positively charged, easy to produce, have tunable physicochemical properties such as charge or polydispersity and once internalized by a cell they are able to escape from the endosome by proton sponge mechanism (16). In order to form nanoscale polyplexes, the addition of genetic material is critical (17). Furthermore, drugs and other molecules such as targeting moieties can be conjugated in the polyplex (18, 19).

NO donors are exogenous agents that once administered are able to release NO and induce potent vasodilator effects (20). In this study, organic nitrates were selected because they have excellent stability and NO release requires enzymes such as cytochrome P450 reductase, aldehyde dehydrogenase-2 or glutathione S-transferase; or reaction with thiols from cysteine and cysteine derivatives (21, 22). Therefore, NO liberation from organic nitrates does not depend on environmental conditions for instance temperature or pH. In this study, NO donor release kinetics was not evaluated due to difficulties associated to *in vivo* intrahepatic measurement. For these reasons, the effect of NO donor NPs was compared to similar NPs lacking the donor and it was assumed that the derived effects were due to the presence of the NO donor. The physicochemical characterization of both NPs revealed that the addition of

an organic NO donor, slightly increased the size and reduced the z-potential of liver-targeted pBAE NPs.

First of all, the specificity of *in vivo* biodistribution was evaluated by i.v. treating cirrhotic rats with ret and non-ret pBAE NPs containing a Cy5 dye and a plasmid encoding for mCherry protein. Most ret pBAE NPs were detected in the liver and spleen as means of positive Cy5 and mCherry. In the liver, Cy5 signal co-localized with mCherry in fiber-like zones. In the spleen, Cy5 signal and mCherry transfection were generalized. Some NPs were found in the kidney but no efficient transfection was detected. Noteworthy, no NPs were found in other organs or in the general circulation. Several studies have demonstrated the feasibility of adding different targeting moieties to the pBAE polyplexes to target cancer cells in the liver (23, 24). In the present investigation, ret was selected as the hepatic-targeting moiety given that the liver is the most important storage for retinoids in the body (25). A previous study from Fornaguera *et al.* showed that adding ret to end-oligopeptide modified pBAE NPs improved hepatic accumulation after i.v. administration in healthy mice (5). In agreement, another class of polymeric particles targeted with ret showed elevated HSC internalization following administration in bile-duct ligated rats (BDL) (26). In decompensated liver disease, the selectivity for the liver is of special importance to prevent potential off-target effects and no further aggravate systemic vasodilation and arterial hypotension. For this reason, Cy5 and mCherry derived fluorescence were also evaluated in the major systemic arteries including carotid, thoracic aorta, abdominal aorta, mesenteric, renal and femoral. No fluorescent signal was detected in any case, further supporting the hepatic-specificity of the NPs.

Clinically significant portal hypertension is defined by an hepatic venous pressure gradient > 10 mm Hg and it is associated to a high risk of decompensation (27). This decompensation involves the worsening of patient prognosis due to a deterioration in the hepatic function and the appearance of complications, being ascites and gastroesophageal varices the most frequent. Non-selective beta blockers (NSBBs) have been used for decades to treat portal hypertension in patients with cirrhosis because they are able to reduce the heart rate, CO and induce splanchnic vasoconstriction. Moreover, several data indicate that NSBBs prevent decompensation and decrease the risk of ascites, bleeding, spontaneous bacterial peritonitis and increase the survival (27). Growing evidence suggests that their indication may be controversial in patients with end-stage cirrhosis (28, 29). Therefore, new therapies aimed to treat portal hypertension in patients with end-stage liver disease are needed. For all these reasons, in the current study, potential effects of a liver-targeted organic NO donor on portal and systemic hemodynamics were evaluated in experimental decompensated cirrhosis. The administration of engineered NO donor ret pBAE NPs did not induce systemic hemodynamic changes including MAP or CO. Of note, the treatment significantly ameliorated PP in cirrhotic rats with ascites. Furthermore, this was accompanied with a reduction in the liver function serum markers LDH and AST in those rats treated with the liver-specific NO donor. Albeit, similar effects in PP reduction have previously been reported with few other liver-specific NO donors, in most of these studies the authors did not evaluate the impact in advanced cirrhosis experimental models, in which PP should be > 10 mm Hg (13, 30). In the case of Moal F *et al.* (31), they did show a reduction in clinical significant portal hypertension, as well as, in fibrosis

development after liver-specific NO donor administration in a BDL cirrhosis model. But, the authors used a quite invasive procedure consisting on osmotic subcutaneous minipumps to administer the therapy. Although more recently, Duong HTT *et al.* (26) did also report attenuation on portal hypertension following a liver-specific NO donor administration in BDL model, they only studied the mechanisms underlying this effect *in vitro* using the human-derived hepatic stellate cell line LX-2.

Subsequent gene expression analysis pointed toward regulation in vascular reactivity as a major driver in portal hypertension improvement in NO donor-treated cirrhotic rats. Stringent gene analysis of alterations in mRNA expression induced by liver-specific NO donor NPs in cirrhotic rats with ascites, considering only those genes showing both statistically and biologically significant downregulation, revealed a group of genes all involved in vascular tone regulation and proinflammatory signaling including *Bdkrb1*, *Ptgs2*, *Ace2* and *Sphk1*.

Potential effects on liver fibrogenesis were also assessed by Sirius red staining and RT-PCR. The treatment had no impact on hepatic collagen deposition. Besides, no changes in the hepatic transcription of *Col1a2*, *Col3a1*, *Acta2*, *Mmp2*, *Mmp9*, or *Timp2* were found after the liver specific NO donor treatment. Previously, Leung TM *et al.* (32), reported that the daily treatment with the NO donor L-arginine for 8 weeks in CCl₄-injected mice resulted in decreased intrahepatic collagen deposition and downregulated the expression of pro-fibrogenic factors such as α SMA, *Cox2*, *Timp1*, *Timp2*, *Mmp2* and *Mmp9*. Similar effects were reported more recently by Sun J *et al.* (13). The treatment with a NO donor linked to ursodeoxycholic acid through threonine in DEN-induced cirrhotic

rats resulted in decreased hydroxyproline content, Sirius red staining and ameliorated fibrosis score. The lack of effect on hepatic fibrosis deposition in the current study could possibly be explained by insufficient treatment exposure time. Strikingly, our liver-targeted NO donor significantly diminished the mRNA expression of *Timp1* in the liver of rats with decompensated cirrhosis. *Timp1* is a glycoprotein that promotes hepatic fibrosis by modulating ECM remodeling via the tight regulation of MMP activity (33, 34). Elevated TIMP1 arterial and venous plasma levels have been found in patients with cirrhosis and they correlate with the severity of the disease and the degree of portal hypertension (35). Additionally, *Timp1* has been involved in apoptosis regulation and its expression has been related to cancer cells survival (36).

Furthermore, liver-specific NO donor treated animals displayed a lesser amount of activated HSC. This was accompanied by a reduction of the expression of proinflammatory genes including *Et-1*, *Nos2*, *Ptgs2*, *Tnfa*, and *Il6*. *Et-1* is the most potent endogenous vasoconstrictor. It has been found that decreased NO bioavailability stimulates the expression of *Et-1* in smooth muscle and endothelial cells, which in turn induces the activation of *Ptgs2* and subsequent formation of prostanoids (37). In this study, *Et-1* downregulation was also associated with reduced *Ptgs2* transcription. *Ptgs2* has been involved in the pathogenesis of liver fibrosis by modulating inflammation, apoptosis and cell senescence (38). Additionally, it has been reported that NO is able to inhibit nuclear factor kappa beta activation (39). The latter is a master regulator of innate and adaptive immunities by the modulation of the expression of various proinflammatory genes as well as the inflammasome (40). In agreement, the expression of the proinflammatory cytokines *Il6* and *Tnfa* along with *Nos2*, was

decreased in the liver of NO donor treated cirrhotic rats. Interestingly, no effects on *Nos3* transcription, the constitutive form of the nitric oxide synthase, were detected.

Altogether suggests that once i.v. administered, NO donor polymeric nanoformulations are avidly internalized by the liver. Liver cells induce the release of NO from the polyplexes and in response, HSC lose the contractile phenotype and induce vasodilation ultimately decreasing portal hypertension and inflammation.

In conclusion, the results of this study suggest that liver-targeted NO donor pBAE NPs may have therapeutic value in attenuating portal hypertension and hepatic inflammation and therefore, complications in decompensated cirrhosis.

REFERENCES

1. Hu LS, George J, Wang JH. Current concepts on the role of nitric oxide in portal hypertension. *World J Gastroenterol*. 2013 Mar;19(11):1707–17.
2. Simonetto DA, Liu M, Kamath PS. Portal Hypertension and Related Complications: Diagnosis and Management. *Mayo Clin Proc*. 2019;94(4):714–26.
3. Morales-Ruiz M, Cejudo-Martín P, Fernández-Varo G, Tugues S, Ros J, Angeli P, et al. Transduction of the liver with activated Akt normalizes portal pressure in cirrhotic rats. *Gastroenterology*. 2003 Aug;125(2):522–31.
4. Iwakiri Y, Kim MY. Nitric oxide in liver diseases. *Trends Pharmacol Sci*. 2015 Aug;36(8):524–36.

5. Fornaguera C, Guerra-Rebollo M, Lázaro MÁ, Cascante A, Rubio N, Blanco J, et al. In Vivo Retargeting of Poly(beta aminoester) (OM-PBAE) Nanoparticles is Influenced by Protein Corona. *Adv Healthc Mater.* 2019 Oct;8(19):e1900849.
6. Clària J, Jiménez W. Experimental models of cirrhosis and ascites. In: *Ascites and Renal Dysfunction in Liver Disease: Pathogenesis Diagnosis and Treatment.* 2nd edition. Blackwell Science Inc; 2005. p. 215–26.
7. Perramón M, Carvajal S, Reichenbach V, Fernández-Varo G, Boix L, Macias-Muñoz L, et al. The pituitary tumour-transforming gene 1/delta-like homologue 1 pathway plays a key role in liver fibrogenesis. *Liver Int.* 2022 Jan 20;42(3):651–62.
8. Stansfield WE, Ranek M, Pendse A, Schisler JC, Wang S, Pulinilkunnil T, et al. Chapter 4 - The Pathophysiology of Cardiac Hypertrophy and Heart Failure. *Cellular and Molecular Pathobiology of Cardiovascular Disease.* Academic Press; 2014, p. 51-78, ISBN 9780124052062. .
9. Herath CB, Warner FJ, Lubel JS, Dean RG, Jia Z, Lew RA, et al. Upregulation of hepatic angiotensin-converting enzyme 2 (ACE2) and angiotensin-(1–7) levels in experimental biliary fibrosis. *J Hepatol.* 2007 Sep; 47(3): 387–395.
10. Ricciotti E, FitzGerald GA. Prostaglandins and Inflammation. *Arteriosclerosis, Thrombosis, and Vascular Biology.* 2011; 31:986–1000.
11. Alshaker H, Sauer L, Monteil D, Ottaviani S, Srivats S, Böhler T, et al. Chapter Six - Therapeutic Potential of Targeting SK1 in Human Cancers. *Advances in Cancer Research.* Academic Press, Volume 117, 2013; p143-200. ISBN 9780123942746.

12. Scatena R, Bottoni P, Pontoglio A, Giardina B. Pharmacological modulation of nitric oxide release: new pharmacological perspectives, potential benefits and risks. *Curr Med Chem*. 2010;17(1):61–73.
13. Sun J, Li M, Fan S, Guo Z, Zhong B, Jin X, et al. A novel liver-targeted nitric oxide donor UDCA-Thr-NO protects against cirrhosis and portal hypertension. *Am J Transl Res*. 2018 Feb 15;10(2):392–401.
14. Fiorucci S, Antonelli E, Morelli O, Mencarelli A, Casini A, Mello T, et al. NCX-1000, a NO-releasing derivative of ursodeoxycholic acid, selectively delivers NO to the liver and protects against development of portal hypertension. *Proc Natl Acad Sci U S A*. 2001 Jul;98(15):8897–902.
15. Liu Y, Li Y, Keskin D, Shi L. Poly(β -Amino Esters): Synthesis, Formulations, and Their Biomedical Applications. *Adv Healthc Mater*. 2019 Jan;8(2):e1801359.
16. Iqbal S, Qu Y, Dong Z, Zhao J, Rauf Khan A, Rehman S, et al. Poly (β -amino esters) based potential drug delivery and targeting polymer; an overview and perspectives (review). *Eur Polym J*. 2020;141:110097.
17. Lynn DM, Langer R. Degradable Poly(β -amino esters): Synthesis, Characterization, and Self-Assembly with Plasmid DNA. *J Am Chem Soc*. 2000 Nov 1;122(44):10761–8. <https://pubs.acs.org/doi/10.1021/ja0015388>
18. Fornaguera C, Guerra-Rebollo M, Ángel Lázaro M, Castells-Sala C, Meca-Cortés O, Ramos-Pérez V, et al. mRNA Delivery System for Targeting Antigen-Presenting Cells In Vivo. *Adv Healthc Mater*. 2018 Sep;7(17):e1800335.
19. Dosta P, Tamargo I, Ramos V, Kumar S, Kang DW, Borrós S, et al. Delivery of Anti-microRNA-712 to Inflamed Endothelial Cells Using Poly(β -amino

- ester) Nanoparticles Conjugated with VCAM-1 Targeting Peptide. *Adv Healthc Mater.* 2021 Aug;10(15):e2001894.
20. Park D, Saravanakumar G, Kim WJ. Chapter 10 - Nitric Oxide-Releasing Functional Nanomaterials for Anticancer Therapy. In: Morbidelli L, Bonavida BBT-TA of NO in C and ID, editors. *Therapeutic Application of Nitric Oxide in Cancer and Inflammatory Disorders.* Academic Press; 2019. p. 191–218.
21. França-Silva MS, Balarini CM, Cruz JC, Khan BA, Rampelotto PH, Braga VA. Organic nitrates: past, present and future. *Molecules.* 2014 Sep;19(9):15314–23.
22. Daiber A, Münzel T. Organic Nitrate Therapy, Nitrate Tolerance, and Nitrate-Induced Endothelial Dysfunction: Emphasis on Redox Biology and Oxidative Stress. *Antioxid Redox Signal.* 2015 Oct;23(11):899–942.
23. Zamboni CG, Kozielski KL, Vaughan HJ, Nakata MM, Kim J, Higgins LJ, et al. Polymeric nanoparticles as cancer-specific DNA delivery vectors to human hepatocellular carcinoma. *J Control Release.* 2017 Oct;263:18–28.
24. Vaughan HJ, Zamboni CG, Radant NP, Bhardwaj P, Revai Lechtich E, Hassan LF, et al. Poly(beta-amino ester) nanoparticles enable tumor-specific TRAIL secretion and a bystander effect to treat liver cancer. *Mol Ther - Oncolytics.* 2021 Jun 25;21:377–88.
25. Shirakami Y, Lee S-A, Clugston RD, Blaner WS. Hepatic metabolism of retinoids and disease associations. *Biochim Biophys Acta.* 2012 Jan;1821(1):124–36.
26. Duong HTT, Dong Z, Su L, Boyer C, George J, Davis TP, et al. The use of nanoparticles to deliver nitric oxide to hepatic stellate cells for treating liver fibrosis and portal hypertension. *Small.* 2015 May;11(19):2291–304.

27. Rodrigues SG, Mendoza YP, Bosch J. Beta-blockers in cirrhosis: Evidence-based indications and limitations. *JHEP reports Innov Hepatol.* 2020 Feb;2(1):100063.
28. Kim SG, Larson JJ, Lee JS, Therneau TM, Kim WR. Beneficial and harmful effects of nonselective beta blockade on acute kidney injury in liver transplant candidates. *Liver Transplant Off Publ Am Assoc Study Liver Dis Int Liver Transplant Soc.* 2017 Jun;23(6):733–40.
29. Sersté T, Melot C, Francoz C, Durand F, Rautou P-E, Valla D, et al. Deleterious effects of beta-blockers on survival in patients with cirrhosis and refractory ascites. *Hepatology.* 2010 Sep;52(3):1017–22.
30. Rodríguez S, Raurell I, Torres-Arauz M, García-Lezana T, Genescà J, Martell M. A Nitric Oxide-Donating Statin Decreases Portal Pressure with a Better Toxicity Profile than Conventional Statins in Cirrhotic Rats. *Sci Rep.* 2017;7(1):40461.
31. Moal F, Veal N, Vuillemin E, Barrière E, Wang J, Fizanne L, et al. Hemodynamic and antifibrotic effects of a selective liver nitric oxide donor V-PYRRO/NO in bile duct ligated rats. *World J Gastroenterol.* 2006 Nov;12(41):6639–45.
32. Leung T-M, Fung M-L, Liong EC, Lau TYH, Nanji AA, Tipoe GL. Role of nitric oxide in the regulation of fibrogenic factors in experimental liver fibrosis in mice. *Histol Histopathol.* 2011 Feb;26(2):201–11.
33. Thiele ND, Wirth JW, Steins D, Koop AC, Ittrich H, Lohse AW, et al. TIMP-1 is upregulated, but not essential in hepatic fibrogenesis and carcinogenesis in mice. *Sci Rep.* 2017 Apr 6;7(1):714.
34. Nie Q-H, Zhang Y-F, Xie Y-M, Luo X-D, Shao B, Li J, et al. Correlation

- between TIMP-1 expression and liver fibrosis in two rat liver fibrosis models. *World J Gastroenterol*. 2006 May 21;12(19):3044–9.
35. Busk TM, Bendtsen F, Nielsen HJ, Jensen V, Brünner N, Møller S. TIMP-1 in patients with cirrhosis: relation to liver dysfunction, portal hypertension, and hemodynamic changes. *Scand J Gastroenterol*. 2014 Sep;49(9):1103–10.
36. Wang K, Lin B, Brems JJ, Gamelli RL. Hepatic apoptosis can modulate liver fibrosis through TIMP1 pathway. *Apoptosis*. 2013;18(5):566–77.
37. Hink U, Münzel T. COX-2, Another Important Player in the Nitric Oxide–Endothelin Cross-Talk: good news for COX-2 inhibitors?. *Circ Res*. 2006 Jun 9;98(11):1344–6.
38. Yang H, Xuefeng Y, Shandong W, Jianhua X. COX-2 in liver fibrosis. *Clin Chim Acta*. 2020;506:196–203.
39. Grumbach IM, Chen W, Mertens SA, Harrison DG. A negative feedback mechanism involving nitric oxide and nuclear factor kappa-B modulates endothelial nitric oxide synthase transcription. *J Mol Cell Cardiol*. 2005 Oct;39(4):595–603.
40. Liu T, Zhang L, Joo D, Sun S-C. NF-κB signaling in inflammation. *Signal Transduct Target Ther*. 2017;2(1):17023.

TABLES AND FIGURES

Table 1. Serum markers of liver function in cirrhotic rats treated with control or NO donor ret pBAE NPs.

	Cirrhotic rats with ascites	
	CT ret NPs (n = 5)	NO donor ret NPs (n = 9)
Body weight (g)	406.2 ± 9.37	420.7 ± 19.1
Ascites (ml)	6.8 ± 2.15	9.22 ± 3.07
Thoracic edema	1 ± 1	2.33 ± 2.21
Alanine transaminase (U/l)	282.7 ± 67.45	191.6 ± 39.46
Aspartate transaminase (U/l)	1384 ± 256.2	671.5 ± 165.2*
Gamma-glutamyl transferase (U/l)	12.76 ± 1.58	7.64 ± 2.27
Lactate dehydrogenase (U/l)	2782 ± 418.2	1101 ± 134***
Total bilirubin (mg/dl)	1.62 ± 0.43	1.84 ± 0.53
Total proteins (g/l)	40.66 ± 2.42	39.47 ± 3.13
Albumin (g/l)	21.76 ± 1.51	23.71 ± 1.54
Triglycerides (mg/dl)	110.2 ± 9.23	80.11 ± 12.53
Total cholesterol (mg/dl)	59.5 ± 4.78	58.29 ± 7.80
Glucose (mg/dl)	68.55 ± 16.89	73.52 ± 13.57
Creatinine (mg/dl)	0.63 ± 0.05	0.57 ± 0.07

*p < 0.05, *** p < 0.001, compared with CT group. Unpaired t-test or Mann Whitney when appropriate. Results are given as means ± S.E.

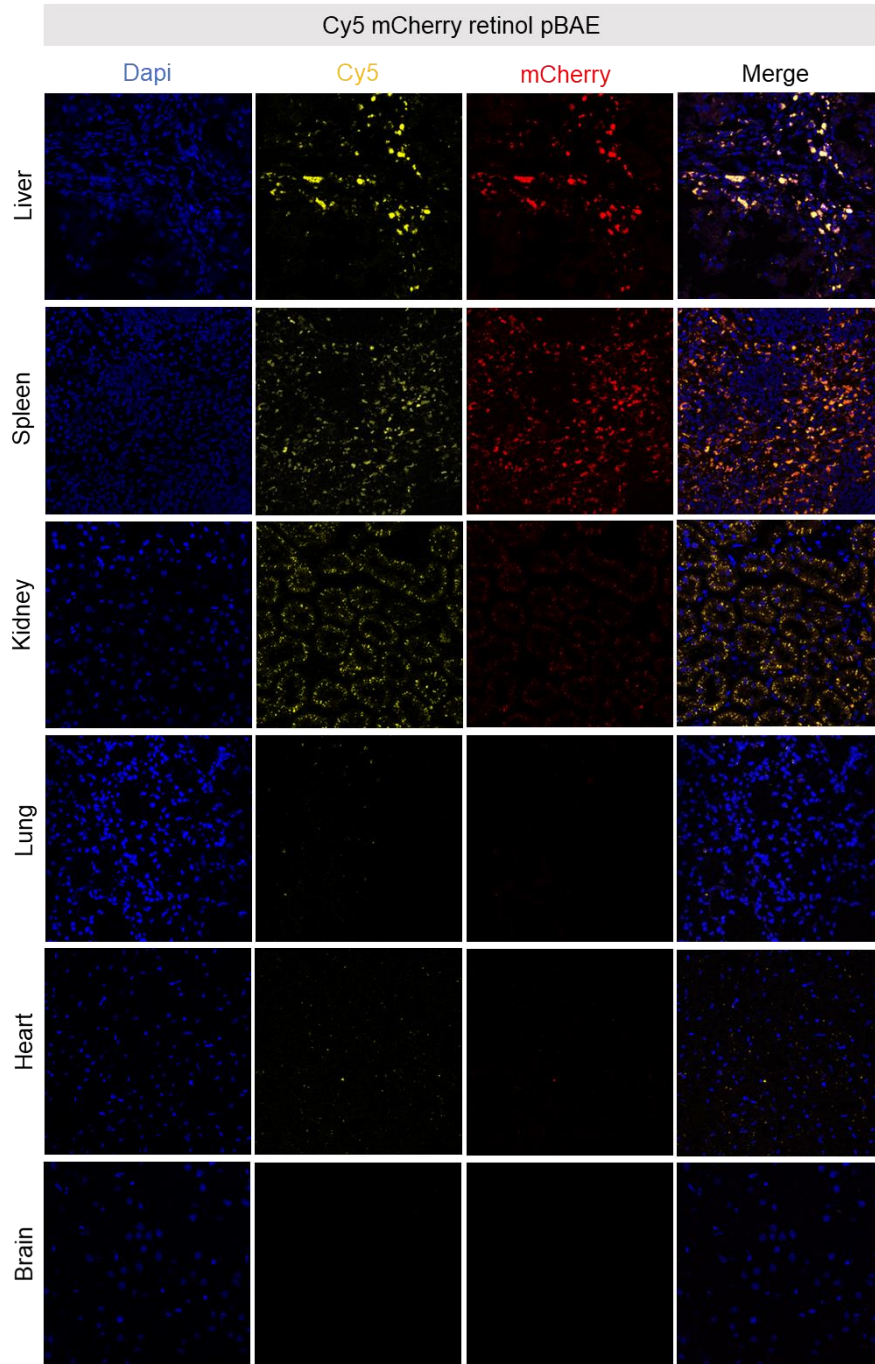


FIGURE 1- Organ biodistribution of Cy5 mCherry ret pBAE NPs. Representative confocal microscopy fluorescence images at 40x of organs collected 3 h after Cy5 mCherry ret pBAE NPs administration in cirrhotic rats. Nuclei are stained in blue.

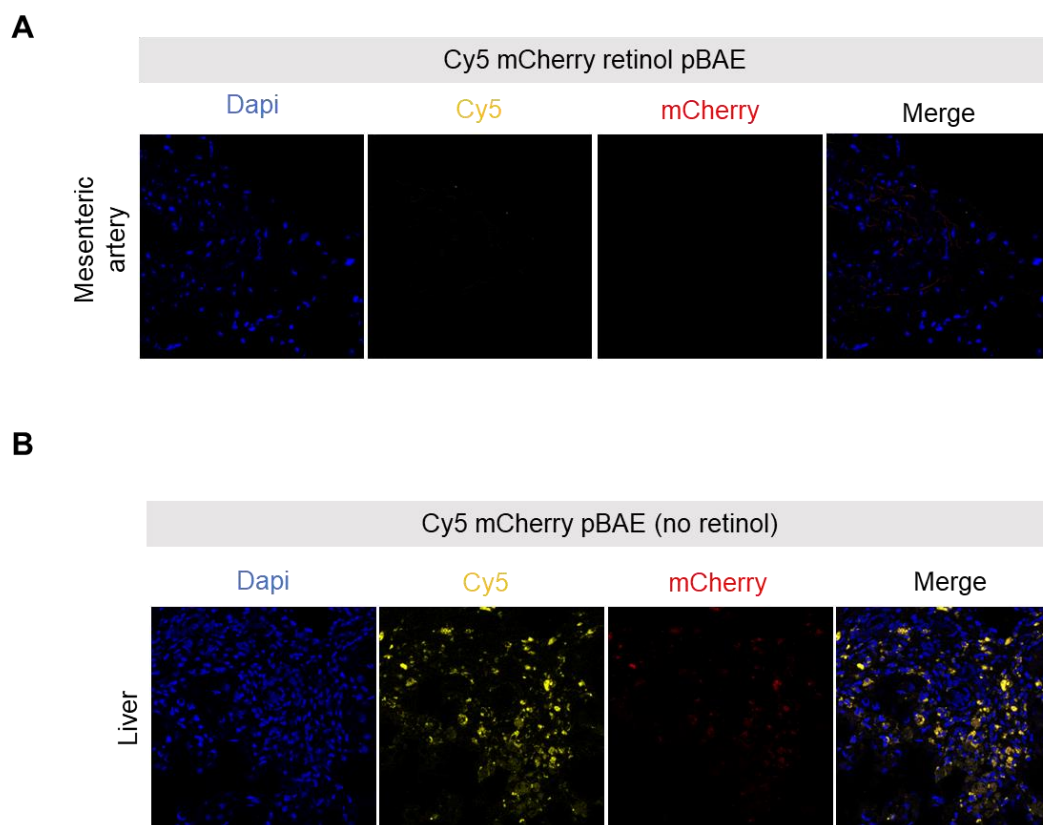


FIGURE 2- Arterial and hepatic distribution of Cy5 mCherry pBAE with and without retinol moiety. Representative confocal microscopy fluorescence images at 40x magnification of samples obtained 3 h after i.v. treatment. Nuclei are stained in blue. (A) Mesenteric artery section of a rat treated with Cy5 mCherry retinol pBAE NPs. (B) Liver section of a rat treated with Cy5 mCherry pBAE without retinol.

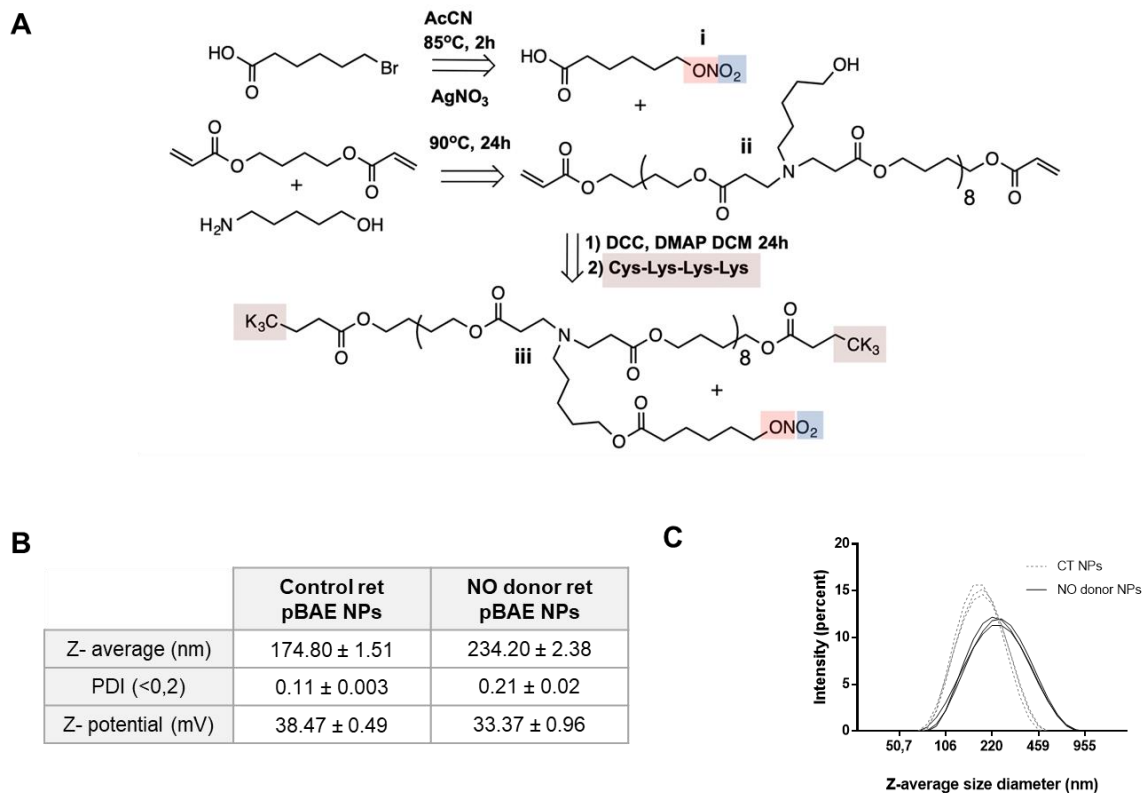


FIGURE 3- Synthesis and characterization of NO donor ret pBAE NPs. (A) Panel of strategy followed to generate a pBAE containing an organic nitrate group: from halide organic acids to its induction through a Steglich esterification reaction using side chain hydroxyls. (B) Z-average size, PDI and Z-potential measured using dynamic light scattering of NPs with and without NO donor. (C) Graphic representing intensity and Z-average size in triplicate measurements of both types of NPs.

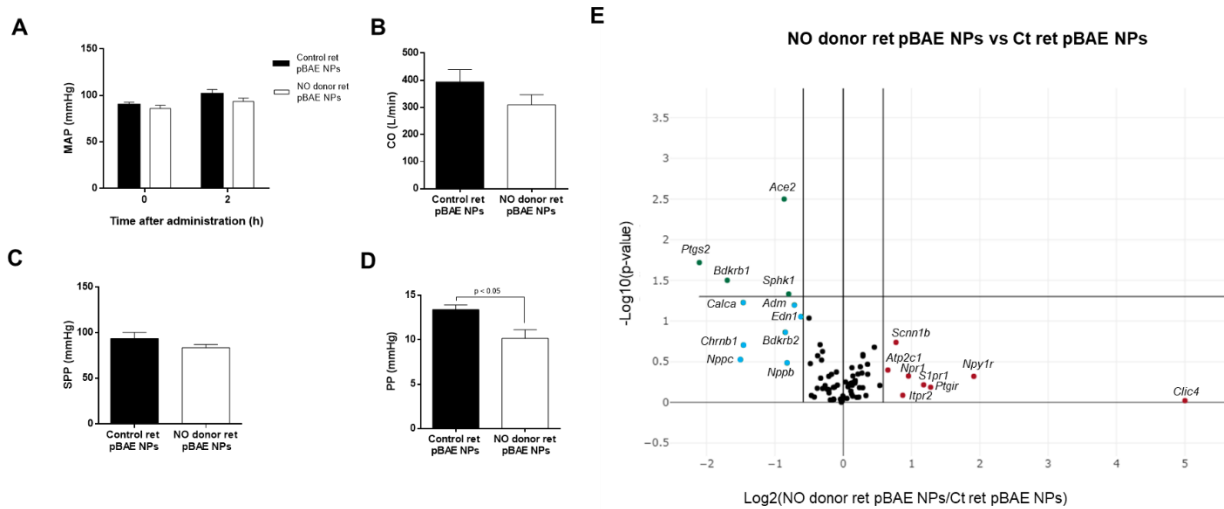


FIGURE 4- Effects of liver-targeted NO donor in systemic and portal hemodynamics of rats with decompensated cirrhosis. Rats with ascites treated with CT (n=5) or NO donor ret pBAE NPs (n=9). (A) MAP measurement before and 2 h after NPs administration. (B) CO measurement at the end of the study. (C) SPP calculated at the end of the study. (D) PP quantification at the end of the study. Results are given as mean \pm S.E. Mann Whitney test. (E) Volcano plot of the differentially expressed genes related to hypertension in a pair-wise comparison in the liver of these rats. Significance was set to a *P* value based on a Student's *t*-test of 0.05 ($-\log_{10} [P\text{-value}] \geq 1.30$), the biological cut-off was set to a fold regulation of ± 1.5 fold ($-1 \geq \log_{1.5} [\text{FC of NO donor ret pBAE NPs/Ct ret pBAE NPs}] \geq 1$). According with these two criteria, the top 19 differentially expressed genes are labeled with their corresponding gene ID. Insignificant (black), biologically but not statistically downregulated (blue) and upregulated (red), and both biologically and statistically significant downregulated (green) genes in cirrhotic rats treated with NO donor ret pBAE NPs.

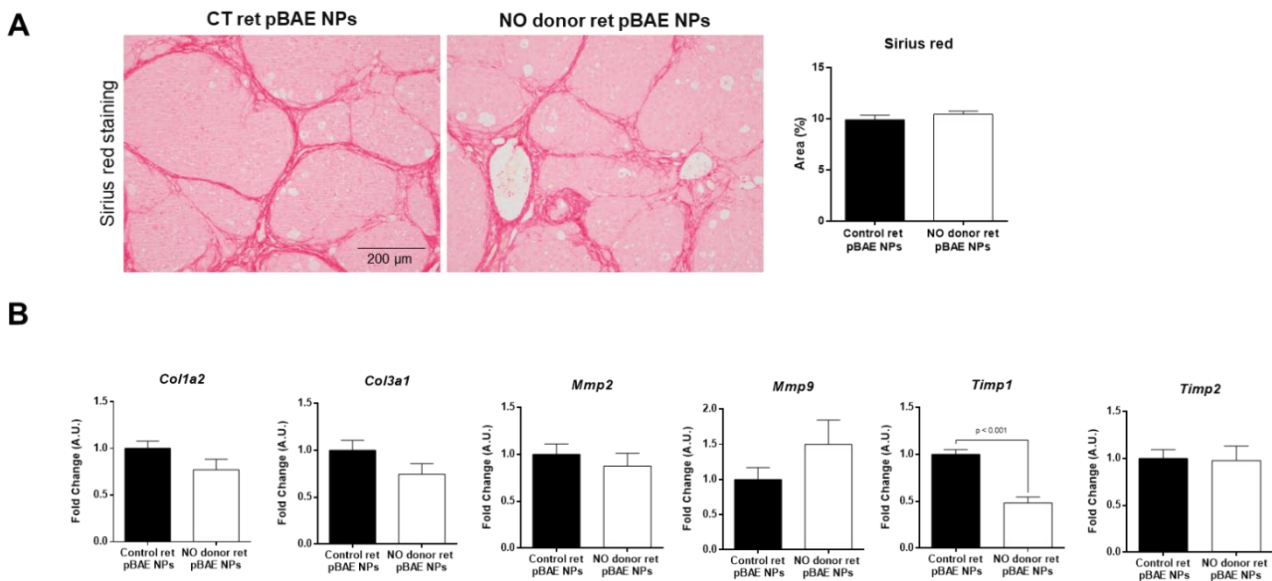


FIGURE 5- Effects of liver-targeted NO donor on fibrosis. Cirrhotic rats treated with CT (n=5) or NO donor ret pBAE NPs (n=9). (A) Representative hepatic liver sections images and morphometric quantification of Sirius red staining at 100x. (B) Hepatic mRNA expression of a panel of genes related to fibrosis including *Col1a2*, *Col3a1*, *Acta2*, *Mmp2*, *Mmp9*, *Timp1*, and *Timp2*. Results are given as mean \pm S.E. Unpaired or Mann Whitney test when appropriate.

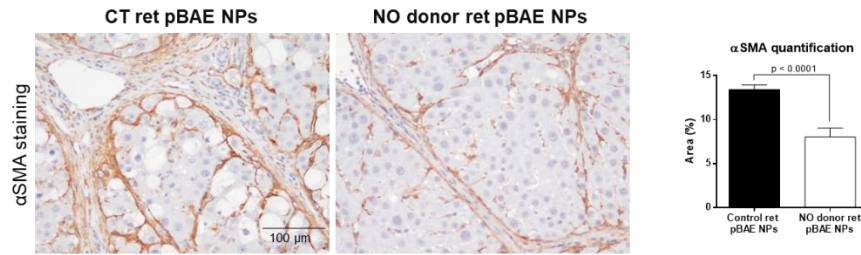
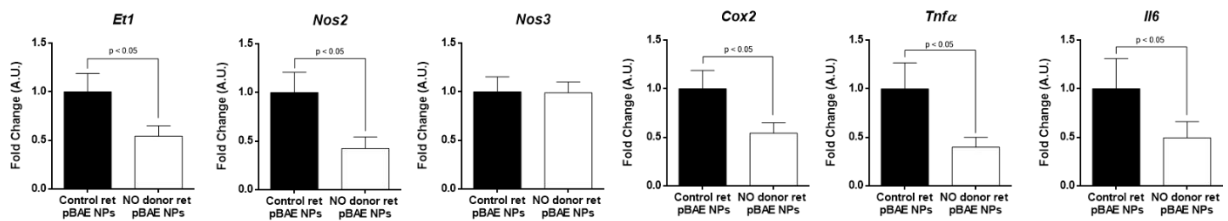
A**B**

FIGURE 6- Effects of liver-targeted NO donor on HSC activation and inflammation. Cirrhotic rats treated with CT (n=5) or NO donor ret pBAE NPs (n=9). (A) Representative hepatic liver sections images and quantification of α SMA staining at 200x. (B) Hepatic mRNA expression of *Et1*, *Nos2*, *Nos3*, *Cox2*, *Tnfa*, and *Il6*. Results are given as mean \pm S.E. Unpaired or Mann Whitney test when appropriate.

DISCUSSION

Liver cirrhosis is the leading cause of hepatic related morbidity and mortality. Identifying an effective antifibrogenic treatment is a major unmet medical need. In the first study of the current doctoral thesis, we aimed to investigate the role of PTTG1/DLK1 signaling in the fibrogenic process and to evaluate *Pttg1* gene silencing as an antifibrogenic treatment to attenuate experimental liver fibrosis.

In the liver of healthy animals, *Pttg1* transcript was almost undetectable, whereas it was augmented in hepatic fibrosis and further in cirrhosis. Besides, the liver was the only organ in which *Pttg1* was augmented in animals with cirrhosis compared to control ones. In accordance, *Dlk1* mRNA was higher in fibrosis than control, positively correlating with collagen deposition. Moreover, the cirrhotic liver was the only organ which significantly overexpressed *Dlk1* compared to the control organ. DLK1 protein levels replicated mRNA expression pattern and diverged from other profibrogenic mediators. Hepatic primary cells isolation revealed augmented *Pttg1* and *Dlk1* transcription in cirrhotic hepatocytes, HSCs and endothelial cells compared to control counterparts. Additionally, whereas control livers did not present positive PTTG1 and DLK1 protein staining, cirrhotic ones showed intense but topologically undefined protein staining. Eventually, hepatic cirrhotic biopsies from patients considerably upregulated *PTTG1* and *DLK1* expression compared to control samples. As far as we know, this is the first study proving *PTTG1* transcript expression in cirrhotic patients. According to previous investigations where *DLK1* has been shown upregulated in HCC but rarely in adjacent non-cancerous tissue (306), we also demonstrated upregulated *DLK1* mRNA in cirrhosis compared to control biopsies. Altogether, this suggests that *PTTG1/DLK1* signaling may be important in the pathogenesis of hepatic fibrosis. This was additionally endorsed by findings using *Pttg1* KO mice. Previously, Buko *et al.* showed that *Pttg1* KO mice presented less thioacetamide-induced bridging fibrosis in comparison to WT mice (81). This conclusion was reaffirmed in the present study using CCl₄-induced liver fibrosis experimental model. Rigorous gene expression analysis comparing the hepatic expression of fibrotic *Pttg1* KO and WT mice showed that disruption of ECM turnover was a key driver governing this phenomenon. Only genes with both statistical and biological significance were considered. The analysis unveiled significant downregulation of *Mmp8*, *Mmp9*, *Timp4* and *Acta2*. Interestingly, this was

accompanied by *Myc* downregulation. *Myc* is a nuclear phosphoprotein that regulates the expression of multiple genes related to cell growth, cycle, differentiation, apoptosis, genomic instability, transformation, and angiogenesis (307). Besides, *Pttg1* has been reported to be a powerful activator of *Myc* (48), which hints that both could interact and play an important role during hepatic fibrogenesis.

Altogether these findings suggest that gene therapy targeting *Pttg1* expression could be a promising approach to interfere with the progression of liver fibrosis. In fact, fibrotic rats treated with a siRNA against *Pttg1* showed weaker liver fibrosis, reduced portal hypertension and decreased number of activated HSCs compared to scrambled siRNA-treated animals, being a reduction of the proportion of activated HSCs the probable responsible of fibrogenesis inhibition. On the other side, the reduction in portal hypertension may be because of the antifibrotic effect. This was accompanied by decreased transcription of *Col1a2*, *Col3a1*, *Tgfb β 1* and *Pdgfr β* . It has been shown that *Pttg1* silencing in ovarian epithelial tumor cells lowered the expression and release of TGF β (308). Here, we report a tendency to decreased *Tgfb β 1* expression following *Pttg1* interference in fibrotic rats. Moreover, previous studies reported diminished *Tgfb β* transcription in the liver of fibrotic *Pttg1* KO compared to WT mice (81).

Administration of *Pttg1* siRNA in CCl₄-induced fibrotic rats was also associated to decreased *Pdgfr β* mRNA. Reduced liver fibrosis was previously reported by intrahepatic PDGFR β pathway blockade using adenoviral vectors (309) and by systemic PDGF antagonism in bile duct ligated rats (310). PDGF is the most potent pro-proliferative mediator in HSCs (311,312). Therefore, inhibition in HSCs proliferation may be responsible for decreased liver fibrosis after *Pttg1* interference.

Both excessive synthesis and decreased ECM degradation contributes to liver fibrosis (313,314). In the current study, ECM remodeling is also affected by *Pttg1* silencing. Hepatic *Col1a2* and *Col3a1* gene expression were upregulated in fibrotic rats receiving scrambled siRNA. Besides *Mmp2* and *Mmp9* transcription was also increased, probably due to a compensatory mechanism aimed to get rid of the excess of scar tissue. *Pttg1* silencing augmented MMPs/TIMPs ratio maybe

as a result of *Timp1* and *Timp2* inhibition. This supports the role of PTTG1 in the regulation of ECM degradation in the fibrotic liver primarily by controlling TIMPs expression.

Noteworthy, most surrogate liver function serum markers in fibrotic rats tended towards the normalization after *Pttg1* siRNA treatment, in exception of transaminases, indicating that *Pttg1* exerts a direct effect in fibrosis generation and not in CCl₄ hepatotoxicity. This phenomenon was reported beforehand in *Pttg1* KO mice (81).

Pttg1 interference mediates several mechanisms in liver fibrosis. Firstly, probably due to post-transcriptional regulation (82), *Dlk1* mRNA expression is prevented by *Pttg1* silencing, resulting in lower HSC activation and fibrosis deposition (112). This suggests that PTTG1/DLK1 network is important during hepatic fibrogenesis. Additionally, both mediators are regulated by histone deacetylases (HDAC). In corticotroph cells, HDAC1 induces proliferation upregulating *Pttg1* expression (315) and in preadipocytes and NIH 3T3 cells, HDAC3 represses *Dlk1* (88). Secondly, *Pttg1* is implicated in ECM remodeling. It has been shown that *Pttg1* induces *Mmp2* expression and secretion (316). MMP2 is a gelatinase involved in the degradation of ECM components such as collagen IV, fibronectin, and laminin (313). In here, we showed that *Mmp2* is augmented in liver fibrosis. Moreover, *Pttg1* silencing reduces *Mmp2* resulting in anti-fibrogenic effect by decreasing normal ECM degradation and inducing HSC activation (317). *Pttg1* silencing also decreases TIMPs expression. Activated HSC highly express *Timp1* and *Timp2*, thereby, reduced *Timp1* and *Timp2* mRNA expression following *Pttg1* interference in fibrotic rats may be due to reduced HSC activation. *Timp1* and *Timp2* also stimulate fibroblast proliferation (318). For this reason, their downregulation could be involved in reduced HSC proliferation. **Figure 20** illustrates a graphical model outlining the proposed mechanism underlying PTTG1/DLK1 axis implication in the pathogenesis of liver fibrosis.

To sum up, this study shows that *Pttg1* gene silencing using a siRNA acts as an anti-fibrotic agent in fibrotic rats. Besides, *Pttg1* interference diminishes upregulated *Dlk1* expression, decreases the activation of HSCs, the expression of

genes related to ECM deposition and remodeling, reduces collagen deposition and eventually, diminishes portal hypertension. Therefore, *PTTG1/DLK1* pathway may be a potential therapeutic target for the prevention and treatment of hepatic fibrogenesis.

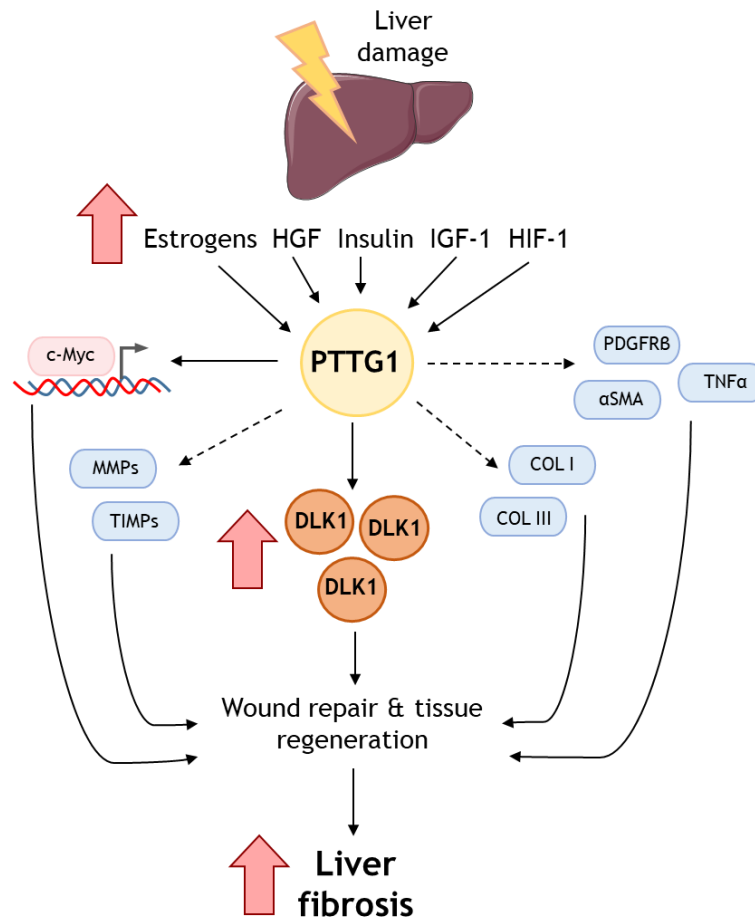


Figure 20. Schematic representation of the proposed mechanism underlying *PTTG1/DLK1* axis role in liver fibrosis induction. The synthesis and release of mediators including estrogens, hepatocyte growth factor (HGF), insulin, insulin growth factor 1 (IGF-1), and hypoxia inducible factor 1 (HIF-1) are augmented following liver injury. These mediators induce the expression of *Pttg1*, a transcriptional activator of *c-myc*. Besides, *Pttg1* indirectly augments the expression of platelet derived growth factor receptor beta (*PDGFRβ*), tumor necrosis factor alpha (*TNFα*), alpha-smooth muscle actin (*αSMA*), collagens I (*COL I*) and III (*COL III*), metalloproteinases (*MMP*), and tissue inhibitors of metalloproteinases (*TIMP*). Noteworthy, *Pttg1* also induces *Dlk1* expression. This contributes to wound repair and tissue regeneration inducing liver fibrosis. Direct effect is shown with continuous arrows and indirect effect by discontinuous ones. Original image from: Perramón M, Carvajal S, Reichenbach V, Fernández-Varo G, Boix L, Macías-Muñoz L, et al. The pituitary tumour-transforming gene 1/delta-like homologue 1 pathway plays a key role in liver fibrogenesis. *Liver Int.* 2022 Mar;42(3):651-662.

In the second study included in the current doctoral thesis, we aimed to evaluate the potential beneficial effects of CeO₂NPs in tumor progression, inflammation, kinase signaling pathways, lipid metabolism, and animal survival in rats with experimental HCC. Despite nanoceria has widely been used for decades to catalyze redox reactions in catalytic exhaust converters and petrochemical industries (253), its use as a therapeutic agent is still a major

concern. Largely due to CeO₂NPs variability in antioxidant response and activity in biological media (319). To overcome these issues, in the present study CeO₂NPs have been coated with albumin resulting in NPs with high stability and monodispersity in physiological media. The formation of large aggregates and protein corona are prevented and thereby, a stable NPs colloidal solution is generated.

An effective systemic HCC treatment remains an unmet clinical need. Oxidative stress, mainly ROS, is a major driver of cancer pathogenesis. It is directly implicated in the initiation and progression of cancer, in addition to decrease the natural antioxidant defenses which are involved in scavenging free radicals (176). For these reasons, antioxidants including different compounds, enzymes and inhibitors have been largely evaluated for the treatment of chronic inflammation and cancer. But to date none of them, as consequence of their low systemic bioavailability, has shown promising results.

In this study, we investigated the potential of the antioxidant CeO₂NPs as a treatment for HCC. Unlike other therapies, CeO₂NPs possess a catalytic self-regenerating antioxidant effect, therefore avoiding the need for periodical administration. Besides, nanoceria is inert in physiological conditions and it is only active when there is oxidative stress.

DEN is a carcinogenic organic compound acting by rising the proliferation of hepatocytes. Once administered, DEN is first hydroxylated by cytochrome (CYP) P450 and then it is oxidized by CYP2E1 to reactive products. The administration of DEN resulted in macroscopically and microscopically alterations of the liver including modification of liver weight, tissue dysplasia and the apparition of fibrotic tracts. Next, we wanted to evaluate the biodistribution following CeO₂NPs administration in rats with HCC. Despite the high tumorigenic activity in the liver, CeO₂NPs preserved their selectivity for liver tissue in rats with DEN-induced HCC.

Besides, HCC rats treated with CeO₂NPs showed decreased activation of parameters related to tissue growth, proliferation, and inflammation. They had increased liver / body weight ratio and reduced the amount of hepatic infiltrating

macrophages and Ki67-positive cells compared to vehicle-treated rats. Ki67 is greatly used as proliferation marker as well as prognostic cancer indicator. Additionally, AFP serum concentration was diminished. AFP is the most used biomarker for hepatocyte dedifferentiation and closely associated to HCC. CeO₂NPs also reduced the expression of proinflammatory M1-related genes. During carcinogenesis, TAMs provide an immunosuppressive microenvironment which facilitates tumor progression (320). Therefore, CeO₂NPs antitumor effects may be partially mediated by the decrease in infiltrating macrophages, due to cell death or chemotaxis inhibition.

Several evidences sustain CeO₂NPs antitumor effects in DEN-induced HCC experimental model. Firstly, nanoceria administration resulted in augmented hepatic apoptosis. This agrees with a previous study from Wang Y *et al.* in which showed that cuprous oxide NPs induce apoptosis of lung melanoma cells (321). Secondly, CeO₂NPs diminished the phosphorylation of ERK1/2. Ras/Raf/MAPK kinase/ERK signaling pathway is one of the most important controlling proliferation, growth, differentiation, survival, angiogenesis, inflammation and glucose and lipid metabolism (322).

Besides, untargeted MS-based proteomics was used to evaluate the effects of CeO₂NPs in HCC cellular phosphorylation. CeO₂NPs significantly affected 9.5% of all detected phosphorylation sites, including augmented and diminished, on the liver of rats with HCC. These effects were in networks related to cell proliferation, apoptosis, migration, and survival. For instance, p21 activated kinase 2, eukaryotic elongation factor 2 kinase, tyrosine kinase 2/focal adhesion kinase 2 and NIMA-related kinase 9. Noteworthy, gene ontology analysis revealed an enrichment of phosphorylation of proteins related to RNA splicing and cell-cell adhesion. Splicing is often disturbed in human tumors and significantly contributes to processes like proliferation, apoptosis, angiogenesis, and migration (323). For that matter, nanoceria effects in altering the phosphorylation of proteins related to splicing may be involved in the decreased hepatic cell proliferation. Besides cell-cell adhesion, involving both tumor suppressors and oncogenes, is a process also deregulated in cancer (324). CeO₂NPs significantly reduced the phosphorylation of cell surface proteins CD44 and Itgb4.

Dysregulation of FA metabolism to support cellular proliferation is one of the hallmarks of cancer (325). Cancer cells have a strong avidity for lipids augmenting both exogenous uptake and endogenous synthesis (326). In agreement, the measurement of lipids circulating in the serum of rats with HCC revealed a reduced amount of triglycerides and cholesterol. Besides, the analysis of principal lipid components in the liver of these rats showed significantly increased CE-derived FAs, which is the most common form of cancer cells to store excessive lipids and cholesterol in LDs (322). NEFA lipid component was also augmented presumably to support tumor growth.

In contrast, the strongest effects of CeO₂NPs in the hepatic lipidome were found in PC-derived FAs. Nanoceria significantly decreased PC-derived FAs because of a great reduction in arachidonic acid. Esterified arachidonic acid is released from cellular phospholipids by phospholipases A₂, C, and D; a pathway already augmented in rats with HCC. Once free, arachidonic acid can be metabolized or act as a second messenger in several networks (327), some of which upregulated in rats with DEN-induced HCC. CeO₂NPs treated animals further decreased esterified PC-derived arachidonic acid, probably related to the increased apoptosis found in these animals since free arachidonic acid can activate sphingomyelinase and induce this process (328).

Additionally, nanoceria significantly diminished one of the most abundant FAs: linoleic acid in TG, NEFA and CE lipid components in the liver of rats with HCC. Brown *J et al.* reported that linoleic acid has an important role in the development of NAFLD-promoted HCC by changing intrahepatic CD4⁺ cells metabolism and inducing apoptosis (328). Anomalous essential FA metabolism involving $\Delta 6$ desaturase induces changes in PUFA profile, which have been related to neoplastic hepatocytes (327). Besides, intracellular redox state regulates the activity and expression of the after mentioned desaturase (329). Therefore, the reduction in oxidative stress after CeO₂NPs treatment could trigger the reactivation of $\Delta 6$ desaturase activity and the restoration to normal linoleic acid hepatic concentrations in rats with HCC.

The effect of nanoceria on survival was further assessed to translate the antitumorigenic effects in a clinically significant improvement. Rats with HCC and

treated with CeO₂NPs significantly increased survival compared to ones receiving vehicle. To treat patients with advanced HCC, several tyrosine kinase inhibitors including sorafenib, lenvatinib, cabozantinib and regorafenib are believed to be effective compounds (330). In our study, similar effects on survival rates were observed after treating DEN-injured rats either with sorafenib or CeO₂NPs, demonstrating that both treatments are equally effective under the studied conditions. The combination of both did not produce further survival amelioration. This could be explained because both treatments lead to similar effects: common signaling pathways are affected as VEGF signaling in angiogenesis, they induce alike ERK1/2 modulation, and phosphorylation state alteration, altogether driving to similar proliferation and apoptosis modification, as reported with sorafenib (331). **Figure 21** illustrates a graphical model outlining the main effects of CeO₂NPs on experimental HCC.

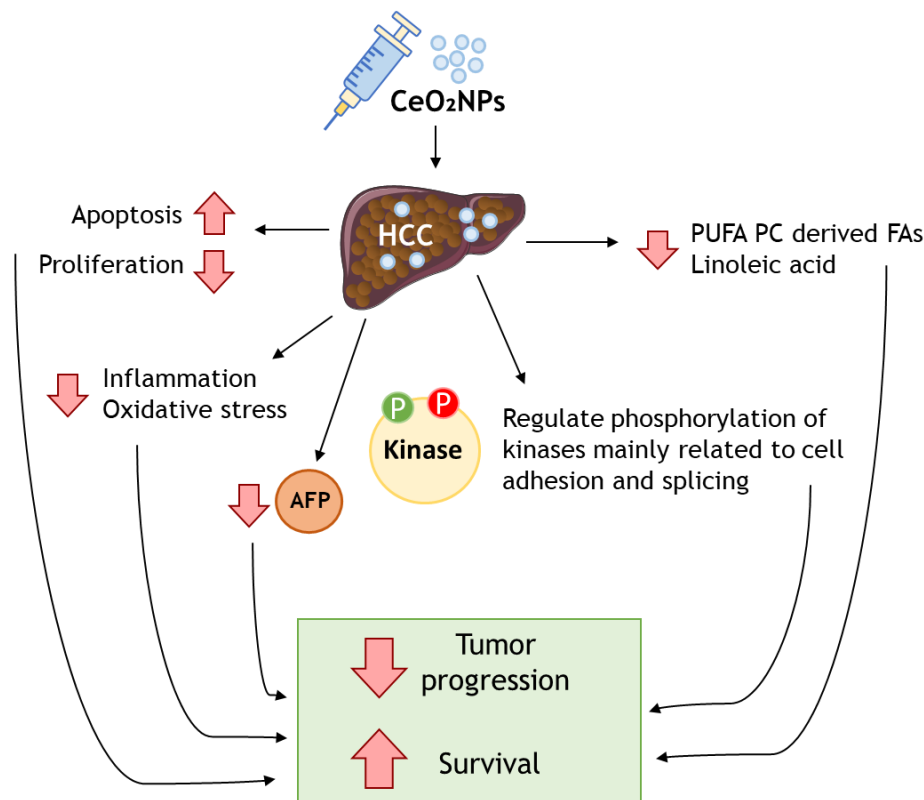


Figure 21. Schematic representation of CeO₂NPs effects on experimental HCC. Following CeO₂NPs intravenous administration, they mainly accumulate in the liver where they increase apoptosis at the same time decrease proliferation. Moreover, CeO₂NPs reduce hepatic inflammation and oxidative stress. CeO₂NPs are also involved in decreasing alpha-fetoprotein (AFP) levels. CeO₂NPs also regulate the phosphorylation of several kinases. Finally, CeO₂NPs treatment ultimately leads to decrease polyunsaturated (PUFA) phosphatidylcholine (PC) derived fatty acids (FAs). Altogether results in the reversion of cellular mechanisms related to tumor progression and improves survival.

Finally, to gain insight on nanoceria behavior in the human liver, we administered CeO₂NPs *ex vivo* to human livers undergoing normothermic

machine perfusion. Following administration, CeO₂NPs rapidly accumulated in the hepatic tissue confirming nanoceria avidity for the human liver. They were observed both within intracellular endosome-like bodies and free in the cytoplasm. Cerium presence was further confirmed by elemental analysis combined with STEM. The human hepatocyte cell line HepG2 reiterated NPs uptake mainly in endosome-like organelles.

In conclusion, the treatment with CeO₂NPs partially reverts tumor progression and significantly augments survival in rats with DEN-induced HCC, suggesting that this antioxidant nanomaterial is a potential effective treatment in experimental HCC. Nanoceria alone or in combination with molecular targeted treatments could be of value attenuating HCC progression in patients.

Portal hypertension is a major complication of advanced liver disease, consequence from increased resistance to the portal blood flow into the liver. The subsequent appearance of clinical life-threatening complications such as ascites or variceal bleeding induce the transition from compensated to a decompensated state. In the third study, we aimed to evaluate the possible therapeutic value of an organic NO donor directed to the liver by retinol decorated pBAE NPs in experimental decompensated cirrhosis.

NO donors are potent compounds with the ability to release NO and facilitate smooth muscle relaxation (332). Organic nitrates are a class of donors widely known for their stability, since NO release does not rely on environmental changes but on enzymatic activities including aldehyde dehydrogenase-2 or cytochrome P450 reductase (333,334). Given that is difficult to measure NO release intrahepatically, their kinetics was not evaluated in the present study. Therefore, similar retinol pBAE NPs but lacking the NO donor were used as control and it was speculated that differences between treatments could be attributed to NO release. NO donor containing retinol pBAE NPs showed a larger hydrodynamic size and a similar positive z-potential compared to control NPs as measured by dynamic light scattering.

To evaluate the potential of pBAE NPs with retinol moiety to specifically target the liver, a biodistribution study was first performed. A Cy5 dye as well as a

plasmid encoding for the protein mCherry were added to the NPs to track their uptake and transfection, respectively. The liver, spleen and kidney showed Cy5 presence. In the hepatic tissue, this signal co-localized with mCherry in fiber-like zones. Besides, both Cy5 and mCherry signals were extensive in the splanchnic tissue. In contrast, mCherry was almost absent in the kidney. Finally, neither Cy5 or mCherry were identified in the heart, brain, or lung. Furthermore, the fluorescence analysis revealed no presence of Cy5 or mCherry protein in thoracic and abdominal aorta, carotid, mesenteric, femoral, and renal arteries. NO donor hepatic selectivity is of major concern in decompensated cirrhosis given that a further increase in systemic vasodilation would have a noxious impact. Other authors had previously employed different ligands to deliver pBAE NPs to hepatic cancer cells (283,303). Here, retinol was selected because the liver plays a central role in retinol storage and distribution (335). Recently, Fornaguera *et al.* reported that the addition of retinol in to end-oligopeptide modified pBAE NPs enabled higher hepatic delivery once injected in control mice (291). In line, Duong HTT *et al.* reported that the decoration with retinol facilitated the delivery of polymeric NPs to HSC in bile-duct ligated rats (232).

Cirrhosis decompensation is characterized by a clinically significant portal hypertension, the worsening of hepatic function and disease progression (132). For several decades, non-selective beta blockers have been the treatment of choice to reduce portal hypertension in patients. These drugs act diminishing the heart rate and CO, in addition to induce splanchnic arteries vasoconstriction. Besides, they have been shown to prevent decompensation and the appearance of clinical complications and therefore, increasing patients' survival (132). Nevertheless, their use in patients with end-stage cirrhosis remains controversial (336,337). Consequently, there is an urge to develop novel therapies intended to reduce the portal hypertension. Here, we evaluated the impact on systemic and portal hemodynamics of our liver-selective nanoformulation conjugated to a NO donor. The treatment with NO donor pBAE NPs decorated with retinol did not influence the mean arterial pressure or the CO. Strikingly, they significantly reduced PP. Other authors have previously shown similar results, but most of them used early fibrosis models which do not recapitulate a clinically significant portal hypertension (338,339). Only two studies have reported the evaluation of

similar treatments in decompensated cirrhosis experimental models. Moal F *et al.* (340) showed a reduction on PP as well as in the development of collateral circulation in n bile duct ligated rats treated with a liver-specific NO donor. Besides, Duong HTT *et al.* (232) reported a decrease in portal hypertension after a liver-targeted NO donor administration in bile duct ligated rats and evaluated the effects *in vitro* in HSCs.

Further knowledge on the hepatic effects of the ret pBAE NPs containing the NO donor in cirrhotic rats with ascites was obtained performing a commercially available array of vasoactive genes. Rigorous analysis revealed that four genes including *Bdkrb1*, *Ptgs2*, *Ace2* and *Sphk1*, were both biologically and statistically significantly downregulated after liver-specific NO treatment.

Next, we evaluated the possible effects of our nanoformulated NO donor on hepatic fibrogenesis. The treatment did not reduce intrahepatic collagen deposition, as means as the morphometric analysis of Sirius red staining. Of note, it significantly decreased the activation of HSCs, measured by α SMA staining. Moreover, the treatment did not induce changes in the mRNA expression of *Col1a2*, *Col3a1*, *Acta2*, *Mmp-2*, *Mmp-9*, or *Timp-2*. Other authors have previously reported fibrogenesis modulation by liver-targeted NO donors. For instance, Leung TM *et al.* (341) showed that the treatment with the NO donor L-arginine induced a downregulation in the transcription of profibrogenic mediators in a CCl₄-induced experimental mice liver fibrosis. In line, Sun J *et al.* (338) described a reduction in Sirius red staining and hydroxyproline content after treating DEN-induced cirrhotic rats with a NO donor linked to ursodeoxycholic acid. These studies reported longer treatment times compared to ours. Hence, the absence of effect in hepatic fibrogenesis in our study could be explained by the short treatment time, which was approximately 3 h.

Remarkably, NO donor pBAE NPs decorated with retinol decreased hepatic transcription of *Timp-1* and *Et-1*. During hepatic injury, TIMP-1 inhibits the activation of the proteolytic enzyme family MMPs to modulate ECM deposition (342,343). Moreover, TIMP-1 is antiapoptotic and has been involved in cellular proliferation promotion (344). In the plasma of patients with cirrhosis, TIMP-1 protein concentration is augmented and correlates with portal hypertension

(345). On the other hand, *ET-1* is a powerful vasoconstrictor, which exerts its functions mainly in endothelial and smooth muscle cells. It is known that NO deficiency induces *ET-1* expression and as a consequence *cyclooxygenase 2* expression and the conversion of arachidonic acid to prostaglandins and thromboxane are stimulated (346). Cyclooxygenase 2 is a mediator that plays an important role in a myriad of biological processes including inflammation, senescence, apoptosis, and autophagy (347). In this study, liver-specific NO donor treatment also resulted in decreased expression of *cyclooxygenase 2* as well as *Il-6*, *Tnfa* and *Nos2* mRNAs. It has been reported that NO inhibits nuclear factor kappa beta activation (348). This transcription factor important for the expression regulation of genes related to the inflammatory response and inflammasome (349). Noteworthy, the treatment did not induce changes in *Nos3* transcription. Finally, the administration of engineered NO donor polymeric NPs reduced the serum concentration of lactate dehydrogenase and aspartate aminotransferase enzyme. Therefore, these evidence suggests that NO donor retinol pBAE NPs efficiently target the liver of cirrhotic rats, where the release of NO is induced. NO in turn triggers 1) the loss of HSC contractile phenotype and 2) hepatic vasodilation. Altogether, this therapy reduces portal hypertension and proinflammatory gene expression.

To sum up, NO donor pBAE NPs decorated with retinol may be useful to mitigate portal hypertension and hepatic inflammation in decompensated cirrhosis.

CONCLUSIONS

1. The progression of rat liver fibrosis is associated to a selective concomitant increase in hepatic *Pttg1* and *Dlk1* mRNA expression.
2. *Pttg1* is upregulated in both cirrhotic rat hepatocytes and HSC compared to controls. *Dlk1* is also increased in both cirrhotic cell types, being more abundant in the former.
3. *PTTG1* and *DLK1* transcripts are augmented in liver biopsies from cirrhotic patients in comparison to non-cirrhotic subjects.
4. *PTTG1* and *DLK1* proteins are present in the hepatic parenchyma and close to portal tracts of cirrhotic rats, whereas they are undetectable in control livers.
5. Liver fibrosis progression correlates with circulating levels of *DLK1*. Besides, *DLK1* serum concentration also positively correlates with hepatic collagen content and portal hypertension.
6. The lack of *Pttg1* in fibrotic mice attenuates liver fibrosis and downregulates the transcript expression of *Dlk1* and genes involved in ECM turnover.
7. Silencing of *Pttg1* in rats with fibrosis significantly reduces hepatic collagen content, HSC activation, and portal hypertension compared to rats receiving scrambled siRNA.
8. CeO₂NPs mainly accumulate in the liver and spleen of rats with HCC that are administered intravenously, and they remain for at least 3 weeks.
9. Albeit CeO₂NPs do not modify hepatic function parameters, they significantly decrease serum AFP concentration and hepatic inflammation.
10. The treatment with CeO₂NPs significantly increases apoptosis and reduces the proliferation rate of hepatocytes in the liver of rats with HCC, probably due to a Ras/MAPK pathway interference.
11. The treatment with CeO₂NPs in DEN-induced HCC has a general effect on the phosphorylation of hepatic proteins, predominantly those related to cell adhesion and RNA splicing.
12. The amount of hepatic phosphatidylcholine-derived PUFAs is reduced in rats with HCC after the treatment with CeO₂NPs, mostly due to a decrease in arachidonic acid. In addition, these NPs normalize the augmented levels of linoleic acid in the principal lipid components from the hepatic tissue of rats with HCC.
13. CeO₂NPs significantly augment survival of DEN chronically administered rats compared to vehicle. Besides, sorafenib and CeO₂NPs have similar benefit and

- the combination of both results in longest survival, although without statistical significance.
14. Human liver can uptake CeO₂NPs from the circulation. In the liver, these NPs are mainly found inside blood vessels, space of Disse and in the cytoplasm and within endosome-like organelles of endothelial and circulating immune cells.
 15. CeO₂NPs are successfully internalized by the human hepatocyte cell line HepG2, and are found attached to the plasmatic membrane, in the cytoplasm and inside endosome-like organelles.
 16. The liver and spleen are the major targets of NO donor retinol pBAE NPs in rats with decompensated cirrhosis.
 17. Liver-targeted NO donor NPs ameliorate serum markers of liver function.
 18. The administration of retinol pBAE NPs containing a NO donor significantly reduce portal hypertension without affecting systemic hemodynamics in cirrhotic rats with ascites.
 19. Liver-targeted NO donor NPs diminish the transcription of genes involved in vascular reactivity.
 20. The activation of HSC and the expression of proinflammatory gene markers is reduced after NO donor containing ret pBAE NPs treatment in rats with decompensated cirrhosis.

According to the results obtained in the current doctoral thesis, it may be concluded that the interference of PTTG1/DLK1 signaling, CeO₂NPs and liver-targeted NO donor polyplexes are three promising nanoscale therapeutic approaches to target liver fibrosis, HCC, or the associated clinical complications, respectively. *Pttg1* and *Dlk1* expression selectively increase in the liver correlating with fibrosis progression in both experimental models and human patients. Moreover, *Pttg1* gene silencing using a siRNA in CCl₄-induced liver fibrosis rat model results in decreased *Dlk1* transcription, reduced collagen deposition, attenuated portal hypertension and diminished fibrosis-related genes expression. Besides, CeO₂NPs behave as strong antioxidants attenuating tumor progression by interfering with kinase pathways and lipid metabolism; ultimately reducing proliferation and inflammation, and at the same time increasing apoptosis in the liver of DEN-induced HCC. CeO₂NPs have similar effects to sorafenib ameliorating rat survival. Moreover, *ex vivo* perfused human liver and *in vitro*

hepatocyte cells can internalize CeO₂NPs both in intracellular endosome-like organelles and free in the cytoplasm. Finally, NO donor pBAE NPs decorated with retinol successfully target the cirrhotic liver. Moreover, pBAE NPs containing a NO donor ameliorate portal hypertension, without affecting systemic hemodynamics in rats with decompensated cirrhosis. Furthermore, these NPs significantly decrease the activation of HSCs and the mRNA expression of proinflammatory genes in the hepatic tissue.

REFERENCES

1. Parola M, Pinzani M. Liver fibrosis: Pathophysiology, pathogenetic targets and clinical issues. *Mol Aspects Med.* 2019 Feb;65:37–55.
2. Paik JM, Golabi P, Younossi Y, Mishra A, Younossi ZM. Changes in the Global Burden of Chronic Liver Diseases From 2012 to 2017: The Growing Impact of Nonalcoholic Fatty Liver Disease. *Hepatology.* 2020 Feb;72(5):1605–16.
3. Byrne CD, Targher G. NAFLD: A multisystem disease. *J Hepatol.* 2015 Apr 1;62(1):S47–64.
4. Eslam M, Newsome PN, Sarin SK, Anstee QM, Targher G, Romero-Gomez M, et al. A new definition for metabolic dysfunction-associated fatty liver disease: An international expert consensus statement. *J Hepatol.* 2020 Jul;73(1):202–9.
5. Sharma A NS. *Chronic Liver Disease.* StatPearls Publishing. 2021.
6. Roehlen N, Crouchet E, Baumert TF. Liver Fibrosis: Mechanistic Concepts and Therapeutic Perspectives. *Cells.* 2020 Apr;9(4).
7. Pinzani M. Pathophysiology of Liver Fibrosis. *Dig Dis.* 2015;33(4):492–7.
8. Ishak K, Baptista A, Bianchi L, Callea F, De Groote J, Gudat F, et al. Histological grading and staging of chronic hepatitis. *J Hepatol.* 1995 Jun;22(6):696–9.
9. Shiha, Gamal; Zalata K. Ishak versus METAVIR: Terminology, Convertibility and Correlation with Laboratory Changes in Chronic Hepatitis C. In: Takahashi KZE-H, editor. *Liver Biopsy.* Rijeka: IntechOpen; 2011.
10. Bedossa P, Poynard T. An algorithm for the grading of activity in chronic hepatitis C. The METAVIR Cooperative Study Group. *Hepatology.* 1996 Aug;24(2):289–93.
11. Sumida Y, Nakajima A, Itoh Y. Limitations of liver biopsy and non-invasive diagnostic tests for the diagnosis of nonalcoholic fatty liver disease/nonalcoholic steatohepatitis. *World J Gastroenterol.* 2014 Jan;20(2):475–85.
12. Hou W, Syn W-K. Role of Metabolism in Hepatic Stellate Cell Activation and Fibrogenesis. *Front Cell Dev Biol.* 2018; 6: 150.
13. Kisseleva T, Brenner D. Molecular and cellular mechanisms of liver fibrosis and its regression. *Nat Rev Gastroenterol Hepatol.* 2021;18(3):151–66.

14. Ying H-Z, Chen Q, Zhang W-Y, Zhang H-H, Ma Y, Zhang S-Z, et al. PDGF signaling pathway in hepatic fibrosis pathogenesis and therapeutics (Review). *Mol Med Rep*. 2017 Dec;16(6):7879–89.
15. van der Heide D, Weiskirchen R, Bansal R. Therapeutic Targeting of Hepatic Macrophages for the Treatment of Liver Diseases. *Front Immunol*. 2019; 10: 2852.
16. Wen Y, Lambrecht J, Ju C, Tacke F. Hepatic macrophages in liver homeostasis and diseases-diversity, plasticity and therapeutic opportunities. *Cell Mol Immunol*. 2021 Jan; 18(1): 45–56.
17. Parola M, Robino G. Oxidative stress-related molecules and liver fibrosis. *J Hepatol*. 2001 Aug;35(2):297–306.
18. Ramos-Tovar E, Muriel P. Molecular Mechanisms That Link Oxidative Stress, Inflammation, and Fibrosis in the Liver. *Antioxidants*. 2020 Dec;9(12):1279.
19. Luangmonkong T, Suriguga S, Mutsaers HAM, Groothuis GMM, Olinga P, Boersema M. Targeting Oxidative Stress for the Treatment of Liver Fibrosis. *Rev Physiol Biochem Pharmacol*. 2018;175:71-102.
20. Elpek GÖ. Cellular and molecular mechanisms in the pathogenesis of liver fibrosis: An update. *World J Gastroenterol*. 2014 Jun;20(23):7260–76.
21. Seki E, Brenner DA. Recent advancement of molecular mechanisms of liver fibrosis. *J Hepatobiliary Pancreat Sci*. 2015 Jul;22(7):512–8.
22. Acharya P, Chouhan K, Weiskirchen S, Weiskirchen R. Cellular Mechanisms of Liver Fibrosis. *Front Pharmacol*. 2021; 12: 671640.
23. Zuo W, Chen Y-G. Specific activation of mitogen-activated protein kinase by transforming growth factor-beta receptors in lipid rafts is required for epithelial cell plasticity. *Mol Biol Cell*. 2009 Feb;20(3):1020–9.
24. Roeb E. Matrix metalloproteinases and liver fibrosis (translational aspects). *Matrix Biol*. 2018;68–69:463–73.
25. Hemmann S, Graf J, Roderfeld M, Roeb E. Expression of MMPs and TIMPs in liver fibrosis – a systematic review with special emphasis on anti-fibrotic strategies. *J Hepatol*. 2007;46(5):955–75.
26. Ramachandran P, Iredale JP. Reversibility of liver fibrosis. *Ann Hepatol*. 2009;8(4):283–91.

27. Murphy FR, Issa R, Zhou X, Ratnarajah S, Arthur MJP, Benyon C, et al. Inhibition of Apoptosis of Activated Hepatic Stellate Cells by Tissue Inhibitor of Metalloproteinase-1 Is Mediated via Effects on Matrix Metalloproteinase Inhibition: IMPLICATIONS FOR REVERSIBILITY OF LIVER FIBROSIS*. *J Biol Chem.* 2002;277(13):11069–76.
28. Viñas O, Bataller R, Sancho-Bru P, Ginès P, Berenguer C, Enrich C, et al. Human hepatic stellate cells show features of antigen-presenting cells and stimulate lymphocyte proliferation. *Hepatology.* 2003 Oct;38(4):919–29.
29. Elpek GÖ. Angiogenesis and liver fibrosis. *World J Hepatol.* 2015 Mar 27;7(3):377–91.
30. Kostallari E, Shah VH. Pericytes in the Liver. *Adv Exp Med Biol.* 2019;1122:153–67.
31. Tsukada S, Parsons CJ, Rippe RA. Mechanisms of liver fibrosis. *Clin Chim Acta.* 2006;364(1):33–60.
32. Rockey DC, Friedman SL. Fibrosis Regression After Eradication of Hepatitis C Virus: From Bench to Bedside. *Gastroenterology.* 2021 Apr;160(5):1502-1520.e1.
33. D'Ambrosio R, Aghemo A, Rumi MG, Ronchi G, Donato MF, Paradis V, et al. A morphometric and immunohistochemical study to assess the benefit of a sustained virological response in hepatitis C virus patients with cirrhosis. *Hepatology.* 2012 Aug;56(2):532–43.
34. Rockey DC. Liver Fibrosis Reversion After Suppression of Hepatitis B Virus. *Clin Liver Dis.* 2016 Nov;20(4):667–79.
35. Ramachandran P, Iredale JP, Fallowfield JA. Resolution of liver fibrosis: basic mechanisms and clinical relevance. *Semin Liver Dis.* 2015 May;35(2):119–31.
36. Wei L, Huang Y-H. Long-term outcomes in patients with chronic hepatitis C in the current era of direct-acting antiviral agents. *Expert Rev Anti Infect Ther.* 2019 May;17(5):311–25.
37. Desmet VJ, Roskams T. Cirrhosis reversal: a duel between dogma and myth. *J Hepatol.* 2004 May;40(5):860–7.
38. Friedman SL, Bansal MB. Reversal of hepatic fibrosis -- fact or fantasy? *Hepatology.* 2006 Feb;43(2 Suppl 1):S82-88.
39. Pei L, Melmed S. Isolation and characterization of a pituitary tumor-transforming gene (PTTG). *Mol Endocrinol.* 1997;11:433–41.

40. Moreno-Mateos MA, Espina ÁG, Torres B, Gámez del Estal MM, Romero-Franco A, Ríos RM, et al. PTTG1/securin modulates microtubule nucleation and cell migration. *Mol Biol Cell*. 2011 Nov;22(22):4302–11.
41. Han X, Poon RYC. Critical differences between isoforms of securin reveal mechanisms of separase regulation. *Mol Cell Biol*. 2013 Sep;33(17):3400–15.
42. Levy D, Ferreira MCMR, Reichert CO, de Almeida LV, Brocardo G, Lage LAPC, et al. Cell Cycle Changes, DNA Ploidy, and PTTG1 Gene Expression in HTLV-1 Patients. *Front Microbiol*. 2020; 11: 1778.
43. Vlotides G, Eigler T, Melmed S. Pituitary tumor-transforming gene: physiology and implications for tumorigenesis. *Endocr Rev*. 2007 Apr;28(2):165–86.
44. Kakar SS. Molecular cloning, genomic organization, and identification of the promoter for the human pituitary tumor transforming gene (PTTG). *Gene*. 1999 Nov;240(2):317–24.
45. Clem AL, Hamid T, Kakar SS. Characterization of the role of Sp1 and NF-Y in differential regulation of PTTG/securin expression in tumor cells. *Gene*. 2003 Dec;322:113–21.
46. Chen P-Y, Yen J-H, Kao R-H, Chen J-H. Down-regulation of the oncogene PTTG1 via the KLF6 tumor suppressor during induction of myeloid differentiation. *PLoS One*. 2013;8(8):e71282.
47. Hamid T, Kakar SS. PTTG and cancer. *Histol Histopathol*. 2003 Jan;18(1):245–51.
48. Pei L. Identification of c-myc as a down-stream target for pituitary tumor-transforming gene. *J Biol Chem*. 2001 Mar;276(11):8484–91.
49. Tong Y, Eigler T. Transcriptional targets for pituitary tumor-transforming gene-1. *J Mol Endocrinol*. 2009 Nov;43(5):179–85.
50. Wang Z, Yu R, Melmed S. Mice lacking pituitary tumor transforming gene show testicular and splenic hypoplasia, thymic hyperplasia, thrombocytopenia, aberrant cell cycle progression, and premature centromere division. *Mol Endocrinol*. 2001 Nov;15(11):1870–9.
51. Chien W, Pei L. A novel binding factor facilitates nuclear translocation and transcriptional activation function of the pituitary tumor-transforming gene product. *J Biol Chem*. 2000 Jun;275(25):19422–7.

52. Wang Z, Moro E, Kovacs K, Yu R, Melmed S. Pituitary tumor transforming gene-null male mice exhibit impaired pancreatic beta cell proliferation and diabetes. *Proc Natl Acad Sci U S A*. 2003 Mar;100(6):3428–32.
53. Wang Z, Melmed S. Characterization of the murine pituitary tumor transforming gene (PTTG) and its promoter. *Endocrinology*. 2000 Feb;141(2):763–71.
54. Sáez C, Japón MA, Ramos-Morales F, Romero F, Segura DI, Tortolero M, et al. hpttg is over-expressed in pituitary adenomas and other primary epithelial neoplasias. *Oncogene*. 1999 Sep;18(39):5473–6.
55. Li H, Yin C, Zhang B, Sun Y, Shi L, Liu N, et al. PTTG1 promotes migration and invasion of human non-small cell lung cancer cells and is modulated by miR-186. *Carcinogenesis*. 2013 Sep;34(9):2145–55.
56. Xiea Y, Wangb R. Pttg1 Promotes Growth of Breast Cancer through P27 Nuclear Exclusion. *Cell Physiol Biochem*. 2016;38(1):393–400.
57. Meng C, Zou Y, Hong W, Bao C, Jia X. Estrogen-regulated PTTG1 promotes breast cancer progression by regulating cyclin kinase expression. *Mol Med*. 2020 Apr;26(1):33.
58. Ren Q, Jin B. The clinical value and biological function of PTTG1 in colorectal cancer. *Biomed Pharmacother*. 2017 May;89:108–15.
59. Zheng Y, Guo J, Zhou J, Lu J, Chen Q, Zhang C, et al. FoxM1 transactivates PTTG1 and promotes colorectal cancer cell migration and invasion. *BMC Med Genomics*. 2015 Aug 12;8:49.
60. Ying H, Furuya F, Zhao L, Araki O, West BL, Hanover JA, et al. Aberrant accumulation of PTTG1 induced by a mutated thyroid hormone beta receptor inhibits mitotic progression. *J Clin Invest*. 2006 Nov;116(11):2972–84.
61. Panguluri SK, Yeakel C, Kakar SS. PTTG: an important target gene for ovarian cancer therapy. *J Ovarian Res*. 2008 Oct;1(1):6.
62. Genkai N, Homma J, Sano M, Tanaka R, Yamanaka R. Increased expression of pituitary tumor-transforming gene (PTTG)-1 is correlated with poor prognosis in glioma patients. *Oncol Rep*. 2006 Jun;15(6):1569–74.
63. Liang M, Chen X, Liu W, Li S, Li C, Jiang L, et al. Role of the pituitary tumor transforming gene 1 in the progression of hepatocellular carcinoma. *Cancer Biol Ther*. 2011 Feb;11(3):337–45.

64. Xiang W, Wu X, Huang C, Wang M, Zhao X, Luo G, et al. PTTG1 regulated by miR-146a-3p promotes bladder cancer migration, invasion, metastasis and growth. *Oncotarget*. 2017 Jan;8(1):664–78.
65. Fraune C, Yehorov S, Luebke AM, Steurer S, Hube-Magg C, Buscheck F, et al. Upregulation of PTTG1 is associated with poor prognosis in prostate cancer. *Pathol Int*. 2020 Apr;70(7):441–51.
66. Xu X, Cao L, Zhang Y, Yin Y, Hu X, Cui Y. Network analysis of DEGs and verification experiments reveal the notable roles of PTTG1 and MMP9 in lung cancer. *Oncol Lett*. 2018 Jan;15(1):257–63.
67. Ma K, Ma L, Jian Z. Pituitary tumor-transforming 1 expression in laryngeal cancer and its association with prognosis. *Oncol Lett*. 2018 Jul;16(1):1107–14.
68. Malik MT, Kakar SS. Regulation of angiogenesis and invasion by human Pituitary tumor transforming gene (PTTG) through increased expression and secretion of matrix metalloproteinase-2 (MMP-2). *Mol Cancer*. 2006 Nov;5:61.
69. Hu C, Huang W, Xiong N, Liu X. SP1-mediated transcriptional activation of PTTG1 regulates the migration and phenotypic switching of aortic vascular smooth muscle cells in aortic dissection through MAPK signaling. *Arch Biochem Biophys*. 2021 Oct;711:109007.
70. Cheng G, Liu X, Li P, Li Y. Down-regulation of PTTG1 suppresses PDGF-BB-induced proliferation, migration and extracellular matrix production of airway smooth muscle cells (ASMCs) by regulating PI3K/AKT/mTOR signaling pathway. *Mol Cell Toxicol*. 2021;17(4):485–92.
71. Thompson AD 3rd, Kakar SS. Insulin and IGF-1 regulate the expression of the pituitary tumor transforming gene (PTTG) in breast tumor cells. *FEBS Lett*. 2005 Jun;579(14):3195–200.
72. Tfelt-Hansen J, Schwarz P, Terwilliger EF, Brown EM, Chattopadhyay N. Calcium-sensing receptor induces messenger ribonucleic acid of human securin, pituitary tumor transforming gene, in rat testicular cancer. *Endocrinology*. 2003 Dec;144(12):5188–93.
73. Akino K, Akita S, Mizuguchi T, Takumi I, Yu R, Wang X, et al. A novel molecular marker of pituitary tumor transforming gene involves in a rat liver regeneration. *J Surg Res*. 2005 Nov;129(1):142–6.
74. Cho-Rok J, Yoo J, Jang YJ, Kim S, Chu I-S, Yeom Y Il, et al. Adenovirus-mediated transfer of siRNA against PTTG1 inhibits liver cancer cell growth in vitro and in vivo. *Hepatology*. 2006 May;43(5):1042–52.

75. Fujii T, Nomoto S, Koshikawa K, Yatabe Y, Teshigawara O, Mori T, et al. Overexpression of pituitary tumor transforming gene 1 in HCC is associated with angiogenesis and poor prognosis. *Hepatology*. 2006 Jun;43(6):1267–75.
76. Liang M, Liu J, Ji H, Chen M, Zhao Y, Li S, et al. A *Aconitum coreanum* polysaccharide fraction induces apoptosis of hepatocellular carcinoma (HCC) cells via pituitary tumor transforming gene 1 (PTTG1)-mediated suppression of the P13K/Akt and activation of p38 MAPK signaling pathway and displays antitumor. *Tumor Biol*. 2015;36(9):7085–91.
77. Huang J-L, Cao S-W, Ou Q-S, Yang B, Zheng S-H, Tang J, et al. The long non-coding RNA PTTG3P promotes cell growth and metastasis via up-regulating PTTG1 and activating PI3K/AKT signaling in hepatocellular carcinoma. *Mol Cancer*. 2018 May;17(1):93.
78. Lee UE, Ghiassi-Nejad Z, Paris AJ, Yea S, Narla G, Walsh M, et al. Tumor suppressor activity of KLF6 mediated by downregulation of the PTTG1 oncogene. *FEBS Lett*. 2010 Mar;584(5):1006–10.
79. Lin X, Yang Y, Guo Y, Liu H, Jiang J, Zheng F, et al. PTTG1 is involved in TNF- α -related hepatocellular carcinoma via the induction of c-myc. *Cancer Med*. 2019 Sep;8(12):5702–15.
80. Molina-Jimenez F, Benedicto I, Murata M, Martin-Vilchez S, Seki T, Antonio Pintor-Toro J, et al. Expression of pituitary tumor-transforming gene 1 (PTTG1)/securin in hepatitis B virus (HBV)-associated liver diseases: evidence for an HBV X protein-mediated inhibition of PTTG1 ubiquitination and degradation. *Hepatology*. 2010 Mar;51(3):777–87.
81. Buko V, Belonovskaya E, Naruta E, Lukivskaya O, Kanyuka O, Zhuk O, et al. Pituitary tumor transforming gene as a novel regulatory factor of liver fibrosis. *Life Sci*. 2015 Jul;132:34–40.
82. Espina AG, Méndez-Vidal C, Moreno-Mateos MA, Sáez C, Romero-Franco A, Japón MA, et al. Induction of Dlk1 by PTTG1 inhibits adipocyte differentiation and correlates with malignant transformation. *Mol Biol Cell*. 2009 Jul;20(14):3353–62.
83. Zhu N-L, Asahina K, Wang J, Ueno A, Lazaro R, Miyaoka Y, et al. Hepatic stellate cell-derived delta-like homolog 1 (DLK1) protein in liver regeneration. *J Biol Chem*. 2012 Mar 23;287(13):10355–67.
84. Falix FA, Tjon-A-Loi MRS, Gaemers IC, Aronson DC, Lamers WH. DLK1 Protein Expression during Mouse Development Provides New Insights into Its Function. Belousov L V, Lardelli M, editors. *ISRN Dev Biol*. 2013;2013.

85. Buccarelli M, Lulli V, Giuliani A, Signore M, Martini M, D'Alessandris QG, et al. Deregulated expression of the imprinted DLK1-DIO3 region in glioblastoma stemlike cells: tumor suppressor role of lncRNA MEG3. *Neuro Oncol.* 2020 Dec 1;22(12):1771–84.
86. da Rocha ST, Edwards CA, Ito M, Ogata T, Ferguson-Smith AC. Genomic imprinting at the mammalian Dlk1-Dio3 domain. *Trends Genet.* 2008 Jun;24(6):306–16.
87. Lu H-P, Lin C-J, Chen W-C, Chang Y-J, Lin S-W, Wang H-H, et al. TRIM28 Regulates Dlk1 Expression in Adipogenesis. *Int J Mol Sci.* 2020 Sep 30;21(19):7245.
88. Li D, Yea S, Li S, Chen Z, Narla G, Banck M, et al. Krüppel-like factor-6 promotes preadipocyte differentiation through histone deacetylase 3-dependent repression of DLK1. *J Biol Chem.* 2005 Jul;280(29):26941–52.
89. Falix FA, Aronson DC, Lamers WH, Gaemers IC. Possible roles of DLK1 in the Notch pathway during development and disease. *Biochim Biophys Acta - Mol Basis Dis.* 2012;1822(6):988–95.
90. Pittaway JFH, Lipsos C, Mariniello K, Guasti L. The role of delta-like non-canonical Notch ligand 1 (DLK1) in cancer. *Endocr Relat Cancer.* 2021 Oct;28(12):R271–87.
91. Smas CM, Chen L, Sul HS. Cleavage of membrane-associated pref-1 generates a soluble inhibitor of adipocyte differentiation. *Mol Cell Biol.* 1997 Feb;17(2):977–88.
92. Liem IK, Indriyanoles of DLK1 in Liver Development and Oncogenesis, Adnindya MR, Nasution AA. Roles of DLK1 in Liver Development and Oncogenesis. *Online J Biol Sci.* 2017 Oct 23;17(4):309–15.
93. Traustadóttir GÁ, Lagoni LV, Ankerstjerne LBS, Bisgaard HC, Jensen CH, Andersen DC. The imprinted gene Delta like non-canonical Notch ligand 1 (Dlk1) is conserved in mammals, and serves a growth modulatory role during tissue development and regeneration through Notch dependent and independent mechanisms. *Cytokine Growth Factor Rev.* 2019;46:17–27.
94. Surmacz B, Noisa P, Risner-Janiczek JR, Hui K, Ungless M, Cui W, et al. DLK1 promotes neurogenesis of human and mouse pluripotent stem cell-derived neural progenitors via modulating Notch and BMP signalling. *Stem cell Rev reports.* 2012 Jun;8(2):459–71.
95. Abdallah BM, Ditzel N, Mahmood A, Isa A, Traustadottir GA, Schilling AF, et al. DLK1 is a novel regulator of bone mass that mediates estrogen deficiency-

- induced bone loss in mice. *J bone Miner Res Off J Am Soc Bone Miner Res.* 2011 Jul;26(7):1457–71.
96. Mitterberger MC, Lechner S, Mattesich M, Kaiser A, Probst D, Wenger N, et al. DLK1(PREF1) is a negative regulator of adipogenesis in CD105+/CD90+/CD34+/CD31-/FABP4- adipose-derived stromal cells from subcutaneous abdominal fat pats of adult women. *Stem Cell Res.* 2012 Jul;9(1):35–48.
97. Moon YS, Smas CM, Lee K, Villena JA, Kim K-H, Yun EJ, et al. Mice lacking paternally expressed Pref-1/Dlk1 display growth retardation and accelerated adiposity. *Mol Cell Biol.* 2002 Aug;22(15):5585–92.
98. Charalambous M, Da Rocha ST, Radford EJ, Medina-Gomez G, Curran S, Pinnock SB, et al. DLK1/PREF1 regulates nutrient metabolism and protects from steatosis. *Proc Natl Acad Sci.* 2014 Nov 11;111(45):16088–93.
99. Jensen CH, Kosmina R, Rydén M, Baun C, Hvidsten S, Andersen MS, et al. The imprinted gene Delta like non-canonical notch ligand 1 (Dlk1) associates with obesity and triggers insulin resistance through inhibition of skeletal muscle glucose uptake. *EBioMedicin.* 2019 Aug 1;46:368–80.
100. Begum A, Kim Y, Lin Q, Yun Z. DLK1, delta-like 1 homolog (Drosophila), regulates tumor cell differentiation in vivo. *Cancer Lett.* 2012 May;318(1):26–33.
101. Yin D, Xie D, Sakajiri S, Miller CW, Zhu H, Popoviciu ML, et al. DLK1: increased expression in gliomas and associated with oncogenic activities. *Oncogene.* 2006 Mar;25(13):1852–61.
102. Xu X, Liu R-F, Zhang X, Huang L-Y, Chen F, Fei Q-L, et al. DLK1 as a potential target against cancer stem/progenitor cells of hepatocellular carcinoma. *Mol Cancer Ther.* 2012 Mar;11(3):629–38.
103. Ceder JA, Jansson L, Helczynski L, Abrahamsson P-A. Delta-like 1 (Dlk-1), a novel marker of prostate basal and candidate epithelial stem cells, is downregulated by notch signalling in intermediate/transit amplifying cells of the human prostate. *Eur Urol.* 2008 Dec;54(6):1344–53.
104. Li L, Tan J, Zhang Y, Han N, Di X, Xiao T, et al. DLK1 promotes lung cancer cell invasion through upregulation of MMP9 expression depending on Notch signaling. *PLoS One.* 2014;9(3):e91509.
105. Lin Q, Yun Z. Impact of the hypoxic tumor microenvironment on the regulation of cancer stem cell characteristics. *Cancer Biol Ther.* 2010 Jun;9(12):949–56.

106. Kim Y, Lin Q, Zelterman D, Yun Z. Hypoxia-regulated delta-like 1 homologue enhances cancer cell stemness and tumorigenicity. *Cancer Res.* 2009 Dec;69(24):9271–80.
107. Grassi ES, Pantazopoulou V, Pietras A. Hypoxia-induced release, nuclear translocation, and signaling activity of a DLK1 intracellular fragment in glioma. *Oncogene.* 2020 May;39(20):4028–44.
108. Lee Y-H, Yun MR, Kim HM, Jeon BH, Park B-C, Lee B-W, et al. Exogenous administration of DLK1 ameliorates hepatic steatosis and regulates gluconeogenesis via activation of AMPK. *Int J Obes (Lond).* 2016 Feb;40(2):356–65.
109. Li H, Cui M, Chen T, Xie H, Cui Y, Tu H, et al. Serum DLK1 is a potential prognostic biomarker in patients with hepatocellular carcinoma. *Tumour Biol J Int Soc Oncodevelopmental Biol Med.* 2015 Nov;36(11):8399–404.
110. Cai C-M, Xiao X, Wu B-H, Wei B-F, Han Z-G. Targeting endogenous DLK1 exerts antitumor effect on hepatocellular carcinoma through initiating cell differentiation. *Oncotarget.* 2016 Nov;7(44):71466–76.
111. Huang J, Zhang X, Zhang M, Zhu J-D, Zhang Y-L, Lin Y, et al. Up-regulation of DLK1 as an imprinted gene could contribute to human hepatocellular carcinoma. *Carcinogenesis.* 2007 May 1;28(5):1094–103.
112. Pan R-L, Wang P, Xiang L-X, Shao J-Z. Delta-like 1 serves as a new target and contributor to liver fibrosis down-regulated by mesenchymal stem cell transplantation. *J Biol Chem.* 2011 Apr;286(14):12340–8.
113. Ramakrishna G, Rastogi A, Trehanpati N, Sen B, Khosla R, Sarin SK. From cirrhosis to hepatocellular carcinoma: new molecular insights on inflammation and cellular senescence. *Liver cancer.* 2013 Aug;2(3–4):367–83.
114. D'Amico G, Bernardi M, Angeli P. Towards a new definition of decompensated cirrhosis. *J Hepatol.* 2022 Jan;76(1):202–7.
115. EASL Clinical Practice Guidelines for the management of patients with decompensated cirrhosis. *J Hepatol.* 2018 Aug;69(2):406–60.
116. Nusrat S, Khan MS, Fazili J, Madhoun MF. Cirrhosis and its complications: evidence based treatment. *World J Gastroenterol.* 2014 May;20(18):5442–60.
117. Shetty A, Jun Yum J, Saab S. The Gastroenterologist's Guide to Preventive Management of Compensated Cirrhosis. *Gastroenterol Hepatol (N Y).* 2019 Aug;15(8):423–30.

118. Iwakiri Y, Trebicka J. Portal hypertension in cirrhosis: Pathophysiological mechanisms and therapy. *JHEP reports Innov Hepatol.* 2021 Aug;3(4):100316.
119. Buob S, Johnston AN, Webster CRL. Portal Hypertension: Pathophysiology, Diagnosis, and Treatment. *J Vet Intern Med.* 2011 Mar 1;25(2):169–86.
120. Suk KT. Hepatic venous pressure gradient: clinical use in chronic liver disease. *Clin Mol Hepatol.* 2014 Mar;20(1):6–14.
121. D’Amico G, Morabito A, D’Amico M, Pasta L, Malizia G, Rebora P, et al. Clinical states of cirrhosis and competing risks. *J Hepatol.* 2018 Mar;68(3):563–76.
122. Pillai AK, Andring B, Patel A, Trimmer C, Kalva SP. Portal hypertension: a review of portosystemic collateral pathways and endovascular interventions. *Clin Radiol.* 2015 Oct;70(10):1047–59.
123. Fernández-Varo G, Ros J, Morales-Ruiz M, Cejudo-Martín P, Arroyo V, Solé M, et al. Nitric oxide synthase 3-dependent vascular remodeling and circulatory dysfunction in cirrhosis. *Am J Pathol.* 2003 Jun;162(6):1985–93.
124. Tsochatzis EA, Bosch J, Burroughs AK. Liver cirrhosis. *Lancet.* 2014 May;383(9930):1749–61.
125. Kim MY, Baik SK, Lee SS. Hemodynamic alterations in cirrhosis and portal hypertension. *Korean J Hepatol.* 2010 Dec;16(4):347–52.
126. Ginès P, Cárdenas A, Arroyo V, Rodés J. Management of cirrhosis and ascites. *N Engl J Med.* 2004 Apr;350(16):1646–54.
127. Martin PY, Ginès P, Schrier RW. Nitric oxide as a mediator of hemodynamic abnormalities and sodium and water retention in cirrhosis. *N Engl J Med.* 1998 Aug;339(8):533–41.
128. Arroyo V. Pathophysiology, diagnosis and treatment of ascites in cirrhosis. *Ann Hepatol.* 2002;1(2):72–9.
129. Ng CKF, Chan MHM, Tai MHL, Lam CWK. Hepatorenal syndrome. *Clin Biochem Rev.* 2007 Feb;28(1):11–7.
130. Crismale JF, Friedman SL. Acute Liver Injury and Decompensated Cirrhosis. *Med Clin North Am.* 2020 Jul;104(4):647–62.
131. Schuppan D, Afdhal NH. Liver cirrhosis. *Lancet.* 2008;371(9615):838–51.

132. Rodrigues SG, Mendoza YP, Bosch J. Beta-blockers in cirrhosis: Evidence-based indications and limitations. *JHEP reports Innov Hepatol.* 2020 Feb;2(1):100063.
133. Langer DA, Shah VH. Nitric oxide and portal hypertension: interface of vasoreactivity and angiogenesis. *J Hepatol.* 2006 Jan;44(1):209–16.
134. McNaughton L, Puttagunta L, Martinez-Cuesta MA, Kneteman N, Mayers I, Moqbel R, et al. Distribution of nitric oxide synthase in normal and cirrhotic human liver. *Proc Natl Acad Sci.* 2002 Dec 24;99(26):17161 LP – 17166.
135. Gross SS. Nitric Oxide Synthases and Their Cofactors. In: Goligorsky MS, Gross SS, editors. *Nitric Oxide and the Kidney: Physiology and Pathophysiology.* Boston, MA: Springer US; 1997. p. 52–65.
136. Wiest R, Groszmann RJ. The paradox of nitric oxide in cirrhosis and portal hypertension: too much, not enough. *Hepatology.* 2002 Feb;35(2):478–91.
137. Leung T-M, Tipoe GL, Liong EC, Lau TYH, Fung M-L, Nanji AA. Endothelial nitric oxide synthase is a critical factor in experimental liver fibrosis. *Int J Exp Pathol.* 2008 Aug;89(4):241–50.
138. Diesen DL, Kuo PC. Nitric oxide and redox regulation in the liver: Part I. General considerations and redox biology in hepatitis. *J Surg Res.* 2010 Jul;162(1):95–109.
139. Morales-Ruiz M, Jiménez W, Pérez-Sala D, Ros J, Leivas A, Lamas S, et al. Increased nitric oxide synthase expression in arterial vessels of cirrhotic rats with ascites. *Hepatology.* 1996 Dec;24(6):1481–6.
140. Schilling K, Opitz N, Wiesenthal A, Oess S, Tikkanen R, Müller-Esterl W, et al. Translocation of endothelial nitric-oxide synthase involves a ternary complex with caveolin-1 and NOSTRIN. *Mol Biol Cell.* 2006 Sep;17(9):3870–80.
141. Hu LS, George J, Wang JH. Current concepts on the role of nitric oxide in portal hypertension. *World J Gastroenterol.* 2013 Mar;19(11):1707–17.
142. Stamler JS, Lamas S, Fang FC. Nitrosylation. the prototypic redox-based signaling mechanism. *Cell.* 2001 Sep;106(6):675–83.
143. Morales-Ruiz M, Rodríguez-Vita J, Ribera J, Jiménez W. Pathophysiology of Portal Hypertension. Lanzer P, editor. *PanVascular Med.* 2015 Jan 23;3631–65.

144. Morales-Ruiz M, Cejudo-Martín P, Fernández-Varo G, Tugues S, Ros J, Angeli P, et al. Transduction of the liver with activated Akt normalizes portal pressure in cirrhotic rats. *Gastroenterology*. 2003 Aug;125(2):522–31.
145. Perri RE, Langer DA, Chatterjee S, Gibbons SJ, Gadgil J, Cao S, et al. Defects in cGMP-PKG pathway contribute to impaired NO-dependent responses in hepatic stellate cells upon activation. *Am J Physiol Liver Physiol*. 2006 Mar 1;290(3):G535–42.
146. Angeli P, Fernández-Varo G, Dalla Libera V, Fasolato S, Galioto A, Arroyo V, et al. The role of nitric oxide in the pathogenesis of systemic and splanchnic vasodilation in cirrhotic rats before and after the onset of ascites. *Liver Int Off J Int Assoc Study Liver*. 2005 Apr;25(2):429–37.
147. Guarner C, Soriano G, Tomas A, Bulbena O, Novella MT, Balanzo J, et al. Increased serum nitrite and nitrate levels in patients with cirrhosis: relationship to endotoxemia. *Hepatology*. 1993 Nov;18(5):1139–43.
148. Fernandez M, Vizzutti F, Garcia-Pagan JC, Rodes J, Bosch J. Anti-VEGF receptor-2 monoclonal antibody prevents portal-systemic collateral vessel formation in portal hypertensive mice. *Gastroenterology*. 2004 Mar;126(3):886–94.
149. Bolognesi M, Di Pascoli M, Verardo A, Gatta A. Splanchnic vasodilation and hyperdynamic circulatory syndrome in cirrhosis. *World J Gastroenterol*. 2014 Mar;20(10):2555–63.
150. Wiest R, Das S, Cadelina G, Garcia-Tsao G, Milstien S, Groszmann RJ. Bacterial translocation in cirrhotic rats stimulates eNOS-derived NO production and impairs mesenteric vascular contractility. *J Clin Invest*. 1999 Nov;104(9):1223–33.
151. Ho H-L, Huang H-C. Molecular mechanisms of circulatory dysfunction in cirrhotic portal hypertension. *J Chin Med Assoc*. 2015 Apr;78(4):195–203.
152. Ahmed F, Perz JF, Kwong S, Jamison PM, Friedman C, Bell BP. National trends and disparities in the incidence of hepatocellular carcinoma, 1998-2003. *Prev Chronic Dis*. 2008 Jul;5(3):A74.
153. Bray F, Ferlay J, Soerjomataram I, Siegel RL, Torre LA, Jemal A. Global cancer statistics 2018: GLOBOCAN estimates of incidence and mortality worldwide for 36 cancers in 185 countries. *CA Cancer J Clin*. 2018 Nov 1;68(6):394–424.
154. Baecker A, Liu X, La Vecchia C, Zhang Z-F. Worldwide incidence of hepatocellular carcinoma cases attributable to major risk factors. *Eur J cancer Prev Off J Eur Cancer Prev Organ*. 2018 May;27(3):205–12.

155. Llovet JM, Kelley RK, Villanueva A, Singal AG, Pikarsky E, Roayaie S, et al. Hepatocellular carcinoma. *Nat Rev Dis Prim.* 2021;7(1):6.
156. Craig AJ, von Felden J, Garcia-Lezana T, Sarcognato S, Villanueva A. Tumour evolution in hepatocellular carcinoma. *Nat Rev Gastroenterol Hepatol.* 2020;17(3):139–52.
157. Reig M, Forner A, Ávila MA, Ayuso C, Mínguez B, Varela M, et al. Diagnosis and treatment of hepatocellular carcinoma. Update of the consensus document of the AEEH, AEC, SEOM, SERAM, SERVEI, and SETH. Vol. 156, *Medicina clinica.* Spain; 2021. p. 463.e1-463.e30.
158. Bialecki ES, Di Bisceglie AM. Diagnosis of hepatocellular carcinoma. *HPB (Oxford).* 2005;7(1):26–34.
159. Villanueva A. Hepatocellular Carcinoma. *N Engl J Med.* 2019 Apr;380(15):1450–62.
160. Bai D-S, Zhang C, Chen P, Jin S-J, Jiang G-Q. The prognostic correlation of AFP level at diagnosis with pathological grade, progression, and survival of patients with hepatocellular carcinoma. *Sci Rep.* 2017;7(1):12870.
161. Forner A, Reig M, Bruix J. Hepatocellular carcinoma. *Lancet.* 2018 Mar;391(10127):1301–14.
162. Bishayee A. The role of inflammation and liver cancer. *Adv Exp Med Biol.* 2014;816:401–35.
163. Kim E, Viatour P. Hepatocellular carcinoma: old friends and new tricks. *Exp Mol Med.* 2020;52(12):1898–907.
164. Keating GM, Santoro A. Sorafenib: A Review of Its Use in Advanced Hepatocellular Carcinoma. *Drugs.* 2009;69(2):223–40.
165. Liu M, Jiang L, Guan X-Y. The genetic and epigenetic alterations in human hepatocellular carcinoma: a recent update. *Protein Cell.* 2014 Sep;5(9):673–91.
166. Nault J-C. Pathogenesis of hepatocellular carcinoma according to aetiology. *Best Pract Res Clin Gastroenterol.* 2014;28(5):937–47.
167. Müller M, Bird TG, Nault J-C. The landscape of gene mutations in cirrhosis and hepatocellular carcinoma. *J Hepatol.* 2020 May;72(5):990–1002.
168. Zucman-Rossi J, Villanueva A, Nault J-C, Llovet JM. Genetic Landscape and Biomarkers of Hepatocellular Carcinoma. *Gastroenterology.* 2015 Oct;149(5):1226-1239.e4.

169. Schulze K, Imbeaud S, Letouzé E, Alexandrov LB, Calderaro J, Rebouissou S, et al. Exome sequencing of hepatocellular carcinomas identifies new mutational signatures and potential therapeutic targets. *Nat Genet.* 2015 May;47(5):505–11.
170. Nault J-C, Ningarhari M, Rebouissou S, Zucman-Rossi J. The role of telomeres and telomerase in cirrhosis and liver cancer. *Nat Rev Gastroenterol Hepatol.* 2019;16(9):544–58.
171. Yang JD, Hainaut P, Gores GJ, Amadou A, Plymoth A, Roberts LR. A global view of hepatocellular carcinoma: trends, risk, prevention and management. *Nat Rev Gastroenterol Hepatol.* 2019 Oct;16(10):589–604.
172. Toh TB, Lim JJ, Chow EK-H. Epigenetics of hepatocellular carcinoma. *Clin Transl Med.* 2019 May 6;8(1):13.
173. Wahid B, Ali A, Rafique S, Idrees M. New Insights into the Epigenetics of Hepatocellular Carcinoma. Scartozzi M, editor. *Biomed Res Int.* 2017;2017:1609575.
174. Schulze K, Nault J-C, Villanueva A. Genetic profiling of hepatocellular carcinoma using next-generation sequencing. *J Hepatol.* 2016 Nov;65(5):1031–42.
175. Yu L-X, Ling Y, Wang H-Y. Role of nonresolving inflammation in hepatocellular carcinoma development and progression. *npj Precis Oncol.* 2018;2(1):6.
176. Waris G, Ahsan H. Reactive oxygen species: role in the development of cancer and various chronic conditions. *J Carcinog.* 2006 May;5:14.
177. Roberts SM, Kehrer JP, Klotz L-O. *Studies on Experimental Toxicology and Pharmacology.* 1st ed. Roberts SM, Kehrer JP, Klotz L-O, editors. Switzerland: Humana Press; 2015. 498 p.
178. Yin H. The role of lipid peroxidation during the progression of human hepatocellular carcinoma (HCC). *Free Radic Biol Med.* 2018;124:563–4.
179. Cichoż-Lach H, Michalak A. Oxidative stress as a crucial factor in liver diseases. *World J Gastroenterol.* 2014;20(25):8082–91.
180. Bian J, Lin J, Long J, Yang X, Yang X, Lu X, et al. T lymphocytes in hepatocellular carcinoma immune microenvironment: insights into human immunology and immunotherapy. *Am J Cancer Res.* 2020;10(12):4585–606.
181. Tian Z, Hou X, Liu W, Han Z, Wei L. Macrophages and hepatocellular carcinoma. *Cell Biosci.* 2019;9:79.

182. Capece D, Fischietti M, Verzella D, Gaggiano A, Ciccirelli G, Tessitore A, et al. The Inflammatory Microenvironment in Hepatocellular Carcinoma: A Pivotal Role for Tumor-Associated Macrophages. Vazquez E, editor. *Biomed Res Int*. 2013;2013:187204.
183. Shirabe K, Mano Y, Muto J, Matono R, Motomura T, Toshima T, et al. Role of tumor-associated macrophages in the progression of hepatocellular carcinoma. *Surg Today*. 2012;42(1):1–7.
184. Lin C-A, Chang L-L, Zhu H, He Q-J, Yang B. Hypoxic microenvironment and hepatocellular carcinoma treatment. *Hepatoma Res*. 2018;4:26.
185. Refolo MG, Messa C, Guerra V, Carr BI, D'Alessandro R. Inflammatory Mechanisms of HCC Development. *Cancers (Basel)*. 2020 Mar;12(3).
186. Morse MA, Sun W, Kim R, He AR, Abada PB, Mynderse M, et al. The Role of Angiogenesis in Hepatocellular Carcinoma. *Clin cancer Res an Off J Am Assoc Cancer Res*. 2019 Feb;25(3):912–20.
187. Pang RWC, Joh JW, Johnson PJ, Monden M, Pawlik TM, Poon RTP. Biology of hepatocellular carcinoma. *Ann Surg Oncol*. 2008 Apr;15(4):962–71.
188. Kalluri R, Weinberg RA. The basics of epithelial-mesenchymal transition. *J Clin Invest*. 2009 Jun;119(6):1420–8.
189. Zhang Q, Liu L, Gong C, Shi H, Zeng Y, Wang X, et al. Prognostic significance of tumor-associated macrophages in solid tumor: a meta-analysis of the literature. *PLoS One*. 2012;7(12):e50946.
190. Ding W, Tan Y, Qian Y, Xue W, Wang Y, Jiang P, et al. Clinicopathologic and prognostic significance of tumor-associated macrophages in patients with hepatocellular carcinoma: A meta-analysis. *PLoS One*. 2019 Oct 16;14(10):e0223971.
191. Wu Y, Zhang J, Zhang X, Zhou H, Liu G, Li Q. Cancer Stem Cells: A Potential Breakthrough in HCC-Targeted Therapy. *Front Pharmacol*. 2020; 11: 198.
192. Sevic I, Spinelli FM, Cantero MJ, Reszegi A, Kovalszky I, García MG, et al. The Role of the Tumor Microenvironment in the Development and Progression of Hepatocellular Carcinoma. In: JEE T-P, editor. *Hepatocellular Carcinoma*. Brisbane: Codon Publications; 2019.
193. Wirth T, Parker N, Ylä-Herttua S. History of gene therapy. *Gene*. 2013 Aug;525(2):162–9.

194. Ramamoorth M, Narvekar A. Non viral vectors in gene therapy- an overview. *J Clin Diagn Res.* 2015 Jan;9(1):GE01-6.
195. Tang R, Xu Z. Gene therapy: a double-edged sword with great powers. *Mol Cell Biochem.* 2020 Nov;474(1-2):73-81.
196. Raper SE, Chirmule N, Lee FS, Wivel NA, Bagg A, Gao G, et al. Fatal systemic inflammatory response syndrome in a ornithine transcarbamylase deficient patient following adenoviral gene transfer. *Mol Genet Metab.* 2003;80(1-2):148-58.
197. Hacein-Bey-Abina S, von Kalle C, Schmidt M, Le Deist F, Wulffraat N, McIntyre E, et al. A Serious Adverse Event after Successful Gene Therapy for X-Linked Severe Combined Immunodeficiency. *N Engl J Med.* 2003 Jan 16;348(3):255-6.
198. Lundstrom K. *Viral Vectors in Gene Therapy.* Dis (Basel, Switzerland). 2018 May;6(2):42.
199. Bulcha JT, Wang Y, Ma H, Tai PWL, Gao G. Viral vector platforms within the gene therapy landscape. *Signal Transduct Target Ther.* 2021;6(1):53.
200. Ylä-Herttuala S. Endgame: glybera finally recommended for approval as the first gene therapy drug in the European union. *Mol Ther.* 2012 Oct;20(10):1831-2.
201. Prado DA, Acosta-Acero M, Maldonado RS. Gene therapy beyond luxturna: a new horizon of the treatment for inherited retinal disease. *Curr Opin Ophthalmol.* 2020 May;31(3):147-54.
202. Schuessler-Lenz M, Enzmann H, Vamvakas S. Regulators' Advice Can Make a Difference: European Medicines Agency Approval of Zynteglo for Beta Thalassemia. *Clin Pharmacol Ther.* 2020 Mar;107(3):492-4.
203. Han D, Xu Z, Zhuang Y, Ye Z, Qian Q. Current Progress in CAR-T Cell Therapy for Hematological Malignancies. *J Cancer.* 2021;12(2):326-34.
204. Riva L, Petrini C. A few ethical issues in translational research for gene and cell therapy. *J Transl Med.* 2019;17(1):395.
205. Delhove J, Osenk I, Prichard I, Donnelley M. Public Acceptability of Gene Therapy and Gene Editing for Human Use: A Systematic Review. *Hum Gene Ther.* 2019 Dec 5;31(1-2):20-46.
206. Dana H, Chalbatani GM, Mahmoodzadeh H, Karimloo R, Rezaiean O, Moradzadeh A, et al. Molecular Mechanisms and Biological Functions of siRNA. *Int J Biomed Sci.* 2017 Jun;13(2):48-57.

207. Thomas CE, Ehrhardt A, Kay MA. Progress and problems with the use of viral vectors for gene therapy. *Nat Rev Genet.* 2003;4(5):346–58.
208. Mellott AJ, Forrest ML, Detamore MS. Physical non-viral gene delivery methods for tissue engineering. *Ann Biomed Eng.* 2013 Mar;41(3):446–68.
209. Patil S, Gao Y-G, Lin X, Li Y, Dang K, Tian Y, et al. The Development of Functional Non-Viral Vectors for Gene Delivery. *Int J Mol Sci.* 2019 Nov;20(21).
210. De Haan P, Van Diemen FR, Toscano MG. Viral gene delivery vectors: the next generation medicines for immune-related diseases. *Hum Vaccin Immunother.* 2021 Jan;17(1):14–21.
211. Flotte TR. Gene Therapy Progress and Prospects: Recombinant adeno-associated virus (rAAV) vectors. *Gene Ther.* 2004;11(10):805–10.
212. Zu H, Gao D. Non-viral Vectors in Gene Therapy: Recent Development, Challenges, and Prospects. *AAPS J.* 2021;23(4):78.
213. Maestro S, Weber ND, Zabaleta N, Aldabe R, Gonzalez-Aseguinolaza G. Novel vectors and approaches for gene therapy in liver diseases. *JHEP Reports.* 2021;3(4):100300.
214. Loh XJ, Lee T-C, Dou Q, Deen GR. Utilising inorganic nanocarriers for gene delivery. *Biomater Sci.* 2016;4(1):70–86.
215. Sainz-Ramos M, Gallego I, Villate-Beitia I, Zarate J, Maldonado I, Puras G, et al. How Far Are Non-Viral Vectors to Come of Age and Reach Clinical Translation in Gene Therapy? *Int J Mol Sci.* 2021 Jul 14;22(14):7545.
216. Williams PD, Kingston PA. Plasmid-mediated gene therapy for cardiovascular disease. *Cardiovasc Res.* 2011 Sep 1;91(4):565–76.
217. Gill DR, Pringle IA, Hyde SC. Progress and Prospects: The design and production of plasmid vectors. *Gene Ther.* 2009;16(2):165–71.
218. Tang X, Zhang S, Fu R, Zhang L, Huang K, Peng H, et al. Therapeutic Prospects of mRNA-Based Gene Therapy for Glioblastoma. *Front Oncol.* 2019 Nov 8;9:1208.
219. Tavernier G, Andries O, Demeester J, Sanders NN, De Smedt SC, Rejman J. mRNA as gene therapeutic: how to control protein expression. *J Control Release.* 2011 Mar;150(3):238–47.

220. Meng Z, O’Keeffe-Ahern J, Lyu J, Pierucci L, Zhou D, Wang W. A new developing class of gene delivery: messenger RNA-based therapeutics. *Biomater Sci.* 2017 Nov;5(12):2381–92.
221. Thijssen MF, Brüggewirth IMA, Gillooly A, Khvorova A, Kowalik TF, Martins PN. Gene Silencing With siRNA (RNA Interference): A New Therapeutic Option During Ex Vivo Machine Liver Perfusion Preservation. *Liver Transplant.* 2019 Jan 1;25(1):140–51.
222. Dong Y, Siegwart DJ, Anderson DG. Strategies, design, and chemistry in siRNA delivery systems. *Adv Drug Deliv Rev.* 2019 Apr;144:133–47.
223. Nikam RR, Gore KR. Journey of siRNA: Clinical Developments and Targeted Delivery. *Nucleic Acid Ther.* 2018 Mar 27;28(4):209–24.
224. Majumdar R, Rajasekaran K, Cary JW. RNA Interference (RNAi) as a Potential Tool for Control of Mycotoxin Contamination in Crop Plants: Concepts and Considerations. *Front Plant Sci.* 2017 Feb 14;8:200.
225. Hu P-F, Xie W-F. Targeted RNA interference for hepatic fibrosis. *Expert Opin Biol Ther.* 2009 Oct;9(10):1305–12.
226. Nguyen TH, Ferry N. Liver gene therapy: advances and hurdles. *Gene Ther.* 2004;11(1):S76–84.
227. Snoeys J, Mertens G, Lievens J, van Berkel T, Collen D, Biessen EAL, et al. Lipid emulsions potently increase transgene expression in hepatocytes after adenoviral transfer. *Mol Ther.* 2006 Jan;13(1):98–107.
228. Kim K-H, Park K-K. Small RNA- and DNA-based gene therapy for the treatment of liver cirrhosis, where we are? *World J Gastroenterol.* 2014 Oct;20(40):14696–705.
229. Cabanes-Creus M, Hallwirth C V, Westhaus A, Ng BH, Liao SHY, Zhu E, et al. Restoring the natural tropism of AAV2 vectors for human liver. *Sci Transl Med.* 2020 Sep;12(560).
230. Jacobs F, Gordts SC, Muthuramu I, De Geest B. The liver as a target organ for gene therapy: state of the art, challenges, and future perspectives. *Pharmaceuticals (Basel).* 2012 Dec;5(12):1372–92.
231. Bartneck M, Warzecha KT, Tacke F. Therapeutic targeting of liver inflammation and fibrosis by nanomedicine. *Hepatobiliary Surg Nutr.* 2014 Dec;3(6):364–76.

232. Duong HTT, Dong Z, Su L, Boyer C, George J, Davis TP, et al. The use of nanoparticles to deliver nitric oxide to hepatic stellate cells for treating liver fibrosis and portal hypertension. *Small*. 2015 May;11(19):2291–304.
233. Wang K, Shang F, Chen D, Cao T, Wang X, Jiao J, et al. Protein liposomes-mediated targeted acetylcholinesterase gene delivery for effective liver cancer therapy. *J Nanobiotechnology*. 2021;19(1):31.
234. Azzam M, El Safy S, Abdelgelil SA, Weiskirchen R, Asimakopoulou A, de Lorenzi F, et al. Targeting Activated Hepatic Stellate Cells Using Collagen-Binding Chitosan Nanoparticles for siRNA Delivery to Fibrotic Livers. *Pharmaceutics*. 2020 Jun;12(6):590.
235. Alonso S. Exploiting the bioengineering versatility of lactobionic acid in targeted nanosystems and biomaterials. *J Control Release*. 2018 Oct;287:216–34.
236. Soares S, Sousa J, Pais A, Vitorino C. Nanomedicine: Principles, Properties, and Regulatory Issues. *Front Chem*. 2018 Aug 20;6:360
237. Wang H, Thorling CA, Liang X, Bridle KR, Grice JE, Zhu Y, et al. Diagnostic imaging and therapeutic application of nanoparticles targeting the liver. *J Mater Chem B*. 2015 Feb;3(6):939–58.
238. Kim BYS, Rutka JT, Chan WCW. Nanomedicine. *N Engl J Med*. 2010 Dec;363(25):2434–43.
239. Donahue ND, Acar H, Wilhelm S. Concepts of nanoparticle cellular uptake, intracellular trafficking, and kinetics in nanomedicine. *Adv Drug Deliv Rev*. 2019;143:68–96.
240. Behzadi S, Serpooshan V, Tao W, Hamaly MA, Alkawareek MY, Dreaden EC, et al. Cellular uptake of nanoparticles: journey inside the cell. *Chem Soc Rev*. 2017 Jul 17;46(14):4218–44.
241. Rampado R, Crotti S, Caliceti P, Pucciarelli S, Agostini M. Recent Advances in Understanding the Protein Corona of Nanoparticles and in the Formulation of “Stealthy” Nanomaterials. *Front Bioeng Biotechnol*. 2020 Apr 3;8:166.
242. Cataldi M, Vigliotti C, Mosca T, Cammarota M, Capone D. Emerging Role of the Spleen in the Pharmacokinetics of Monoclonal Antibodies, Nanoparticles and Exosomes. *Int J Mol Sci*. 2017 Jun;18(6).
243. Zhang Y-N, Poon W, Tavares AJ, McGilvray ID, Chan WCW. Nanoparticle–liver interactions: Cellular uptake and hepatobiliary elimination. *J Control Release*. 2016;240:332–48.

244. Tsoi KM, MacParland SA, Ma X-Z, Spetzler VN, Echeverri J, Ouyang B, et al. Mechanism of hard-nanomaterial clearance by the liver. *Nat Mater*. 2016 Nov;15(11):1212–21.
245. Cheng S-H, Li F-C, Souris JS, Yang C-S, Tseng F-G, Lee H-S, et al. Visualizing dynamics of sub-hepatic distribution of nanoparticles using intravital multiphoton fluorescence microscopy. *ACS Nano*. 2012 May;6(5):4122–31.
246. Moghimi SM, Hunter AC, Andresen TL. Factors controlling nanoparticle pharmacokinetics: an integrated analysis and perspective. *Annu Rev Pharmacol Toxicol*. 2012;52:481–503.
247. Hamzeh M, Hosseinimehr SJ, Karimpour A, Mohammadi HR, Khalatbary AR, Talebpour Amiri F. Cerium Oxide Nanoparticles Protect Cyclophosphamide-induced Testicular Toxicity in Mice. *Int J Prev Med*. 2019 Jan 15;10:5.
248. Hardas SS, Sultana R, Warriar G, Dan M, Wu P, Grulke EA, et al. Rat hippocampal responses up to 90 days after a single nanoceria dose extends a hierarchical oxidative stress model for nanoparticle toxicity. *Nanotoxicology*. 2014 Aug;8 Suppl 1:155–66.
249. Sadowska-Bartosz I, Bartosz G. Redox nanoparticles: synthesis, properties and perspectives of use for treatment of neurodegenerative diseases. *J Nanobiotechnology*. 2018 Nov 3;16(1):87.
250. Rzigalinski BA, Carfagna CS, Ehrich M. Cerium oxide nanoparticles in neuroprotection and considerations for efficacy and safety. *Wiley Interdiscip Rev Nanomed Nanobiotechnol*. 2017;9(4):e1444
251. Dhall A, Self W. Cerium Oxide Nanoparticles: A Brief Review of Their Synthesis Methods and Biomedical Applications. *Antioxidants*. 2018 Jul;7(8).
252. Chen J, Patil S, Seal S, McGinnis JF. Rare earth nanoparticles prevent retinal degeneration induced by intracellular peroxides. *Nat Nanotechnol*. 2006 Nov;1(2):142–50.
253. Reed K, Cormack A, Kulkarni A, Mayton M, Sayle D, Klaessig F, et al. Exploring the properties and applications of nanoceria: is there still plenty of room at the bottom? *Environ Sci Nano*. 2014;1(5):390–405.
254. Ivanov VK, Shcherbakov AB, Usatenko A V. Structure-sensitive properties and biomedical applications of nanodispersed cerium dioxide. *Russ Chem Rev*. 2009;78(9):855–71.

255. Sun C, Li H, Chen L. Nanostructured ceria-based materials: synthesis, properties, and applications. *Energy Environ Sci.* 2012;5(9):8475–505.
256. Jung H, Kittelson DB, Zachariah MR. The influence of a cerium additive on ultrafine diesel particle emissions and kinetics of oxidation. *Combust Flame.* 2005;142(3):276–88.
257. Casals E, Gusta MF, Piella J, Casals G, Jiménez W, Puntès V. Intrinsic and Extrinsic Properties Affecting Innate Immune Responses to Nanoparticles: The Case of Cerium Oxide. *Front Immunol.* 2017;8:970.
258. Nemmar A, Al-Salam S, Al Ansari Z, Alkharas ZA, Al Ahbabi RM, Beegam S, et al. Impact of Pulmonary Exposure to Cerium Oxide Nanoparticles on Experimental Acute Kidney Injury. *Cell Physiol Biochem Int J Exp Cell Physiol Biochem Pharmacol.* 2019;52(3):439–54.
259. Tseng MT, Lu X, Duan X, Hardas SS, Sultana R, Wu P, et al. Alteration of hepatic structure and oxidative stress induced by intravenous nanoceria. *Toxicol Appl Pharmacol.* 2012 Apr;260(2):173–82.
260. Pourkhalili N, Hosseini A, Nili-Ahmadabadi A, Hassani S, Pakzad M, Baeeri M, et al. Biochemical and cellular evidence of the benefit of a combination of cerium oxide nanoparticles and selenium to diabetic rats. *World J Diabetes.* 2011 Nov 15;2(11):204–10.
261. Hirst SM, Karakoti AS, Tyler RD, Sriranganathan N, Seal S, Reilly CM. Anti-inflammatory properties of cerium oxide nanoparticles. *Nanotherapeutics.* 2009;5(24):2848–56.
262. Niu J, Azfer A, Rogers LM, Wang X, Kolattukudy PE. Cardioprotective effects of cerium oxide nanoparticles in a transgenic murine model of cardiomyopathy. *Cardiovasc Res.* 2007 Feb;73(3):549–59.
263. Alili L, Sack M, Karakoti AS, Teuber S, Puschmann K, Hirst SM, et al. Combined cytotoxic and anti-invasive properties of redox-active nanoparticles in tumor-stroma interactions. *Biomaterials.* 2011;32(11):2918–29.
264. Casals G, Perramón M, Casals E, Portolés I, Fernández-Varo G, Morales-Ruiz M, et al. Cerium Oxide Nanoparticles: A New Therapeutic Tool in Liver Diseases. *Antioxidants (Basel).* 2021 Apr 24;10(5):660.
265. Oró D, Yudina T, Fernández-Varo G, Casals E, Reichenbach V, Casals G, et al. Cerium oxide nanoparticles reduce steatosis, portal hypertension and display anti-inflammatory properties in rats with liver fibrosis. *J Hepatol.* 2016 Mar;64(3):691–8.

266. Córdoba-Jover B, Arce-Cerezo A, Ribera J, Pauta M, Oró D, Casals G, et al. Cerium oxide nanoparticles improve liver regeneration after acetaminophen-induced liver injury and partial hepatectomy in rats. *J Nanobiotechnology*. 2019 Oct;17(1):112.
267. Fernández-Varo G, Perramón M, Carvajal S, Oró D, Casals E, Boix L, et al. Bespoke Nanoceria: An Effective Treatment in Experimental Hepatocellular Carcinoma. *Hepatology*. 2020 Oct;72(4):1267–82.
268. Hirst SM, Karakoti A, Singh S, Self W, Tyler R, Seal S, et al. Bio-distribution and In Vivo Antioxidant Effects of Cerium Oxide Nanoparticles in Mice. *Environ Toxicol*. 2011;28(2):107–18.
269. Yokel RA, Tseng MT, Dan M, Unrine JM, Graham UM, Wu P, et al. Biodistribution and biopersistence of ceria engineered nanomaterials: size dependence. *Nanomedicine*. 2013 Apr;9(3):398–407.
270. Ni D, Wei H, Chen W, Bao Q, Rosenkrans ZT, Barnhart TE, et al. Ceria Nanoparticles Meet Hepatic Ischemia-Reperfusion Injury: The Perfect Imperfection. *Adv Mater*. 2019 Oct;31(40):e1902956.
271. Parra-Robert M, Casals E, Massana N, Zeng M, Perramón M, Fernández-Varo G, et al. Beyond the Scavenging of Reactive Oxygen Species (ROS): Direct Effect of Cerium Oxide Nanoparticles in Reducing Fatty Acids Content in an In Vitro Model of Hepatocellular Steatosis. *Biomolecules*. 2019 Aug;9(9).
272. Ribera J, Rodríguez-Vita J, Cordoba B, Portolés I, Casals G, Casals E, et al. Functionalized cerium oxide nanoparticles mitigate the oxidative stress and pro-inflammatory activity associated to the portal vein endothelium of cirrhotic rats. *PLoS One*. 2019 Jun 24;14(6):e0218716.
273. Carvajal S, Perramón M, Casals G, Oró D, Ribera J, Morales-Ruiz M, et al. Cerium Oxide Nanoparticles Protect against Oxidant Injury and Interfere with Oxidative Mediated Kinase Signaling in Human-Derived Hepatocytes. *Int J Mol Sci*. 2019 Nov;20(23).
274. Ibrahim HG, Attia N, Hashem FEZA, El Heneidy MAR. Cerium oxide nanoparticles: In pursuit of liver protection against doxorubicin-induced injury in rats. *Biomed Pharmacother*. 2018 Jul;103:773–81.
275. Eilenberger C, Selinger F, Rothbauer M, Lin Y, Limbeck A, Schädl B, et al. Cytotoxicity, Retention, and Anti-inflammatory Effects of a CeO₂ Nanoparticle-Based Supramolecular Complex in a 3D Liver Cell Culture Model. *ACS Pharmacol Transl Sci*. 2021 Feb 12;4(1):101–6.

276. Kobyliak N, Virchenko O, Falalyeyeva T, Kondro M, Beregova T, Bodnar P, et al. Cerium dioxide nanoparticles possess anti-inflammatory properties in the conditions of the obesity-associated NAFLD in rats. *Biomed Pharmacother.* 2017 Jun;90:608–14.
277. Carvajal S, Perramón M, Oró D, Casals E, Fernández-Varo G, Casals G, et al. Cerium oxide nanoparticles display antilipogenic effect in rats with non-alcoholic fatty liver disease. *Sci Rep.* 2019 Sep;9(1):12848.
278. Wasef L, Nassar AMK, El-Sayed YS, Samak D, Noreldin A, Elshony N, et al. The potential ameliorative impacts of cerium oxide nanoparticles against fipronil-induced hepatic steatosis. *Sci Rep.* 2021 Jan;11(1):1310.
279. Parra-Robert M, Zeng M, Shu Y, Fernández-Varo G, Perramón M, Desai D, et al. Mesoporous silica coated CeO₂ nanozymes with combined lipid-lowering and antioxidant activity induce long-term improvement of the metabolic profile in obese Zucker rats. *Nanoscale.* 2021 May;13(18):8452–66.
280. Adebayo OA, Akinloye O, Adaramoye OA. Cerium Oxide Nanoparticles Attenuate Oxidative Stress and Inflammation in the Liver of Diethylnitrosamine-Treated Mice. *Biol Trace Elem Res.* 2020;193(1):214–25.
281. Lynn DM, Langer R. Degradable Poly(β -amino esters): Synthesis, Characterization, and Self-Assembly with Plasmid DNA. *J Am Chem Soc.* 2000 Nov 1;122(44):10761–8.
282. Liu Y, Li Y, Keskin D, Shi L. Poly(β -Amino Esters): Synthesis, Formulations, and Their Biomedical Applications. *Adv Healthc Mater.* 2019 Jan;8(2):e1801359.
283. Zamboni CG, Kozielski KL, Vaughan HJ, Nakata MM, Kim J, Higgins LJ, et al. Polymeric nanoparticles as cancer-specific DNA delivery vectors to human hepatocellular carcinoma. *J Control Release.* 2017 Oct;263:18–28.
284. Iqbal S, Qu Y, Dong Z, Zhao J, Rauf Khan A, Rehman S, et al. Poly (β -amino esters) based potential drug delivery and targeting polymer; an overview and perspectives (review). *Eur Polym J.* 2020;141:110097.
285. Tzeng SY, Green JJ. Subtle changes to polymer structure and degradation mechanism enable highly effective nanoparticles for siRNA and DNA delivery to human brain cancer. *Adv Healthc Mater.* 2013 Mar;2(3):468–80.
286. Karlsson J, Rhodes KR, Green JJ, Tzeng SY. Poly(beta-amino ester)s as gene delivery vehicles: challenges and opportunities. *Expert Opin Drug Deliv.* 2020 Oct;17(10):1395–410.

287. Segovia N, Dosta P, Cascante A, Ramos V, Borrós S. Oligopeptide-terminated poly(β -amino ester)s for highly efficient gene delivery and intracellular localization. *Acta Biomater.* 2014 May;10(5):2147–58.
288. Freeman EC, Weiland LM, Meng WS. Modeling the proton sponge hypothesis: examining proton sponge effectiveness for enhancing intracellular gene delivery through multiscale modeling. *J Biomater Sci Polym Ed.* 2013;24(4):398–416.
289. Shenoy D, Little S, Langer R, Amiji M. Poly(ethylene oxide)-modified poly(beta-amino ester) nanoparticles as a pH-sensitive system for tumor-targeted delivery of hydrophobic drugs. 1. In vitro evaluations. *Mol Pharm.* 2005;2(5):357–66.
290. Jones CH, Chen M, Ravikrishnan A, Reddinger R, Zhang G, Hakansson AP, et al. Mannosylated poly(beta-amino esters) for targeted antigen presenting cell immune modulation. *Biomaterials.* 2015 Jan;37:333–44.
291. Fornaguera C, Guerra-Rebollo M, Lázaro MÁ, Cascante A, Rubio N, Blanco J, et al. In Vivo Retargeting of Poly(beta aminoester) (OM-PBAE) Nanoparticles is Influenced by Protein Corona. *Adv Healthc Mater.* 2019 Oct;8(19):e1900849.
292. Green JJ, Chiu E, Leshchiner ES, Shi J, Langer R, Anderson DG. Electrostatic ligand coatings of nanoparticles enable ligand-specific gene delivery to human primary cells. *Nano Lett.* 2007 Apr;7(4):874–9.
293. Ávila-Ortega A, Carrillo-Cocom LM, Olán-Noverola CE, Nic-Can GI, Vilchis-Nestor AR, Talavera-Pech WA. Increased Toxicity of Doxorubicin Encapsulated into pH-Responsive Poly(β -Amino Ester)-Functionalized MCM-41 Silica Nanoparticles. *Curr Drug Deliv.* 2020;17(9):799–805.
294. Moffett HF, Coon ME, Radtke S, Stephan SB, McKnight L, Lambert A, et al. Hit-and-run programming of therapeutic cytoreagents using mRNA nanocarriers. *Nat Commun.* 2017;8(1):389.
295. Mastorakos P, da Silva AL, Chisholm J, Song E, Choi WK, Boyle MP, et al. Highly compacted biodegradable DNA nanoparticles capable of overcoming the mucus barrier for inhaled lung gene therapy. *Proc Natl Acad Sci.* 2015 Jul 14;112(28):8720 LP – 8725.
296. Kaczmarek JC, Kauffman KJ, Fenton OS, Sadtler K, Patel AK, Heartlein MW, et al. Optimization of a Degradable Polymer–Lipid Nanoparticle for Potent Systemic Delivery of mRNA to the Lung Endothelium and Immune Cells. *Nano Lett.* 2018 Oct 10;18(10):6449–54.

297. Perni S, Prokopovich P. Optimisation and feature selection of poly-beta-amino-ester as a drug delivery system for cartilage. *J Mater Chem B*. 2020 Jun;8(23):5096–108.
298. Karlsson J, Rui Y, Kozielski KL, Placone AL, Choi O, Tzeng SY, et al. Engineered nanoparticles for systemic siRNA delivery to malignant brain tumours. *Nanoscale*. 2019 Nov;11(42):20045–57.
299. Gregory J V, Kadiyala P, Doherty R, Cadena M, Habel S, Ruoslahti E, et al. Systemic brain tumor delivery of synthetic protein nanoparticles for glioblastoma therapy. *Nat Commun*. 2020 Nov;11(1):5687.
300. Segovia N, Pont M, Oliva N, Ramos V, Borrós S, Artzi N. Hydrogel doped with nanoparticles for local sustained release of siRNA in breast cancer. *Adv Healthc Mater*. 2015 Jan;4(2):271–80.
301. Zhu D, Shen H, Tan S, Hu Z, Wang L, Yu L, et al. Nanoparticles Based on Poly (β -Amino Ester) and HPV16-Targeting CRISPR/shRNA as Potential Drugs for HPV16-Related Cervical Malignancy. *Mol Ther*. 2018 Oct;26(10):2443–55.
302. Tzeng SY, Patel KK, Wilson DR, Meyer RA, Rhodes KR, Green JJ. In situ genetic engineering of tumors for long-lasting and systemic immunotherapy. *Proc Natl Acad Sci*. 2020 Feb 25;117(8):4043 LP – 4052.
303. Vaughan HJ, Zamboni CG, Radant NP, Bhardwaj P, Revai Lechtich E, Hassan LF, et al. Poly(beta-amino ester) nanoparticles enable tumor-specific TRAIL secretion and a bystander effect to treat liver cancer. *Mol Ther - Oncolytics*. 2021 Jun 25;21:377–88.
304. Sharma BC, Gluud LL, Sarin SK. Beta-blocker plus nitrates for secondary prevention of variceal bleeding. Vol. 2017, *The Cochrane Database of Systematic Reviews*. 2017. p. CD006709.
305. Mela M, Mancuso A, Burroughs A. Drug treatment for portal hypertension. *Ann Hepatol*. 2002;1(3):102–20.
306. Huang J, Zhang X, Zhang M, Zhu J-D, Zhang Y-L, Lin Y, et al. Up-regulation of DLK1 as an imprinted gene could contribute to human hepatocellular carcinoma. *Carcinogenesis*. 2007 May 1;28(5):1094–103.
307. Chakravorty D, Jana T, Das Mandal S, Seth A, Bhattacharya A, Saha S. MYCbase: a database of functional sites and biochemical properties of Myc in both normal and cancer cells. *BMC Bioinformatics*. 2017 Apr;18(1):224.

308. Shah PP, Kakar SS. Pituitary tumor transforming gene induces epithelial to mesenchymal transition by regulation of Twist, Snail, Slug, and E-cadherin. *Cancer Lett.* 2011 Dec;311(1):66–76.
309. Reichenbach V, Fernández-Varo G, Casals G, Oró D, Ros J, Melgar-Lesmes P, et al. Adenoviral dominant-negative soluble PDGFR β improves hepatic collagen, systemic hemodynamics, and portal pressure in fibrotic rats. *J Hepatol.* 2012 Nov;57(5):967–73.
310. Borkham-Kamphorst E, Herrmann J, Stoll D, Treptau J, Gressner AM, Weiskirchen R. Dominant-negative soluble PDGF-beta receptor inhibits hepatic stellate cell activation and attenuates liver fibrosis. *Lab Invest.* 2004 Jun;84(6):766–77.
311. Pinzani M. PDGF and signal transduction in hepatic stellate cells. *Front Biosci.* 2002 Aug;7:d1720-6.
312. Friedman SL. Mechanisms of hepatic fibrogenesis. *Gastroenterology.* 2008 May;134(6):1655–69.
313. Murphy G, Cockett MI, Ward R V, Docherty AJ. Matrix metalloproteinase degradation of elastin, type IV collagen and proteoglycan. A quantitative comparison of the activities of 95 kDa and 72 kDa gelatinases, stromelysins-1 and -2 and punctuated metalloproteinase (PUMP). *Biochem J.* 1991 Jul;277 (Pt 1(Pt 1):277–9.
314. Arthur MJ. Fibrogenesis II. Metalloproteinases and their inhibitors in liver fibrosis. *Am J Physiol Gastrointest Liver Physiol.* 2000 Aug;279(2):G245-9.
315. Hagiwara R, Kageyama K, Niioka K, Takayasu S, Tasso M, Daimon M. Involvement of histone deacetylase 1/2 in adrenocorticotrophic hormone synthesis and proliferation of corticotroph tumor AtT-20 cells. *Peptides.* 2021 Feb;136:170441.
316. Yan H, Wang W, Dou C, Tian F, Qi S. Securin promotes migration and invasion via matrix metalloproteinases in glioma cells. *Oncol Lett.* 2015 Jun;9(6):2895–901.
317. Alcolado R, Arthur MJ, Iredale JP. Pathogenesis of liver fibrosis. Vol. 92, *Clinical science* (London, England: 1979). England; 1997. p. 103–12.
318. Madtes DK, Elston AL, Kaback LA, Clark JG. Selective induction of tissue inhibitor of metalloproteinase-1 in bleomycin-induced pulmonary fibrosis. *Am J Respir Cell Mol Biol.* 2001 May;24(5):599–607.

319. Casals E, Gonzalez E, Puentes VF. Reactivity of inorganic nanoparticles in biological environments: insights into nanotoxicity mechanisms. *J Phys D Appl Phys*. 2012;45(44):443001.
320. Krenkel O, Tacke F. Liver macrophages in tissue homeostasis and disease. *Nat Rev Immunol*. 2017 May;17(5):306–21.
321. Wang Y, Yang F, Zhang HX, Zi XY, Pan XH, Chen F, et al. Cuprous oxide nanoparticles inhibit the growth and metastasis of melanoma by targeting mitochondria. *Cell Death Dis*. 2013 Aug;4(8):e783.
322. Asati V, Mahapatra DK, Bharti SK. PI3K/Akt/mTOR and Ras/Raf/MEK/ERK signaling pathways inhibitors as anticancer agents: Structural and pharmacological perspectives. *Eur J Med Chem*. 2016 Feb;109:314–41.
323. Czuby A, Piekietko-Witkowska A. Protein kinases that phosphorylate splicing factors: Roles in cancer development, progression and possible therapeutic options. *Int J Biochem Cell Biol*. 2017 Oct;91(Pt B):102–15.
324. Fearnley GW, Young KA, Edgar JR, Antrobus R, Hay IM, Liang W-C, et al. The homophilic receptor PTPRK selectively dephosphorylates multiple junctional regulators to promote cell-cell adhesion. *Elife*. 2019 Mar;8.
325. Röhrig F, Schulze A. The multifaceted roles of fatty acid synthesis in cancer. *Nat Rev Cancer*. 2016 Nov;16(11):732–49.
326. Bechmann LP, Hannivoort RA, Gerken G, Hotamisligil GS, Trauner M, Canbay A. The interaction of hepatic lipid and glucose metabolism in liver diseases. *J Hepatol*. 2012 Apr;56(4):952–64.
327. Abel S, Smuts CM, de Villiers C, Gelderblom WC. Changes in essential fatty acid patterns associated with normal liver regeneration and the progression of hepatocyte nodules in rat hepatocarcinogenesis. *Carcinogenesis*. 2001 May;22(5):795–804.
328. Brown ZJ, Fu Q, Ma C, Kruhlak M, Zhang H, Luo J, et al. Carnitine palmitoyltransferase gene upregulation by linoleic acid induces CD4(+) T cell apoptosis promoting HCC development. *Cell Death Dis*. 2018 May;9(6):620.
329. Valenzuela R, Echeverria F, Ortiz M, Rincón-Cervera MÁ, Espinosa A, Hernandez-Rodas MC, et al. Hydroxytyrosol prevents reduction in liver activity of Δ -5 and Δ -6 desaturases, oxidative stress, and depletion in long chain polyunsaturated fatty acid content in different tissues of high-fat diet fed mice. *Lipids Health Dis*. 2017 Apr;16(1):64.

330. Bruix J, Reig M, Sherman M. Evidence-Based Diagnosis, Staging, and Treatment of Patients With Hepatocellular Carcinoma. *Gastroenterology*. 2016 Apr;150(4):835–53.
331. Wilhelm SM, Adnane L, Newell P, Villanueva A, Llovet JM, Lynch M. Preclinical overview of sorafenib, a multikinase inhibitor that targets both Raf and VEGF and PDGF receptor tyrosine kinase signaling. *Mol Cancer Ther*. 2008 Oct;7(10):3129–40.
332. Park D, Saravanakumar G, Kim WJ. Chapter 10 - Nitric Oxide-Releasing Functional Nanomaterials for Anticancer Therapy. In: Morbidelli L, Bonavida BBT-TA of NO in C and ID, editors. *Therapeutic Application of Nitric Oxide in Cancer and Inflammatory Disorders*. Academic Press; 2019. p. 191–218.
333. França-Silva MS, Balarini CM, Cruz JC, Khan BA, Rampelotto PH, Braga VA. Organic nitrates: past, present and future. *Molecules*. 2014 Sep;19(9):15314–23.
334. Daiber A, Münzel T. Organic Nitrate Therapy, Nitrate Tolerance, and Nitrate-Induced Endothelial Dysfunction: Emphasis on Redox Biology and Oxidative Stress. *Antioxid Redox Signal*. 2015 Oct;23(11):899–942.
335. Shirakami Y, Lee S-A, Clugston RD, Blaner WS. Hepatic metabolism of retinoids and disease associations. *Biochim Biophys Acta*. 2012 Jan;1821(1):124–36.
336. Kim SG, Larson JJ, Lee JS, Therneau TM, Kim WR. Beneficial and harmful effects of nonselective beta blockade on acute kidney injury in liver transplant candidates. *Liver Transplant Off Publ Am Assoc Study Liver Dis Int Liver Transplant Soc*. 2017 Jun;23(6):733–40.
337. Sersté T, Melot C, Francoz C, Durand F, Rautou P-E, Valla D, et al. Deleterious effects of beta-blockers on survival in patients with cirrhosis and refractory ascites. *Hepatology*. 2010 Sep;52(3):1017–22.
338. Sun J, Li M, Fan S, Guo Z, Zhong B, Jin X, et al. A novel liver-targeted nitric oxide donor UDCA-Thr-NO protects against cirrhosis and portal hypertension. *Am J Transl Res*. 2018 Feb 15;10(2):392–401.
339. Rodríguez S, Raurell I, Torres-Arauz M, García-Lezana T, Genescà J, Martell M. A Nitric Oxide-Donating Statin Decreases Portal Pressure with a Better Toxicity Profile than Conventional Statins in Cirrhotic Rats. *Sci Rep*. 2017;7(1):40461.
340. Moal F, Veal N, Vuillemin E, Barrière E, Wang J, Fizanne L, et al. Hemodynamic and antifibrotic effects of a selective liver nitric oxide donor V-

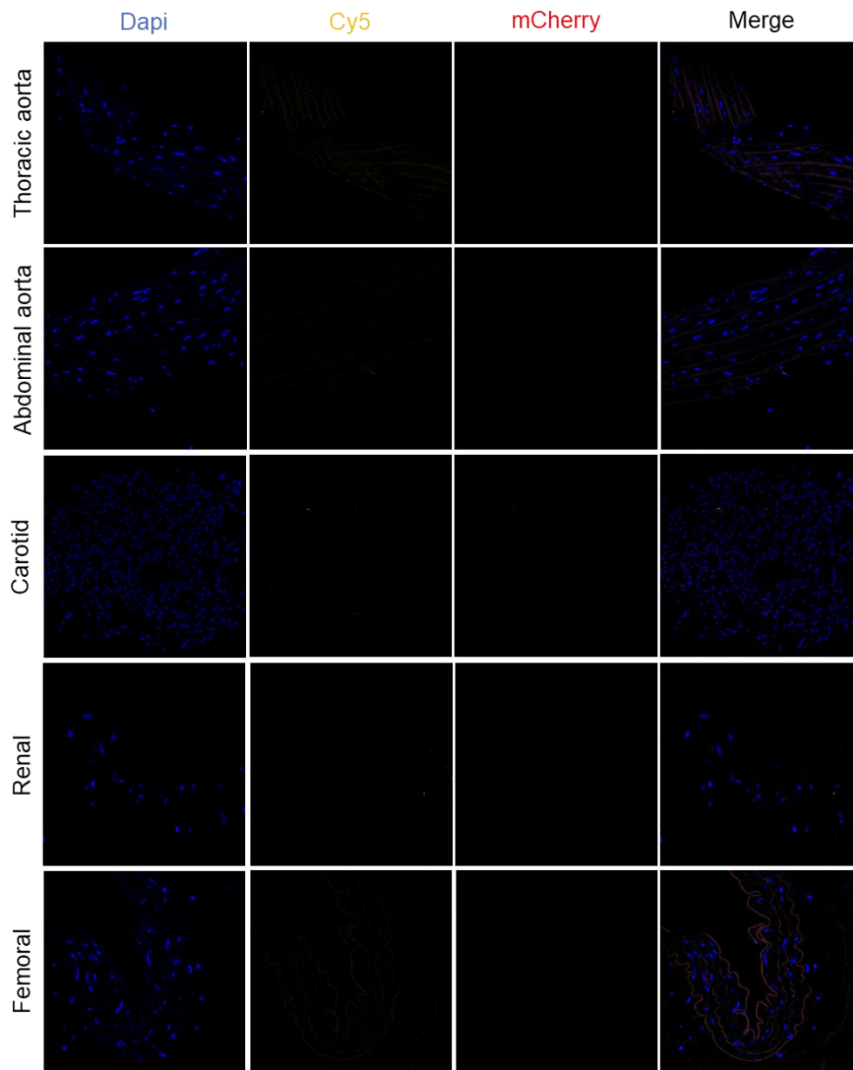
- PYRRO/NO in bile duct ligated rats. *World J Gastroenterol.* 2006 Nov;12(41):6639–45.
341. Leung T-M, Fung M-L, Liong EC, Lau TYH, Nanji AA, Tipoe GL. Role of nitric oxide in the regulation of fibrogenic factors in experimental liver fibrosis in mice. *Histol Histopathol.* 2011 Feb;26(2):201–11.
342. Thiele ND, Wirth JW, Steins D, Koop AC, Ittrich H, Lohse AW, et al. TIMP-1 is upregulated, but not essential in hepatic fibrogenesis and carcinogenesis in mice. *Sci Rep.* 2017 Apr 6;7(1):714.
343. Nie Q-H, Zhang Y-F, Xie Y-M, Luo X-D, Shao B, Li J, et al. Correlation between TIMP-1 expression and liver fibrosis in two rat liver fibrosis models. *World J Gastroenterol.* 2006 May 21;12(19):3044–9.
344. Wang K, Lin B, Brems JJ, Gamelli RL. Hepatic apoptosis can modulate liver fibrosis through TIMP1 pathway. *Apoptosis.* 2013;18(5):566–77.
345. Busk TM, Bendtsen F, Nielsen HJ, Jensen V, Brüner N, Møller S. TIMP-1 in patients with cirrhosis: relation to liver dysfunction, portal hypertension, and hemodynamic changes. *Scand J Gastroenterol.* 2014 Sep;49(9):1103–10.
346. Hink U, Münzel T. COX-2, Another Important Player in the Nitric Oxide–Endothelin Cross-Talk. *Circ Res.* 2006 Jun 9;98(11):1344–6.
347. Yang H, Xuefeng Y, Shandong W, Jianhua X. COX-2 in liver fibrosis. *Clin Chim Acta.* 2020;506:196–203.
348. Grumbach IM, Chen W, Mertens SA, Harrison DG. A negative feedback mechanism involving nitric oxide and nuclear factor kappa-B modulates endothelial nitric oxide synthase transcription. *J Mol Cell Cardiol.* 2005 Oct;39(4):595–603.
349. Liu T, Zhang L, Joo D, Sun S-C. NF- κ B signaling in inflammation. *Signal Transduct Target Ther.* 2017;2(1):17023.

**LIVER-TARGETED NANOPARTICLES DELIVERING NITRIC OXIDE
REDUCE PORTAL HYPERTENSION IN CIRRHOTIC RATS**

Meritxell Perramón, María Navalón-López, Guillermo Fernández-Varo, Alazne Moreno-Lanceta, Cristina Fornaguera, Pedro Melgar-Lesmes, Salvador Borrós, Wladimiro Jiménez

Table of contents

Supplementary figure 12



SUPPLEMENTARY FIGURE 1- Main arteries from the general circulation of cirrhotic rats treated with pBAE NPs with ret moiety. Representative confocal microscopy fluorescence images at 40x of arteries collected 3 h after Cy5 mCherry ret pBAE NPs administration in a cirrhotic rat with ascites. Nuclei are stained in blue.

DISCUSSION

Liver cirrhosis is the leading cause of hepatic related morbidity and mortality. Identifying an effective antifibrogenic treatment is a major unmet medical need. In the first study of the current doctoral thesis, we aimed to investigate the role of PTTG1/DLK1 signaling in the fibrogenic process and to evaluate *Pttg1* gene silencing as an antifibrogenic treatment to attenuate experimental liver fibrosis.

In the liver of healthy animals, *Pttg1* transcript was almost undetectable, whereas it was augmented in hepatic fibrosis and further in cirrhosis. Besides, the liver was the only organ in which *Pttg1* was augmented in animals with cirrhosis compared to control ones. In accordance, *Dlk1* mRNA was higher in fibrosis than control, positively correlating with collagen deposition. Moreover, the cirrhotic liver was the only organ which significantly overexpressed *Dlk1* compared to the control organ. DLK1 protein levels replicated mRNA expression pattern and diverged from other profibrogenic mediators. Hepatic primary cells isolation revealed augmented *Pttg1* and *Dlk1* transcription in cirrhotic hepatocytes, HSCs and endothelial cells compared to control counterparts. Additionally, whereas control livers did not present positive PTTG1 and DLK1 protein staining, cirrhotic ones showed intense but topologically undefined protein staining. Eventually, hepatic cirrhotic biopsies from patients considerably upregulated *PTTG1* and *DLK1* expression compared to control samples. As far as we know, this is the first study proving *PTTG1* transcript expression in cirrhotic patients. According to previous investigations where *DLK1* has been shown upregulated in HCC but rarely in adjacent non-cancerous tissue (306), we also demonstrated upregulated *DLK1* mRNA in cirrhosis compared to control biopsies. Altogether, this suggests that *PTTG1/DLK1* signaling may be important in the pathogenesis of hepatic fibrosis. This was additionally endorsed by findings using *Pttg1* KO mice. Previously, Buko *et al.* showed that *Pttg1* KO mice presented less thioacetamide-induced bridging fibrosis in comparison to WT mice (81). This conclusion was reaffirmed in the present study using CCl₄-induced liver fibrosis experimental model. Rigorous gene expression analysis comparing the hepatic expression of fibrotic *Pttg1* KO and WT mice showed that disruption of ECM turnover was a key driver governing this phenomenon. Only genes with both statistical and biological significance were considered. The analysis unveiled significant downregulation of *Mmp8*, *Mmp9*, *Timp4* and *Acta2*. Interestingly, this was

accompanied by *Myc* downregulation. *Myc* is a nuclear phosphoprotein that regulates the expression of multiple genes related to cell growth, cycle, differentiation, apoptosis, genomic instability, transformation, and angiogenesis (307). Besides, *Pttg1* has been reported to be a powerful activator of *Myc* (48), which hints that both could interact and play an important role during hepatic fibrogenesis.

Altogether these findings suggest that gene therapy targeting *Pttg1* expression could be a promising approach to interfere with the progression of liver fibrosis. In fact, fibrotic rats treated with a siRNA against *Pttg1* showed weaker liver fibrosis, reduced portal hypertension and decreased number of activated HSCs compared to scrambled siRNA-treated animals, being a reduction of the proportion of activated HSCs the probable responsible of fibrogenesis inhibition. On the other side, the reduction in portal hypertension may be because of the antifibrotic effect. This was accompanied by decreased transcription of *Col1a2*, *Col3a1*, *Tgfb β 1* and *Pdgfr β* . It has been shown that *Pttg1* silencing in ovarian epithelial tumor cells lowered the expression and release of TGF β (308). Here, we report a tendency to decreased *Tgfb β 1* expression following *Pttg1* interference in fibrotic rats. Moreover, previous studies reported diminished *Tgfb β* transcription in the liver of fibrotic *Pttg1* KO compared to WT mice (81).

Administration of *Pttg1* siRNA in CCl₄-induced fibrotic rats was also associated to decreased *Pdgfr β* mRNA. Reduced liver fibrosis was previously reported by intrahepatic PDGFR β pathway blockade using adenoviral vectors (309) and by systemic PDGF antagonism in bile duct ligated rats (310). PDGF is the most potent pro-proliferative mediator in HSCs (311,312). Therefore, inhibition in HSCs proliferation may be responsible for decreased liver fibrosis after *Pttg1* interference.

Both excessive synthesis and decreased ECM degradation contributes to liver fibrosis (313,314). In the current study, ECM remodeling is also affected by *Pttg1* silencing. Hepatic *Col1a2* and *Col3a1* gene expression were upregulated in fibrotic rats receiving scrambled siRNA. Besides *Mmp2* and *Mmp9* transcription was also increased, probably due to a compensatory mechanism aimed to get rid of the excess of scar tissue. *Pttg1* silencing augmented MMPs/TIMPs ratio maybe

as a result of *Timp1* and *Timp2* inhibition. This supports the role of PTTG1 in the regulation of ECM degradation in the fibrotic liver primarily by controlling TIMPs expression.

Noteworthy, most surrogate liver function serum markers in fibrotic rats tended towards the normalization after *Pttg1* siRNA treatment, in exception of transaminases, indicating that *Pttg1* exerts a direct effect in fibrosis generation and not in CCl₄ hepatotoxicity. This phenomenon was reported beforehand in *Pttg1* KO mice (81).

Pttg1 interference mediates several mechanisms in liver fibrosis. Firstly, probably due to post-transcriptional regulation (82), *Dlk1* mRNA expression is prevented by *Pttg1* silencing, resulting in lower HSC activation and fibrosis deposition (112). This suggests that PTTG1/DLK1 network is important during hepatic fibrogenesis. Additionally, both mediators are regulated by histone deacetylases (HDAC). In corticotroph cells, HDAC1 induces proliferation upregulating *Pttg1* expression (315) and in preadipocytes and NIH 3T3 cells, HDAC3 represses *Dlk1* (88). Secondly, *Pttg1* is implicated in ECM remodeling. It has been shown that *Pttg1* induces *Mmp2* expression and secretion (316). MMP2 is a gelatinase involved in the degradation of ECM components such as collagen IV, fibronectin, and laminin (313). In here, we showed that *Mmp2* is augmented in liver fibrosis. Moreover, *Pttg1* silencing reduces *Mmp2* resulting in anti-fibrogenic effect by decreasing normal ECM degradation and inducing HSC activation (317). *Pttg1* silencing also decreases TIMPs expression. Activated HSC highly express *Timp1* and *Timp2*, thereby, reduced *Timp1* and *Timp2* mRNA expression following *Pttg1* interference in fibrotic rats may be due to reduced HSC activation. *Timp1* and *Timp2* also stimulate fibroblast proliferation (318). For this reason, their downregulation could be involved in reduced HSC proliferation. **Figure 20** illustrates a graphical model outlining the proposed mechanism underlying PTTG1/DLK1 axis implication in the pathogenesis of liver fibrosis.

To sum up, this study shows that *Pttg1* gene silencing using a siRNA acts as an anti-fibrotic agent in fibrotic rats. Besides, *Pttg1* interference diminishes upregulated *Dlk1* expression, decreases the activation of HSCs, the expression of

genes related to ECM deposition and remodeling, reduces collagen deposition and eventually, diminishes portal hypertension. Therefore, *PTTG1/DLK1* pathway may be a potential therapeutic target for the prevention and treatment of hepatic fibrogenesis.

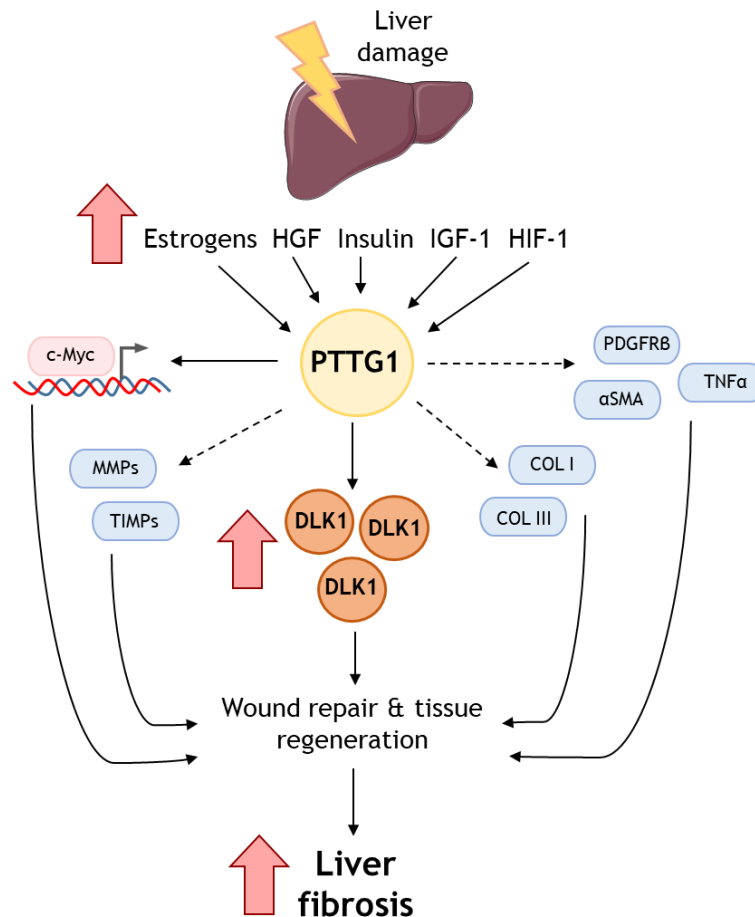


Figure 1. Schematic representation of the proposed mechanism underlying *PTTG1/DLK1* axis role in liver fibrosis induction. The synthesis and release of mediators including estrogens, hepatocyte growth factor (HGF), insulin, insulin growth factor 1 (IGF-1), and hypoxia inducible factor 1 (HIF-1) are augmented following liver injury. These mediators induce the expression of *Pttg1*, a transcriptional activator of *c-myc*. Besides, *Pttg1* indirectly augments the expression of platelet derived growth factor receptor beta (*PDGFRβ*), tumor necrosis factor alpha (*TNFα*), alpha-smooth muscle actin (*αSMA*), collagens I (*COL I*) and III (*COL III*), metalloproteinases (*MMP*), and tissue inhibitors of metalloproteinases (*TIMP*). Noteworthy, *Pttg1* also induces *Dlk1* expression. This contributes to wound repair and tissue regeneration inducing liver fibrosis. Direct effect is shown with continuous arrows and indirect effect by discontinuous ones. Original image from: Perramón M, Carvajal S, Reichenbach V, Fernández-Varo G, Boix L, Macías-Muñoz L, et al. The pituitary tumour-transforming gene 1/delta-like homologue 1 pathway plays a key role in liver fibrogenesis. *Liver Int.* 2022 Mar;42(3):651-662.

In the second study included in the current doctoral thesis, we aimed to evaluate the potential beneficial effects of CeO₂NPs in tumor progression, inflammation, kinase signaling pathways, lipid metabolism, and animal survival in rats with experimental HCC. Despite nanoceria has widely been used for decades to catalyze redox reactions in catalytic exhaust converters and petrochemical industries (253), its use as a therapeutic agent is still a major

concern. Largely due to CeO₂NPs variability in antioxidant response and activity in biological media (319). To overcome these issues, in the present study CeO₂NPs have been coated with albumin resulting in NPs with high stability and monodispersity in physiological media. The formation of large aggregates and protein corona are prevented and thereby, a stable NPs colloidal solution is generated.

An effective systemic HCC treatment remains an unmet clinical need. Oxidative stress, mainly ROS, is a major driver of cancer pathogenesis. It is directly implicated in the initiation and progression of cancer, in addition to decrease the natural antioxidant defenses which are involved in scavenging free radicals (176). For these reasons, antioxidants including different compounds, enzymes and inhibitors have been largely evaluated for the treatment of chronic inflammation and cancer. But to date none of them, as consequence of their low systemic bioavailability, has shown promising results.

In this study, we investigated the potential of the antioxidant CeO₂NPs as a treatment for HCC. Unlike other therapies, CeO₂NPs possess a catalytic self-regenerating antioxidant effect, therefore avoiding the need for periodical administration. Besides, nanoceria is inert in physiological conditions and it is only active when there is oxidative stress.

DEN is a carcinogenic organic compound acting by rising the proliferation of hepatocytes. Once administered, DEN is first hydroxylated by cytochrome (CYP) P450 and then it is oxidized by CYP2E1 to reactive products. The administration of DEN resulted in macroscopically and microscopically alterations of the liver including modification of liver weight, tissue dysplasia and the apparition of fibrotic tracts. Next, we wanted to evaluate the biodistribution following CeO₂NPs administration in rats with HCC. Despite the high tumorigenic activity in the liver, CeO₂NPs preserved their selectivity for liver tissue in rats with DEN-induced HCC.

Besides, HCC rats treated with CeO₂NPs showed decreased activation of parameters related to tissue growth, proliferation, and inflammation. They had increased liver / body weight ratio and reduced the amount of hepatic infiltrating

macrophages and Ki67-positive cells compared to vehicle-treated rats. Ki67 is greatly used as proliferation marker as well as prognostic cancer indicator. Additionally, AFP serum concentration was diminished. AFP is the most used biomarker for hepatocyte dedifferentiation and closely associated to HCC. CeO₂NPs also reduced the expression of proinflammatory M1-related genes. During carcinogenesis, TAMs provide an immunosuppressive microenvironment which facilitates tumor progression (320). Therefore, CeO₂NPs antitumor effects may be partially mediated by the decrease in infiltrating macrophages, due to cell death or chemotaxis inhibition.

Several evidences sustain CeO₂NPs antitumor effects in DEN-induced HCC experimental model. Firstly, nanoceria administration resulted in augmented hepatic apoptosis. This agrees with a previous study from Wang Y *et al.* in which showed that cuprous oxide NPs induce apoptosis of lung melanoma cells (321). Secondly, CeO₂NPs diminished the phosphorylation of ERK1/2. Ras/Raf/MAPK kinase/ERK signaling pathway is one of the most important controlling proliferation, growth, differentiation, survival, angiogenesis, inflammation and glucose and lipid metabolism (322).

Besides, untargeted MS-based proteomics was used to evaluate the effects of CeO₂NPs in HCC cellular phosphorylation. CeO₂NPs significantly affected 9.5% of all detected phosphorylation sites, including augmented and diminished, on the liver of rats with HCC. These effects were in networks related to cell proliferation, apoptosis, migration, and survival. For instance, p21 activated kinase 2, eukaryotic elongation factor 2 kinase, tyrosine kinase 2/focal adhesion kinase 2 and NIMA-related kinase 9. Noteworthy, gene ontology analysis revealed an enrichment of phosphorylation of proteins related to RNA splicing and cell-cell adhesion. Splicing is often disturbed in human tumors and significantly contributes to processes like proliferation, apoptosis, angiogenesis, and migration (323). For that matter, nanoceria effects in altering the phosphorylation of proteins related to splicing may be involved in the decreased hepatic cell proliferation. Besides cell-cell adhesion, involving both tumor suppressors and oncogenes, is a process also deregulated in cancer (324). CeO₂NPs significantly reduced the phosphorylation of cell surface proteins CD44 and Itgb4.

Dysregulation of FA metabolism to support cellular proliferation is one of the hallmarks of cancer (325). Cancer cells have a strong avidity for lipids augmenting both exogenous uptake and endogenous synthesis (326). In agreement, the measurement of lipids circulating in the serum of rats with HCC revealed a reduced amount of triglycerides and cholesterol. Besides, the analysis of principal lipid components in the liver of these rats showed significantly increased CE-derived FAs, which is the most common form of cancer cells to store excessive lipids and cholesterol in LDs (322). NEFA lipid component was also augmented presumably to support tumor growth.

In contrast, the strongest effects of CeO₂NPs in the hepatic lipidome were found in PC-derived FAs. Nanoceria significantly decreased PC-derived FAs because of a great reduction in arachidonic acid. Esterified arachidonic acid is released from cellular phospholipids by phospholipases A₂, C, and D; a pathway already augmented in rats with HCC. Once free, arachidonic acid can be metabolized or act as a second messenger in several networks (327), some of which upregulated in rats with DEN-induced HCC. CeO₂NPs treated animals further decreased esterified PC-derived arachidonic acid, probably related to the increased apoptosis found in these animals since free arachidonic acid can activate sphingomyelinase and induce this process (328).

Additionally, nanoceria significantly diminished one of the most abundant FAs: linoleic acid in TG, NEFA and CE lipid components in the liver of rats with HCC. Brown *J et al.* reported that linoleic acid has an important role in the development of NAFLD-promoted HCC by changing intrahepatic CD4⁺ cells metabolism and inducing apoptosis (328). Anomalous essential FA metabolism involving $\Delta 6$ desaturase induces changes in PUFA profile, which have been related to neoplastic hepatocytes (327). Besides, intracellular redox state regulates the activity and expression of the after mentioned desaturase (329). Therefore, the reduction in oxidative stress after CeO₂NPs treatment could trigger the reactivation of $\Delta 6$ desaturase activity and the restoration to normal linoleic acid hepatic concentrations in rats with HCC.

The effect of nanoceria on survival was further assessed to translate the antitumorigenic effects in a clinically significant improvement. Rats with HCC and

treated with CeO₂NPs significantly increased survival compared to ones receiving vehicle. To treat patients with advanced HCC, several tyrosine kinase inhibitors including sorafenib, lenvatinib, cabozantinib and regorafenib are believed to be effective compounds (330). In our study, similar effects on survival rates were observed after treating DEN-injured rats either with sorafenib or CeO₂NPs, demonstrating that both treatments are equally effective under the studied conditions. The combination of both did not produce further survival amelioration. This could be explained because both treatments lead to similar effects: common signaling pathways are affected as VEGF signaling in angiogenesis, they induce alike ERK1/2 modulation, and phosphorylation state alteration, altogether driving to similar proliferation and apoptosis modification, as reported with sorafenib (331). **Figure 21** illustrates a graphical model outlining the main effects of CeO₂NPs on experimental HCC.

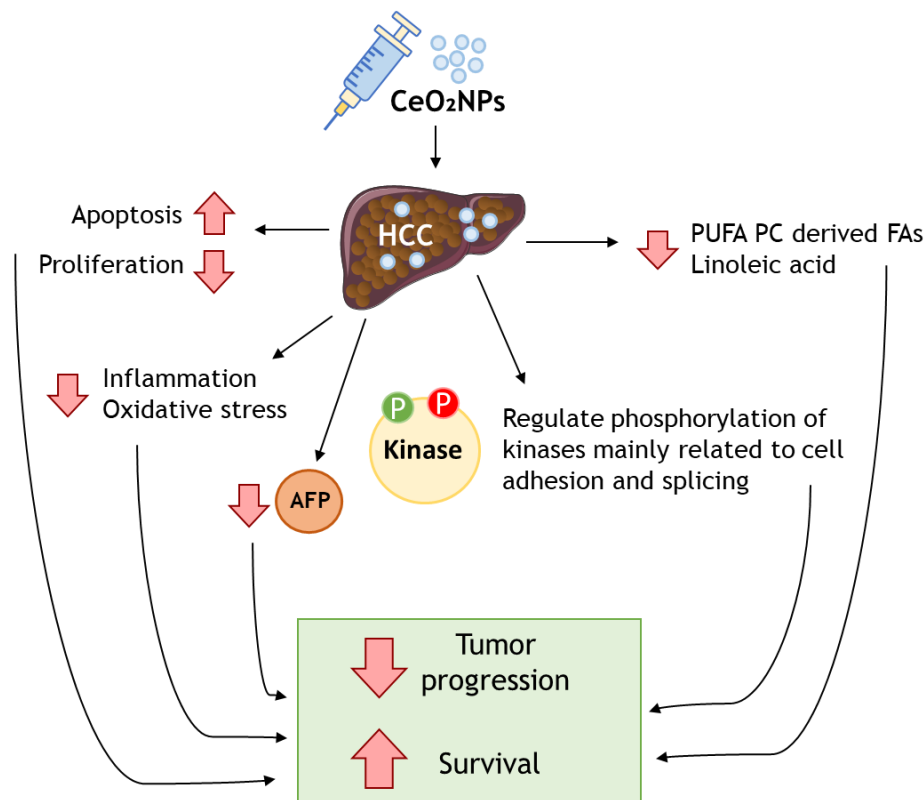


Figure 2. Schematic representation of CeO₂NPs effects on experimental HCC. Following CeO₂NPs intravenous administration, they mainly accumulate in the liver where they increase apoptosis at the same time decrease proliferation. Moreover, CeO₂NPs reduce hepatic inflammation and oxidative stress. CeO₂NPs are also involved in decreasing alpha-fetoprotein (AFP) levels. CeO₂NPs also regulate the phosphorylation of several kinases. Finally, CeO₂NPs treatment ultimately leads to decrease polyunsaturated (PUFA) phosphatidylcholine (PC) derived fatty acids (FAs). Altogether results in the reversion of cellular mechanisms related to tumor progression and improves survival.

Finally, to gain insight on nanoceria behavior in the human liver, we administered CeO₂NPs *ex vivo* to human livers undergoing normothermic

machine perfusion. Following administration, CeO₂NPs rapidly accumulated in the hepatic tissue confirming nanoceria avidity for the human liver. They were observed both within intracellular endosome-like bodies and free in the cytoplasm. Cerium presence was further confirmed by elemental analysis combined with STEM. The human hepatocyte cell line HepG2 reiterated NPs uptake mainly in endosome-like organelles.

In conclusion, the treatment with CeO₂NPs partially reverts tumor progression and significantly augments survival in rats with DEN-induced HCC, suggesting that this antioxidant nanomaterial is a potential effective treatment in experimental HCC. Nanoceria alone or in combination with molecular targeted treatments could be of value attenuating HCC progression in patients.

Portal hypertension is a major complication of advanced liver disease, consequence from increased resistance to the portal blood flow into the liver. The subsequent appearance of clinical life-threatening complications such as ascites or variceal bleeding induce the transition from compensated to a decompensated state. In the third study, we aimed to evaluate the possible therapeutic value of an organic NO donor directed to the liver by retinol decorated pBAE NPs in experimental decompensated cirrhosis.

NO donors are potent compounds with the ability to release NO and facilitate smooth muscle relaxation (332). Organic nitrates are a class of donors widely known for their stability, since NO release does not rely on environmental changes but on enzymatic activities including aldehyde dehydrogenase-2 or cytochrome P450 reductase (333,334). Given that is difficult to measure NO release intrahepatically, their kinetics was not evaluated in the present study. Therefore, similar retinol pBAE NPs but lacking the NO donor were used as control and it was speculated that differences between treatments could be attributed to NO release. NO donor containing retinol pBAE NPs showed a larger hydrodynamic size and a similar positive z-potential compared to control NPs as measured by dynamic light scattering.

To evaluate the potential of pBAE NPs with retinol moiety to specifically target the liver, a biodistribution study was first performed. A Cy5 dye as well as a

plasmid encoding for the protein mCherry were added to the NPs to track their uptake and transfection, respectively. The liver, spleen and kidney showed Cy5 presence. In the hepatic tissue, this signal co-localized with mCherry in fiber-like zones. Besides, both Cy5 and mCherry signals were extensive in the splanchnic tissue. In contrast, mCherry was almost absent in the kidney. Finally, neither Cy5 or mCherry were identified in the heart, brain, or lung. Furthermore, the fluorescence analysis revealed no presence of Cy5 or mCherry protein in thoracic and abdominal aorta, carotid, mesenteric, femoral, and renal arteries. NO donor hepatic selectivity is of major concern in decompensated cirrhosis given that a further increase in systemic vasodilation would have a noxious impact. Other authors had previously employed different ligands to deliver pBAE NPs to hepatic cancer cells (283,303). Here, retinol was selected because the liver plays a central role in retinol storage and distribution (335). Recently, Fornaguera *et al.* reported that the addition of retinol in to end-oligopeptide modified pBAE NPs enabled higher hepatic delivery once injected in control mice (291). In line, Duong HTT *et al.* reported that the decoration with retinol facilitated the delivery of polymeric NPs to HSC in bile-duct ligated rats (232).

Cirrhosis decompensation is characterized by a clinically significant portal hypertension, the worsening of hepatic function and disease progression (132). For several decades, non-selective beta blockers have been the treatment of choice to reduce portal hypertension in patients. These drugs act diminishing the heart rate and CO, in addition to induce splanchnic arteries vasoconstriction. Besides, they have been shown to prevent decompensation and the appearance of clinical complications and therefore, increasing patients' survival (132). Nevertheless, their use in patients with end-stage cirrhosis remains controversial (336,337). Consequently, there is an urge to develop novel therapies intended to reduce the portal hypertension. Here, we evaluated the impact on systemic and portal hemodynamics of our liver-selective nanoformulation conjugated to a NO donor. The treatment with NO donor pBAE NPs decorated with retinol did not influence the mean arterial pressure or the CO. Strikingly, they significantly reduced PP. Other authors have previously shown similar results, but most of them used early fibrosis models which do not recapitulate a clinically significant portal hypertension (338,339). Only two studies have reported the evaluation of

similar treatments in decompensated cirrhosis experimental models. Moal F *et al.* (340) showed a reduction on PP as well as in the development of collateral circulation in n bile duct ligated rats treated with a liver-specific NO donor. Besides, Duong HTT *et al.* (232) reported a decrease in portal hypertension after a liver-targeted NO donor administration in bile duct ligated rats and evaluated the effects *in vitro* in HSCs.

Further knowledge on the hepatic effects of the ret pBAE NPs containing the NO donor in cirrhotic rats with ascites was obtained performing a commercially available array of vasoactive genes. Rigorous analysis revealed that four genes including *Bdkrb1*, *Ptgs2*, *Ace2* and *Sphk1*, were both biologically and statistically significantly downregulated after liver-specific NO treatment.

Next, we evaluated the possible effects of our nanoformulated NO donor on hepatic fibrogenesis. The treatment did not reduce intrahepatic collagen deposition, as means as the morphometric analysis of Sirius red staining. Of note, it significantly decreased the activation of HSCs, measured by α SMA staining. Moreover, the treatment did not induce changes in the mRNA expression of *Col1a2*, *Col3a1*, *Acta2*, *Mmp-2*, *Mmp-9*, or *Timp-2*. Other authors have previously reported fibrogenesis modulation by liver-targeted NO donors. For instance, Leung TM *et al.* (341) showed that the treatment with the NO donor L-arginine induced a downregulation in the transcription of profibrogenic mediators in a CCl₄-induced experimental mice liver fibrosis. In line, Sun J *et al.* (338) described a reduction in Sirius red staining and hydroxyproline content after treating DEN-induced cirrhotic rats with a NO donor linked to ursodeoxycholic acid. These studies reported longer treatment times compared to ours. Hence, the absence of effect in hepatic fibrogenesis in our study could be explained by the short treatment time, which was approximately 3 h.

Remarkably, NO donor pBAE NPs decorated with retinol decreased hepatic transcription of *Timp-1* and *Et-1*. During hepatic injury, TIMP-1 inhibits the activation of the proteolytic enzyme family MMPs to modulate ECM deposition (342,343). Moreover, TIMP-1 is antiapoptotic and has been involved in cellular proliferation promotion (344). In the plasma of patients with cirrhosis, TIMP-1 protein concentration is augmented and correlates with portal hypertension

(345). On the other hand, *ET-1* is a powerful vasoconstrictor, which exerts its functions mainly in endothelial and smooth muscle cells. It is known that NO deficiency induces *ET-1* expression and as a consequence *cyclooxygenase 2* expression and the conversion of arachidonic acid to prostaglandins and thromboxane are stimulated (346). Cyclooxygenase 2 is a mediator that plays an important role in a myriad of biological processes including inflammation, senescence, apoptosis, and autophagy (347). In this study, liver-specific NO donor treatment also resulted in decreased expression of *cyclooxygenase 2* as well as *Il-6*, *Tnfa* and *Nos2* mRNAs. It has been reported that NO inhibits nuclear factor kappa beta activation (348). This transcription factor important for the expression regulation of genes related to the inflammatory response and inflammasome (349). Noteworthy, the treatment did not induce changes in *Nos3* transcription. Finally, the administration of engineered NO donor polymeric NPs reduced the serum concentration of lactate dehydrogenase and aspartate aminotransferase enzyme. Therefore, these evidence suggests that NO donor retinol pBAE NPs efficiently target the liver of cirrhotic rats, where the release of NO is induced. NO in turn triggers 1) the loss of HSC contractile phenotype and 2) hepatic vasodilation. Altogether, this therapy reduces portal hypertension and proinflammatory gene expression.

To sum up, NO donor pBAE NPs decorated with retinol may be useful to mitigate portal hypertension and hepatic inflammation in decompensated cirrhosis.

CONCLUSIONS

1. The progression of rat liver fibrosis is associated to a selective concomitant increase in hepatic *Pttg1* and *Dlk1* mRNA expression.
2. *Pttg1* is upregulated in both cirrhotic rat hepatocytes and HSC compared to controls. *Dlk1* is also increased in both cirrhotic cell types, being more abundant in the former.
3. *PTTG1* and *DLK1* transcripts are augmented in liver biopsies from cirrhotic patients in comparison to non-cirrhotic subjects.
4. *PTTG1* and *DLK1* proteins are present in the hepatic parenchyma and close to portal tracts of cirrhotic rats, whereas they are undetectable in control livers.
5. Liver fibrosis progression correlates with circulating levels of *DLK1*. Besides, *DLK1* serum concentration also positively correlates with hepatic collagen content and portal hypertension.
6. The lack of *Pttg1* in fibrotic mice attenuates liver fibrosis and downregulates the transcript expression of *Dlk1* and genes involved in ECM turnover.
7. Silencing of *Pttg1* in rats with fibrosis significantly reduces hepatic collagen content, HSC activation, and portal hypertension compared to rats receiving scrambled siRNA.
8. CeO_2NPs mainly accumulate in the liver and spleen of rats with HCC that are administered intravenously, and they remain for at least 3 weeks.
9. Albeit CeO_2NPs do not modify hepatic function parameters, they significantly decrease serum AFP concentration and hepatic inflammation.
10. The treatment with CeO_2NPs significantly increases apoptosis and reduces the proliferation rate of hepatocytes in the liver of rats with HCC, probably due to a Ras/MAPK pathway interference.
11. The treatment with CeO_2NPs in DEN-induced HCC has a general effect on the phosphorylation of hepatic proteins, predominantly those related to cell adhesion and RNA splicing.
12. The amount of hepatic phosphatidylcholine-derived PUFAs is reduced in rats with HCC after the treatment with CeO_2NPs , mostly due to a decrease in arachidonic acid. In addition, these NPs normalize the augmented levels of linoleic acid in the principal lipid components from the hepatic tissue of rats with HCC.
13. CeO_2NPs significantly augment survival of DEN chronically administered rats compared to vehicle. Besides, sorafenib and CeO_2NPs have similar benefit and

- the combination of both results in longest survival, although without statistical significance.
14. Human liver can uptake CeO₂NPs from the circulation. In the liver, these NPs are mainly found inside blood vessels, space of Disse and in the cytoplasm and within endosome-like organelles of endothelial and circulating immune cells.
 15. CeO₂NPs are successfully internalized by the human hepatocyte cell line HepG2, and are found attached to the plasmatic membrane, in the cytoplasm and inside endosome-like organelles.
 16. The liver and spleen are the major targets of NO donor retinol pBAE NPs in rats with decompensated cirrhosis.
 17. Liver-targeted NO donor NPs ameliorate serum markers of liver function.
 18. The administration of retinol pBAE NPs containing a NO donor significantly reduce portal hypertension without affecting systemic hemodynamics in cirrhotic rats with ascites.
 19. Liver-targeted NO donor NPs diminish the transcription of genes involved in vascular reactivity.
 20. The activation of HSC and the expression of proinflammatory gene markers is reduced after NO donor containing ret pBAE NPs treatment in rats with decompensated cirrhosis.

According to the results obtained in the current doctoral thesis, it may be concluded that the interference of PTTG1/DLK1 signaling, CeO₂NPs and liver-targeted NO donor polyplexes are three promising nanoscale therapeutic approaches to target liver fibrosis, HCC, or the associated clinical complications, respectively. *Pttg1* and *Dlk1* expression selectively increase in the liver correlating with fibrosis progression in both experimental models and human patients. Moreover, *Pttg1* gene silencing using a siRNA in CCl₄-induced liver fibrosis rat model results in decreased *Dlk1* transcription, reduced collagen deposition, attenuated portal hypertension and diminished fibrosis-related genes expression. Besides, CeO₂NPs behave as strong antioxidants attenuating tumor progression by interfering with kinase pathways and lipid metabolism; ultimately reducing proliferation and inflammation, and at the same time increasing apoptosis in the liver of DEN-induced HCC. CeO₂NPs have similar effects to sorafenib ameliorating rat survival. Moreover, *ex vivo* perfused human liver and *in vitro*

hepatocyte cells can internalize CeO₂NPs both in intracellular endosome-like organelles and free in the cytoplasm. Finally, NO donor pBAE NPs decorated with retinol successfully target the cirrhotic liver. Moreover, pBAE NPs containing a NO donor ameliorate portal hypertension, without affecting systemic hemodynamics in rats with decompensated cirrhosis. Furthermore, these NPs significantly decrease the activation of HSCs and the mRNA expression of proinflammatory genes in the hepatic tissue.

REFERENCES

1. Parola M, Pinzani M. Liver fibrosis: Pathophysiology, pathogenetic targets and clinical issues. *Mol Aspects Med.* 2019 Feb;65:37–55.
2. Paik JM, Golabi P, Younossi Y, Mishra A, Younossi ZM. Changes in the Global Burden of Chronic Liver Diseases From 2012 to 2017: The Growing Impact of Nonalcoholic Fatty Liver Disease. *Hepatology.* 2020 Feb;72(5):1605–16.
3. Byrne CD, Targher G. NAFLD: A multisystem disease. *J Hepatol.* 2015 Apr 1;62(1):S47–64.
4. Eslam M, Newsome PN, Sarin SK, Anstee QM, Targher G, Romero-Gomez M, et al. A new definition for metabolic dysfunction-associated fatty liver disease: An international expert consensus statement. *J Hepatol.* 2020 Jul;73(1):202–9.
5. Sharma A NS. *Chronic Liver Disease.* StatPearls Publishing. 2021.
6. Roehlen N, Crouchet E, Baumert TF. Liver Fibrosis: Mechanistic Concepts and Therapeutic Perspectives. *Cells.* 2020 Apr;9(4).
7. Pinzani M. Pathophysiology of Liver Fibrosis. *Dig Dis.* 2015;33(4):492–7.
8. Ishak K, Baptista A, Bianchi L, Callea F, De Groote J, Gudat F, et al. Histological grading and staging of chronic hepatitis. *J Hepatol.* 1995 Jun;22(6):696–9.
9. Shiha, Gamal; Zalata K. Ishak versus METAVIR: Terminology, Convertibility and Correlation with Laboratory Changes in Chronic Hepatitis C. In: Takahashi KZE-H, editor. *Liver Biopsy.* Rijeka: IntechOpen; 2011.
10. Bedossa P, Poynard T. An algorithm for the grading of activity in chronic hepatitis C. The METAVIR Cooperative Study Group. *Hepatology.* 1996 Aug;24(2):289–93.
11. Sumida Y, Nakajima A, Itoh Y. Limitations of liver biopsy and non-invasive diagnostic tests for the diagnosis of nonalcoholic fatty liver disease/nonalcoholic steatohepatitis. *World J Gastroenterol.* 2014 Jan;20(2):475–85.
12. Hou W, Syn W-K. Role of Metabolism in Hepatic Stellate Cell Activation and Fibrogenesis. *Front Cell Dev Biol.* 2018; 6: 150.
13. Kisseleva T, Brenner D. Molecular and cellular mechanisms of liver fibrosis and its regression. *Nat Rev Gastroenterol Hepatol.* 2021;18(3):151–66.

14. Ying H-Z, Chen Q, Zhang W-Y, Zhang H-H, Ma Y, Zhang S-Z, et al. PDGF signaling pathway in hepatic fibrosis pathogenesis and therapeutics (Review). *Mol Med Rep*. 2017 Dec;16(6):7879–89.
15. van der Heide D, Weiskirchen R, Bansal R. Therapeutic Targeting of Hepatic Macrophages for the Treatment of Liver Diseases. *Front Immunol*. 2019; 10: 2852.
16. Wen Y, Lambrecht J, Ju C, Tacke F. Hepatic macrophages in liver homeostasis and diseases-diversity, plasticity and therapeutic opportunities. *Cell Mol Immunol*. 2021 Jan; 18(1): 45–56.
17. Parola M, Robino G. Oxidative stress-related molecules and liver fibrosis. *J Hepatol*. 2001 Aug;35(2):297–306.
18. Ramos-Tovar E, Muriel P. Molecular Mechanisms That Link Oxidative Stress, Inflammation, and Fibrosis in the Liver. *Antioxidants*. 2020 Dec;9(12):1279.
19. Luangmonkong T, Suriguga S, Mutsaers HAM, Groothuis GMM, Olinga P, Boersema M. Targeting Oxidative Stress for the Treatment of Liver Fibrosis. *Rev Physiol Biochem Pharmacol*. 2018;175:71-102.
20. Elpek GÖ. Cellular and molecular mechanisms in the pathogenesis of liver fibrosis: An update. *World J Gastroenterol*. 2014 Jun;20(23):7260–76.
21. Seki E, Brenner DA. Recent advancement of molecular mechanisms of liver fibrosis. *J Hepatobiliary Pancreat Sci*. 2015 Jul;22(7):512–8.
22. Acharya P, Chouhan K, Weiskirchen S, Weiskirchen R. Cellular Mechanisms of Liver Fibrosis. *Front Pharmacol*. 2021; 12: 671640.
23. Zuo W, Chen Y-G. Specific activation of mitogen-activated protein kinase by transforming growth factor-beta receptors in lipid rafts is required for epithelial cell plasticity. *Mol Biol Cell*. 2009 Feb;20(3):1020–9.
24. Roeb E. Matrix metalloproteinases and liver fibrosis (translational aspects). *Matrix Biol*. 2018;68–69:463–73.
25. Hemmann S, Graf J, Roderfeld M, Roeb E. Expression of MMPs and TIMPs in liver fibrosis – a systematic review with special emphasis on anti-fibrotic strategies. *J Hepatol*. 2007;46(5):955–75.
26. Ramachandran P, Iredale JP. Reversibility of liver fibrosis. *Ann Hepatol*. 2009;8(4):283–91.

27. Murphy FR, Issa R, Zhou X, Ratnarajah S, Arthur MJP, Benyon C, et al. Inhibition of Apoptosis of Activated Hepatic Stellate Cells by Tissue Inhibitor of Metalloproteinase-1 Is Mediated via Effects on Matrix Metalloproteinase Inhibition: IMPLICATIONS FOR REVERSIBILITY OF LIVER FIBROSIS*. *J Biol Chem.* 2002;277(13):11069–76.
28. Viñas O, Bataller R, Sancho-Bru P, Ginès P, Berenguer C, Enrich C, et al. Human hepatic stellate cells show features of antigen-presenting cells and stimulate lymphocyte proliferation. *Hepatology.* 2003 Oct;38(4):919–29.
29. Elpek GÖ. Angiogenesis and liver fibrosis. *World J Hepatol.* 2015 Mar 27;7(3):377–91.
30. Kostallari E, Shah VH. Pericytes in the Liver. *Adv Exp Med Biol.* 2019;1122:153–67.
31. Tsukada S, Parsons CJ, Rippe RA. Mechanisms of liver fibrosis. *Clin Chim Acta.* 2006;364(1):33–60.
32. Rockey DC, Friedman SL. Fibrosis Regression After Eradication of Hepatitis C Virus: From Bench to Bedside. *Gastroenterology.* 2021 Apr;160(5):1502-1520.e1.
33. D'Ambrosio R, Aghemo A, Rumi MG, Ronchi G, Donato MF, Paradis V, et al. A morphometric and immunohistochemical study to assess the benefit of a sustained virological response in hepatitis C virus patients with cirrhosis. *Hepatology.* 2012 Aug;56(2):532–43.
34. Rockey DC. Liver Fibrosis Reversion After Suppression of Hepatitis B Virus. *Clin Liver Dis.* 2016 Nov;20(4):667–79.
35. Ramachandran P, Iredale JP, Fallowfield JA. Resolution of liver fibrosis: basic mechanisms and clinical relevance. *Semin Liver Dis.* 2015 May;35(2):119–31.
36. Wei L, Huang Y-H. Long-term outcomes in patients with chronic hepatitis C in the current era of direct-acting antiviral agents. *Expert Rev Anti Infect Ther.* 2019 May;17(5):311–25.
37. Desmet VJ, Roskams T. Cirrhosis reversal: a duel between dogma and myth. *J Hepatol.* 2004 May;40(5):860–7.
38. Friedman SL, Bansal MB. Reversal of hepatic fibrosis -- fact or fantasy? *Hepatology.* 2006 Feb;43(2 Suppl 1):S82-88.
39. Pei L, Melmed S. Isolation and characterization of a pituitary tumor-transforming gene (PTTG). *Mol Endocrinol.* 1997;11:433–41.

40. Moreno-Mateos MA, Espina ÁG, Torres B, Gámez del Estal MM, Romero-Franco A, Ríos RM, et al. PTTG1/securin modulates microtubule nucleation and cell migration. *Mol Biol Cell*. 2011 Nov;22(22):4302–11.
41. Han X, Poon RYC. Critical differences between isoforms of securin reveal mechanisms of separase regulation. *Mol Cell Biol*. 2013 Sep;33(17):3400–15.
42. Levy D, Ferreira MCMR, Reichert CO, de Almeida LV, Brocardo G, Lage LAPC, et al. Cell Cycle Changes, DNA Ploidy, and PTTG1 Gene Expression in HTLV-1 Patients. *Front Microbiol*. 2020; 11: 1778.
43. Vlotides G, Eigler T, Melmed S. Pituitary tumor-transforming gene: physiology and implications for tumorigenesis. *Endocr Rev*. 2007 Apr;28(2):165–86.
44. Kakar SS. Molecular cloning, genomic organization, and identification of the promoter for the human pituitary tumor transforming gene (PTTG). *Gene*. 1999 Nov;240(2):317–24.
45. Clem AL, Hamid T, Kakar SS. Characterization of the role of Sp1 and NF-Y in differential regulation of PTTG/securin expression in tumor cells. *Gene*. 2003 Dec;322:113–21.
46. Chen P-Y, Yen J-H, Kao R-H, Chen J-H. Down-regulation of the oncogene PTTG1 via the KLF6 tumor suppressor during induction of myeloid differentiation. *PLoS One*. 2013;8(8):e71282.
47. Hamid T, Kakar SS. PTTG and cancer. *Histol Histopathol*. 2003 Jan;18(1):245–51.
48. Pei L. Identification of c-myc as a down-stream target for pituitary tumor-transforming gene. *J Biol Chem*. 2001 Mar;276(11):8484–91.
49. Tong Y, Eigler T. Transcriptional targets for pituitary tumor-transforming gene-1. *J Mol Endocrinol*. 2009 Nov;43(5):179–85.
50. Wang Z, Yu R, Melmed S. Mice lacking pituitary tumor transforming gene show testicular and splenic hypoplasia, thymic hyperplasia, thrombocytopenia, aberrant cell cycle progression, and premature centromere division. *Mol Endocrinol*. 2001 Nov;15(11):1870–9.
51. Chien W, Pei L. A novel binding factor facilitates nuclear translocation and transcriptional activation function of the pituitary tumor-transforming gene product. *J Biol Chem*. 2000 Jun;275(25):19422–7.

52. Wang Z, Moro E, Kovacs K, Yu R, Melmed S. Pituitary tumor transforming gene-null male mice exhibit impaired pancreatic beta cell proliferation and diabetes. *Proc Natl Acad Sci U S A*. 2003 Mar;100(6):3428–32.
53. Wang Z, Melmed S. Characterization of the murine pituitary tumor transforming gene (PTTG) and its promoter. *Endocrinology*. 2000 Feb;141(2):763–71.
54. Sáez C, Japón MA, Ramos-Morales F, Romero F, Segura DI, Tortolero M, et al. hpttg is over-expressed in pituitary adenomas and other primary epithelial neoplasias. *Oncogene*. 1999 Sep;18(39):5473–6.
55. Li H, Yin C, Zhang B, Sun Y, Shi L, Liu N, et al. PTTG1 promotes migration and invasion of human non-small cell lung cancer cells and is modulated by miR-186. *Carcinogenesis*. 2013 Sep;34(9):2145–55.
56. Xiea Y, Wangb R. Pttg1 Promotes Growth of Breast Cancer through P27 Nuclear Exclusion. *Cell Physiol Biochem*. 2016;38(1):393–400.
57. Meng C, Zou Y, Hong W, Bao C, Jia X. Estrogen-regulated PTTG1 promotes breast cancer progression by regulating cyclin kinase expression. *Mol Med*. 2020 Apr;26(1):33.
58. Ren Q, Jin B. The clinical value and biological function of PTTG1 in colorectal cancer. *Biomed Pharmacother*. 2017 May;89:108–15.
59. Zheng Y, Guo J, Zhou J, Lu J, Chen Q, Zhang C, et al. FoxM1 transactivates PTTG1 and promotes colorectal cancer cell migration and invasion. *BMC Med Genomics*. 2015 Aug 12;8:49.
60. Ying H, Furuya F, Zhao L, Araki O, West BL, Hanover JA, et al. Aberrant accumulation of PTTG1 induced by a mutated thyroid hormone beta receptor inhibits mitotic progression. *J Clin Invest*. 2006 Nov;116(11):2972–84.
61. Panguluri SK, Yeakel C, Kakar SS. PTTG: an important target gene for ovarian cancer therapy. *J Ovarian Res*. 2008 Oct;1(1):6.
62. Genkai N, Homma J, Sano M, Tanaka R, Yamanaka R. Increased expression of pituitary tumor-transforming gene (PTTG)-1 is correlated with poor prognosis in glioma patients. *Oncol Rep*. 2006 Jun;15(6):1569–74.
63. Liang M, Chen X, Liu W, Li S, Li C, Jiang L, et al. Role of the pituitary tumor transforming gene 1 in the progression of hepatocellular carcinoma. *Cancer Biol Ther*. 2011 Feb;11(3):337–45.

64. Xiang W, Wu X, Huang C, Wang M, Zhao X, Luo G, et al. PTTG1 regulated by miR-146a-3p promotes bladder cancer migration, invasion, metastasis and growth. *Oncotarget*. 2017 Jan;8(1):664–78.
65. Fraune C, Yehorov S, Luebke AM, Steurer S, Hube-Magg C, Buscheck F, et al. Upregulation of PTTG1 is associated with poor prognosis in prostate cancer. *Pathol Int*. 2020 Apr;70(7):441–51.
66. Xu X, Cao L, Zhang Y, Yin Y, Hu X, Cui Y. Network analysis of DEGs and verification experiments reveal the notable roles of PTTG1 and MMP9 in lung cancer. *Oncol Lett*. 2018 Jan;15(1):257–63.
67. Ma K, Ma L, Jian Z. Pituitary tumor-transforming 1 expression in laryngeal cancer and its association with prognosis. *Oncol Lett*. 2018 Jul;16(1):1107–14.
68. Malik MT, Kakar SS. Regulation of angiogenesis and invasion by human Pituitary tumor transforming gene (PTTG) through increased expression and secretion of matrix metalloproteinase-2 (MMP-2). *Mol Cancer*. 2006 Nov;5:61.
69. Hu C, Huang W, Xiong N, Liu X. SP1-mediated transcriptional activation of PTTG1 regulates the migration and phenotypic switching of aortic vascular smooth muscle cells in aortic dissection through MAPK signaling. *Arch Biochem Biophys*. 2021 Oct;711:109007.
70. Cheng G, Liu X, Li P, Li Y. Down-regulation of PTTG1 suppresses PDGF-BB-induced proliferation, migration and extracellular matrix production of airway smooth muscle cells (ASMCs) by regulating PI3K/AKT/mTOR signaling pathway. *Mol Cell Toxicol*. 2021;17(4):485–92.
71. Thompson AD 3rd, Kakar SS. Insulin and IGF-1 regulate the expression of the pituitary tumor transforming gene (PTTG) in breast tumor cells. *FEBS Lett*. 2005 Jun;579(14):3195–200.
72. Tfelt-Hansen J, Schwarz P, Terwilliger EF, Brown EM, Chattopadhyay N. Calcium-sensing receptor induces messenger ribonucleic acid of human securin, pituitary tumor transforming gene, in rat testicular cancer. *Endocrinology*. 2003 Dec;144(12):5188–93.
73. Akino K, Akita S, Mizuguchi T, Takumi I, Yu R, Wang X, et al. A novel molecular marker of pituitary tumor transforming gene involves in a rat liver regeneration. *J Surg Res*. 2005 Nov;129(1):142–6.
74. Cho-Rok J, Yoo J, Jang YJ, Kim S, Chu I-S, Yeom Y Il, et al. Adenovirus-mediated transfer of siRNA against PTTG1 inhibits liver cancer cell growth in vitro and in vivo. *Hepatology*. 2006 May;43(5):1042–52.

75. Fujii T, Nomoto S, Koshikawa K, Yatabe Y, Teshigawara O, Mori T, et al. Overexpression of pituitary tumor transforming gene 1 in HCC is associated with angiogenesis and poor prognosis. *Hepatology*. 2006 Jun;43(6):1267–75.
76. Liang M, Liu J, Ji H, Chen M, Zhao Y, Li S, et al. A *Aconitum coreanum* polysaccharide fraction induces apoptosis of hepatocellular carcinoma (HCC) cells via pituitary tumor transforming gene 1 (PTTG1)-mediated suppression of the P13K/Akt and activation of p38 MAPK signaling pathway and displays antitumor. *Tumor Biol*. 2015;36(9):7085–91.
77. Huang J-L, Cao S-W, Ou Q-S, Yang B, Zheng S-H, Tang J, et al. The long non-coding RNA PTTG3P promotes cell growth and metastasis via up-regulating PTTG1 and activating PI3K/AKT signaling in hepatocellular carcinoma. *Mol Cancer*. 2018 May;17(1):93.
78. Lee UE, Ghiassi-Nejad Z, Paris AJ, Yea S, Narla G, Walsh M, et al. Tumor suppressor activity of KLF6 mediated by downregulation of the PTTG1 oncogene. *FEBS Lett*. 2010 Mar;584(5):1006–10.
79. Lin X, Yang Y, Guo Y, Liu H, Jiang J, Zheng F, et al. PTTG1 is involved in TNF- α -related hepatocellular carcinoma via the induction of c-myc. *Cancer Med*. 2019 Sep;8(12):5702–15.
80. Molina-Jimenez F, Benedicto I, Murata M, Martin-Vilchez S, Seki T, Antonio Pintor-Toro J, et al. Expression of pituitary tumor-transforming gene 1 (PTTG1)/securin in hepatitis B virus (HBV)-associated liver diseases: evidence for an HBV X protein-mediated inhibition of PTTG1 ubiquitination and degradation. *Hepatology*. 2010 Mar;51(3):777–87.
81. Buko V, Belonovskaya E, Naruta E, Lukivskaya O, Kanyuka O, Zhuk O, et al. Pituitary tumor transforming gene as a novel regulatory factor of liver fibrosis. *Life Sci*. 2015 Jul;132:34–40.
82. Espina AG, Méndez-Vidal C, Moreno-Mateos MA, Sáez C, Romero-Franco A, Japón MA, et al. Induction of Dlk1 by PTTG1 inhibits adipocyte differentiation and correlates with malignant transformation. *Mol Biol Cell*. 2009 Jul;20(14):3353–62.
83. Zhu N-L, Asahina K, Wang J, Ueno A, Lazaro R, Miyaoka Y, et al. Hepatic stellate cell-derived delta-like homolog 1 (DLK1) protein in liver regeneration. *J Biol Chem*. 2012 Mar 23;287(13):10355–67.
84. Falix FA, Tjon-A-Loi MRS, Gaemers IC, Aronson DC, Lamers WH. DLK1 Protein Expression during Mouse Development Provides New Insights into Its Function. Belousov L V, Lardelli M, editors. *ISRN Dev Biol*. 2013;2013.

85. Buccarelli M, Lulli V, Giuliani A, Signore M, Martini M, D'Alessandris QG, et al. Deregulated expression of the imprinted DLK1-DIO3 region in glioblastoma stemlike cells: tumor suppressor role of lncRNA MEG3. *Neuro Oncol.* 2020 Dec 1;22(12):1771–84.
86. da Rocha ST, Edwards CA, Ito M, Ogata T, Ferguson-Smith AC. Genomic imprinting at the mammalian Dlk1-Dio3 domain. *Trends Genet.* 2008 Jun;24(6):306–16.
87. Lu H-P, Lin C-J, Chen W-C, Chang Y-J, Lin S-W, Wang H-H, et al. TRIM28 Regulates Dlk1 Expression in Adipogenesis. *Int J Mol Sci.* 2020 Sep 30;21(19):7245.
88. Li D, Yea S, Li S, Chen Z, Narla G, Banck M, et al. Krüppel-like factor-6 promotes preadipocyte differentiation through histone deacetylase 3-dependent repression of DLK1. *J Biol Chem.* 2005 Jul;280(29):26941–52.
89. Falix FA, Aronson DC, Lamers WH, Gaemers IC. Possible roles of DLK1 in the Notch pathway during development and disease. *Biochim Biophys Acta - Mol Basis Dis.* 2012;1822(6):988–95.
90. Pittaway JFH, Lipsos C, Mariniello K, Guasti L. The role of delta-like non-canonical Notch ligand 1 (DLK1) in cancer. *Endocr Relat Cancer.* 2021 Oct;28(12):R271–87.
91. Smas CM, Chen L, Sul HS. Cleavage of membrane-associated pref-1 generates a soluble inhibitor of adipocyte differentiation. *Mol Cell Biol.* 1997 Feb;17(2):977–88.
92. Liem IK, Indriyanoles of DLK1 in Liver Development and Oncogenesis, Adnindya MR, Nasution AA. Roles of DLK1 in Liver Development and Oncogenesis. *Online J Biol Sci.* 2017 Oct 23;17(4):309–15.
93. Traustadóttir GÁ, Lagoni LV, Ankerstjerne LBS, Bisgaard HC, Jensen CH, Andersen DC. The imprinted gene Delta like non-canonical Notch ligand 1 (Dlk1) is conserved in mammals, and serves a growth modulatory role during tissue development and regeneration through Notch dependent and independent mechanisms. *Cytokine Growth Factor Rev.* 2019;46:17–27.
94. Surmacz B, Noisa P, Risner-Janiczek JR, Hui K, Ungless M, Cui W, et al. DLK1 promotes neurogenesis of human and mouse pluripotent stem cell-derived neural progenitors via modulating Notch and BMP signalling. *Stem cell Rev reports.* 2012 Jun;8(2):459–71.
95. Abdallah BM, Ditzel N, Mahmood A, Isa A, Traustadottir GA, Schilling AF, et al. DLK1 is a novel regulator of bone mass that mediates estrogen deficiency-

- induced bone loss in mice. *J bone Miner Res Off J Am Soc Bone Miner Res.* 2011 Jul;26(7):1457–71.
96. Mitterberger MC, Lechner S, Mattesich M, Kaiser A, Probst D, Wenger N, et al. DLK1(PREF1) is a negative regulator of adipogenesis in CD105+/CD90+/CD34+/CD31-/FABP4- adipose-derived stromal cells from subcutaneous abdominal fat pats of adult women. *Stem Cell Res.* 2012 Jul;9(1):35–48.
97. Moon YS, Smas CM, Lee K, Villena JA, Kim K-H, Yun EJ, et al. Mice lacking paternally expressed Pref-1/Dlk1 display growth retardation and accelerated adiposity. *Mol Cell Biol.* 2002 Aug;22(15):5585–92.
98. Charalambous M, Da Rocha ST, Radford EJ, Medina-Gomez G, Curran S, Pinnock SB, et al. DLK1/PREF1 regulates nutrient metabolism and protects from steatosis. *Proc Natl Acad Sci.* 2014 Nov 11;111(45):16088–93.
99. Jensen CH, Kosmina R, Rydén M, Baun C, Hvidsten S, Andersen MS, et al. The imprinted gene Delta like non-canonical notch ligand 1 (Dlk1) associates with obesity and triggers insulin resistance through inhibition of skeletal muscle glucose uptake. *EBioMedicin.* 2019 Aug 1;46:368–80.
100. Begum A, Kim Y, Lin Q, Yun Z. DLK1, delta-like 1 homolog (Drosophila), regulates tumor cell differentiation in vivo. *Cancer Lett.* 2012 May;318(1):26–33.
101. Yin D, Xie D, Sakajiri S, Miller CW, Zhu H, Popoviciu ML, et al. DLK1: increased expression in gliomas and associated with oncogenic activities. *Oncogene.* 2006 Mar;25(13):1852–61.
102. Xu X, Liu R-F, Zhang X, Huang L-Y, Chen F, Fei Q-L, et al. DLK1 as a potential target against cancer stem/progenitor cells of hepatocellular carcinoma. *Mol Cancer Ther.* 2012 Mar;11(3):629–38.
103. Ceder JA, Jansson L, Helczynski L, Abrahamsson P-A. Delta-like 1 (Dlk-1), a novel marker of prostate basal and candidate epithelial stem cells, is downregulated by notch signalling in intermediate/transit amplifying cells of the human prostate. *Eur Urol.* 2008 Dec;54(6):1344–53.
104. Li L, Tan J, Zhang Y, Han N, Di X, Xiao T, et al. DLK1 promotes lung cancer cell invasion through upregulation of MMP9 expression depending on Notch signaling. *PLoS One.* 2014;9(3):e91509.
105. Lin Q, Yun Z. Impact of the hypoxic tumor microenvironment on the regulation of cancer stem cell characteristics. *Cancer Biol Ther.* 2010 Jun;9(12):949–56.

106. Kim Y, Lin Q, Zelterman D, Yun Z. Hypoxia-regulated delta-like 1 homologue enhances cancer cell stemness and tumorigenicity. *Cancer Res.* 2009 Dec;69(24):9271–80.
107. Grassi ES, Pantazopoulou V, Pietras A. Hypoxia-induced release, nuclear translocation, and signaling activity of a DLK1 intracellular fragment in glioma. *Oncogene.* 2020 May;39(20):4028–44.
108. Lee Y-H, Yun MR, Kim HM, Jeon BH, Park B-C, Lee B-W, et al. Exogenous administration of DLK1 ameliorates hepatic steatosis and regulates gluconeogenesis via activation of AMPK. *Int J Obes (Lond).* 2016 Feb;40(2):356–65.
109. Li H, Cui M, Chen T, Xie H, Cui Y, Tu H, et al. Serum DLK1 is a potential prognostic biomarker in patients with hepatocellular carcinoma. *Tumour Biol J Int Soc Oncodevelopmental Biol Med.* 2015 Nov;36(11):8399–404.
110. Cai C-M, Xiao X, Wu B-H, Wei B-F, Han Z-G. Targeting endogenous DLK1 exerts antitumor effect on hepatocellular carcinoma through initiating cell differentiation. *Oncotarget.* 2016 Nov;7(44):71466–76.
111. Huang J, Zhang X, Zhang M, Zhu J-D, Zhang Y-L, Lin Y, et al. Up-regulation of DLK1 as an imprinted gene could contribute to human hepatocellular carcinoma. *Carcinogenesis.* 2007 May 1;28(5):1094–103.
112. Pan R-L, Wang P, Xiang L-X, Shao J-Z. Delta-like 1 serves as a new target and contributor to liver fibrosis down-regulated by mesenchymal stem cell transplantation. *J Biol Chem.* 2011 Apr;286(14):12340–8.
113. Ramakrishna G, Rastogi A, Trehanpati N, Sen B, Khosla R, Sarin SK. From cirrhosis to hepatocellular carcinoma: new molecular insights on inflammation and cellular senescence. *Liver cancer.* 2013 Aug;2(3–4):367–83.
114. D'Amico G, Bernardi M, Angeli P. Towards a new definition of decompensated cirrhosis. *J Hepatol.* 2022 Jan;76(1):202–7.
115. EASL Clinical Practice Guidelines for the management of patients with decompensated cirrhosis. *J Hepatol.* 2018 Aug;69(2):406–60.
116. Nusrat S, Khan MS, Fazili J, Madhoun MF. Cirrhosis and its complications: evidence based treatment. *World J Gastroenterol.* 2014 May;20(18):5442–60.
117. Shetty A, Jun Yum J, Saab S. The Gastroenterologist's Guide to Preventive Management of Compensated Cirrhosis. *Gastroenterol Hepatol (N Y).* 2019 Aug;15(8):423–30.

118. Iwakiri Y, Trebicka J. Portal hypertension in cirrhosis: Pathophysiological mechanisms and therapy. *JHEP reports Innov Hepatol.* 2021 Aug;3(4):100316.
119. Buob S, Johnston AN, Webster CRL. Portal Hypertension: Pathophysiology, Diagnosis, and Treatment. *J Vet Intern Med.* 2011 Mar 1;25(2):169–86.
120. Suk KT. Hepatic venous pressure gradient: clinical use in chronic liver disease. *Clin Mol Hepatol.* 2014 Mar;20(1):6–14.
121. D’Amico G, Morabito A, D’Amico M, Pasta L, Malizia G, Rebora P, et al. Clinical states of cirrhosis and competing risks. *J Hepatol.* 2018 Mar;68(3):563–76.
122. Pillai AK, Andring B, Patel A, Trimmer C, Kalva SP. Portal hypertension: a review of portosystemic collateral pathways and endovascular interventions. *Clin Radiol.* 2015 Oct;70(10):1047–59.
123. Fernández-Varo G, Ros J, Morales-Ruiz M, Cejudo-Martín P, Arroyo V, Solé M, et al. Nitric oxide synthase 3-dependent vascular remodeling and circulatory dysfunction in cirrhosis. *Am J Pathol.* 2003 Jun;162(6):1985–93.
124. Tsochatzis EA, Bosch J, Burroughs AK. Liver cirrhosis. *Lancet.* 2014 May;383(9930):1749–61.
125. Kim MY, Baik SK, Lee SS. Hemodynamic alterations in cirrhosis and portal hypertension. *Korean J Hepatol.* 2010 Dec;16(4):347–52.
126. Ginès P, Cárdenas A, Arroyo V, Rodés J. Management of cirrhosis and ascites. *N Engl J Med.* 2004 Apr;350(16):1646–54.
127. Martin PY, Ginès P, Schrier RW. Nitric oxide as a mediator of hemodynamic abnormalities and sodium and water retention in cirrhosis. *N Engl J Med.* 1998 Aug;339(8):533–41.
128. Arroyo V. Pathophysiology, diagnosis and treatment of ascites in cirrhosis. *Ann Hepatol.* 2002;1(2):72–9.
129. Ng CKF, Chan MHM, Tai MHL, Lam CWK. Hepatorenal syndrome. *Clin Biochem Rev.* 2007 Feb;28(1):11–7.
130. Crismale JF, Friedman SL. Acute Liver Injury and Decompensated Cirrhosis. *Med Clin North Am.* 2020 Jul;104(4):647–62.
131. Schuppan D, Afdhal NH. Liver cirrhosis. *Lancet.* 2008;371(9615):838–51.

132. Rodrigues SG, Mendoza YP, Bosch J. Beta-blockers in cirrhosis: Evidence-based indications and limitations. *JHEP reports Innov Hepatol.* 2020 Feb;2(1):100063.
133. Langer DA, Shah VH. Nitric oxide and portal hypertension: interface of vasoreactivity and angiogenesis. *J Hepatol.* 2006 Jan;44(1):209–16.
134. McNaughton L, Puttagunta L, Martinez-Cuesta MA, Kneteman N, Mayers I, Moqbel R, et al. Distribution of nitric oxide synthase in normal and cirrhotic human liver. *Proc Natl Acad Sci.* 2002 Dec 24;99(26):17161 LP – 17166.
135. Gross SS. Nitric Oxide Synthases and Their Cofactors. In: Goligorsky MS, Gross SS, editors. *Nitric Oxide and the Kidney: Physiology and Pathophysiology.* Boston, MA: Springer US; 1997. p. 52–65.
136. Wiest R, Groszmann RJ. The paradox of nitric oxide in cirrhosis and portal hypertension: too much, not enough. *Hepatology.* 2002 Feb;35(2):478–91.
137. Leung T-M, Tipoe GL, Liong EC, Lau TYH, Fung M-L, Nanji AA. Endothelial nitric oxide synthase is a critical factor in experimental liver fibrosis. *Int J Exp Pathol.* 2008 Aug;89(4):241–50.
138. Diesen DL, Kuo PC. Nitric oxide and redox regulation in the liver: Part I. General considerations and redox biology in hepatitis. *J Surg Res.* 2010 Jul;162(1):95–109.
139. Morales-Ruiz M, Jiménez W, Pérez-Sala D, Ros J, Leivas A, Lamas S, et al. Increased nitric oxide synthase expression in arterial vessels of cirrhotic rats with ascites. *Hepatology.* 1996 Dec;24(6):1481–6.
140. Schilling K, Opitz N, Wiesenthal A, Oess S, Tikkanen R, Müller-Esterl W, et al. Translocation of endothelial nitric-oxide synthase involves a ternary complex with caveolin-1 and NOSTRIN. *Mol Biol Cell.* 2006 Sep;17(9):3870–80.
141. Hu LS, George J, Wang JH. Current concepts on the role of nitric oxide in portal hypertension. *World J Gastroenterol.* 2013 Mar;19(11):1707–17.
142. Stamler JS, Lamas S, Fang FC. Nitrosylation. the prototypic redox-based signaling mechanism. *Cell.* 2001 Sep;106(6):675–83.
143. Morales-Ruiz M, Rodríguez-Vita J, Ribera J, Jiménez W. Pathophysiology of Portal Hypertension. Lanzer P, editor. *PanVascular Med.* 2015 Jan 23;3631–65.

144. Morales-Ruiz M, Cejudo-Martín P, Fernández-Varo G, Tugues S, Ros J, Angeli P, et al. Transduction of the liver with activated Akt normalizes portal pressure in cirrhotic rats. *Gastroenterology*. 2003 Aug;125(2):522–31.
145. Perri RE, Langer DA, Chatterjee S, Gibbons SJ, Gadgil J, Cao S, et al. Defects in cGMP-PKG pathway contribute to impaired NO-dependent responses in hepatic stellate cells upon activation. *Am J Physiol Liver Physiol*. 2006 Mar 1;290(3):G535–42.
146. Angeli P, Fernández-Varo G, Dalla Libera V, Fasolato S, Galioto A, Arroyo V, et al. The role of nitric oxide in the pathogenesis of systemic and splanchnic vasodilation in cirrhotic rats before and after the onset of ascites. *Liver Int Off J Int Assoc Study Liver*. 2005 Apr;25(2):429–37.
147. Guarner C, Soriano G, Tomas A, Bulbena O, Novella MT, Balanzo J, et al. Increased serum nitrite and nitrate levels in patients with cirrhosis: relationship to endotoxemia. *Hepatology*. 1993 Nov;18(5):1139–43.
148. Fernandez M, Vizzutti F, Garcia-Pagan JC, Rodes J, Bosch J. Anti-VEGF receptor-2 monoclonal antibody prevents portal-systemic collateral vessel formation in portal hypertensive mice. *Gastroenterology*. 2004 Mar;126(3):886–94.
149. Bolognesi M, Di Pascoli M, Verardo A, Gatta A. Splanchnic vasodilation and hyperdynamic circulatory syndrome in cirrhosis. *World J Gastroenterol*. 2014 Mar;20(10):2555–63.
150. Wiest R, Das S, Cadelina G, Garcia-Tsao G, Milstien S, Groszmann RJ. Bacterial translocation in cirrhotic rats stimulates eNOS-derived NO production and impairs mesenteric vascular contractility. *J Clin Invest*. 1999 Nov;104(9):1223–33.
151. Ho H-L, Huang H-C. Molecular mechanisms of circulatory dysfunction in cirrhotic portal hypertension. *J Chin Med Assoc*. 2015 Apr;78(4):195–203.
152. Ahmed F, Perz JF, Kwong S, Jamison PM, Friedman C, Bell BP. National trends and disparities in the incidence of hepatocellular carcinoma, 1998-2003. *Prev Chronic Dis*. 2008 Jul;5(3):A74.
153. Bray F, Ferlay J, Soerjomataram I, Siegel RL, Torre LA, Jemal A. Global cancer statistics 2018: GLOBOCAN estimates of incidence and mortality worldwide for 36 cancers in 185 countries. *CA Cancer J Clin*. 2018 Nov 1;68(6):394–424.
154. Baecker A, Liu X, La Vecchia C, Zhang Z-F. Worldwide incidence of hepatocellular carcinoma cases attributable to major risk factors. *Eur J cancer Prev Off J Eur Cancer Prev Organ*. 2018 May;27(3):205–12.

155. Llovet JM, Kelley RK, Villanueva A, Singal AG, Pikarsky E, Roayaie S, et al. Hepatocellular carcinoma. *Nat Rev Dis Prim.* 2021;7(1):6.
156. Craig AJ, von Felden J, Garcia-Lezana T, Sarcognato S, Villanueva A. Tumour evolution in hepatocellular carcinoma. *Nat Rev Gastroenterol Hepatol.* 2020;17(3):139–52.
157. Reig M, Forner A, Ávila MA, Ayuso C, Mínguez B, Varela M, et al. Diagnosis and treatment of hepatocellular carcinoma. Update of the consensus document of the AEEH, AEC, SEOM, SERAM, SERVEI, and SETH. Vol. 156, *Medicina clinica.* Spain; 2021. p. 463.e1-463.e30.
158. Bialecki ES, Di Bisceglie AM. Diagnosis of hepatocellular carcinoma. *HPB (Oxford).* 2005;7(1):26–34.
159. Villanueva A. Hepatocellular Carcinoma. *N Engl J Med.* 2019 Apr;380(15):1450–62.
160. Bai D-S, Zhang C, Chen P, Jin S-J, Jiang G-Q. The prognostic correlation of AFP level at diagnosis with pathological grade, progression, and survival of patients with hepatocellular carcinoma. *Sci Rep.* 2017;7(1):12870.
161. Forner A, Reig M, Bruix J. Hepatocellular carcinoma. *Lancet.* 2018 Mar;391(10127):1301–14.
162. Bishayee A. The role of inflammation and liver cancer. *Adv Exp Med Biol.* 2014;816:401–35.
163. Kim E, Viatour P. Hepatocellular carcinoma: old friends and new tricks. *Exp Mol Med.* 2020;52(12):1898–907.
164. Keating GM, Santoro A. Sorafenib: A Review of Its Use in Advanced Hepatocellular Carcinoma. *Drugs.* 2009;69(2):223–40.
165. Liu M, Jiang L, Guan X-Y. The genetic and epigenetic alterations in human hepatocellular carcinoma: a recent update. *Protein Cell.* 2014 Sep;5(9):673–91.
166. Nault J-C. Pathogenesis of hepatocellular carcinoma according to aetiology. *Best Pract Res Clin Gastroenterol.* 2014;28(5):937–47.
167. Müller M, Bird TG, Nault J-C. The landscape of gene mutations in cirrhosis and hepatocellular carcinoma. *J Hepatol.* 2020 May;72(5):990–1002.
168. Zucman-Rossi J, Villanueva A, Nault J-C, Llovet JM. Genetic Landscape and Biomarkers of Hepatocellular Carcinoma. *Gastroenterology.* 2015 Oct;149(5):1226-1239.e4.

169. Schulze K, Imbeaud S, Letouzé E, Alexandrov LB, Calderaro J, Rebouissou S, et al. Exome sequencing of hepatocellular carcinomas identifies new mutational signatures and potential therapeutic targets. *Nat Genet.* 2015 May;47(5):505–11.
170. Nault J-C, Ningarhari M, Rebouissou S, Zucman-Rossi J. The role of telomeres and telomerase in cirrhosis and liver cancer. *Nat Rev Gastroenterol Hepatol.* 2019;16(9):544–58.
171. Yang JD, Hainaut P, Gores GJ, Amadou A, Plymoth A, Roberts LR. A global view of hepatocellular carcinoma: trends, risk, prevention and management. *Nat Rev Gastroenterol Hepatol.* 2019 Oct;16(10):589–604.
172. Toh TB, Lim JJ, Chow EK-H. Epigenetics of hepatocellular carcinoma. *Clin Transl Med.* 2019 May 6;8(1):13.
173. Wahid B, Ali A, Rafique S, Idrees M. New Insights into the Epigenetics of Hepatocellular Carcinoma. Scartozzi M, editor. *Biomed Res Int.* 2017;2017:1609575.
174. Schulze K, Nault J-C, Villanueva A. Genetic profiling of hepatocellular carcinoma using next-generation sequencing. *J Hepatol.* 2016 Nov;65(5):1031–42.
175. Yu L-X, Ling Y, Wang H-Y. Role of nonresolving inflammation in hepatocellular carcinoma development and progression. *npj Precis Oncol.* 2018;2(1):6.
176. Waris G, Ahsan H. Reactive oxygen species: role in the development of cancer and various chronic conditions. *J Carcinog.* 2006 May;5:14.
177. Roberts SM, Kehrer JP, Klotz L-O. *Studies on Experimental Toxicology and Pharmacology.* 1st ed. Roberts SM, Kehrer JP, Klotz L-O, editors. Switzerland: Humana Press; 2015. 498 p.
178. Yin H. The role of lipid peroxidation during the progression of human hepatocellular carcinoma (HCC). *Free Radic Biol Med.* 2018;124:563–4.
179. Cichoż-Lach H, Michalak A. Oxidative stress as a crucial factor in liver diseases. *World J Gastroenterol.* 2014;20(25):8082–91.
180. Bian J, Lin J, Long J, Yang X, Yang X, Lu X, et al. T lymphocytes in hepatocellular carcinoma immune microenvironment: insights into human immunology and immunotherapy. *Am J Cancer Res.* 2020;10(12):4585–606.
181. Tian Z, Hou X, Liu W, Han Z, Wei L. Macrophages and hepatocellular carcinoma. *Cell Biosci.* 2019;9:79.

182. Capece D, Fischietti M, Verzella D, Gaggiano A, Ciccirelli G, Tessitore A, et al. The Inflammatory Microenvironment in Hepatocellular Carcinoma: A Pivotal Role for Tumor-Associated Macrophages. Vazquez E, editor. *Biomed Res Int*. 2013;2013:187204.
183. Shirabe K, Mano Y, Muto J, Matono R, Motomura T, Toshima T, et al. Role of tumor-associated macrophages in the progression of hepatocellular carcinoma. *Surg Today*. 2012;42(1):1–7.
184. Lin C-A, Chang L-L, Zhu H, He Q-J, Yang B. Hypoxic microenvironment and hepatocellular carcinoma treatment. *Hepatoma Res*. 2018;4:26.
185. Refolo MG, Messa C, Guerra V, Carr BI, D'Alessandro R. Inflammatory Mechanisms of HCC Development. *Cancers (Basel)*. 2020 Mar;12(3).
186. Morse MA, Sun W, Kim R, He AR, Abada PB, Mynderse M, et al. The Role of Angiogenesis in Hepatocellular Carcinoma. *Clin cancer Res an Off J Am Assoc Cancer Res*. 2019 Feb;25(3):912–20.
187. Pang RWC, Joh JW, Johnson PJ, Monden M, Pawlik TM, Poon RTP. Biology of hepatocellular carcinoma. *Ann Surg Oncol*. 2008 Apr;15(4):962–71.
188. Kalluri R, Weinberg RA. The basics of epithelial-mesenchymal transition. *J Clin Invest*. 2009 Jun;119(6):1420–8.
189. Zhang Q, Liu L, Gong C, Shi H, Zeng Y, Wang X, et al. Prognostic significance of tumor-associated macrophages in solid tumor: a meta-analysis of the literature. *PLoS One*. 2012;7(12):e50946.
190. Ding W, Tan Y, Qian Y, Xue W, Wang Y, Jiang P, et al. Clinicopathologic and prognostic significance of tumor-associated macrophages in patients with hepatocellular carcinoma: A meta-analysis. *PLoS One*. 2019 Oct 16;14(10):e0223971.
191. Wu Y, Zhang J, Zhang X, Zhou H, Liu G, Li Q. Cancer Stem Cells: A Potential Breakthrough in HCC-Targeted Therapy. *Front Pharmacol*. 2020; 11: 198.
192. Sevic I, Spinelli FM, Cantero MJ, Reszegi A, Kovalszky I, García MG, et al. The Role of the Tumor Microenvironment in the Development and Progression of Hepatocellular Carcinoma. In: JEE T-P, editor. *Hepatocellular Carcinoma*. Brisbane: Codon Publications; 2019.
193. Wirth T, Parker N, Ylä-Herttuala S. History of gene therapy. *Gene*. 2013 Aug;525(2):162–9.

194. Ramamoorth M, Narvekar A. Non viral vectors in gene therapy- an overview. *J Clin Diagn Res.* 2015 Jan;9(1):GE01-6.
195. Tang R, Xu Z. Gene therapy: a double-edged sword with great powers. *Mol Cell Biochem.* 2020 Nov;474(1-2):73-81.
196. Raper SE, Chirmule N, Lee FS, Wivel NA, Bagg A, Gao G, et al. Fatal systemic inflammatory response syndrome in a ornithine transcarbamylase deficient patient following adenoviral gene transfer. *Mol Genet Metab.* 2003;80(1-2):148-58.
197. Hacein-Bey-Abina S, von Kalle C, Schmidt M, Le Deist F, Wulffraat N, McIntyre E, et al. A Serious Adverse Event after Successful Gene Therapy for X-Linked Severe Combined Immunodeficiency. *N Engl J Med.* 2003 Jan 16;348(3):255-6.
198. Lundstrom K. *Viral Vectors in Gene Therapy.* Dis (Basel, Switzerland). 2018 May;6(2):42.
199. Bulcha JT, Wang Y, Ma H, Tai PWL, Gao G. Viral vector platforms within the gene therapy landscape. *Signal Transduct Target Ther.* 2021;6(1):53.
200. Ylä-Herttuala S. Endgame: glybera finally recommended for approval as the first gene therapy drug in the European union. *Mol Ther.* 2012 Oct;20(10):1831-2.
201. Prado DA, Acosta-Acero M, Maldonado RS. Gene therapy beyond luxturna: a new horizon of the treatment for inherited retinal disease. *Curr Opin Ophthalmol.* 2020 May;31(3):147-54.
202. Schuessler-Lenz M, Enzmann H, Vamvakas S. Regulators' Advice Can Make a Difference: European Medicines Agency Approval of Zynteglo for Beta Thalassemia. *Clin Pharmacol Ther.* 2020 Mar;107(3):492-4.
203. Han D, Xu Z, Zhuang Y, Ye Z, Qian Q. Current Progress in CAR-T Cell Therapy for Hematological Malignancies. *J Cancer.* 2021;12(2):326-34.
204. Riva L, Petrini C. A few ethical issues in translational research for gene and cell therapy. *J Transl Med.* 2019;17(1):395.
205. Delhove J, Osenk I, Prichard I, Donnelley M. Public Acceptability of Gene Therapy and Gene Editing for Human Use: A Systematic Review. *Hum Gene Ther.* 2019 Dec 5;31(1-2):20-46.
206. Dana H, Chalbatani GM, Mahmoodzadeh H, Karimloo R, Rezaiean O, Moradzadeh A, et al. Molecular Mechanisms and Biological Functions of siRNA. *Int J Biomed Sci.* 2017 Jun;13(2):48-57.

207. Thomas CE, Ehrhardt A, Kay MA. Progress and problems with the use of viral vectors for gene therapy. *Nat Rev Genet.* 2003;4(5):346–58.
208. Mellott AJ, Forrest ML, Detamore MS. Physical non-viral gene delivery methods for tissue engineering. *Ann Biomed Eng.* 2013 Mar;41(3):446–68.
209. Patil S, Gao Y-G, Lin X, Li Y, Dang K, Tian Y, et al. The Development of Functional Non-Viral Vectors for Gene Delivery. *Int J Mol Sci.* 2019 Nov;20(21).
210. De Haan P, Van Diemen FR, Toscano MG. Viral gene delivery vectors: the next generation medicines for immune-related diseases. *Hum Vaccin Immunother.* 2021 Jan;17(1):14–21.
211. Flotte TR. Gene Therapy Progress and Prospects: Recombinant adeno-associated virus (rAAV) vectors. *Gene Ther.* 2004;11(10):805–10.
212. Zu H, Gao D. Non-viral Vectors in Gene Therapy: Recent Development, Challenges, and Prospects. *AAPS J.* 2021;23(4):78.
213. Maestro S, Weber ND, Zabaleta N, Aldabe R, Gonzalez-Aseguinolaza G. Novel vectors and approaches for gene therapy in liver diseases. *JHEP Reports.* 2021;3(4):100300.
214. Loh XJ, Lee T-C, Dou Q, Deen GR. Utilising inorganic nanocarriers for gene delivery. *Biomater Sci.* 2016;4(1):70–86.
215. Sainz-Ramos M, Gallego I, Villate-Beitia I, Zarate J, Maldonado I, Puras G, et al. How Far Are Non-Viral Vectors to Come of Age and Reach Clinical Translation in Gene Therapy? *Int J Mol Sci.* 2021 Jul 14;22(14):7545.
216. Williams PD, Kingston PA. Plasmid-mediated gene therapy for cardiovascular disease. *Cardiovasc Res.* 2011 Sep 1;91(4):565–76.
217. Gill DR, Pringle IA, Hyde SC. Progress and Prospects: The design and production of plasmid vectors. *Gene Ther.* 2009;16(2):165–71.
218. Tang X, Zhang S, Fu R, Zhang L, Huang K, Peng H, et al. Therapeutic Prospects of mRNA-Based Gene Therapy for Glioblastoma. *Front Oncol.* 2019 Nov 8;9:1208.
219. Tavernier G, Andries O, Demeester J, Sanders NN, De Smedt SC, Rejman J. mRNA as gene therapeutic: how to control protein expression. *J Control Release.* 2011 Mar;150(3):238–47.

220. Meng Z, O’Keeffe-Ahern J, Lyu J, Pierucci L, Zhou D, Wang W. A new developing class of gene delivery: messenger RNA-based therapeutics. *Biomater Sci*. 2017 Nov;5(12):2381–92.
221. Thijssen MF, Brüggewirth IMA, Gillooly A, Khvorova A, Kowalik TF, Martins PN. Gene Silencing With siRNA (RNA Interference): A New Therapeutic Option During Ex Vivo Machine Liver Perfusion Preservation. *Liver Transplant*. 2019 Jan 1;25(1):140–51.
222. Dong Y, Siegwart DJ, Anderson DG. Strategies, design, and chemistry in siRNA delivery systems. *Adv Drug Deliv Rev*. 2019 Apr;144:133–47.
223. Nikam RR, Gore KR. Journey of siRNA: Clinical Developments and Targeted Delivery. *Nucleic Acid Ther*. 2018 Mar 27;28(4):209–24.
224. Majumdar R, Rajasekaran K, Cary JW. RNA Interference (RNAi) as a Potential Tool for Control of Mycotoxin Contamination in Crop Plants: Concepts and Considerations. *Front Plant Sci*. 2017 Feb 14;8:200.
225. Hu P-F, Xie W-F. Targeted RNA interference for hepatic fibrosis. *Expert Opin Biol Ther*. 2009 Oct;9(10):1305–12.
226. Nguyen TH, Ferry N. Liver gene therapy: advances and hurdles. *Gene Ther*. 2004;11(1):S76–84.
227. Snoeys J, Mertens G, Lievens J, van Berkel T, Collen D, Biessen EAL, et al. Lipid emulsions potently increase transgene expression in hepatocytes after adenoviral transfer. *Mol Ther*. 2006 Jan;13(1):98–107.
228. Kim K-H, Park K-K. Small RNA- and DNA-based gene therapy for the treatment of liver cirrhosis, where we are? *World J Gastroenterol*. 2014 Oct;20(40):14696–705.
229. Cabanes-Creus M, Hallwirth C V, Westhaus A, Ng BH, Liao SHY, Zhu E, et al. Restoring the natural tropism of AAV2 vectors for human liver. *Sci Transl Med*. 2020 Sep;12(560).
230. Jacobs F, Gordts SC, Muthuramu I, De Geest B. The liver as a target organ for gene therapy: state of the art, challenges, and future perspectives. *Pharmaceuticals (Basel)*. 2012 Dec;5(12):1372–92.
231. Bartneck M, Warzecha KT, Tacke F. Therapeutic targeting of liver inflammation and fibrosis by nanomedicine. *Hepatobiliary Surg Nutr*. 2014 Dec;3(6):364–76.

232. Duong HTT, Dong Z, Su L, Boyer C, George J, Davis TP, et al. The use of nanoparticles to deliver nitric oxide to hepatic stellate cells for treating liver fibrosis and portal hypertension. *Small*. 2015 May;11(19):2291–304.
233. Wang K, Shang F, Chen D, Cao T, Wang X, Jiao J, et al. Protein liposomes-mediated targeted acetylcholinesterase gene delivery for effective liver cancer therapy. *J Nanobiotechnology*. 2021;19(1):31.
234. Azzam M, El Safy S, Abdelgelil SA, Weiskirchen R, Asimakopoulou A, de Lorenzi F, et al. Targeting Activated Hepatic Stellate Cells Using Collagen-Binding Chitosan Nanoparticles for siRNA Delivery to Fibrotic Livers. *Pharmaceutics*. 2020 Jun;12(6):590.
235. Alonso S. Exploiting the bioengineering versatility of lactobionic acid in targeted nanosystems and biomaterials. *J Control Release*. 2018 Oct;287:216–34.
236. Soares S, Sousa J, Pais A, Vitorino C. Nanomedicine: Principles, Properties, and Regulatory Issues. *Front Chem*. 2018 Aug 20;6:360
237. Wang H, Thorling CA, Liang X, Bridle KR, Grice JE, Zhu Y, et al. Diagnostic imaging and therapeutic application of nanoparticles targeting the liver. *J Mater Chem B*. 2015 Feb;3(6):939–58.
238. Kim BYS, Rutka JT, Chan WCW. Nanomedicine. *N Engl J Med*. 2010 Dec;363(25):2434–43.
239. Donahue ND, Acar H, Wilhelm S. Concepts of nanoparticle cellular uptake, intracellular trafficking, and kinetics in nanomedicine. *Adv Drug Deliv Rev*. 2019;143:68–96.
240. Behzadi S, Serpooshan V, Tao W, Hamaly MA, Alkawareek MY, Dreaden EC, et al. Cellular uptake of nanoparticles: journey inside the cell. *Chem Soc Rev*. 2017 Jul 17;46(14):4218–44.
241. Rampado R, Crotti S, Caliceti P, Pucciarelli S, Agostini M. Recent Advances in Understanding the Protein Corona of Nanoparticles and in the Formulation of “Stealthy” Nanomaterials. *Front Bioeng Biotechnol*. 2020 Apr 3;8:166.
242. Cataldi M, Vigliotti C, Mosca T, Cammarota M, Capone D. Emerging Role of the Spleen in the Pharmacokinetics of Monoclonal Antibodies, Nanoparticles and Exosomes. *Int J Mol Sci*. 2017 Jun;18(6).
243. Zhang Y-N, Poon W, Tavares AJ, McGilvray ID, Chan WCW. Nanoparticle–liver interactions: Cellular uptake and hepatobiliary elimination. *J Control Release*. 2016;240:332–48.

244. Tsoi KM, MacParland SA, Ma X-Z, Spetzler VN, Echeverri J, Ouyang B, et al. Mechanism of hard-nanomaterial clearance by the liver. *Nat Mater*. 2016 Nov;15(11):1212–21.
245. Cheng S-H, Li F-C, Souris JS, Yang C-S, Tseng F-G, Lee H-S, et al. Visualizing dynamics of sub-hepatic distribution of nanoparticles using intravital multiphoton fluorescence microscopy. *ACS Nano*. 2012 May;6(5):4122–31.
246. Moghimi SM, Hunter AC, Andresen TL. Factors controlling nanoparticle pharmacokinetics: an integrated analysis and perspective. *Annu Rev Pharmacol Toxicol*. 2012;52:481–503.
247. Hamzeh M, Hosseinimehr SJ, Karimpour A, Mohammadi HR, Khalatbary AR, Talebpour Amiri F. Cerium Oxide Nanoparticles Protect Cyclophosphamide-induced Testicular Toxicity in Mice. *Int J Prev Med*. 2019 Jan 15;10:5.
248. Hardas SS, Sultana R, Warriar G, Dan M, Wu P, Grulke EA, et al. Rat hippocampal responses up to 90 days after a single nanoceria dose extends a hierarchical oxidative stress model for nanoparticle toxicity. *Nanotoxicology*. 2014 Aug;8 Suppl 1:155–66.
249. Sadowska-Bartosz I, Bartosz G. Redox nanoparticles: synthesis, properties and perspectives of use for treatment of neurodegenerative diseases. *J Nanobiotechnology*. 2018 Nov 3;16(1):87.
250. Rzigalinski BA, Carfagna CS, Ehrich M. Cerium oxide nanoparticles in neuroprotection and considerations for efficacy and safety. *Wiley Interdiscip Rev Nanomed Nanobiotechnol*. 2017;9(4):e1444
251. Dhall A, Self W. Cerium Oxide Nanoparticles: A Brief Review of Their Synthesis Methods and Biomedical Applications. *Antioxidants*. 2018 Jul;7(8).
252. Chen J, Patil S, Seal S, McGinnis JF. Rare earth nanoparticles prevent retinal degeneration induced by intracellular peroxides. *Nat Nanotechnol*. 2006 Nov;1(2):142–50.
253. Reed K, Cormack A, Kulkarni A, Mayton M, Sayle D, Klaessig F, et al. Exploring the properties and applications of nanoceria: is there still plenty of room at the bottom? *Environ Sci Nano*. 2014;1(5):390–405.
254. Ivanov VK, Shcherbakov AB, Usatenko A V. Structure-sensitive properties and biomedical applications of nanodispersed cerium dioxide. *Russ Chem Rev*. 2009;78(9):855–71.

255. Sun C, Li H, Chen L. Nanostructured ceria-based materials: synthesis, properties, and applications. *Energy Environ Sci.* 2012;5(9):8475–505.
256. Jung H, Kittelson DB, Zachariah MR. The influence of a cerium additive on ultrafine diesel particle emissions and kinetics of oxidation. *Combust Flame.* 2005;142(3):276–88.
257. Casals E, Gusta MF, Piella J, Casals G, Jiménez W, Puentes V. Intrinsic and Extrinsic Properties Affecting Innate Immune Responses to Nanoparticles: The Case of Cerium Oxide. *Front Immunol.* 2017;8:970.
258. Nemmar A, Al-Salam S, Al Ansari Z, Alkharas ZA, Al Ahbabi RM, Beegam S, et al. Impact of Pulmonary Exposure to Cerium Oxide Nanoparticles on Experimental Acute Kidney Injury. *Cell Physiol Biochem Int J Exp Cell Physiol Biochem Pharmacol.* 2019;52(3):439–54.
259. Tseng MT, Lu X, Duan X, Hardas SS, Sultana R, Wu P, et al. Alteration of hepatic structure and oxidative stress induced by intravenous nanoceria. *Toxicol Appl Pharmacol.* 2012 Apr;260(2):173–82.
260. Pourkhalili N, Hosseini A, Nili-Ahmadabadi A, Hassani S, Pakzad M, Baeeri M, et al. Biochemical and cellular evidence of the benefit of a combination of cerium oxide nanoparticles and selenium to diabetic rats. *World J Diabetes.* 2011 Nov 15;2(11):204–10.
261. Hirst SM, Karakoti AS, Tyler RD, Sriranganathan N, Seal S, Reilly CM. Anti-inflammatory properties of cerium oxide nanoparticles. *Nanotherapeutics.* 2009;5(24):2848–56.
262. Niu J, Azfer A, Rogers LM, Wang X, Kolattukudy PE. Cardioprotective effects of cerium oxide nanoparticles in a transgenic murine model of cardiomyopathy. *Cardiovasc Res.* 2007 Feb;73(3):549–59.
263. Alili L, Sack M, Karakoti AS, Teuber S, Puschmann K, Hirst SM, et al. Combined cytotoxic and anti-invasive properties of redox-active nanoparticles in tumor-stroma interactions. *Biomaterials.* 2011;32(11):2918–29.
264. Casals G, Perramón M, Casals E, Portolés I, Fernández-Varo G, Morales-Ruiz M, et al. Cerium Oxide Nanoparticles: A New Therapeutic Tool in Liver Diseases. *Antioxidants (Basel).* 2021 Apr 24;10(5):660.
265. Oró D, Yudina T, Fernández-Varo G, Casals E, Reichenbach V, Casals G, et al. Cerium oxide nanoparticles reduce steatosis, portal hypertension and display anti-inflammatory properties in rats with liver fibrosis. *J Hepatol.* 2016 Mar;64(3):691–8.

266. Córdoba-Jover B, Arce-Cerezo A, Ribera J, Pauta M, Oró D, Casals G, et al. Cerium oxide nanoparticles improve liver regeneration after acetaminophen-induced liver injury and partial hepatectomy in rats. *J Nanobiotechnology*. 2019 Oct;17(1):112.
267. Fernández-Varo G, Perramón M, Carvajal S, Oró D, Casals E, Boix L, et al. Bespoke Nanoceria: An Effective Treatment in Experimental Hepatocellular Carcinoma. *Hepatology*. 2020 Oct;72(4):1267–82.
268. Hirst SM, Karakoti A, Singh S, Self W, Tyler R, Seal S, et al. Biodistribution and In Vivo Antioxidant Effects of Cerium Oxide Nanoparticles in Mice. *Environ Toxicol*. 2011;28(2):107–18.
269. Yokel RA, Tseng MT, Dan M, Unrine JM, Graham UM, Wu P, et al. Biodistribution and biopersistence of ceria engineered nanomaterials: size dependence. *Nanomedicine*. 2013 Apr;9(3):398–407.
270. Ni D, Wei H, Chen W, Bao Q, Rosenkrans ZT, Barnhart TE, et al. Ceria Nanoparticles Meet Hepatic Ischemia-Reperfusion Injury: The Perfect Imperfection. *Adv Mater*. 2019 Oct;31(40):e1902956.
271. Parra-Robert M, Casals E, Massana N, Zeng M, Perramón M, Fernández-Varo G, et al. Beyond the Scavenging of Reactive Oxygen Species (ROS): Direct Effect of Cerium Oxide Nanoparticles in Reducing Fatty Acids Content in an In Vitro Model of Hepatocellular Steatosis. *Biomolecules*. 2019 Aug;9(9).
272. Ribera J, Rodríguez-Vita J, Cordoba B, Portolés I, Casals G, Casals E, et al. Functionalized cerium oxide nanoparticles mitigate the oxidative stress and pro-inflammatory activity associated to the portal vein endothelium of cirrhotic rats. *PLoS One*. 2019 Jun 24;14(6):e0218716.
273. Carvajal S, Perramón M, Casals G, Oró D, Ribera J, Morales-Ruiz M, et al. Cerium Oxide Nanoparticles Protect against Oxidant Injury and Interfere with Oxidative Mediated Kinase Signaling in Human-Derived Hepatocytes. *Int J Mol Sci*. 2019 Nov;20(23).
274. Ibrahim HG, Attia N, Hashem FEZA, El Heneidy MAR. Cerium oxide nanoparticles: In pursuit of liver protection against doxorubicin-induced injury in rats. *Biomed Pharmacother*. 2018 Jul;103:773–81.
275. Eilenberger C, Selinger F, Rothbauer M, Lin Y, Limbeck A, Schädl B, et al. Cytotoxicity, Retention, and Anti-inflammatory Effects of a CeO₂ Nanoparticle-Based Supramolecular Complex in a 3D Liver Cell Culture Model. *ACS Pharmacol Transl Sci*. 2021 Feb 12;4(1):101–6.

276. Kobyliak N, Virchenko O, Falalyeyeva T, Kondro M, Beregova T, Bodnar P, et al. Cerium dioxide nanoparticles possess anti-inflammatory properties in the conditions of the obesity-associated NAFLD in rats. *Biomed Pharmacother.* 2017 Jun;90:608–14.
277. Carvajal S, Perramón M, Oró D, Casals E, Fernández-Varo G, Casals G, et al. Cerium oxide nanoparticles display antilipogenic effect in rats with non-alcoholic fatty liver disease. *Sci Rep.* 2019 Sep;9(1):12848.
278. Wasef L, Nassar AMK, El-Sayed YS, Samak D, Noreldin A, Elshony N, et al. The potential ameliorative impacts of cerium oxide nanoparticles against fipronil-induced hepatic steatosis. *Sci Rep.* 2021 Jan;11(1):1310.
279. Parra-Robert M, Zeng M, Shu Y, Fernández-Varo G, Perramón M, Desai D, et al. Mesoporous silica coated CeO₂ nanozymes with combined lipid-lowering and antioxidant activity induce long-term improvement of the metabolic profile in obese Zucker rats. *Nanoscale.* 2021 May;13(18):8452–66.
280. Adebayo OA, Akinloye O, Adaramoye OA. Cerium Oxide Nanoparticles Attenuate Oxidative Stress and Inflammation in the Liver of Diethylnitrosamine-Treated Mice. *Biol Trace Elem Res.* 2020;193(1):214–25.
281. Lynn DM, Langer R. Degradable Poly(β -amino esters): Synthesis, Characterization, and Self-Assembly with Plasmid DNA. *J Am Chem Soc.* 2000 Nov 1;122(44):10761–8.
282. Liu Y, Li Y, Keskin D, Shi L. Poly(β -Amino Esters): Synthesis, Formulations, and Their Biomedical Applications. *Adv Healthc Mater.* 2019 Jan;8(2):e1801359.
283. Zamboni CG, Kozielski KL, Vaughan HJ, Nakata MM, Kim J, Higgins LJ, et al. Polymeric nanoparticles as cancer-specific DNA delivery vectors to human hepatocellular carcinoma. *J Control Release.* 2017 Oct;263:18–28.
284. Iqbal S, Qu Y, Dong Z, Zhao J, Rauf Khan A, Rehman S, et al. Poly (β -amino esters) based potential drug delivery and targeting polymer; an overview and perspectives (review). *Eur Polym J.* 2020;141:110097.
285. Tzeng SY, Green JJ. Subtle changes to polymer structure and degradation mechanism enable highly effective nanoparticles for siRNA and DNA delivery to human brain cancer. *Adv Healthc Mater.* 2013 Mar;2(3):468–80.
286. Karlsson J, Rhodes KR, Green JJ, Tzeng SY. Poly(beta-amino ester)s as gene delivery vehicles: challenges and opportunities. *Expert Opin Drug Deliv.* 2020 Oct;17(10):1395–410.

287. Segovia N, Dosta P, Cascante A, Ramos V, Borrós S. Oligopeptide-terminated poly(β -amino ester)s for highly efficient gene delivery and intracellular localization. *Acta Biomater.* 2014 May;10(5):2147–58.
288. Freeman EC, Weiland LM, Meng WS. Modeling the proton sponge hypothesis: examining proton sponge effectiveness for enhancing intracellular gene delivery through multiscale modeling. *J Biomater Sci Polym Ed.* 2013;24(4):398–416.
289. Shenoy D, Little S, Langer R, Amiji M. Poly(ethylene oxide)-modified poly(beta-amino ester) nanoparticles as a pH-sensitive system for tumor-targeted delivery of hydrophobic drugs. 1. In vitro evaluations. *Mol Pharm.* 2005;2(5):357–66.
290. Jones CH, Chen M, Ravikrishnan A, Reddinger R, Zhang G, Hakansson AP, et al. Mannosylated poly(beta-amino esters) for targeted antigen presenting cell immune modulation. *Biomaterials.* 2015 Jan;37:333–44.
291. Fornaguera C, Guerra-Rebollo M, Lázaro MÁ, Cascante A, Rubio N, Blanco J, et al. In Vivo Retargeting of Poly(beta aminoester) (OM-PBAE) Nanoparticles is Influenced by Protein Corona. *Adv Healthc Mater.* 2019 Oct;8(19):e1900849.
292. Green JJ, Chiu E, Leshchiner ES, Shi J, Langer R, Anderson DG. Electrostatic ligand coatings of nanoparticles enable ligand-specific gene delivery to human primary cells. *Nano Lett.* 2007 Apr;7(4):874–9.
293. Ávila-Ortega A, Carrillo-Cocom LM, Olán-Noverola CE, Nic-Can GI, Vilchis-Nestor AR, Talavera-Pech WA. Increased Toxicity of Doxorubicin Encapsulated into pH-Responsive Poly(β -Amino Ester)-Functionalized MCM-41 Silica Nanoparticles. *Curr Drug Deliv.* 2020;17(9):799–805.
294. Moffett HF, Coon ME, Radtke S, Stephan SB, McKnight L, Lambert A, et al. Hit-and-run programming of therapeutic cytoreagents using mRNA nanocarriers. *Nat Commun.* 2017;8(1):389.
295. Mastorakos P, da Silva AL, Chisholm J, Song E, Choi WK, Boyle MP, et al. Highly compacted biodegradable DNA nanoparticles capable of overcoming the mucus barrier for inhaled lung gene therapy. *Proc Natl Acad Sci.* 2015 Jul 14;112(28):8720 LP – 8725.
296. Kaczmarek JC, Kauffman KJ, Fenton OS, Sadtler K, Patel AK, Heartlein MW, et al. Optimization of a Degradable Polymer–Lipid Nanoparticle for Potent Systemic Delivery of mRNA to the Lung Endothelium and Immune Cells. *Nano Lett.* 2018 Oct 10;18(10):6449–54.

297. Perni S, Prokopovich P. Optimisation and feature selection of poly-beta-amino-ester as a drug delivery system for cartilage. *J Mater Chem B*. 2020 Jun;8(23):5096–108.
298. Karlsson J, Rui Y, Kozielski KL, Placone AL, Choi O, Tzeng SY, et al. Engineered nanoparticles for systemic siRNA delivery to malignant brain tumours. *Nanoscale*. 2019 Nov;11(42):20045–57.
299. Gregory J V, Kadiyala P, Doherty R, Cadena M, Habel S, Ruoslahti E, et al. Systemic brain tumor delivery of synthetic protein nanoparticles for glioblastoma therapy. *Nat Commun*. 2020 Nov;11(1):5687.
300. Segovia N, Pont M, Oliva N, Ramos V, Borrós S, Artzi N. Hydrogel doped with nanoparticles for local sustained release of siRNA in breast cancer. *Adv Healthc Mater*. 2015 Jan;4(2):271–80.
301. Zhu D, Shen H, Tan S, Hu Z, Wang L, Yu L, et al. Nanoparticles Based on Poly (β -Amino Ester) and HPV16-Targeting CRISPR/shRNA as Potential Drugs for HPV16-Related Cervical Malignancy. *Mol Ther*. 2018 Oct;26(10):2443–55.
302. Tzeng SY, Patel KK, Wilson DR, Meyer RA, Rhodes KR, Green JJ. In situ genetic engineering of tumors for long-lasting and systemic immunotherapy. *Proc Natl Acad Sci*. 2020 Feb 25;117(8):4043 LP – 4052.
303. Vaughan HJ, Zamboni CG, Radant NP, Bhardwaj P, Revai Lechtich E, Hassan LF, et al. Poly(beta-amino ester) nanoparticles enable tumor-specific TRAIL secretion and a bystander effect to treat liver cancer. *Mol Ther - Oncolytics*. 2021 Jun 25;21:377–88.
304. Sharma BC, Gluud LL, Sarin SK. Beta-blocker plus nitrates for secondary prevention of variceal bleeding. Vol. 2017, *The Cochrane Database of Systematic Reviews*. 2017. p. CD006709.
305. Mela M, Mancuso A, Burroughs A. Drug treatment for portal hypertension. *Ann Hepatol*. 2002;1(3):102–20.
306. Huang J, Zhang X, Zhang M, Zhu J-D, Zhang Y-L, Lin Y, et al. Up-regulation of DLK1 as an imprinted gene could contribute to human hepatocellular carcinoma. *Carcinogenesis*. 2007 May 1;28(5):1094–103.
307. Chakravorty D, Jana T, Das Mandal S, Seth A, Bhattacharya A, Saha S. MYCbase: a database of functional sites and biochemical properties of Myc in both normal and cancer cells. *BMC Bioinformatics*. 2017 Apr;18(1):224.

308. Shah PP, Kakar SS. Pituitary tumor transforming gene induces epithelial to mesenchymal transition by regulation of Twist, Snail, Slug, and E-cadherin. *Cancer Lett.* 2011 Dec;311(1):66–76.
309. Reichenbach V, Fernández-Varo G, Casals G, Oró D, Ros J, Melgar-Lesmes P, et al. Adenoviral dominant-negative soluble PDGFR β improves hepatic collagen, systemic hemodynamics, and portal pressure in fibrotic rats. *J Hepatol.* 2012 Nov;57(5):967–73.
310. Borkham-Kamphorst E, Herrmann J, Stoll D, Treptau J, Gressner AM, Weiskirchen R. Dominant-negative soluble PDGF-beta receptor inhibits hepatic stellate cell activation and attenuates liver fibrosis. *Lab Invest.* 2004 Jun;84(6):766–77.
311. Pinzani M. PDGF and signal transduction in hepatic stellate cells. *Front Biosci.* 2002 Aug;7:d1720-6.
312. Friedman SL. Mechanisms of hepatic fibrogenesis. *Gastroenterology.* 2008 May;134(6):1655–69.
313. Murphy G, Cockett MI, Ward R V, Docherty AJ. Matrix metalloproteinase degradation of elastin, type IV collagen and proteoglycan. A quantitative comparison of the activities of 95 kDa and 72 kDa gelatinases, stromelysins-1 and -2 and punctuated metalloproteinase (PUMP). *Biochem J.* 1991 Jul;277 (Pt 1(Pt 1):277–9.
314. Arthur MJ. Fibrogenesis II. Metalloproteinases and their inhibitors in liver fibrosis. *Am J Physiol Gastrointest Liver Physiol.* 2000 Aug;279(2):G245-9.
315. Hagiwara R, Kageyama K, Niioka K, Takayasu S, Tasso M, Daimon M. Involvement of histone deacetylase 1/2 in adrenocorticotrophic hormone synthesis and proliferation of corticotroph tumor AtT-20 cells. *Peptides.* 2021 Feb;136:170441.
316. Yan H, Wang W, Dou C, Tian F, Qi S. Securin promotes migration and invasion via matrix metalloproteinases in glioma cells. *Oncol Lett.* 2015 Jun;9(6):2895–901.
317. Alcolado R, Arthur MJ, Iredale JP. Pathogenesis of liver fibrosis. Vol. 92, *Clinical science* (London, England: 1979). England; 1997. p. 103–12.
318. Madtes DK, Elston AL, Kaback LA, Clark JG. Selective induction of tissue inhibitor of metalloproteinase-1 in bleomycin-induced pulmonary fibrosis. *Am J Respir Cell Mol Biol.* 2001 May;24(5):599–607.

319. Casals E, Gonzalez E, Puentes VF. Reactivity of inorganic nanoparticles in biological environments: insights into nanotoxicity mechanisms. *J Phys D Appl Phys*. 2012;45(44):443001.
320. Krenkel O, Tacke F. Liver macrophages in tissue homeostasis and disease. *Nat Rev Immunol*. 2017 May;17(5):306–21.
321. Wang Y, Yang F, Zhang HX, Zi XY, Pan XH, Chen F, et al. Cuprous oxide nanoparticles inhibit the growth and metastasis of melanoma by targeting mitochondria. *Cell Death Dis*. 2013 Aug;4(8):e783.
322. Asati V, Mahapatra DK, Bharti SK. PI3K/Akt/mTOR and Ras/Raf/MEK/ERK signaling pathways inhibitors as anticancer agents: Structural and pharmacological perspectives. *Eur J Med Chem*. 2016 Feb;109:314–41.
323. Czuby A, Piekietko-Witkowska A. Protein kinases that phosphorylate splicing factors: Roles in cancer development, progression and possible therapeutic options. *Int J Biochem Cell Biol*. 2017 Oct;91(Pt B):102–15.
324. Fearnley GW, Young KA, Edgar JR, Antrobus R, Hay IM, Liang W-C, et al. The homophilic receptor PTPRK selectively dephosphorylates multiple junctional regulators to promote cell-cell adhesion. *Elife*. 2019 Mar;8.
325. Röhrig F, Schulze A. The multifaceted roles of fatty acid synthesis in cancer. *Nat Rev Cancer*. 2016 Nov;16(11):732–49.
326. Bechmann LP, Hannivoort RA, Gerken G, Hotamisligil GS, Trauner M, Canbay A. The interaction of hepatic lipid and glucose metabolism in liver diseases. *J Hepatol*. 2012 Apr;56(4):952–64.
327. Abel S, Smuts CM, de Villiers C, Gelderblom WC. Changes in essential fatty acid patterns associated with normal liver regeneration and the progression of hepatocyte nodules in rat hepatocarcinogenesis. *Carcinogenesis*. 2001 May;22(5):795–804.
328. Brown ZJ, Fu Q, Ma C, Kruhlak M, Zhang H, Luo J, et al. Carnitine palmitoyltransferase gene upregulation by linoleic acid induces CD4(+) T cell apoptosis promoting HCC development. *Cell Death Dis*. 2018 May;9(6):620.
329. Valenzuela R, Echeverria F, Ortiz M, Rincón-Cervera MÁ, Espinosa A, Hernandez-Rodas MC, et al. Hydroxytyrosol prevents reduction in liver activity of Δ -5 and Δ -6 desaturases, oxidative stress, and depletion in long chain polyunsaturated fatty acid content in different tissues of high-fat diet fed mice. *Lipids Health Dis*. 2017 Apr;16(1):64.

330. Bruix J, Reig M, Sherman M. Evidence-Based Diagnosis, Staging, and Treatment of Patients With Hepatocellular Carcinoma. *Gastroenterology*. 2016 Apr;150(4):835–53.
331. Wilhelm SM, Adnane L, Newell P, Villanueva A, Llovet JM, Lynch M. Preclinical overview of sorafenib, a multikinase inhibitor that targets both Raf and VEGF and PDGF receptor tyrosine kinase signaling. *Mol Cancer Ther*. 2008 Oct;7(10):3129–40.
332. Park D, Saravanakumar G, Kim WJ. Chapter 10 - Nitric Oxide-Releasing Functional Nanomaterials for Anticancer Therapy. In: Morbidelli L, Bonavida BBT-TA of NO in C and ID, editors. *Therapeutic Application of Nitric Oxide in Cancer and Inflammatory Disorders*. Academic Press; 2019. p. 191–218.
333. França-Silva MS, Balarini CM, Cruz JC, Khan BA, Rampelotto PH, Braga VA. Organic nitrates: past, present and future. *Molecules*. 2014 Sep;19(9):15314–23.
334. Daiber A, Münzel T. Organic Nitrate Therapy, Nitrate Tolerance, and Nitrate-Induced Endothelial Dysfunction: Emphasis on Redox Biology and Oxidative Stress. *Antioxid Redox Signal*. 2015 Oct;23(11):899–942.
335. Shirakami Y, Lee S-A, Clugston RD, Blaner WS. Hepatic metabolism of retinoids and disease associations. *Biochim Biophys Acta*. 2012 Jan;1821(1):124–36.
336. Kim SG, Larson JJ, Lee JS, Therneau TM, Kim WR. Beneficial and harmful effects of nonselective beta blockade on acute kidney injury in liver transplant candidates. *Liver Transplant Off Publ Am Assoc Study Liver Dis Int Liver Transplant Soc*. 2017 Jun;23(6):733–40.
337. Sersté T, Melot C, Francoz C, Durand F, Rautou P-E, Valla D, et al. Deleterious effects of beta-blockers on survival in patients with cirrhosis and refractory ascites. *Hepatology*. 2010 Sep;52(3):1017–22.
338. Sun J, Li M, Fan S, Guo Z, Zhong B, Jin X, et al. A novel liver-targeted nitric oxide donor UDCA-Thr-NO protects against cirrhosis and portal hypertension. *Am J Transl Res*. 2018 Feb 15;10(2):392–401.
339. Rodríguez S, Raurell I, Torres-Arauz M, García-Lezana T, Genescà J, Martell M. A Nitric Oxide-Donating Statin Decreases Portal Pressure with a Better Toxicity Profile than Conventional Statins in Cirrhotic Rats. *Sci Rep*. 2017;7(1):40461.
340. Moal F, Veal N, Vuillemin E, Barrière E, Wang J, Fizanne L, et al. Hemodynamic and antifibrotic effects of a selective liver nitric oxide donor V-

- PYRRO/NO in bile duct ligated rats. *World J Gastroenterol*. 2006 Nov;12(41):6639–45.
341. Leung T-M, Fung M-L, Liong EC, Lau TYH, Nanji AA, Tipoe GL. Role of nitric oxide in the regulation of fibrogenic factors in experimental liver fibrosis in mice. *Histol Histopathol*. 2011 Feb;26(2):201–11.
342. Thiele ND, Wirth JW, Steins D, Koop AC, Ittrich H, Lohse AW, et al. TIMP-1 is upregulated, but not essential in hepatic fibrogenesis and carcinogenesis in mice. *Sci Rep*. 2017 Apr 6;7(1):714.
343. Nie Q-H, Zhang Y-F, Xie Y-M, Luo X-D, Shao B, Li J, et al. Correlation between TIMP-1 expression and liver fibrosis in two rat liver fibrosis models. *World J Gastroenterol*. 2006 May 21;12(19):3044–9.
344. Wang K, Lin B, Brems JJ, Gamelli RL. Hepatic apoptosis can modulate liver fibrosis through TIMP1 pathway. *Apoptosis*. 2013;18(5):566–77.
345. Busk TM, Bendtsen F, Nielsen HJ, Jensen V, Brüner N, Møller S. TIMP-1 in patients with cirrhosis: relation to liver dysfunction, portal hypertension, and hemodynamic changes. *Scand J Gastroenterol*. 2014 Sep;49(9):1103–10.
346. Hink U, Münzel T. COX-2, Another Important Player in the Nitric Oxide–Endothelin Cross-Talk. *Circ Res*. 2006 Jun 9;98(11):1344–6.
347. Yang H, Xuefeng Y, Shandong W, Jianhua X. COX-2 in liver fibrosis. *Clin Chim Acta*. 2020;506:196–203.
348. Grumbach IM, Chen W, Mertens SA, Harrison DG. A negative feedback mechanism involving nitric oxide and nuclear factor kappa-B modulates endothelial nitric oxide synthase transcription. *J Mol Cell Cardiol*. 2005 Oct;39(4):595–603.
349. Liu T, Zhang L, Joo D, Sun S-C. NF- κ B signaling in inflammation. *Signal Transduct Target Ther*. 2017;2(1):17023.